UNIVERSITÀ DEGLI STUDI DI CAMERINO

SCHOOL OF ADVANCED STUDIES

DOCTORAL COURSE IN

SCIENCES AND TECHNOLOGY

XXXIV CYCLE

Tectonic escape of Sicily micro plate in the framework of the Tyrrhenian-Apennine system evolution

PHD STUDENT

GIULIA PENZA

SUPERVISOR

PIETRO PAOLO PIERANTONI

Contents

Abstract

The opening of the Tyrrhenian basin and the contemporary formation of the Apennine chain are described through the application of techniques of deformable plate kinematics and modeled with several dedicated software (Chapter 1). These methods have proven to be suitable to describe complex tectonic processes, such as those observed along the Africa–Europe collision belt, characterized by passive subduction processes. These results from the subduction of the residual Alpine Tethys and the Ionian lithosphere, and from the fragmentation of the Adriatic plate.

As a first step, described in Chapter 2, the area of the Apennine Chain and of the Tyrrhenian basin have been divided into deformable polygons through a careful observation of the regional structures. The polygons are distinguished on the basis of sets of extensional structures that are coherent with unique Euler pole grids. The boundaries between these polygons coincide with large tectonic lineaments that characterize the Tyrrhenian–Apennine area. The tectonic style along these structures reflects the variability of relative velocity vectors between two adjacent blocks. The deformation of tectonic elements is accomplished, allowing different rotation velocities of lines that compose these blocks about the same stable stage poles. The angular velocities of extension are determined on the basis of the stratigraphic records of syn-rift sequences, while the finite rotation angles are obtained by crustal balancing. From north to south, the polygons are: (1) Northern Apennine; (2) Umbria–Marche Apennine Arc; (3) Southern Apennine; (4) Calabrian Arc; (5) Sicilian Chain.

Then, to understand the geodynamic processes that guided the opening of Tyrrhenian back-arc basin, the geometry of the Adriatic-Ionian slab has been reconstructed and presented in Chapter 3. The slab is constituted by Liguride and Ionian oceans and by the Apulian-Adriatic continental margin. It is segmented by STEP faults, propagated along the COB of the Liguride and Ionian oceans and along the fracture zones of the Apulian-Adriatic margin, formed during the Triassic-Jurassic rifting. The continental lithosphere begins to subduct starting from the North and proceeds to the South with time intervals determined by the articulation of the Adriatic COB line. To the South, where the continental lithosphere is absent or scarce, the slab segments keep sinking into the upper mantle; on the contrary, the northernmost segments progressively decrease their sinking with the incoming of continental lithosphere into the subduction zone, until the buoyancy equilibrium is reached. A strong relationship between upper plate evolution and asynchronous subduction has been considered in the proposed kinematic model.

Chapter 4 is dedicated to the specific aim of this PhD thesis: reconstruct the kinematic evolution of Sicily, considered as an independent plate starting from 4.5 Ma ago, and its role in the framework of the Tyrrhenian-Apennine System. Sicily is involved in a process of escape towards east-southeast induced by the African plate acting as an intender pushing toward north, during its convergence with the European plate, and by the Malta escarpment STEP fault, due to the retreat of the African-Ionian slab that created space toward east.

The plates and microplates that I consider involved during the evolution of the last 4.5 Ma are Europe, Africa, Calabria and Tunisia. This last microplate is strictly related to the evolution of Sicily. The boundaries of the Sicily and Tunisia microplates are lithospheric structures known from the literature and identifiable from geological and geophysical datasets: high resolution bathymetric maps, seismic sections, geodetic data, focal mechanism of recent earthquakes, gravimetric maps, Moho depth maps and so on.

The margin between Sicily and Europe is along the Drepano-Elimi chain (Ustica ridge), a E-W trending morpho-structure with a general transpressive kinematics; the margin with the Calabrian microplate is along the right-lateral Taormina line first and then along the ‘‘Aeolian-Tindari-Letojanni” line; the margin with Africa is expressed along part of the Malta Escarpment and along the Sicily Channel, where a series of troughs (Pantelleria, Linosa and Malta) were interpreted in literature as rift basins or as pull-apart basins related to a dextral shear zone. The margins of Tunisia instead follow the N-S and NE-SW structures that characterize the Central Atlas.

Several attempts have been tried to obtain the Euler pole of rotation between Sicily and Africa, starting from the structures in the Sicily Channel and using the GPlates software. Then, also Sicily-Europe, Sicily-Calabria and Sicily-Tunisia poles and the respective velocity vectors have been derived and compared with the geological data.

Finally, the proposed kinematic model of the Tyrrhenian-Apennine system, including Sicily and Tunisia, is shown in Appendix 1 and Movie 1, and described in 5 phases in Chapter 5. Briefly, during the first phase (19–12 Ma), an extension strip divided the proto-Apennine chain from Sardinia while a northern Apennine arc and a central Apennine arc were separated from an extensional area, in transverse direction, covered by top-wedge sediments. The Calabrian arc was divided in north Calabria and south Calabria–Peloritani mounts, separated by the Catanzaro Trough. The second phase (12–7 Ma) is marked by the separation of the Western Sicily chain from the Calabrian arc and the beginning of extension in the Caltanissetta basin; this, is still active in

phase 3, for the whole Messinian age. Phase 3 (7–4.5 Ma) was characterized by the formation of the Vavilov basin, which records major changes in the Ionian slab-retreat process. A new nascent sector, the Southern Apennine Sector, including the Lazio–Abruzzi platform, was separated from the Apennine Arc by the Ancona–Anzio Line and rotated around a very close pole, located at the northern tip of the Vavilov Basin. During phase 4 (4.5-2.5 Ma) Sicily and Tunisia start to rotate around their poles: Tunisia is pushed upward while Sicily starts a clockwise rotation that produces extension in the northernmost part of the Sicily Channel. At this time the Taormina line is active as the boundary between Sicily and Calabria. At the beginning of the last phase (2.5-0 Ma) extension jumped eastwards of the Vavilov basin and the southern branch of the triple junction of the Southern Tyrrhenian rifts started to form the Marsili basin. A dextral shear zone is active in the Sicily channel and the movement between Sicily and Calabria jumps from the Taormina line to the ‘‘Aeolian-Tindari-Letojanni” line. At the end of this phase the Ionian STEP fault intersected the Malta Escarpment and the tear fault began to propagate along this structure.

General Introduction

This PhD thesis is part of an extensive research focused on the evolution of the Tyrrhenian-Apennine system (PRIN Turco, prot. 2008YWPCWB). The research group has been working in this direction for years, aiming to create a kinematic model that reconciles the kinematic constraints with the geological-geophysical data recorded in the central Mediterranean area.

The ultimate goal of my PhD project was the characterization of the Sicily microplate and its kinematic reconstruction. The novelty of this project consists in the fact that until now Sicily had not been considered an independent microplate but as part of Africa/Europe.

The idea of an independent Sicily microplate was born thinking about the relationship between Upper and Lower plates; the paper Pierantoni et al. (2020) shows a first result about the influence of the Lower plate on the Upper plate, then resumed and improved in Turco et al. (2021).

This last article, for which I contributed in the improving of the method, investigation and data curation, but above all for the modeling with PCME and GPlates software, represents the integration of all the data collected in recent years (excluding Sicily) in a single kinematic model.

In this thesis, the kinematic evolution of Sicily have been integrated inside the evolution of the Tyrrhenian-Apennine system that we published with the paper Turco et al. (2021).

The movie included in this work (Appendix 1 and Movie 1) puts together the kinematic model of Turco et al. (2021) with the kinematic model for Sicily microplate and can contribute to our better knowledge of the Central Mediterranean area.

Chapter 1 - Plate tectonics: Tools and methods

Ch.1.1 - Introduction

Plate kinematics is the fundamental tool to describe, on a global scale, the processes affecting the Earth's lithosphere. The relative motions and interactions of tectonic plates, the opening and closure of oceanic basins and the formation or destruction of continents can all be reconstructed modeling the rotations of spherical caps about Eulerian poles (*Greiner, 1999; Schettino, 2014*). The results obtained from modeling are paleogeographic maps of the past which, if used in time-sequence, can provide kinematic information and insights on the geodynamic processes active in a selected time frame.

The quantity of geological and geophysical data needed is huge, at local scale as well as at regional and global scale. Geological data can constrain the model about the kind of process in place and timing, and assess its reliability. Geophysical data provide an estimate of the modulus and direction of plate motion and of the amount of deformation (stretching or shortening) along plate boundaries.
The collected data are integrated in appropriate software to obtain a synthetic plate motion model. The essential objects to be included in the model are the tectonic elements, delimited by plate boundaries or other geologic features (e.g. tectonic lineaments) and a rotation model that specifies relative positions and orientations for each pair of plates, in the form of total reconstruction poles (*Cox and Hart, 1986*), at selected times, usually coinciding with times of principal identified marine magnetic anomalies.

The kinematic parameters that can be obtained dealing with oceanic plate boundaries are due to the study of fracture zones and magnetic anomalies. The first ones allow to obtain the geometry of motion (rotation axes) fitting small circle arcs to fracture zone segments, the second ones allow to determine the timing of each rotation, through a pattern of magnetic stripes, on both sides of the mid-ocean ridge (*Vine and Matthews, 1963*).

In the absence of this kind of data, structural geology can contribute to determine some fundamental parameters that must be specified to apply the plate kinematics approach, such as plate boundaries, kinematic indicators, useful to determine rotation poles, and angles of rotation. It is important to specify that the kind of structural data that can be useful, for determining rotation poles, must be observed on geological structures at the same scale of the model that is

being constructed. For example, single slip vectors observed along the Dead Sea fault zone cannot be used for determining the rotation pole of a microplate like Sinai. In fact, due to the heterogeneity of the rocks, these data record only strains generated by local stresses. Instead, the structural parameters that can be useful for determining rotation poles must be observed on geological structures at the same scale of the model that is being constructed.

Ch.1.2 - Tectonic Elements

Tectonic elements are semi-rigid lithospheric blocks, bounded by faults, which have had an independent kinematic history in a certain time interval (*Ross and Scotese, 1988*). Specialized GIS software, such as GlobalMapper™ and thematic base maps (gravity or magnetic anomaly maps, topography,bathymetry, geologic maps, structural maps, etc.) allow to define and digitize them in order to reconstruct sequences of past plate configurations (*Schettino, 2014*). Another important attribute that needs to be specified is the temporal range of activity of tectonic elements along their boundary.

Oceanic plate boundaries are easily recognizable observing fracture zones and mid-ocean ridges. Continent-Ocean boundaries (COBs) are defined on the basis of geophysical constraints, for example they were associated with the maximum horizontal gradient of the gravity anomaly field (*Schettino & Scotese, 2005*) (Fig. 1.1) or identified through magnetic anomalies that border volcanic ocean-continent transitions (OCTs). In the past, the shape of isobaths was assumed as representative of the COB (*Bullard et al., 1965*). Such method returns good results only at the beginning of the ocean opening since the subsequent sediment deposition strongly affects the shape of bathymetry contour lines and decreases the initial goodness of fit.

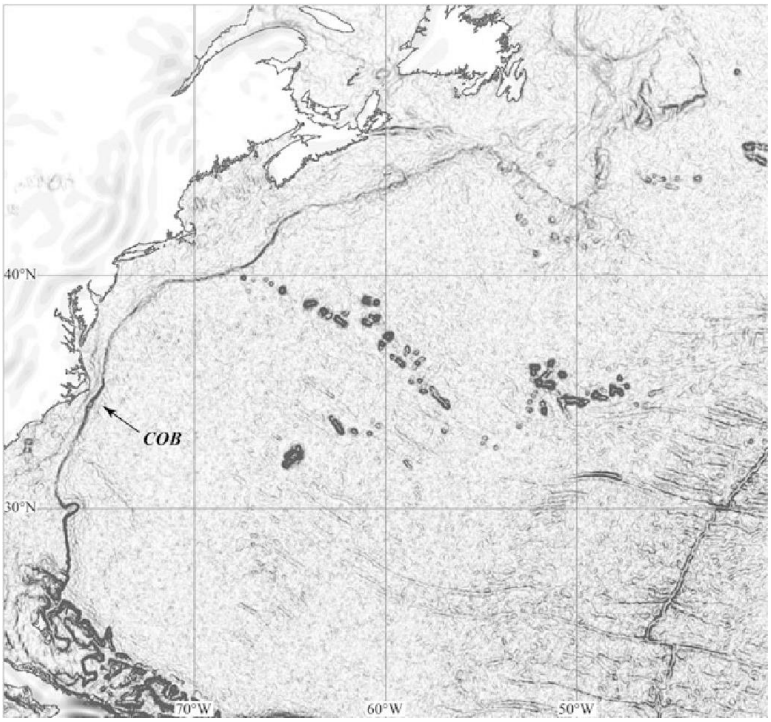

Figure. 1.1 - Eastern North American COB, based on the maximum horizontal gradient of the free-air gravity anomaly field, from Sandwell and Smith 1997.

Ch.1.3 - Modeling

During the modeling phase tectonic elements are considered as 2D objects moving on the earth surface, thus as polygonal regions that move on the unit sphere. (*Schettino, 1998; 1999a; 1999b*). The geographic coordinates ((θ, φ), latitude and longitude) of the vertices of the tectonic elements represent their current position and orientation. Cartesian coordinates (*x*, *y*, *z*), built setting the *z*-axis oriented as the Earth's spin axis, the *x*-axis directed towards the Greenwich meridian (φ = 0) and the *y*-axis intersected with the Earth's surface at 90°E, are then obtained by the following Equation:

$$\begin{cases} x = cos\lambda cos\varphi \\ y = cos\lambda sin\varphi \\ z = sin\lambda \end{cases}$$

This geocentric reference system is valid to describe the past relative position of an object (tectonic element A) compared to the current position of another object (tectonic element B) called reference plate. Thus, applying a finite rotation to the object A around an axis α, of an angle Ω, the object A is moved from the current position to the position assumed at time t, with respect to object B (fixed in the current geographic system).

A finite rotation is the result of the combination of three elementary rotations, respectively about the *z*, *x* and *y*-axis. Each rotation can be described by a 3x3 orthogonal matrix, and the total rotation is associated to the 3x3 orthogonal matrix that results from the product of these matrices. Hence, any re-orientation of A can be described as a rotation about a unique axis *α* and angle of rotation *Ω* (*Schettino, 2014*).

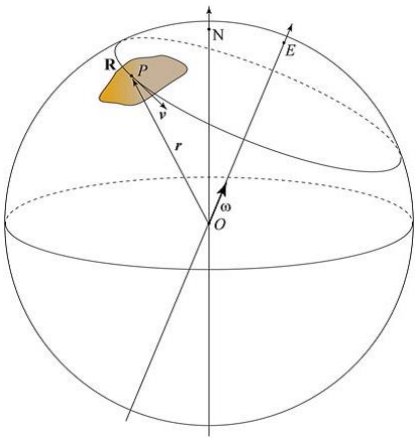

Figure. 1.2 - Geometry of the instantaneous motion of a tectonic plate R. E is the Euler pole, N is the North Pole. P is a representative point on R, whose instantaneous linear velocity is v. ω is the Euler vector of R; from *Schettino (2014).*

The point where the finite positive rotation semi-axis intersects the Earth's surface is called the Euler pole (Fig. 1.2). The corresponding rotation matrix will be indicated as $R_{AB}(t)$. If e = (e_x,e_y,e_z) are the Cartesian coordinates of the Euler pole, then $R_{AB}(t)$ is given by Cox and Hart (1986):

$$R = \begin{bmatrix} e_x^2(1-cos\Omega)+cos\Omega & e_xe_y(1-cos\Omega)-e_zsin\Omega & e_xe_z(1-cos\Omega)+e_ysin\Omega \\ e_xe_y(1-cos\Omega)+e_zsin\Omega & e_y^2(1-cos\Omega)+cos\Omega & e_ye_z(1-cos\Omega)-e_xsin\Omega \\ e_xe_z(1-cos\Omega)-e_ysin\Omega & e_ye_z(1-cos\Omega)+e_xsin\Omega & e_z^2(1-cos\Omega)+cos\Omega \end{bmatrix}$$

Euler pole of finite rotations can be calculated in many other different ways, according to the specific tectonic setting:

* conjugate isochrons can be moved using interactive computer software until a best match to calculate the resulting finite pole of rotation;
* fracture zones and strike slip faults can be modeled as small circle arcs about axis α. Great circles, drawn perpendicular to these structures meet at the pole, with some scatter. Rotation angle Ω and timing are then determined geologically (*Cox and Hart, 1986*);
* small fragments of continental lithosphere: this method mostly relies on geological constraints; it was used by *Turco et al. (2013; 2021*) for the kinematic model of the Tyrrhenian-Apennine system and will be discussed in detail in Chapter 2. Two principles need to be applied: the model must be consistent with the kinematics of the surrounding plates and the original geometry of fragments must be restored through the construction of crustal-scale mass balanced profiles (*Macchiavelli, 2014*);
* Engebretson and Cox (*1984*) method: useful when a starting finite rotation is known, but no isochrons pairs are available for earlier times. This is a method of analysis based on the equation:

$$R_{AB}(t_2) = S_{AB}(t_1, t_2)R_{AB}(t_1)$$

Where $t_1 < t_2$. It allows the calculation of stage poles and, indirectly, finite rotations from a one-sided dataset of magnetic anomalies and fracture zones.

A stage rotation represents the rotation that is necessary to carry a plate A from the relative position assumed at time t_1 to the position assumed at time t_2 relatively to a reference plate B that is kept fixed to the present day location (Fig. 1.3). It is assumed that an Euler pole remains fixed during the stage and jumps between successive stages. It is important to notice that finite reconstructions are the combined result of many instantaneous or stage rotations.

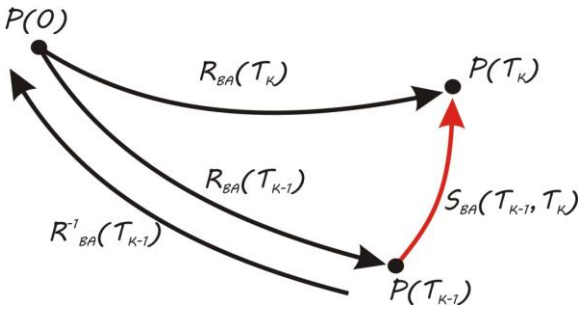

Figure. 1.3 - Relationship between stage rotations and finite reconstructions. To move a point P from the location at time T_{k-1} to that at time T_k, it is possible to go first to the present day through an inverse finite reconstruction, then to time T_k through a direct finite transformation; modified from *Schettino (2014)*.

All the kinematic information that is needed to reconstruct the plate motions and the tectonic history at regional or global scale, for the considered time interval, are stored in a rotation model. Rotation model is a table that contains all the known Euler poles, expressed as coordinates (Latitude, Longitude) of the pole, and angle of rotation for each couple of plates (Fig. 1.4).

- Plate ID number;
- Age;
- Euler Pole Latitude;
- Euler Pole Longitude;
- Finite rotation angle;
- Reference (Fixed) Plate ID number;
- Comments.

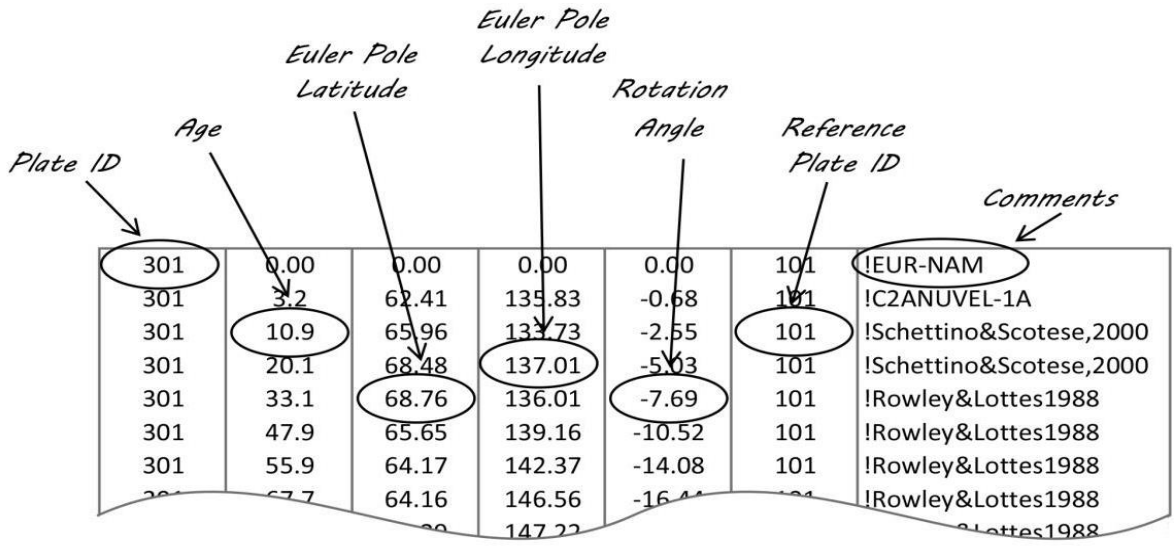

Figure. 1.4 - A fragment of a rotation model.

Ch.1.3.1 - GPlates

GPlates is a desktop software for the interactive visualization of plate tectonics. It combines interactive plate tectonic reconstructions, geographic information system (GIS) functionality and raster data visualization. GPlates enables both the display and the manipulation of plate tectonic reconstructions and associated data through geological time (*Müller et al., 2018*).

This software is an essential tool for Euler Poles calculation, to verify the fitting with geological structures, calibrate the movements derived from the obtained poles and identify for each boundary the kinematic associated to the specific pole. It was used to create the proposed kinematic model (Ch.5) and the movie included in this work (Appendix 1 and Movie 1). Each tectonic element of the kinematic reconstruction has been created and modeled in Gplates and then re-drawn in Corel Draw for a better image resolution (Fig. 1.5).

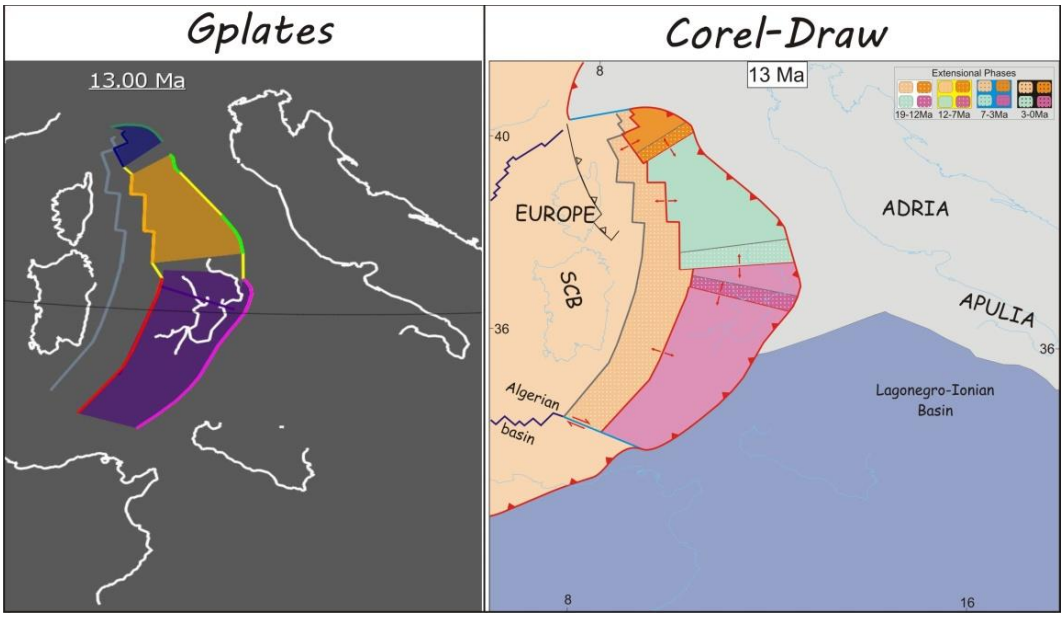

Figure. 1.5 – Example of GPlates product compared with finite product in Corel-Draw.

The used tools are:

- Digitise tool: it enables the user to digitise features on the globe as polylines, polygons and multi-point geometries and to add them to new or existing feature collections. Once the feature is created it is possible to assign a plate ID number, that is a number with three or more digit that represents the name of a specific plate, a type (e.g. Fault, Basin, Volcano) and various properties (e.g. age of appearance and disappearance). When combined with a rotation file, tectonic elements with an assigned ID number can be digitised at any time in the past and then reconstructed backwards and forwards through time.

- Pole manipulation: there are different tools to modify poles, the most used allows to drag a tectonic element from the current position to a past position, for example to determine the pole between two isochrons with this tool is possible to overlap one isochrons on the other, considered fixed, and obtain the geographical coordinates of the Euler pole that describes this movement.
- Small circle features: a useful tool to detect the direction of relative motion of a tectonic element at any point on the boundary. They are parallels of latitude about the Euler pole. Small circles can be drawn with the mouse directly on the globe or map, explicitly specified by the user or generated from a stage-pole calculation.

  During the modeling phase, small circles have been superimposed on high resolution bathymetry in GPlates or in Global Mapper, to verify the fitting between structures along the boundary and the kinematics associated to the poles. It was also used to determine the poles using the technique with fracture zones and strike slip faults described above.
- Topology tool: topological features are features which do not have a geometry defined of their own. Instead of a single fixed geometry their geometry is based on the parts of other features. This tool was used to build, in the movie, the semi-rigid blocks described by *Turco et al. (2021*) and in Chapter 2. In particular, thrust fronts are lengthened as they migrate toward East and blocks are changing shape interacting with each other.
- Motion Paths tool: creates arrows that show the absolute motion of a tectonic element over time, either with respect to the anchor plate, or with respect to some other specified plate, based on the used rotation file.

Ch.1.3.2 - Global Mapper

Global Mapper is a GIS software package developed by Blue Marble Geographics for Windows OS. It is capable of displaying and handling raster and elevation and vector datasets, allowing users to easily export the data in multiple formats.

It was mostly used in the bathymetric interpretation, first loading a high resolution bathymetry of the area and then inspecting large scale structures. Also Euler rotation poles obtained with GPlates were loaded in Global Mapper and compared with the observed structures. Finally it was used to create points, lines and areas and export in DWG or SHP formats the objects used in the final movie.

Ch.1.3.3 - P.C.M.E. software © (Schettino, 1998)

It was used by *Turco et al.* (*2012, 2013*) to create a first kinematic reconstruction of the Tyrrenian-Appenine system. The PCME user-interface permits paleogeographic reconstructions for any time interval. In the map editor it is possible to create multipolygon map files (.mpf) that represent paleogeographic or paleotectonic features. A multipolygon map file is a file containing sequences of vertices for any set of polygons representing shelf margins, coastlines, topographic contours or tectonic lines. Supported data are in the formats: PCME binary map files, ASCII text files (lists of the latitudinal and longitudinal coordinates of geographic elements) and geographic data files in the format of the PALEOMAP project (*Schettino, 1998*). Having one or more MPF files with the present day position of tectonic elements, it is possible to rotate them in their ancient position with the Finite Rotation Tool. Here the user can specify either an Euler pole and a rotation angle or a paleomagnetic pole and a longitude shift.

The rotation of an entire set of tectonic elements from the present day position to the past position at a given time requires a standard rotation model, similar to the one described in Chapter 1.3.

Other modeling tools, useful to access geophysical data, are: a contouring module and an isochrone generator, allow the user to extract respectively ocean floor polygons or isochrons from the Ocean Floor Agegrid (*Müller et al., 1997*); a contouring module, for the extraction of topographic/bathymetric contours; a module for the computation of geometric parameters (area and inertial tensor components) of tectonic plate polygons or plate boundaries.

All the rotated tectonic elements are then assembled into continental margin polygons, representing the boundaries of the shallow seas and containing information about the limit between oceanic and continental crust. Also, polygons for the ancient landmass shorelines and for the mountain (non-deposition area) contours must be defined. Finally, the definition of a set of tectonic lines for ridges, active plate margins, fractures etc. completes a standard paleogeographic framework.

Once a complete set of maps has been created, it is possible to generate and display reconstructions and compare the terrestrial paleogeography at different ages (*Macchiavelli, 2014*).

Ch.1.4 - References

Bullard, E. C.; Everett, J. E. and Smith, A. G. 1965. The fit of the continents around the Atlantic: a symposium on continental drift, Phil. Trans. R. Soc. London, Ser. A, 258, pp. 41-51.

Cox, A. and Hart, R. B. 1986. Plate Tectonics: How It Works, 392 pp., Blackwell Scientific Publications, Palo Alto, Calif.

Engebretson, D. C.; Cox, A. and Gordon, R. G. 1984. Relative motions between oceanic plates of the Pacific basin, J. Geophys. Res., 89(B12), 10, 291-10, 310 pp.

Greiner, B. 1999. Euler rotations in plate-tectonic reconstructions. Comput. Geosci. 25, pp. 209–216.

Kearey, P.and Vine, F.J. 1990. Global Tectonics; Wiley-Blackwell: Hoboken, NJ, USA.

Macchiavelli, C. 2014. Tectonic reconstruction of Sicily in the framework of the Central Mediterranean geological evolution. Phd thesis

Müller, R.D.; Roest, W. R; Royer, J.Y.; Gahagan, L. M. and Sclater, J. G. 1997. Digital isochrons of the world's ocean floor, J. Geophys. Res., 102(B2), pp. 3211-3214.

Müller, R.D.; Cannon, J.; Qin, X.; Watson, R.J.; Gurnis, M.; Williams, S.; Pfaffelmoser, T.; Seton, M.; Russell, S.H.J.; Zahirovic, S. GPlates: Building a virtual Earth through deep time. Geochem. Geophys. Geosystems 2018, 19, doi:10.1029/2018GC007584.

Ross, M.I. and Scotese, C.R. 1988 A hierarchical tectonic model of the Gulf of Mexico and Caribbean region. Tectonophysics 155(1–4), pp. 139–168.

Sandwell, D.T., Smith, W.H.F. 1997. Marine gravity anomaly from Geosat and ERS 1 satellite altimetry. J GeophysRes 102:10039–10054.

Schettino, A. 1998. Computer aided paleogeographic reconstructions, Computers and Geosciences, 24(3), pp. 259-267.

Schettino, A. 1999a. Polygon intersections in spherical topology: Application to Plate Tectonics, Computers and Geosciences, 25(1), pp. 61-69.

Schettino, A. 1999b. Computational methods for calculating geometric parameters of tectonic plates, Computers and Geosciences, 25(8), pp. 897-907.

Schettino, A. 2014. Quantitative plate tectonics. Physics of the Earth–Plate Kinematics–Geodynamics, 1st ed.; Springer International Publishing: New York, NY, USA.

Schettino, A. and Scotese, C.R. 2005. Apparent polar wander paths for the major continents (200 Ma – present day): a paleomagnetic reference frame for global plate tectonic reconstructions. Geophys J Int 163(2), pp. 727–759.

Turco, E.; Schettino, A.; Pierantoni, P.P. and Santarelli, G. 2006. The Pleistocene extension of the Campania Plain in the framework of the southern Tyrrhenian tectonic evolution: Morphotectonic analysis, kinematic model and implications for volcanism. In Volcanism in the Campania Plain: Vesuvius, Campi Flegrei and Ignimbrites; De Vivo, B., Ed.; Elsevier: Amsterdam, The Netherlands; Volume 9, pp. 27–51.

Turco, E.; Macchiavelli, C.; Mazzoli, S.; Schettino, A. and Pierantoni, P.P. 2012. Kinematic evolution of the Alpine Corsica in the framework of Mediterranean mountain belts. Tectonophysics, 579, pp. 193–206.

Turco, E.; Schettino, A.; Macchiavelli, C. and Pierantoni, P.P. 2013. A plate kinematics approach to the tectonic analysis of the Tyrrhenian–Apennines System. Geophys. Res. Abstr., 29, pp. 187–190.

Turco, E.; Macchiavelli, C.; Penza, G.; Schettino, A. and Pierantoni, P.P. 2021. Kinematics of Deformable Blocks: Application to the Opening of the Tyrrhenian Basin and the Formation of the Apennine Chain. Geosciences, 11, 177. https://doi.org/10.3390/geosciences11040177.

Vine, F. J. and Matthews, D. H. 1963. Magnetic anomalies over oceanic ridges, Nature, 199, 947-949.

Chapter 2 - Kinematics of Deformable Blocks: Application to the Opening of the Tyrrhenian Basin and the Formation of the Apennine Chain

Ch.2.1 - Introduction

The peri-Tyrrhenian orogenic belt, which is formed by the Apennine Chain, the Calabrian arc, and the Sicily Chain, is the most recent expression of the geodynamic process that created the western Mediterranean basin after the Europe–Africa collision (Fig. 2.1).

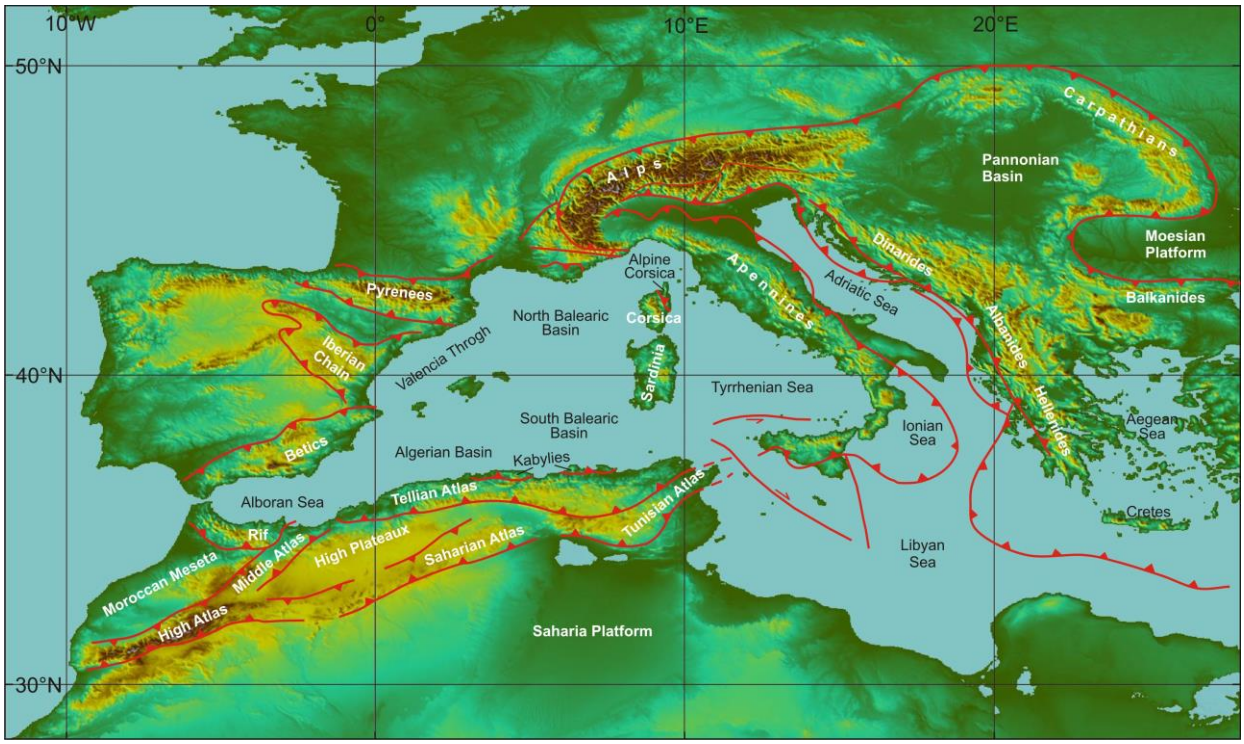

Figure. 2.1 - Digital terrain model (ASTER images, 1.5 s) of the western Mediterranean region with major, simplified, tectonic lineaments; modified after *Turco et al. (2012).*

Large-scale extensional tectonics, coupled with orogenic processes, formed the Tyrrhenian basin, while the thrust belt–foredeep system of the Apennine chain continued migrating towards the present-day Adriatic–Ionian foreland. The Tyrrhenian margin of the Apennine chain experienced widespread extensional tectonics, characterized by formation of several marine basins, intramontane troughs, and intense magmatism. The Tyrrhenian Sea, which developed since Middle Tortonian times, is the youngest basin of the western Mediterranean region (*Sartori et al., 2004*). It has been extensively studied since the 1960s. In spite of the huge amount of available data, the geodynamic evolution of the Tyrrhenian basin and surrounding regions are not yet coherently described and have been subject to controversial interpretations (*Biju-Duval et al.,*

1977; Dercourt et al., 1986; Malinverno & Ryan, 1986; Kastens & Mascle, 1987; Dewey et al., 1989; Boccaletti et al., 1990; Carmignani et al., 1995; Lavecchia et al., 1995; Faccenna et al., 1996; Ferranti et al., 1996; Turco & Zuppetta, 1998; Jolivet & Faccenna, 2000; Faccenna et al., 2001; Rosenbaum & Lister, 2002; Lavecchia et al., 2003; Peccerillo & Turco, 2004).

In particular, the kinematic relationships between extension in the Tyrrhenian Sea, basin formation along the Tyrrhenian margin of the Apennine chain, migration of the Apennine arcs, and volcanism still remain to be determined.

The main reason for the existence of controversial interpretations is due to the complexity of the geodynamic processes that generated the Tyrrhenian–Apennine system. It belongs to the Africa–Europe collision belt along which the fragmentation of the Adriatic plate started (*Schettino & Turco, 2011*) since the upper Cretaceous, followed by upper Oligocene slab-retreat events. All these processes have produced an articulated Africa–Europe collision front, which includes back-arc basins and the Apennine chain. Most models proposed so far for the description of the evolution of the Tyrrhenian–Apennine system are based on stratigraphic and structural analyses of transects, not always correctly oriented along the flow lines of relative motion. Tectonic reconstructions obtained with such a 2D method often neglect important 3D kinematic constraints expressed by structures that are transversal to the chain (*Malinverno & Ryan, 1986; Johnston & Mazzoli, 2009; Carminati et al., 2012; Le Breton et al., 2017)*. Only a few authors have followed an approach based on the laws of plate kinematics (*Rosenbaum et al., 2002; Rosenbaum & Lister, 2004; Hosseinpour et al., 2016; Müller et al., 2019; Van Hinsbergen et al., 2020*).

A quantitative method for describing the evolution of a system of deformable tectonic elements in the context of a back-arc extension and associated building of an accretionary wedge mountain belt is here proposed. The technique is then applied to the kinematic reconstruction of the Tyrrhenian–Apennine region. Previous works (*Dewey et al., 1989; Turco et al., 2013; Pierantoni et al., 2020*) have described the tectonic evolution of this area in the rigid plate kinematics approximation. *Turco et al., (2021*) uses the same kinematic framework but allow internal deformation of the blocks during their motion. This approach provides a better representation of the geological processes associated with the formation of back-arc basins, in particular the existence of transverse structures along the axis of the accretionary wedge. Finally, the resulting model supports the formation of at least three STEP (Subduction-Transform- Edge-Propagator) faults along the subducting slabs, as shown in Chapter 3.

Ch.2.2 - Geological Setting

Ch.2.2.1 - The Apennine Chain

The Apennine–Maghreb chain is a Neogene thrust belt, which comprises Mesozoic to Paleogene sedimentary rocks, derived from different basins and shelf located in paleogeographic domains of the Adria continental margin (*Turco et al., 2013; and reference therein*).

According to (*Turco et al., 2012*), when the Sardinian-Corsica block (SCB) started separating from the European plate, a long trench was present in the Central-Western Mediterranean region, where Liguride-Tethys lithosphere was subducting. It is known that the polarity of subduction flipped from NW below the Calabrian Arc-Kabylies to SE below Alpine Corsica (AlC) and the Western Alpine Arc (WAA). Such a structure always determines the formation of a transform fault that links the two branches of the subduction zone (*Schettino et al., 2014*). The rotation of the Sardinian-Corsican block accompanied this process, favouring the sinistral transpressional character of the plate boundary between Adria and Sardinia-Corsica block (yellow line A, Fig. 2.2). At the end of the Sardinia-Corsica rotation, such a lithosphere fault reached its maximum length of ~500 km (Fig. 2.3).

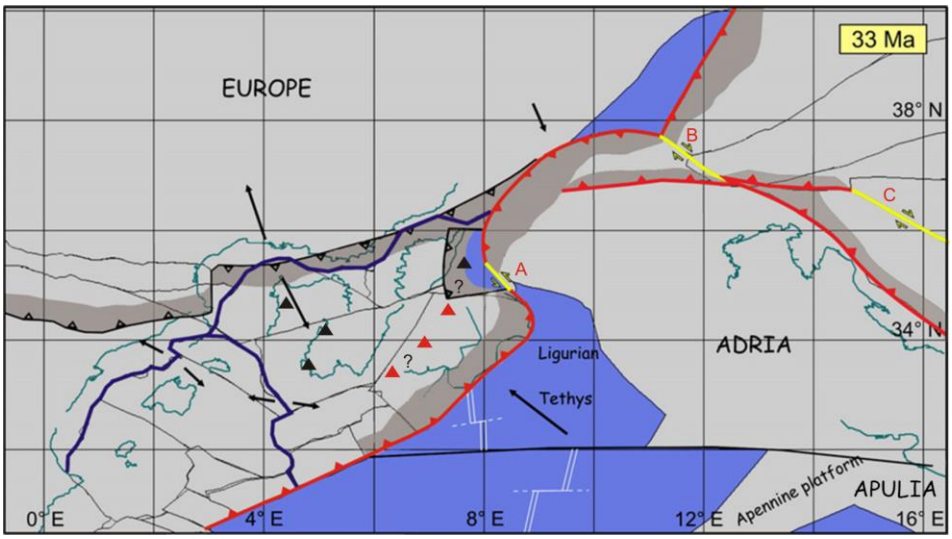

Figure. 2.2 - Plate reconstruction of the western Mediterranean region at 33 Ma. The distribution of the continental lithosphere is shown in gray. Present-day coastlines are shown for reference. Black arrows represent direction and magnitude of relative motion. Strike–slip faults are shown in yellow, labeled A,B,C. Red lines are convergent boundaries. Blue lines are divergent boundaries. White lines represent extinct spreading centers. Red triangles are volcanoes associated with the Tethys subduction; black triangles are volcanoes probably associated with the pyrenaic subduction. AlC: Alpine Corsica; SCB: Sardinian-Corsican block; WAA: Western Alpine Arc; modified after *Turco et al., (2012).*

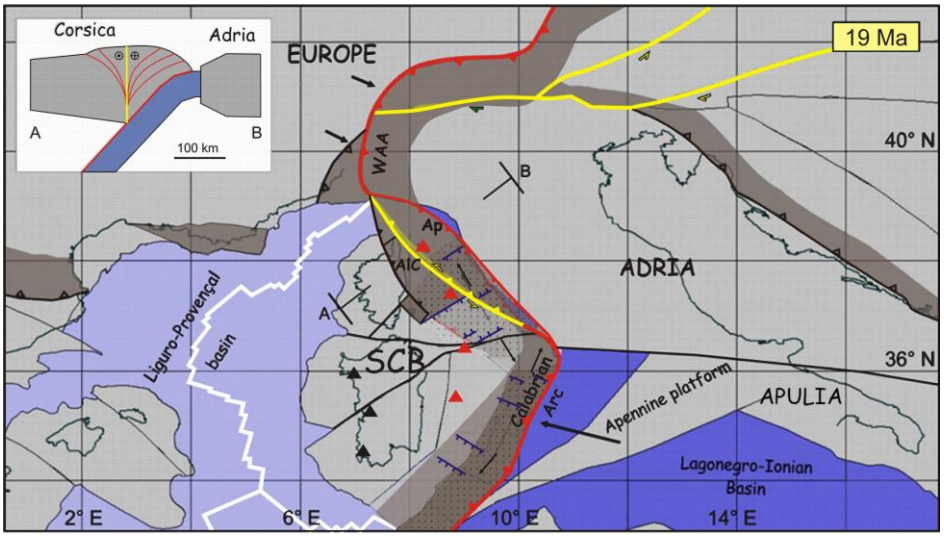

Figure. 2.3 - Plate reconstruction of the western Mediterranean region at 19 Ma (late Aquitanian). Dotted areas indicate wedge-top basins. Lower Miocene Chains are shown in dark gray, the Africa-Adria continental lithosphere is in light gray, the oceanic crust is in blue. Red lines are active boundaries. Black lines are inactive boundaries. Yellow lines are strike-slip faults. Red triangles are volcanoes associated with the Tethys subduction; black triangles are volcanoes probably associated with the pyrenaic subduction. AlC: Alpine Corsica; Ap: proto-Apennine chain; SCB: Sardini-an-Corsican block; WAA: Western Alpine Arc. Other symbols are the same from Figure 2.2; modified after *Turco et al., (2012).*

At the end of the rotation, the Liguride slab was juxtaposed to the Corsica block and had dragged with it the deepest parts of the Calabrian accretion wedge, thereby a mélange of rocks belonging to the accretion wedge formed along the transpressive boundary. Complex structures, probably associated to the transpression, formed top-wedge basins, filled by sediments of the external Liguride flysch, today outcropping along the Tyrrhenian margin from Liguria to northern Calabria (*Knott, 1987*). During the Burdigalian, the extension jumped from the western to the eastern margin of the Sardinian-Corsican block (future Tyrrhenian area) and the construction of the Apennine Chain continued further East. Therefore, the process of Tyrrhenian extension is strictly connected to the formation of the Apennine Chain. In current literature, the Apennine Chain extends from the Sestri-Voltaggio line to the Sangineto line (northern Calabria) (*Ogniben, 1969; Elter & Perusati, 1973; Amodio-Morelli et al., 1976; Patacca & Scandone, 1989*) (Fig. 2.4) and, on the basis of the paleogeographic domains involved in its structuring, it is subdivided in: 1) Northern Apennine, where the Ligurian allochthonous units extensively crop out (*Barchi, 1998; Barchi, 2010; Boccaletti et al., 1990; Carmignani et al., 2001; Centamore et al., 2009; Elter et al., 1975; Marroni et al., 2017*), 2) Umbria-Marche Apennine, where sediments of the homonymous continental paleogeographic basin outcrop (*Parotto & Praturlon, 1975; Boccaletti et al., 1990;*

Deiana & Pialli, 1994; Calamita et al., 1995; Centamore et al., 2009), 3) Lazio-Abruzzi Apennine, characterized by the presence of the homonymous Cretaceous carbonatic platform (*Scarsella, 1951; Cosentino et al., 1991; Piana, 1991; Centamore, 1992; Capotorti et al., 1995; Civitelli & Brandano, 2005*), and 4) Southern Apennine, which resulted from the deformation of the Campania-Lucania platform and the Lagonegro Basin (*Patacca & Scandone, 1991, 2007; Ferranti et al., 1996; Cello & Mazzoli, 1998; Pescatore et al., 1999; Mazzoli et al., 2001*). The lateral continuity of the Apennine units is interrupted by the Calabrian arc along the Sangineto line and finds again its lateral continuity in the Maghrebide belt, which starts outcropping in Sicily west of the Taormina line (*Amodio-Morelli et al., 1976; Van Dijk et al., 2000; Bonardi et al., 2000*) (Fig. 2.4).

It is important to note the following key peculiarities of the Apennine chain: a) the basement of the Adriatic margin is never involved in the structuring of the chain; b) although the chain is exclusively made up of carbonate rocks deriving from the Adriatic domain, the foredeep and top-wedge sediments have a composition mainly referable to continental basement rocks (*Finetti, 2005*); c) during its structuring, while the Apennine chain grows along the Adriatic front, it is subject to extension along the Tyrrhenian side.

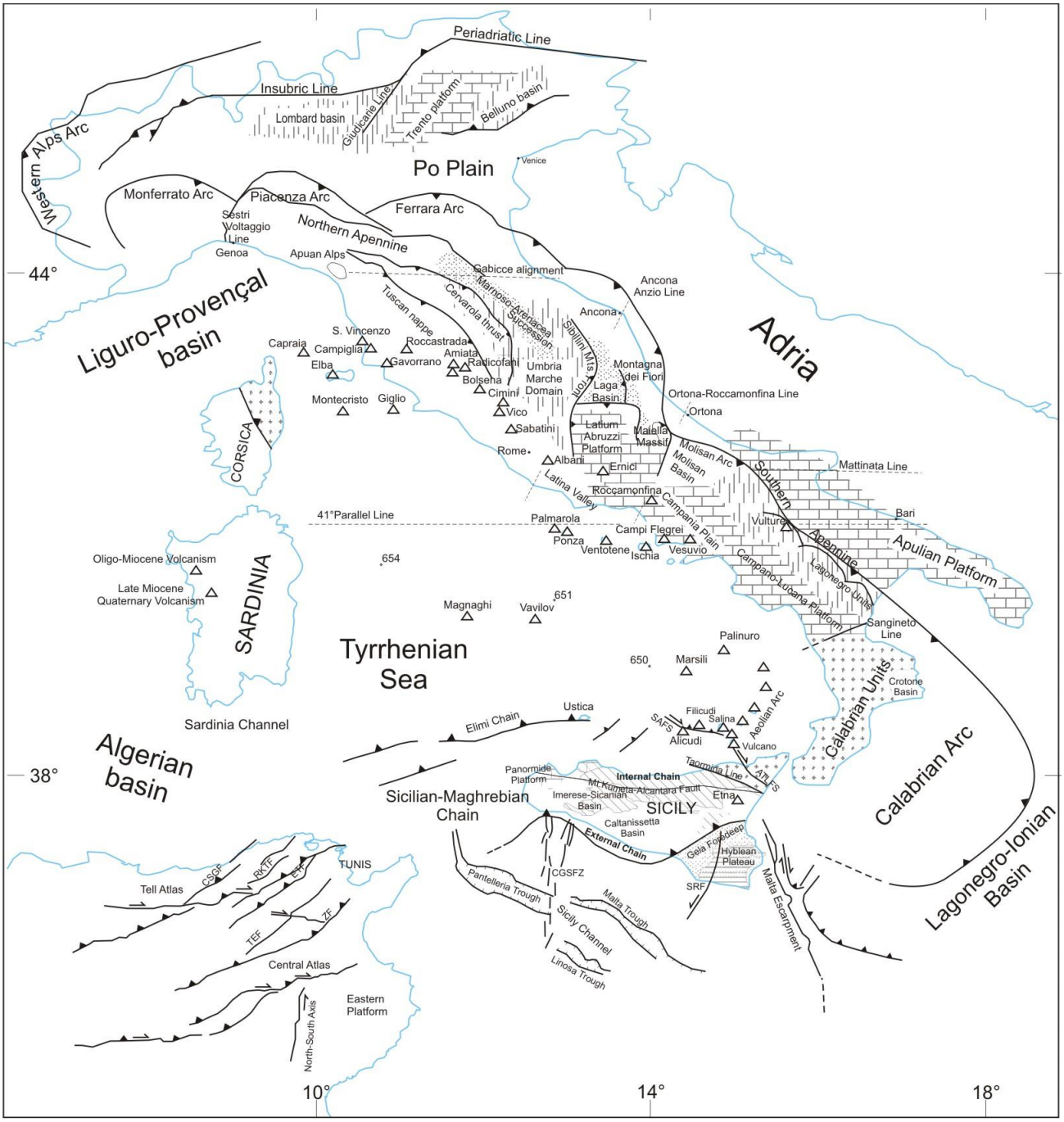

Figure. 2.4 - Location map of the main paleogeographic and structural units, modified after Pierantoni et al., (2020). ATLFS: Aeolian-Tindari-Letojanni Fault System; CGSFZ: Capo Granitola-Sciacca Fault Zone; SAFS: Sisifo-Alicudi Fault System; SRF: Scicli-Ragusa Fault; CSGF: Cap Serrat-Gardimaou Fault; ETF: El Alia-Teboursouk Fault; RKTF: Ras El Kouran-Thibar Fault; TEF: Tunis Elles Fault; ZF: Zaghouan Fault.

Ch.2.2.2 - The Tyrrhenian Sea

The Tyrrhenian Sea has a triangular shape, and its northern vertex is located in the proximity of Elba Island. Starting from the northern tip of the triangle, the Ligurian-Provençal Sea extends westwards. From the end of the 1960s and up to the entire decade of the 1980s, the Tyrrhenian basin has been the subject of many scientific cruises (DSDP, ODP, and various seismic explorations). Its formation started after the cessation of sea floor spreading in the Ligurian–Provencal basin and, according to *Malinverno and Ryan (1986)* and *Faccenna et al. (1996)*, it was due to rollback of the subducting Ionian lithosphere and migration of the Calabrian Arc towards the southeast.

An E–W lineament extending from northern Sardinia to the Campania margin, known as the 41st parallel line, is suggested to be a lithospheric left-lateral transform fault that separates the Tyrrhenian Sea in two sectors (*Selli, 1981*). The amount and directions of extension, as well as crustal and lithospheric thicknesses, are different to the north of the line with respect to the southern region (Fig. 2.5).

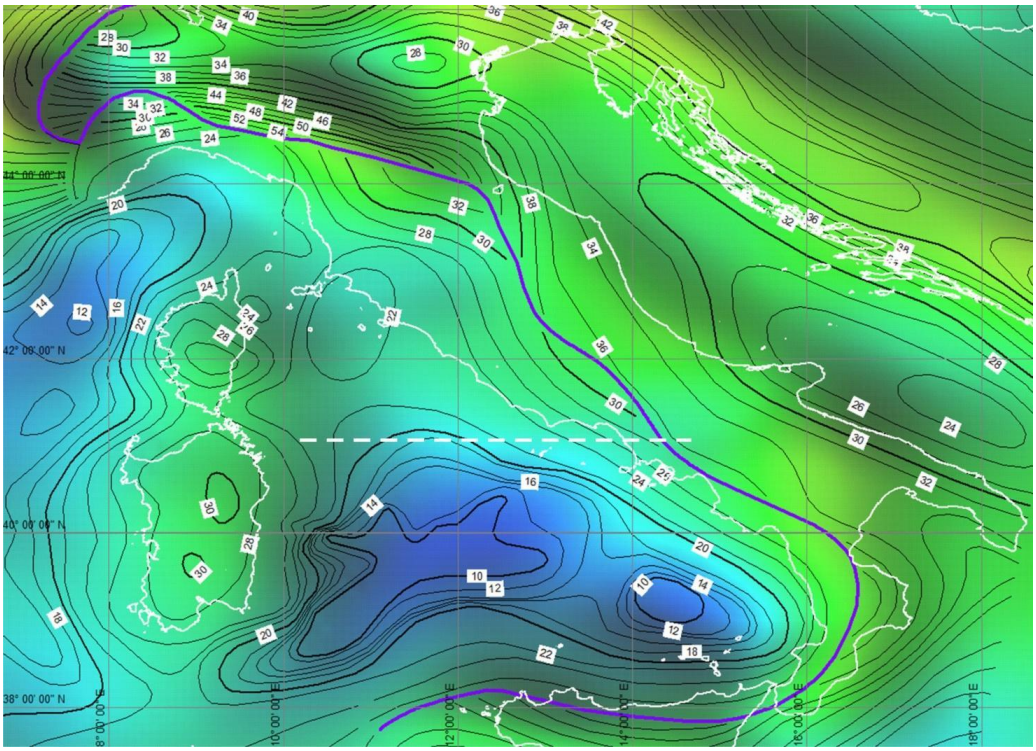

Figure. 2.5 - Moho map showing the difference of crustal thickness to the north and south of the 41° parallel line. White dashed line is the 41°parallel line, the violet line is the Moho discontinuity (*Grad & Tire, 2009*).

In the sector north of the 41st parallel line, the continental crust is 20–25 Km thick and the lithosphere thickness is ~50–60 Km (*Panza & Calcagnile, 1979-1980; Nicolich, 1981; Panza, 1984*). ODP site 654 (*Kastens & Mascle, 1987)* shows conglomerates covered by Tortonian, Messinian, and Plio-Pleistocene deposits. Conversely, the southern sector includes the Vavilov and Marsili basins, more than 3500 m deep, which have thin crust (25–10 Km or less) and lithosphere (30–50 Km) (*Panza & Calcagnile, 1979-1980; Nicolich, 1981; Panza, 1984*). The Vavilov basin is characterized by a triangular shape, while the Marsili basin is almost squared. Both basins show magnetic lineaments comparable with the structural lineaments and the geometric shape of the basins (Fig. 2.6).

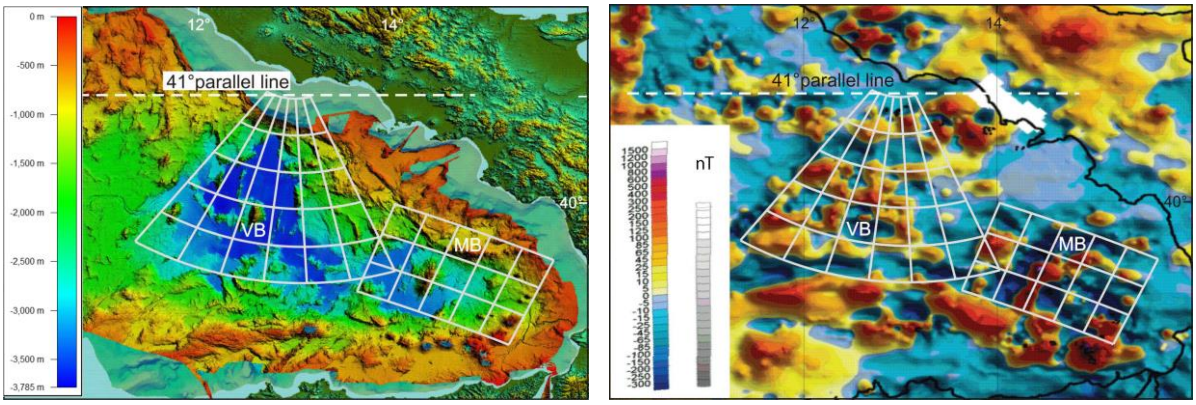

Figure. 2.6 - (**a**) Bathymetry (Marani & Gamberi, 2004) and (**b**) magnetic anomalies (Meloni et al., 2007) for the Tyrrhenian basin. White lines show the grid of the rotation pole for: Vavilov (VB) and Marsili (MB) basins. Both basins show magnetic anomalies comparable with the structural lineaments and the geometric shape of the basins.

According to some authors (*Sartori, 1990, 2003; Spadini et al., 1995; Rosenbaum & Lister, 2004*), rifting processes in this sector started along the Sardinia margin at ~10 Ma and then migrated eastward forming the Vavilov basin first (at 5.5 Ma) and later the Marsili basin (2.0–1.8 Ma). Despite the remarkable extension, the presence of oceanic crust is likely to be restricted within these two basins (*Marani, 2004; Sartori, 2004; Milia et al., 2017;*), as testified by the ODP sites 651 and 650. The first one shows, from the top, a 388 m thick Pliocene–Pleistocene succession (bio-zone MPL6/NN18, 2 Ma) above 39-m thick succession of dolostones, lying on 29 m of highly serpentinized peridotites covered by a 134 m thick succession of basalts (lava flows and breccia). The second borehole displays, starting from the bottom, 32 m of vesicular basalts followed by dolostones and a 602-m thick succession of Plio-Pleistocene deposits (bio zone MPL6/NN18, 2.0 Ma) (Fig. 2.7).

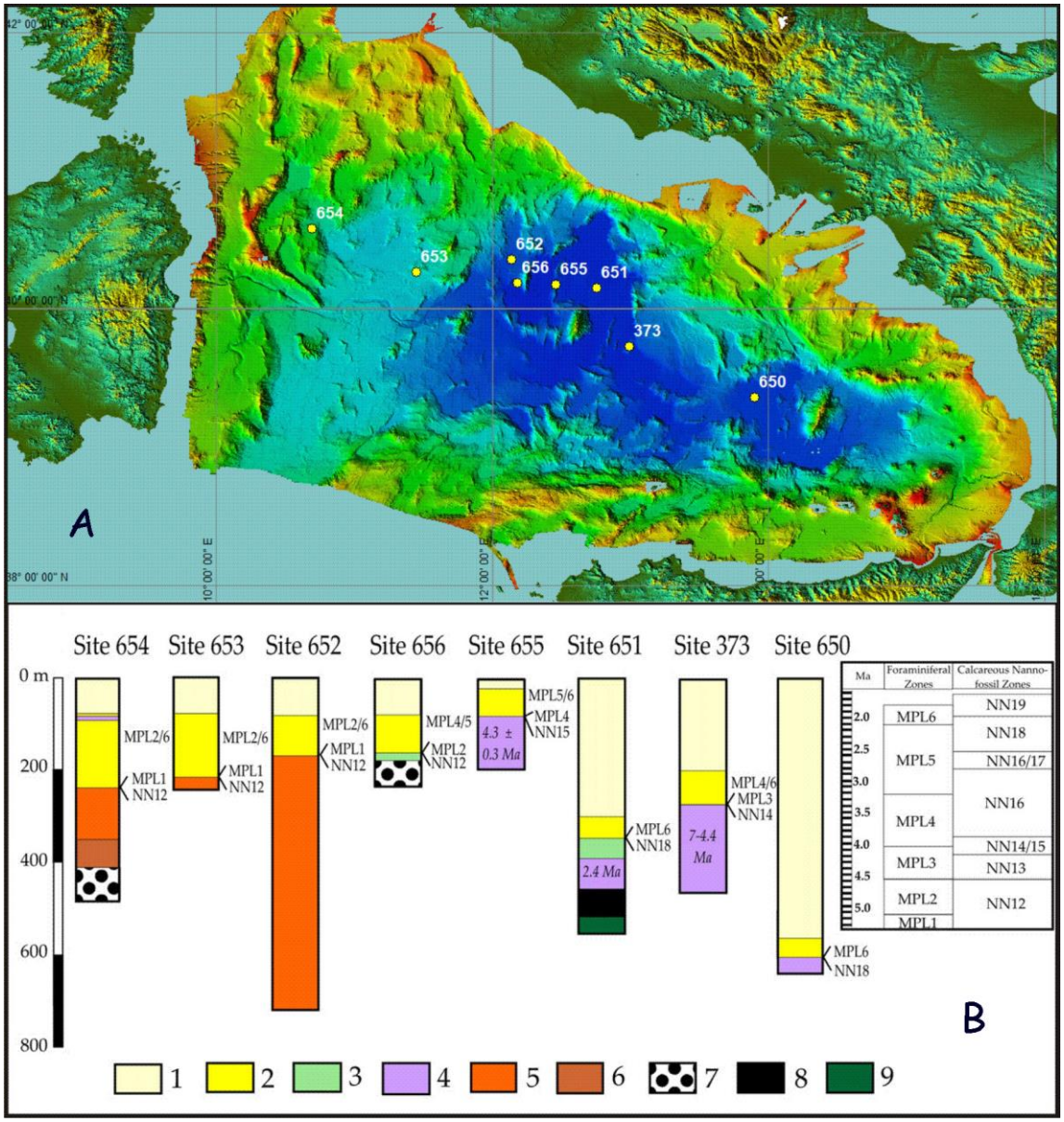

Figure. 2.7 - (**a**) Index map of Italy and Vavilov basin and DSDP and ODP well sites (**b**) Stratigraphic logs of the DSDP and ODP sites. (**1**) Pleistocene deposits; (**2**) Pliocene deposits; (**3**) dolostones; (**4**) basalts; (**5**)Messinian deposits; (**6**) Tortonian deposits; (**7**) conglomerates; (**8**) breccias; (**9**) serpentinized peridotites; after *Milia et al., (2017).*

Despite the great commitment in the exploration of the Tyrrhenian basin, the start time of the Tyrrhenian extension process is not well constrained. According to some authors (*Dewey et al., 1989; Schettino & Turco, 2006*), the time of cessation of sea floor spreading in the Ligure–Provençal basin is 19 Ma. Conversely, *Speranza et al. (1999)* proposed that the rotation of the Sardinian-Corsican block ended at 15 Ma. These ages are important because they put a constraint on the timing of roll-back for the Adriatic slab. The end of sea-floor spreading in the Ligure–Provençal basin and the Algerian basin was determined by *Marani (2004)* on the basis of marine magnetic anomalies. The end of rotation of the Sardinian–Corsica block can be also constrained by

paleomagnetic data. While *Marani (2004)* confirmed the age obtained by the analysis of marine magnetic anomalies (19 Ma) on the basis of a compilation of quality paleopoles, *Gattacceca et al. (2007)* proposed a younger age of 15 Ma on the basis of new paleomagnetic data and 40Ar/39Ar dating. For the beginning of the Tyrrhenian extension, several authors used the ages of the stratigraphic successions from wells and seismic correlations to suggest that it took place during the Middle Tortonian times (~12 Ma) (*Kastens & Mascle, 1987; Sartori, 1990; Milia & Torrente, 2014*). Therefore, the time elapsed between the end of the rotation of the Sardinian–Corsican block and the beginning of the Tyrrhenian rift is not sufficiently determined so far. However, it is important to note that the elapsed time between the onset of Tyrrhenian rifting and the beginning of sedimentation in the basin depends on the speed of extension in the rift and on the original thickness of the crust.

Ch.2.3 - Methods

Plate kinematics has always encountered major obstacles in being used to represent deformation processes at the scale of mountain ranges, continental rifts and transcurrent boundaries, in the absence of magnetic isochrons. For this reason, palinspastic reconstructions along cross-sections at the macro-scale rely on the methods of structural geology. Retro-deformation (or crustal balancing) methods are well-known tools for the analysis of single transects, but are hardly applicable in complex areas characterized by the presence of triple junctions or polyphase systems. In these situations, the techniques of plate kinematics provide a convenient set of tools for describing the tectonic evolution and quantify the deformation of complex areas, while structural geology provides the fundamental parameters necessary to determine rotation poles. For example, normal faults associated with an active rift such as the Tyrrhenian Sea represent a record that reflects the kinematics of extension. They exhibit sharp morpho-structural lineaments, easily observable on high-resolution DTMs or multibeam bathymetry. These features are generally devoid of “structural noise” generated by local paleo-stresses.

A shuttle radar topography mission (SRTM) image of the Tyrrhenian region shows lineaments that can be grouped into fan-shaped sets characterizing specific sectors of the Tyrrhenian and Apennine areas (Fig. 2.8). Thus, considering that these lineaments are expressions of several systems of normal faults associated with the Tyrrhenian extension, a set of Euler poles that describes the relative motion of different sectors of the Apennine chain can be determined. The classic rules of plate kinematics allow to assign these Euler poles on the basis of an estimate of the location of the convergence point of the observed lineaments. All the Euler poles identified using this method describe the opening of the Tyrrhenian Sea in a European (Corsica–Sardinia) reference frame.

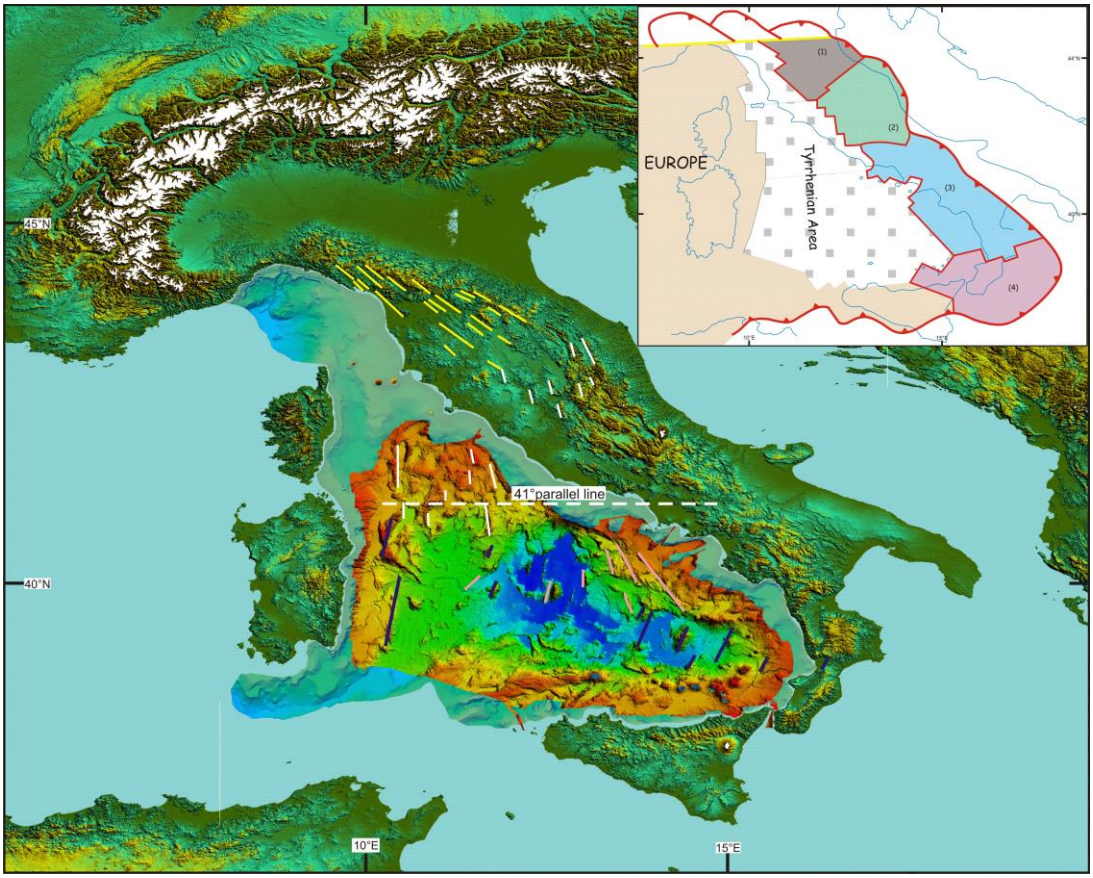

Figure. 2.8 - Morpho-tectonic map of the Tyrrhenian-Apennine system showing lineaments that can be grouped into fan-shaped sets characterizing specific sectors. Lineaments of the Northern Apennine sector are in (yellow); (white) lines are for northern Tyrrhenian basin and Central Apennine sector; (blue and pink) lines are for Calabrian and Southern sectors respectively. The multibeam bathymetry is after *Marani & Gamberi (2004)*. The insert box shows the deformable blocks identified: (1) Northern sector in (dark beige), (2) Central Sector in (green), (3) southern sector in (blue); (4) Calabrian Arc Sector in (pink). Dotted areas are in extension; (white dotted) area is the extended Tyrrhenian area.

Ch.2.3.1 - How to Identify Tectonic Elements in the Apennine Domain

Every single block of the Apennine area is characterized by boundaries that are divergent along the Tyrrhenian side and convergent along the Adriatic–Ionian side. They result from rotations about fixed Euler poles in the Corsica–Sardinia reference frame. The boundary between two adjacent blocks is represented by structural systems, usually transversal to the chain, that are the expression of continuously changing Euler poles in the same reference frame. The faults associated with the Tyrrhenian side boundaries represent eastward migrating fan-shaped extensional systems. On the Adriatic side, the frontal segments of the Apennine chain represent the eastern boundaries of the tectonic elements. On the basis of the lineaments identified for the Tyrrhenian area, *Turco et al. (2021)* defined the deformable blocks shown in Figure 2.8, which

extend along the Tyrrhenian side and grow by accretion along the Adriatic margin. Boundaries between adjacent blocks are not easily identified, because the Euler pole of relative motion is always changing and depends on the ratio of angular velocities (in the Sardinia–Corsica reference system) between pairs of tectonic elements. Boundaries with extensional kinematics produce systems of faults that break the continuity of the chain, forming transversal basins that are simultaneously included in the Apennine orogenic system and TTR-like and FTR-like triple junctions (Fig. 2.9). Boundaries with strike-slip kinematics produce more complex structures and can form pull-apart basins or depressions. In some cases, for example the Ancona–Anzio line (Fig. 2.4), the boundary can have compressive or transpressive kinematics. On the Tyrrhenian side, RRR-like triple junctions form at the intersection of rift axes (Fig. 2.9).

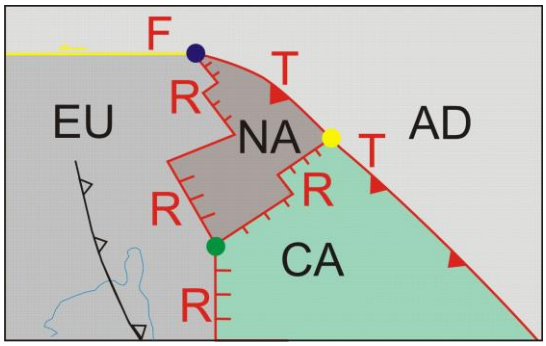

Figure. 2.9 - Scheme showing TTR-like (Trench-Trench-Ridge) and FTR-like (Fault-Trench-Ridge) triple junctions of the Apennine and RRR-like (Ridge-Ridge-Ridge) triple junction of the Tyrrhenian side. AD: Adria, CA: Central Apennine, EU: Europe, NA: North Apennine, T = Trench, R = Ridge, F: Fault; (yellow dot) is the TTR-like triple junction; (green dot) is the RRR-like triple junction, (blue dot) is the FTR triple junction.

The blocks identified in this way are highly deformable and it is not possible to identify any portion inside them that can be considered rigid. In general, the eastward migrating extensional axes overlap with some delay to the compressional structures, determining their collapse. Conversely, in global tectonics the deformed areas along plate margins represent bands with negligible surface compared to that of the entire rigid lithospheric plate. Therefore, the tectonic elements considered here behave like portions of large plate margins devoid of their rigid counterpart. However, considering the scale of the tectonic reconstructions, the internal deformation of the tectonic elements is not relevant for the application of the method. The boundaries of the Apennine blocks cannot therefore be considered fixed over time; tectonic elements do not represent rigid polygons but are characterized by the rotation pole about which the lines and points contained in them rotate.

Ch.2.3.2 - How to Determine Rotation Poles of Apennine Blocks

The stage poles between conjugate oceanic plates are determined by building magnetic isochrons. In continental tectonics, where magnetic lineaments are not available, the rotation pole between two divergent plates is generally determined qualitatively tracing central meridians of at least two parallels passing from conjugate points on the two undeformed margins. Then, the Euler pole is the central point of a cloud of intersection points between meridians. Unfortunately, this method cannot be applied to the Tyrrhenian area, as it is not possible to recognize conjugate points belonging to the margins of Corsica–Sardinia and the Apennine domain, while there are no clear magnetic lineaments in the Tyrrhenian Sea. Therefore, the finite poles of rotation of the Apennine blocks can only be estimated by taking intersections of great circle arcs associated with morpho-structural lineaments of the Tyrrhenian rift. Finally, specialized software for plate kinematics (e.g., PCME-Paleo Continental Map Editor (*Schettino, 1998*) or GPlates (*Müller et al., 2018*)) can be used to build Euler pole grids that show parallels and meridians about every single rotation pole. Parallel circles represent flow lines of relative motion, while meridians represent the trend of extensional structures. These grids can be superimposed on the observed morpho-structures to assess the correctness of the Euler poles.

Ch.2.3.3 - How to Determine an Angle of Finite Rotation and the Start and End Times of Rotation

The angle of rotation about a Euler pole is a function of finite strain and can be determined through crustal balancing of transects along flow lines of relative motion, granted that an estimate of the initial thickness is available. The technique is described in (*Schettino, 2014*) and can be easily applied to the restoration of rifted continental margins and the reconstruction of pre-rift configurations. In the case of migrating mountain belts, the angle of rotation does not need to be determined through crustal balancing, because it can be observed directly measuring the angular distance between the present day location of a point along the thrust front and a homologous point along the estimated location of the thrust at an earlier age. Two points along the thrust front at different ages are considered homologous when the more recent point can be obtained rotating the older one about the Euler pole. In this instance, crustal balancing can be applied a posteriori to obtain the initial thickness of the chain. For example, the estimated initial thickness for the central Apennine chain through the crustal balancing procedure, illustrated in Figure 2.10, is of ~42 km. A reference point in the Sardinian–Corsican block (blue point FPL in Fig. 2.10), located at the western end of the extensional area, and a homologous point along the Sibillini mountains

(red point ML00 in Fig. 2.10), representative of the eastern end of the rift, have been considered. The angular distance between these two points is 13°, corresponding to 180 km along the small circle arc linking the two points. The crustal balancing procedure was performed using the Moho depths of *Grad & Tire (2009)* (Fig. 2.5), which have an uncertainty of 2–4 km in this area.

To determine the velocity vectors, it is also necessary to know the timing of deformation. This parameter can be estimated by the analysis of stratigraphic successions that record the syn-rift tectonic activity. There is a wide array of literature for the Tyrrhenian basin with data deriving from well stratigraphy, seismic surveys, and dredging (Fig. 2.7) (*Kastens & Mascle, 1990; Sartori, 2003, 2004; Pascucci et al., 2007; Thinon et al., 2016*). Furthermore, there are many other data on successions of the Apennine and foredeep basins that have recorded the time of tectonic activity of the chain (*Pascucci, 2002; Barchi, 2010*).

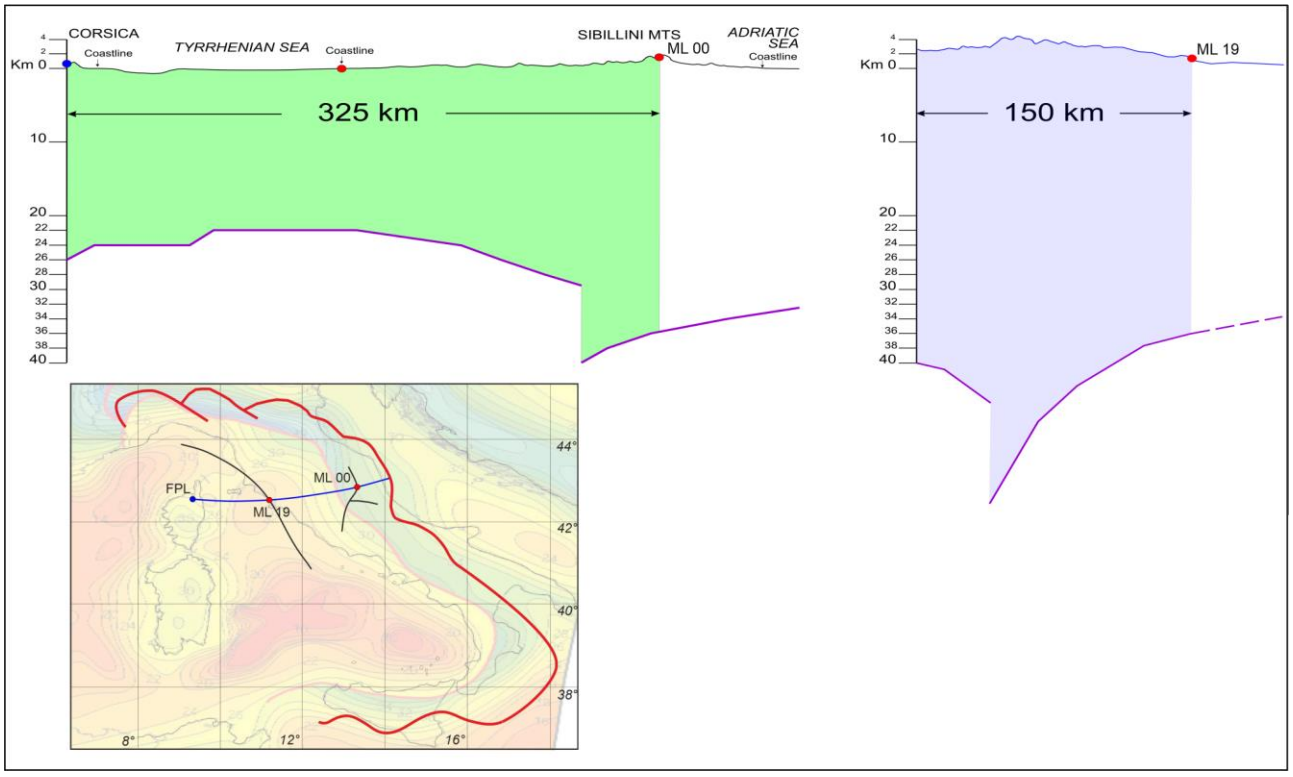

Figure. 2.10 -Crustal balancing technique for the Central Apennine. FPL: Fixed Pin Line (Blue); ML19: Mobile Line (Red), corresponding to the eastern extensional margin at 19 Ma; ML00: Mobile Line, corresponding to the active extensional margin. Between the Sibillini mountains (ML00) and the Corsica coastline (FPL) there are about 325 km. Considering the depth of the actual Moho the green area in the picture measures 8808 Km^2; the same area can be obtained between FPL and ML19 estimating a medium depth of 50 km for a chain of about 4000 m.

Ch.2.3.4 - Apennine Chain and Tyrrhenian Sea Sectors

Six groups of homogeneous structural systems, which characterize chain sectors, have been distinguished. From north to south, they are: (1) Northern Apennine; (2) Umbria–Marche Apennine Arc; (3) Southern Apennine; (4) Calabrian Arc; (5) Sicilian Chain (*Turco et al., 2013*).

1. The Northern Sector

The Northern sector extends north of Elba Island and includes eastern Ligurian Sea, Northern Apennine and the area of the Tuscan rift. The Northern Apennine has been identified as the northern limb of the Umbria–Marche Apennine Arc, running from the Sestri–Voltaggio line to the Gabicce alignment (Figure 2.4) and formed by chaotic sediments deriving from oceanic covers and boudins-like structures of Liguride ophiolites and their thick terrigenous top-wedge successions. The chain front of this sector is buried under Po river valley sediments. In the Corsica basin, syn-rift sediments are aged between Messinian and Oligocene (*Pascucci, 2002;* Sartori, 2004; *Thinon et al., 2016)*. The rift area is also characterized by the well-known Tyrrhenian-Tuscan magmatism; the age of the magmatism grows from east to west. From the structural point of view, this sector shows a fan of lineaments converging towards NW. The resulting Euler pole is located at 45.45°N, 8.40°E (Fig. 2.11).

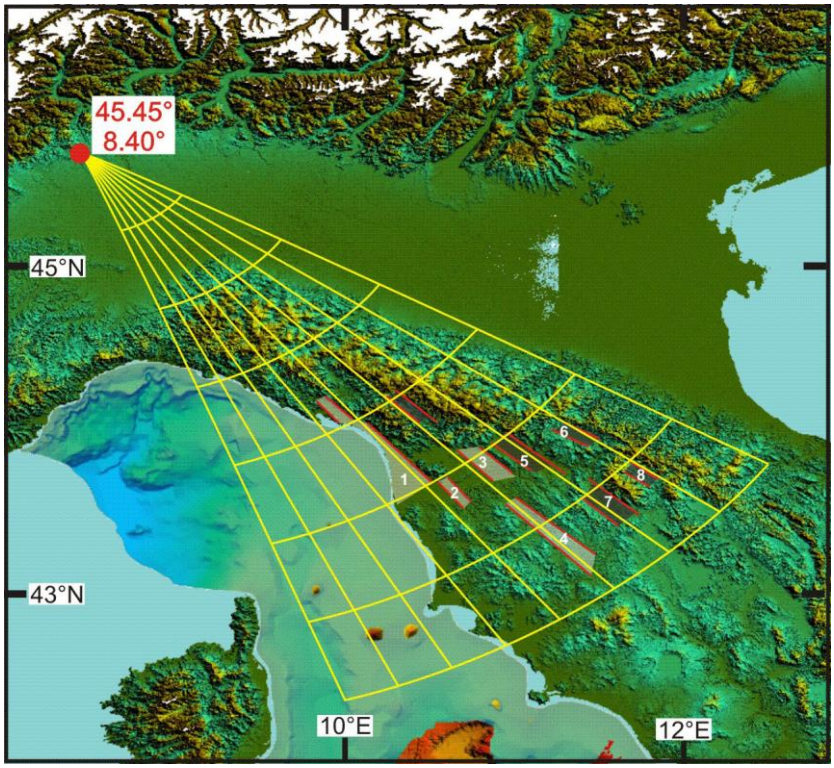

Figure. 2.11 - Morpho-structural lineaments of the northern Apennine and Euler pole of relative motion with respect to Sardinia-Corsica (red dot). The Euler pole grid shows the goodness of fit between kinematic model and geological structures. Some basins associated with the Tyrrhenian extension are also shown. Mio-Pliocene basins are in (light gray), Plio-Pleistocene basins are in (dark gray). (1) Viareggio basin, (2) Volterra basin, (3) Elsa basin, (4) Siena basin, (5) Firenze basin, (6) Mugello basin, (7) Valdarno basin, (8) Casentino basin.

2. Central Sector

The Central Sector extends from Elba Island to the 41° parallel and includes the northern Tyrrhenian Sea, the Umbria–Marche-Abruzzi Apennine Arc and the areas of Umbria-Lazio and Southern Tuscan rifts. The Umbria–Marche Apennine Arc is located between the Gabicce alignment (Fig. 2.4) and the Ancona–Anzio line and is composed of deposits from the Adriatic margin (the well-known Umbria–Marche succession). The Umbria-Marche succession consists of Jurassic-Middle Miocene basinal sediments. The eastern part of the arc is the Ancona-Anzio line during the first phase of evolution and lately the Maiella front, also called "Ortona-Roccamonfina line" (*Patacca & Scandone, 1989, 1991; Di Bucci & Tozzi, 1999*) (Fig. 2.4). Between the two lines there is a thick Mesozoic carbonate platform succession known as Lazio–Abruzzi platform. Tyrrhenian rift structures in this sector form lineaments converging toward north (Lat. 48.9°; Long. 10.4°; Fig. 2.12). The Lazio margin of this sector is also affected by a Pleistocene–Oligocene volcanism.

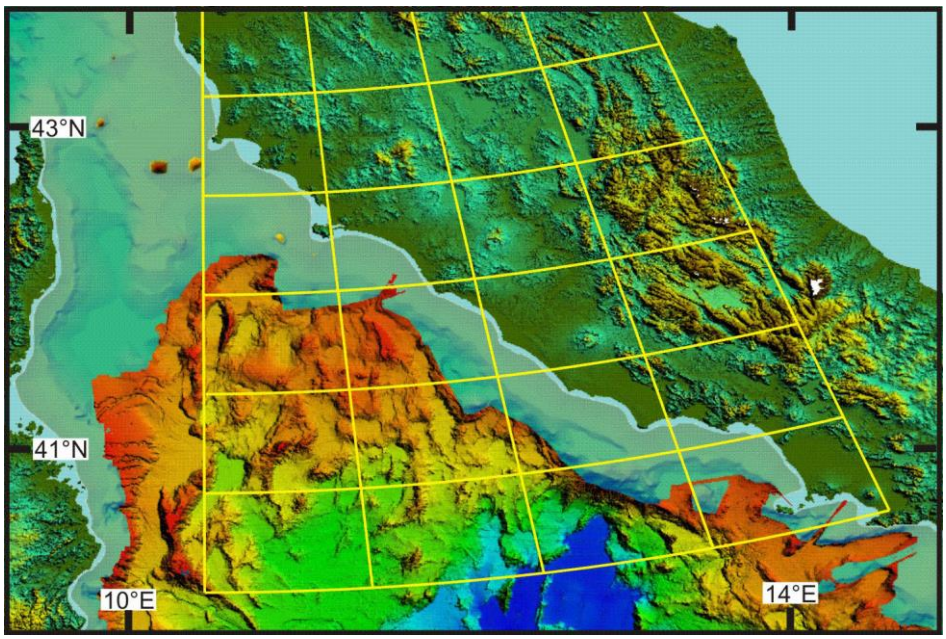

Figure. 2.12 - Morpho-structural lineaments of the central Apennine and Euler pole grid of relative motion with respect to Sardinia-Corsica. The Euler pole grid shows the goodness of fit between kinematic model and geological structures. The Euler pole has coordinates: 48.9°−10.4°.

The interaction between the northern and central sectors is responsible for the formation of transversal lineaments (orthogonal features) that created rectangular basins and depressions (chocolate bar), e.g., the Trasimeno Lake (*Caricchi et al., 2014)* (Fig. 2.13).

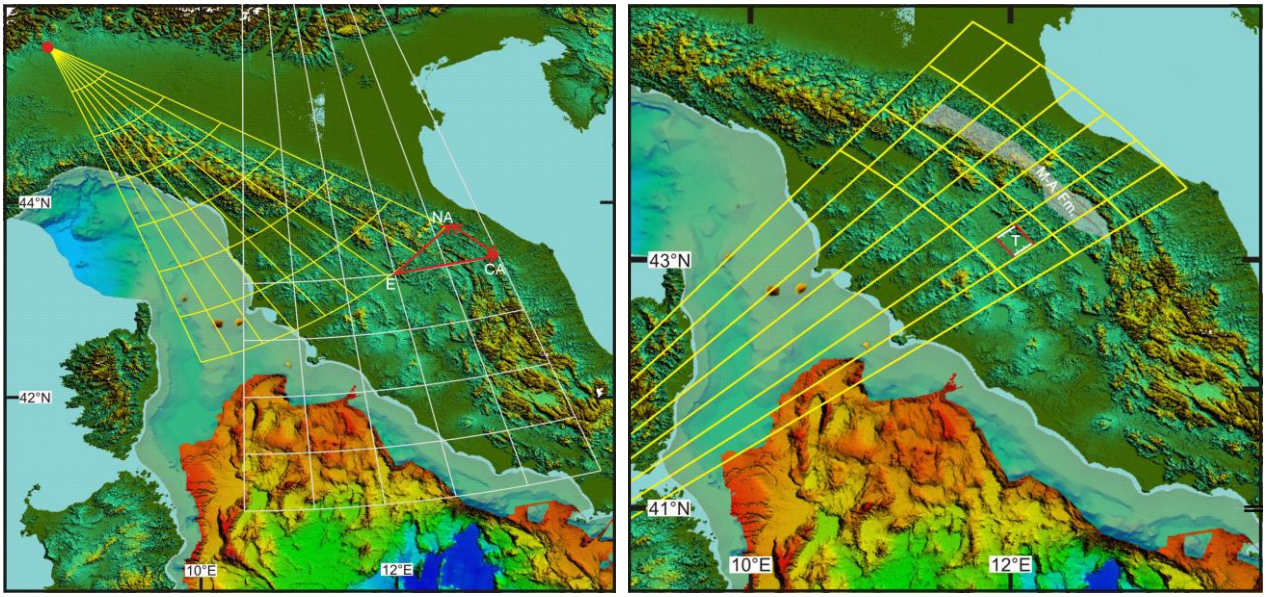

(**a**) (**b**)

Figure. 2.13 - (a) Interaction between northern (yellow grid) and central (white grid) sectors. Red arrows are velocity vectors of the relative motion between the two sectors. E: Europe, NA: Northern Apennine, CA: Central Apennine. (b) Comparison between morpho-structures and the Stage pole grid valid from 5 Ma to present, between Northern Apennine and Central Apennine sectors. T: Trasimeno Lake, M-A Fm: Marnoso-Arenacea Formation. The Euler pole has coordinates: 38.95°−5.61°.

3. Southern Sector

The southern sector runs from south of the 41° parallel to the Sangineto line (northern Calabria) and includes the Vavilov basin and the entire Southern Apennine. The Southern Apennine is composed, from the bottom to the top, of Middle Triassic—Lower Cretaceous Lagonegro units and of carbonatic Upper Triassic—Eocene Panormide units. In some places, the Panormide units are overlapped by ophiolites and oceanic sediments of the Liguride basin, covered by lower Miocene top-wedge sediments (*Zuppetta & Mazzoli, 1995; Cesarano et al., 2002*). On the external chain front, at the boundary with the Central sector, there is a minor arc known as “Molise arc”, extended from the Maiella front to the Vulture volcano. It is made of Jurassic-Cretaceous pelagic successions and of carbonate platforms, overlapped by Mio-Pliocene chaotic and top-wedge successions (*Patacca & Scandone, 2007*). Structures of the Tyrrhenian rift of this sector form a fan

of lineaments that draw the triangular shape of the Vavilov basin, whose vertex is located at 41.23°N,13.01°E (Figs. 2.14 and 2.8).

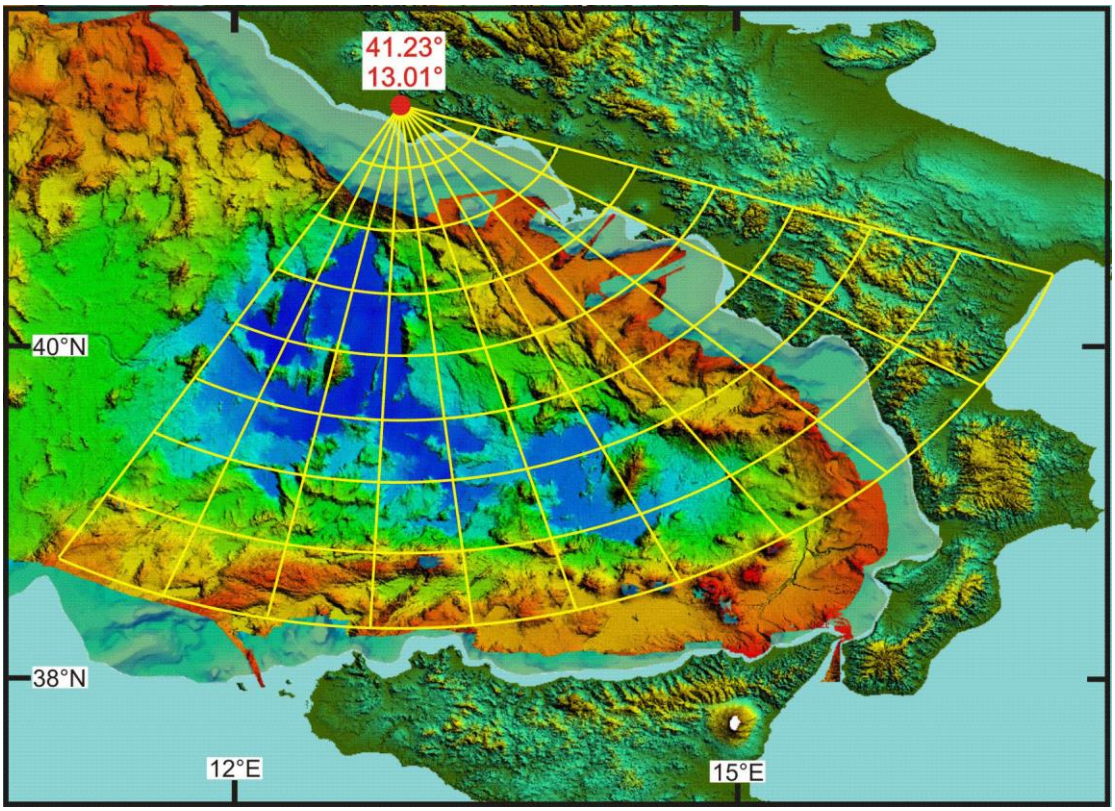

Figure. 2.14 - Morpho-structural lineaments of the southern sector and Euler pole of relative motion with respect to Corsica (red dot). The Euler pole grid shows the goodness of fit between kinematic model and geological structures.

The interaction between the southern and central sectors is responsible for the formation of transversal lineaments (ex. Gran Sasso front, Ancona–Anzio line) and basins (Laga basin) (Fig. 2.15a). The southern sector is also characterized by complex extensional structures expressed by transverse features that cut, on the Apennine margin, the fan of the Vavilov basin. The transverse structures are the result of the interaction with the Calabrian arc sector and form basins and depressions since the Pleistocene. Some of these contain considerable thicknesses of sediment (ex. Sant'Arcangelo basin) (*Capalbo et al., 2010; Patacca & Scandone, 2001*, and reference therein) (Fig. 2.15b). The southern sector also shows a strong magmatism, both on the Tyrrhenian portion and on the Campania margin. A volcano located in the Apulian foredeep of the chain (Mount Vulture) belongs to this sector.

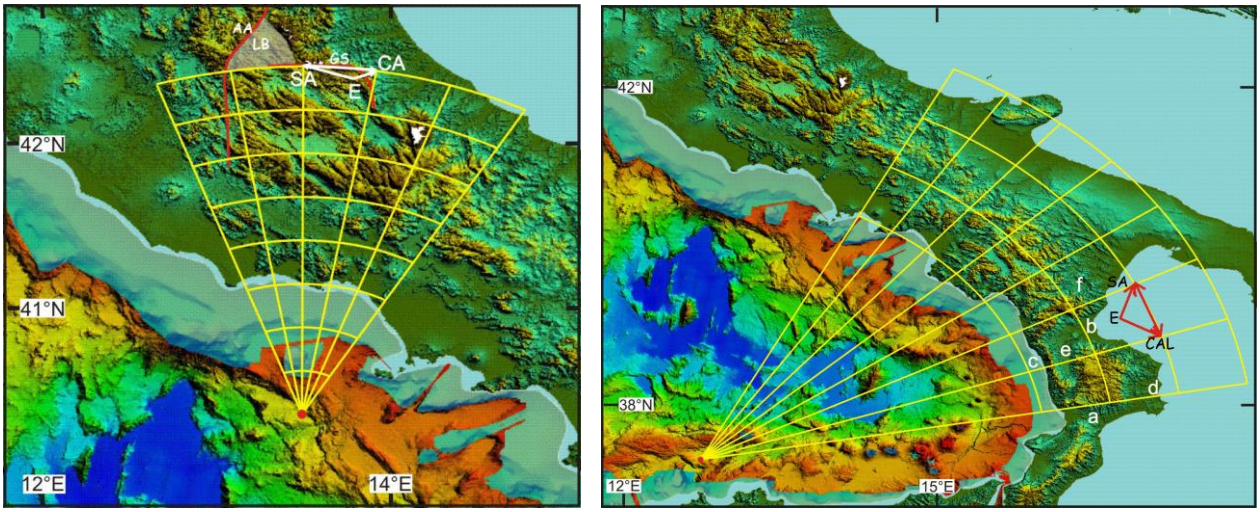

(**a**) (**b**)

Figure. 2.15 - Comparison between morpho-structures and the Stage pole grid valid from 5 Ma to present, between: (a) Central Apennine and southern sectors. The Euler pole has coordinates: 40.48°−13.52° (b) southern and Calabrian arc sectors. The Euler pole has coordinates: 38.43°−12.80°. a: Catanzaro trough, b: Sibari basin, c: Paola basin, d: Crotone basin, e: Crati valley, f: Sant' Arcangelo basin. Red and white arrows are velocity vectors of the relative motion between sectors. AA: Ancona-Anzio line, CA: Central Apennine, CAL: Calabrian Arc, E: Europe, LB: Laga Basin, GS: Gran Sasso front, SA: Southern Apennine.

4. Calabrian Arc Sector

The Calabrian Arc sector is bordered to the north by the Sangineto line and to the south by the Taormina line and includes the southern Tyrrhenian Sea (Marsili Basin). Structural lineaments converge towards SW. The Calabrian Arc includes the Coastal Chain, the Sila Massif, Le Serre, Aspromonte and Paleoritani mountains in Sicily. This segment of the chain is an accretion wedge formed, from bottom to top, by: Apennine carbonatic units, ophiolites (Liguride units), units consisting of low-grade metamorphic rocks with high-grade rocks on top, derived from continental crust with local covers of Upper Trias–Upper Cretaceous sedimentary deposits. The Tyrrhenian extensional structures are represented by the lineaments that characterize the Marsili basin, the southern Calabria and the Strait of Messina. These lineaments form a mild fan with vertex towards SW (Lat. 21.85°; Long. 6.28°; Fig. 2.16), which can be superimposed to the magnetic lineaments of the Marsili basin (Fig. 2.6b). The Calabrian arc is also characterized by important transverse features that express extensional structures, essentially present in Northern Calabria. The most evident have generated the Catanzaro trough, the Sibari basin and also the Paola basin, the Crotonese Basin, and the Crati Valley, which are delimited by structures transversal to the arc and by high-angle N-S trending structures (Fig. 2.15b).

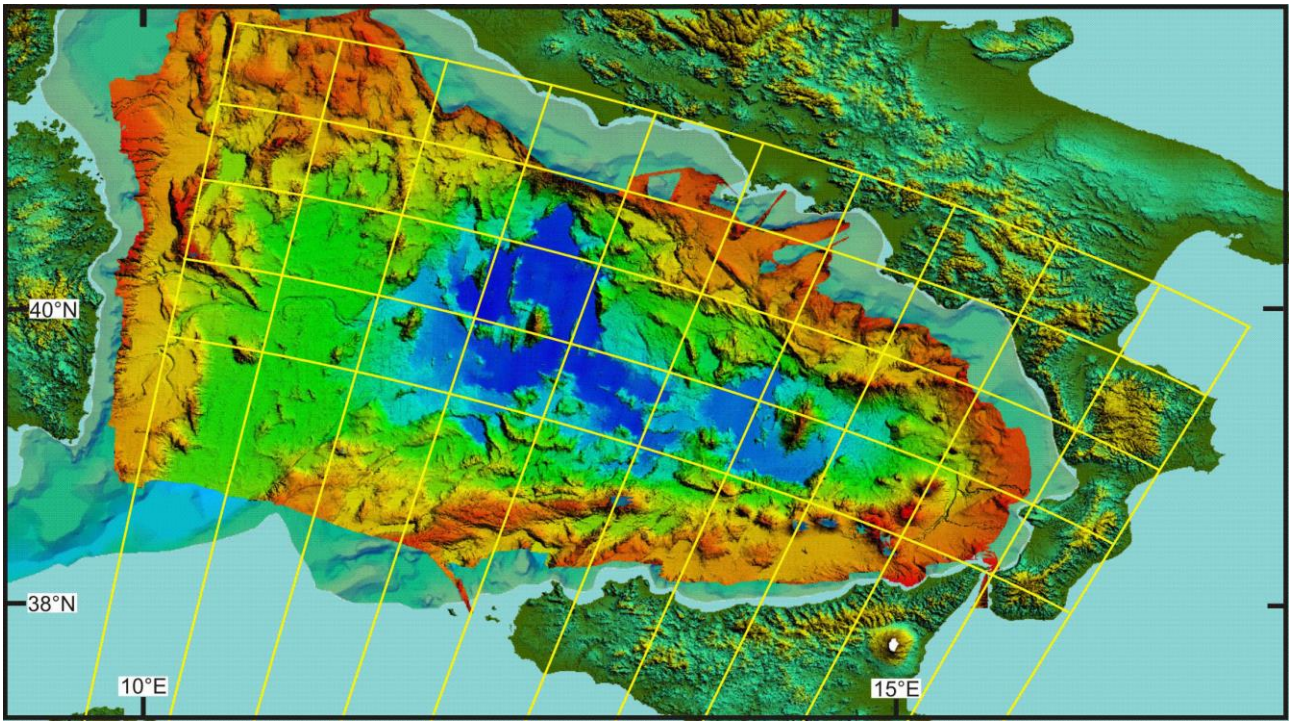

Figure. 2.16 - Morpho-structural lineaments of the southern Tyrrhenian and Euler pole grid of relative motion with respect to Sardinia-Corsica. The Euler pole grid shows the goodness of fit between kinematic model and geological structures. The Euler pole has coordinates: 21.85° 6.28°.

5. Sicilian Sector

The Sicilian sector is represented by the chain located west of the Taormina line. It is made up of Meso-Cenozoic basin and carbonate platform deposits, belonging to the African margin, overlapped by: sediments of the Middle Triassic-Jurassic/Cretaceous Imerese basin, sediments belonging to the Late Triassic-Eocene Panormide carbonatic platform, and Sicilidi Units covered by Oligo-Miocene sediments (*Ghisetti & Vezzani, 1984; Roure et al., 1990; Catalano et al., 2013; Butler et al., 2019*).

The Sicilian chain, with southern vergence, is sharply divided in a northern internal sector and a southern external one by a long E-W trending lineament, known as “Monte Kumeta-Alcantara fault”. This is considered a high-angle strike-slip structure with right-lateral kinematics (*Ghisetti & Vezzani, 1981*), formed from the interaction of the Calabrian arc sector and the Sicilian sector (Figs. 2.17-2.18).

The internal sector includes Nebrodi Mounts, Madonie and Palermo Mounts. The external sector includes Trapanese and Saccense Units, covered by sediments that filled the great depression of the Caltanissetta basin that ends south on the Gela foredeep. On the west side the foredeep is

sharply interrupted in the proximity of Sciacca Mounts. To the East it passes through the Ragusa foreland and ends at Etna Mount. The Caltanissetta basin is filled by thick Messinian and Pliocene successions and is highlighted by a strong gravimetric anomaly (2.18). This evidence suggests the presence of extensional structures that delimited the basin to the West and East (*Catalano et al., 2013*).

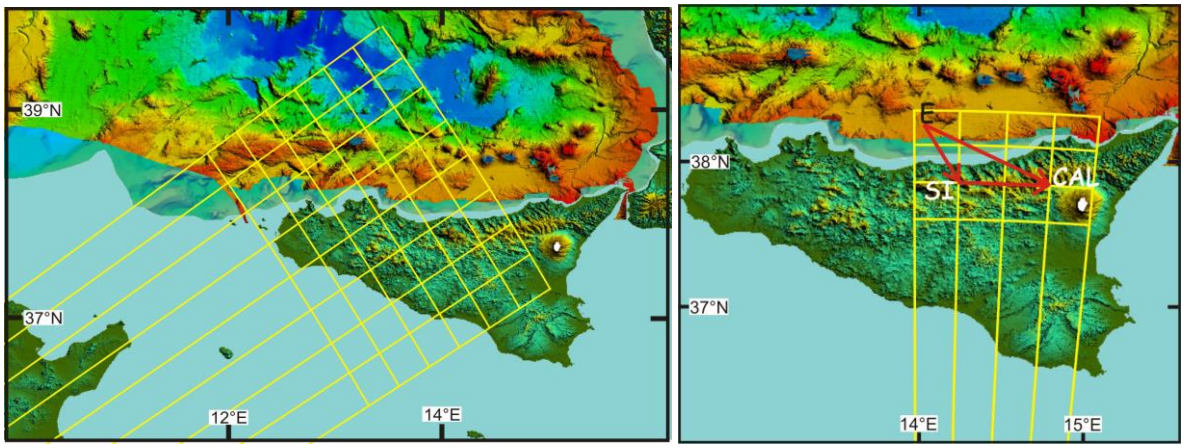

(**a**) (**b**)

Figure. 2.17 –Stage pole grid valid from 12 Ma to present of: a) the Sicilian sector with respect to Sardinia-Corsica. The Euler pole has coordinates: 23.21° 120.84°.b) Sicilian sector and Calabrian arc sectors. The Euler pole has coordinates: 26.63° 13.99°. CAL: Calabrian Arc, E: Europe, SI: Sicilian sector.

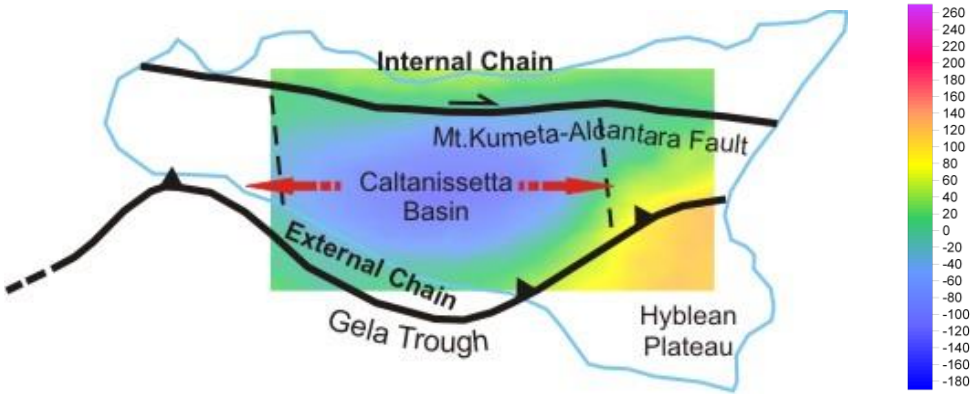

Figure. 2.18 - Schematic tectonic evolution of the Caltanissetta Basin. (Red arrows) show the direction of extension. The Bouguer gravity map is after (ISPRA, ENI, OGS 2009), Cartografia Gravimetrica Digitale d'Italia alla scala 1:250.000).

The Sicilian sector, despite the Apennine sectors that show very visible and clear Tyrrhenian extensional structures, is characterized by complex structures. The Tyrrhenian offshore includes post-Messinian basins interposed between the Elimi chain and the Sicilian northern margin. The chain, E-W oriented, ends to the East with Ustica Island, where volcanic islands (Alicudi, Filicudi,

Salina) mark the continuation of the lineament towards the East (Figure 2.4). Morpho-structures along the chain show characteristics similar to transpressive structures. Seismic profiles (*Catalano et al., 2013*) and compressive earthquakes confirm this hypothesis. Therefore, the Tyrrhenian margin of Sicily, unlike the Apennine one, is characterized by a second phase with transpressive kinematics.

Ch.2.3.5 - Rotation Model

The tectonic reconstructions proposed here can be considered as a refinement of the regional kinematic model of the western Tethys proposed by (*Schettino & Turco 2011; Turco et al., 2012, 2013; Pierantoni et al., 2020*). They were made using interactive computer software for plate kinematic modeling (*Schettino, 1998;* Müller et al., 2018). These software allow to create and maintain data sets of plate boundaries and relative plate positions, and to test the predicted plate motions through the generation of velocity fields and inferred tectonic structures.

As explained above in this chapter, the classic techniques of rigid plate kinematics are not applicable in the Tyrrhenian-Apennine area. To release the block rigidity constraint, polygons were not used to represent the different Apennine blocks. The classic polygons were replaced by linear elements that allowed to implicitly define areas with changing geometry. Therefore, each sector in the rotational model includes two separate objects that rotate about the same pole but with different angles of rotation. The western side of a block rotates with a velocity defined by the local amount of Tyrrhenian extension, while the eastern side of the arc front rotates by a higher angle that represents the accretion rate of the corresponding sector. Euler poles for the Apennine sectors are shown in Figure 2.19 and can be found in Table 2.1.

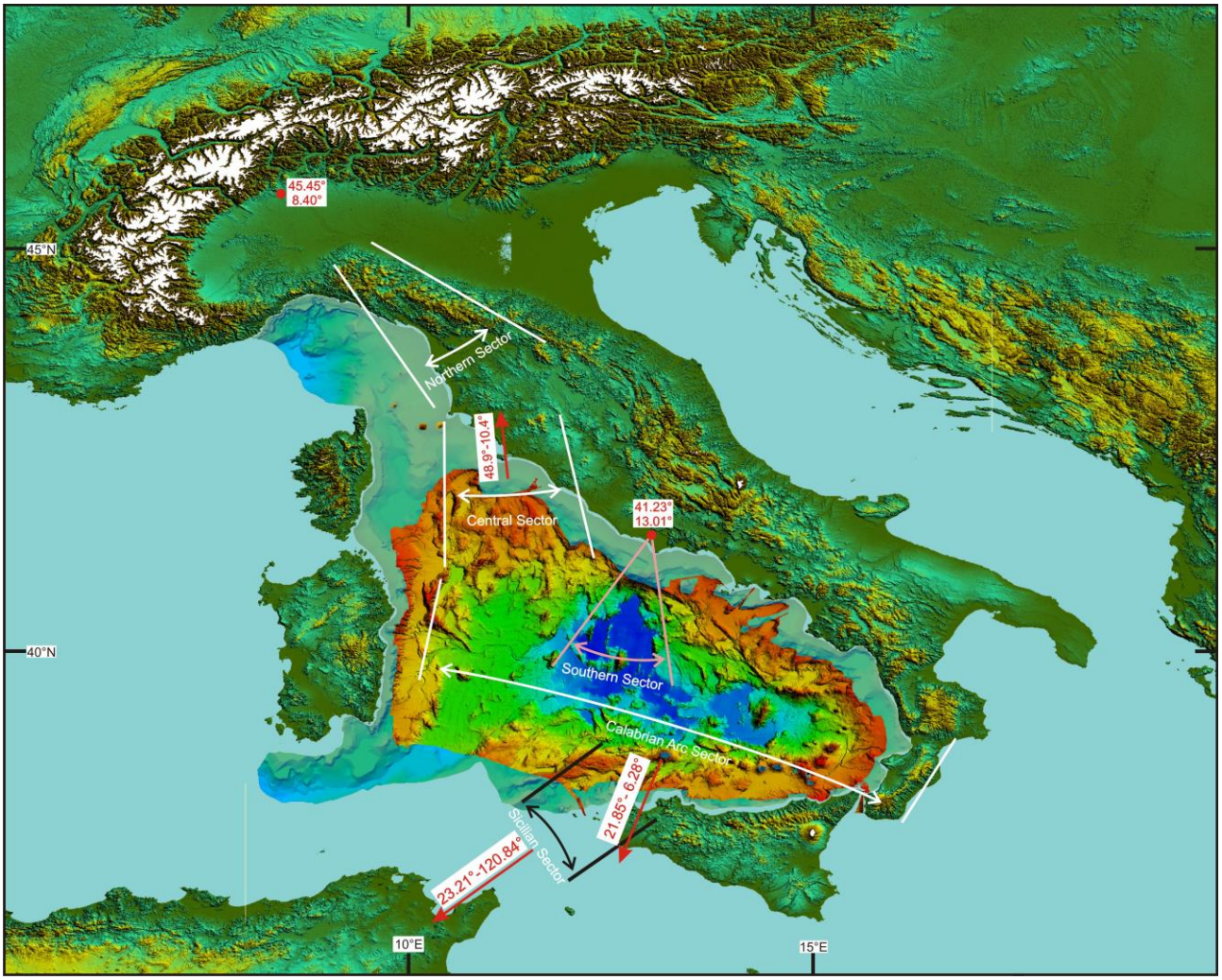

Figure. 2.19 - Morpho-tectonic map and multibeam bathymetry of the Tyrrhenian-Apennine system, showing extension directions in the Tyrrhenian Basin. (White, black and pink lines) show extension started respectively 19 Ma, 12 Ma and 7 Ma. (Red points) are Euler poles. (Red arrows) indicate the Euler poles out of the figure, coordinates of these poles are shown. Real angle of rotation is shown for each pole. Modified after Turco et al., (2013). The multibeam bathymetry is after *Marani et al., (2004).*

The construction of the rotation model of Table 2.1 was performed as follows. Although the Euler poles associated with each tectonic stage could be determined by fitting the observed morpho-structures, the corresponding angles with the exception of the rotation angle of the central Apennine with respect to Sardinia-Corsica, were not known a priori. Therefore, first the ratios between the stage angles, fitting the predicted relative motion between adjacent sectors to the observed geologic structures, have been determined.

Therefore, with the exception of the central sector, the rotation angles of the other tectonic elements forming the Apennine chain were determined considering the velocity ratios between adjacent blocks, which control the kinematics and the trend of the structural associations that

characterize the boundaries. In practice, the rotation angles were chosen in such a way that the resulting velocity ratios were compatible with the observed geological structures along the boundaries. Figures 2.20 and 2.21 summarize the timing of deformation and amount of extension on the basis of the available literature and the proposed kinematic model.

Table 2.1 - Finite reconstruction parameters, from *Turco et al., (2013).*

NAME	PLATE ID	TIME.	LAT.	LONG.	ANGLE	REF. ID
Northern Sector Rear	384	19	45.45	8.40	-20	301
North. Sect. Front	387	19	45.45	8.40	-38	301
Central Sector Rear	360	19	48.90	10.40	-13	301
Cent. Sect. Front	357	19	48.90	10.40	-18	301
Southern Sector Rear	383	7	41.23	13.01	-45.00	301
South. Sect. Front	390	7	41.23	13.01	-54	301
Calabrian Arc Rear	381	1	21.85	6.28	+0.46	301
Calabrian Arc Rear	381	7	21.85	6.28	+7.0	301
Calabrian Arc Rear	381	19	21.85	6.28	+12.00	301
Calab. Arc Front	388	1	21.85	6.28	+0.507	301
Calab. Arc Front	388	7	21.85	6.28	+8.75	301
Calab. Arc Front	388	19	21.85	6.28	+15	301
Sicilian Sector	382	4	-27.345	-167.653	4.469	381
Sicilian Sector	382	7	-27.653	-165.988	8.194	381
Sicilian Sector	382	12	-26.63	-166.009	9.312	381

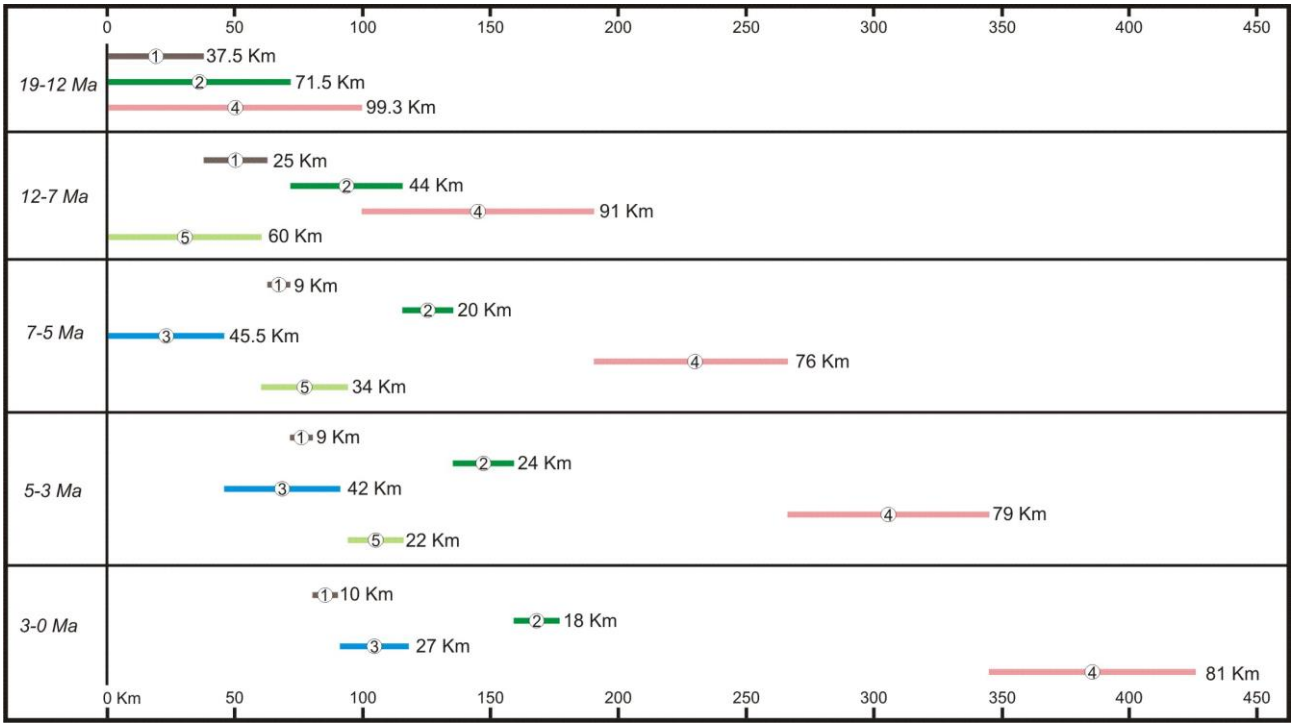

Figure. 2.20 – Estimated extension and timing along representative small circle arcs about the Euler poles of sectors 1–5 with respect to Sardinia-Corsica. Brown line (1): Northern sector, dark green line (2): Central sector, blue line (3): Southern sector, pink line (4): Calabrian arc sector, light green line (5): Sicilian sector.

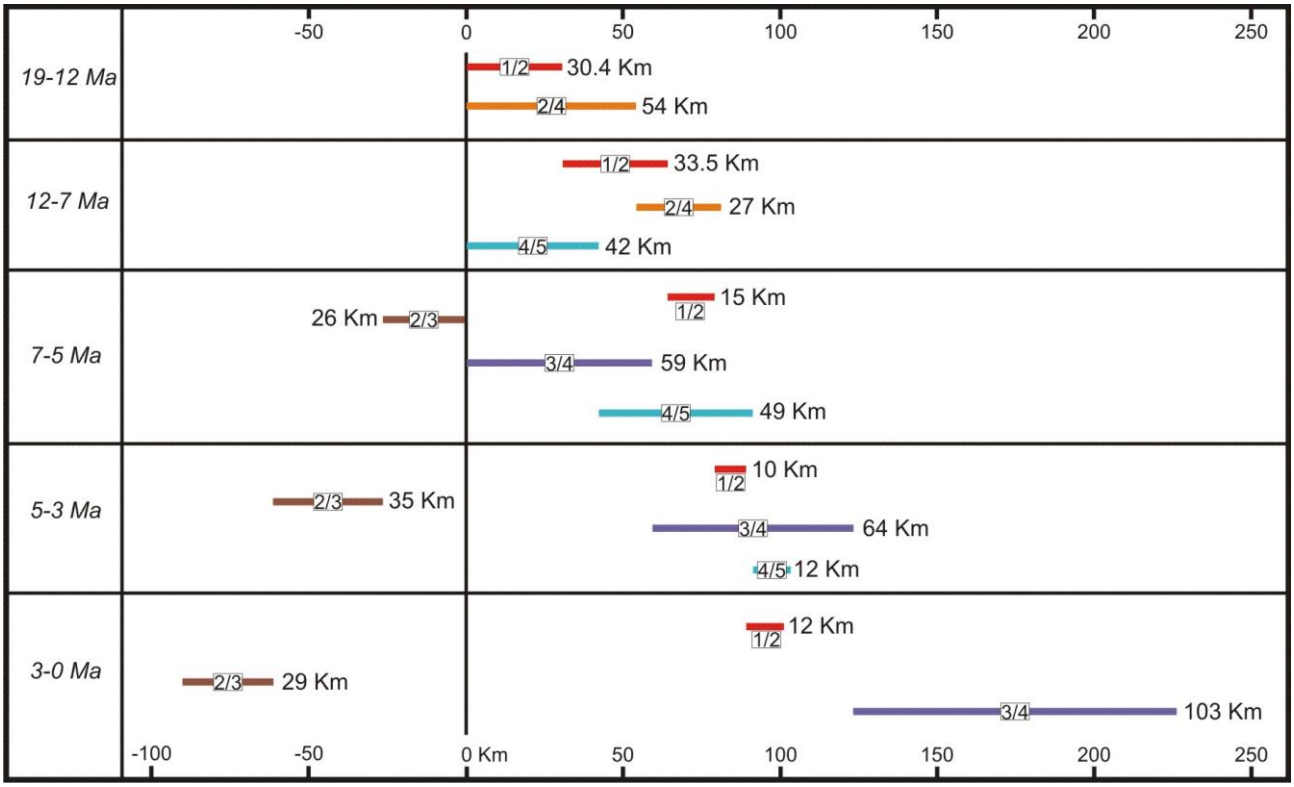

Figure. 2.21 - Estimated total shortening/extension and timing between adjacent sectors of Figure 2.20.

Ch.2.4 - References

Amodio-Morelli, L.; Bonardi, G.; Colonna, V.; Dietrich, D.; Giunta, G.; Ippolito, F.; Liguorl, V.; Lorenzoni, S.; Paglionico, A.; Perrone, V.; et al. 1976. L'arco calabro-peloritano nell'orogene appenninico-maghrebide. Mem. Soc. Geol. Ital., 17, pp. 1–60.

Barchi, M. 1998. The CROP 03 profile: A synthesis of results on deep structures of the Northern Apennines. Mem. Soc. Geol. It., 52, pp. 383–400.

Barchi, M. 2010. The Neogene-Quaternary evolution of the Northern Apennines: Crustal structure, style of deformation and seismicity. J. Virtual Explor., Volume 36 (10), doi:10.3809/jvirtex.2010.00220.

Biju-Duval, B.; Dercourt, J.; Le Pichon, X. 1977. From the Tethys Ocean to the Mediterranean Seas: A plate tectonic model of the evolution of the Western Alpine system. In Structural History of the Mediterranean Basins, Proceedings of the International Symposium on the Structural History of the Mediterranean Basins, Split, 1976, Paris, France, 25–29 October 1977; Biju-Duval, B., Montadert, L., Eds.; Editions Technip: Paris, France; pp. 143–164.

Boccaletti, M.; Ciranafi, N.; Cosentino, D.; Deiana, G.; Gelati, R.; Lentini, F.; Massari, F.; Moratti, G.; Pescatore, T.; Lucchi, F.R.; et al., 1990. Palinspastic restoration and paleogeographic reconstruction of the perithyrrenian area during the Neogene. Palaeogeogr. Palaeoclimatol. Palaeoecol., 77, pp. 41–50.

Bonardi, G.; Cavazza, W.; Perrone, V.; Rossi, S. 2001. Calabria-Peloritani terrane and northern Ionian Sea. In Anatomy of an Orogen: The Apennines and Adjacent Mediterranean Basins; Vai, G.B.; Martini, I.P., Eds.; Springer: Dordrecht, The Netherlands, doi:10.1007/978–94–015–9829–3_17.

Butler, R.W.H.; Maniscalco, R.; Pinter, P.R. 2019. Syn-kinematic sedimentary systems as constraints on the structural response of thrust belts: Re-examining the structural style of the Maghrebian thrust belt of Eastern Sicily. Ital. J. Geosci., 138, pp. 371–389.

Calamita, F.; Centamore, E.; Deiana, G.; Ridolfi, M. 1995. Caratterizzazione geologico-strutturale dell'area marchigiano-abruzzese esterna (Appennino centrale). Studi Geol. Camerti, pp. 171–182, doi:10.15165/studgeocam-896.

Capalbo, A.; Ascione, A.; Aucelli, P.P.; Mazzoli, S. 2010.Valutazione del tasso di erosione in Appennino Meridionale da dati geologico-geomorfologici. Ital. J. Quat. Sci., 23, pp. 75–90.

Capotorti, F.; Fumanti, F.; Mariotti, G. 1995. Evoluzione tettonico-sedimentaria e strutturazione del settore di piattaforma carbonatica laziale-abruzzese nell'alta Valle del F. Velino. Studi Geol. Camerti, pp. 101–111, doi:10.15165/studgeocam-923.

Caricchi, C.; F.; Cifelli, L.; Sagnotti, F.; Sani, F.; Speranza, M. Mattei. 2014. Paleomagnetic evidence for a post-Eocene 90° CCW rotation of internal Apennine units: A linkage with Corsica-Sardinia rotation? Tectonics, 33, pp. 374–392, doi:10.1002/2013TC003364.

Carmignani, L.; Decandia, F.A.; Disperati, L.; Fantozzi, P.L.; Lazzarotto, A.; Liotta, D.; Oggiano, G. 1995. Relationships between the tertiary structural evolution of the Sardinia-Corsica-Provencal Domain and the Northern Apennines. Terra Nova, 7, pp. 128–137.

Carmignani, L.; Decandia, F.A.; Disperati, L.; Fantozzi, P.L.; Kligfield, R.; Lazzarotto, A.; Liotta, D.; Meccheri, M. 2001. Inner northern Apennines. In Anatomy of an Orogen: The Apennines and Adjacent Mediterranean Basins; Vai, G.B., Martini, I.P., Ed.; Kluwer Academic, Dordrecht, The Netherlands, pp. 197–213.

Carminati, E.; Lustrino, M.; Doglioni, C. 2012. Geodynamic evolution of the central and western Mediterranean: Tectonics versus igneous petrology constraints. Tectonophysics, 579, pp. 173–192.

Catalano, S.; De Guidi, G.; Lanzafame, G.; Monaco, C.; Tortorici, L. 2009 Late Quaternary deformation on the island on Pantelleria: New constraints for the recent tectonic evolution of the Sicily Channel Rift (southern Italy). J. Geodyn., 48, pp. 75–82.

Catalano, R.; Valenti, V.; Albanese, C.; Accaino, F.; Sulli, A.; Tinivella, U.; Morticelli, G.M.; Zanolla, C.; Giustiniani, M. 2013. Sicily's fold-thrust belt and slab roll-back: The SI.RI.PRO. seismic crustal transect. Geol. Soc. Lond. Mem., 170, pp. 451–464, doi:10.1144/jgs2012–099.

Cello, G.; Mazzoli, S. 1998. Apennine tectonics in southern Italy: A review. J. Geodyn., 27, pp. 191–211.

Centamore, E. 1992. Carta Geologica dei Bacini della Laga e del Cellino e dei Rilievi Carbonatici Circostanti (Marche Meridionali, Lazio Nord-Orientale, Abruzzo Settentrionale; Università degli studi di Camerino: Camerino, Italy.

Centamore, E.; Rossi, D.; Tavernelli, E. 2009. Geometry and kinematics of Triassic to Recent structures in the Northern-Central Apennines: A review and an original working hypothesis. Ital. J. Geosci., 128, pp. 419–432.

Cesarano, M.; Pierantoni, P.P.; Turco, E. 2002. Structural analysis of the Albidona Formation in the Alessandria del Carretto–Plataci area (Calabro-Lucanian Apennines, Southern Italy). Ital. J. Geosci., 1, pp.669–676.

Civitelli, G.; Brandano, M. 2005. Atlante delle litofacies e modello deposizionale dei Calcari a Briozoi e Litotamni nella Piattaforma carbonatica laziale-abruzzese. Boll. Soc. Geol. Ital., 124, 611.

Cosentino, D.; Scoppola, C.; Scrocca, D.; Vecchia, P. 1991. Stile strutturale dei Monti Reatini e dei Monti Sabini settentrionali (Appennino centrale) a confronto. Studi Geol. Camerti, pp. 55–61, doi:10.15165/studgeocam-962.

Deiana, G.; Pialli, G. 1994. The structural provinces of the Umbro-Marchean Apennines. Mem. Soc. Geol. Ital., 48, pp. 473–484.

Dercourt, J.; Zonenshain, L.P.; Ricou, L.E.; Kazmin, V.G.; Le Pichon, X.; Knipper, A.L.; Grandjacquet, C.; Sbortshikov, I.M.; Geyssant, J.; Lepvrier, C.; et al. 1986. Geological evolution of the Tethys belt from the Atlantic to the Pamirs since the Lias. Tectonophysics, 123, pp. 241–315.

Dewey, J.F.; Helman, M.L.; Turco, E.; Hutton, D.H.W.; Knott, S.D. 1989. Kinematics of theWestern Mediterranean. In Alpine Tectonics; Coward, M.P., Dietrich, D., Park, R.G., Eds.; Geological Society: London, UK; Volume 45, pp. 265–283.

Di Bucci, D.; Tozzi, M. 1991. La linea "Ortona-Roccamonfina": Revisione dei dati esistenti e nuovi contributi per il settore settentrionale (media valle del Sangro). Studi Geol. Camerti, pp. 397–406, doi:10.15165/studgeocam-1036.

Elter, P., Perusati, P. 1973. Considerazioni sul limite Alpi-Appennino e sulle sue relazioni con l'arco delle Alpi occidentali. Mem. Soc. Geol. Ita., 12, pp. 359–375.

Elter, P., Gilgia, G., Tonigiorgi, M., Trevisan, L. 1975. Tensional and compressional areas in the recent (Tortonian to present) evolution of the northern Apennines. Boll. Di Geof. Teor. Appl., 17, pp. 3–18.

Faccenna, C.; Davy, P.; Brun, J.-P.; Funiciello, R.; Giardini, D.; Mattei, M.; Nalpas, T. 1996. The dynamics of back-arc extensions: An experimental approach to the opening of the Tyrrhenian Sea. Geophys. J. Int., 126, pp. 781–795.

Faccenna, C.; Becker, T.W.; Lucente, F.P.; Jolivet, L.; Rossetti, F. 2001. History of subduction and back-arc extension in the Central Mediterranean. Geophys. J. Int., 145, pp. 809–820.

Ferranti, L.; Oldow, J.S.; Sacchi, M. 1996. Pre-Quaternary orogen-parallel extension in the Southern Apennine Belt, Italy. Tectonophysics, 260, pp. 325–347.

Finetti, I.R. 2005. CROP Project: Deep Seismic Exploration of the Central Mediterranean and Italy; Elsevier: Amsterdam, The Netherlands.

Gattacceca, J.; Deino, A.; Rizzo, R.; Jones, D.S.; Henry, B.; Beaudoin, B.; Vadeboin, F. 2007. Miocene rotation of Sardinia: New paleomagnetic and geochronological constraints and geodynamic implications. Earth Planet. Sci. Lett., 258, pp. 359–377.

Ghisetti, F.; Vezzani, L. 1981. Contribution of structural analysis to understanding the geodynamic evolution of the Calabrian arc (Southern Italy). J. Struct. Geol., 3, pp. 371–381.

Ghisetti, F.; Vezzani, L. 1984. Thin-skinned deformations of the western Sicily thrust belt and relationships with crustal short-ening; mesostructural data on the Mt. Kumeta-Alcantara fault zone and related structures. Boll. Soc. Geol. Ital., 103, pp. 129–157.

Grad, M.; Tire, T.2009. ESC Working Group. The Moho depth map of the European Plate. Geophys. J. Int., 176, pp. 279–292, doi:10.1111/j.1365-246X.2008.03919.x.

Hosseinpour, M.; Williams, S.; Seton, M.; Barnett-Moore, N.; Müller, R.D. 2016. Tectonic evolution of Western Tethys from Jurassic to present day: Coupling geological and geophysical data with seismic tomography models. Int. Geol. Rev., 58, pp. 1616–1645.

Johnston, S.T.; Mazzoli, S. 2009. The Calabrian Orocline: Buckling of a previously more linear orogen. Geol. Soc. Lond. Mem., 327, pp. 113–125.

Jolivet, L.; Faccenna, C. 2000 Mediterranean extension and the Africa-Eurasia collision. Tectonics, 19, pp. 1095–1107.

Kastens, K.A.; Mascle, J. 1987. Site 654: Upper sardinian margin. Proc. ODP Init. Rep., pp. 107, 772.

Kastens, K.A.; Mascle, J. 1990. The geological evolution of the Tyrrhenian Sea: An introduction to the scientific results of ODP Leg 107. Proc. ODP Sci. Results, Volume 107(3), 26.

Kearey, P.; Vine, F.J. 1990. Global Tectonics; Wiley-Blackwell: Hoboken, NJ, USA.

Knott, S.D. 1987. The Liguride complex of southern Italy—A Cretaceous to Paleogene accretionary wedge. Tectonophysics, 142, pp. 217–226.

Lavecchia, G.; Federico, C.; Stoppa, F.; Karner, G. 1995. La distensione tosco-tirrenica come possibile motore della compressione appenninica. Studi Geol. Camerti, pp. 489–497.

Lavecchia, G.; Boncio, P.; Creati, N.; Brozzetti, F. 2003. Some aspects of the Italian geology not fitting with a subduction scenario. J. Virtual Explor., 10, pp. 1–14.

Le Breton, E.; Handy, M.R.; Molli, G.; Ustaszewski, K. 2017. Post-20 Ma motion of the Adriatic Plate: New constraints from surrounding orogens and implications for crust-mantle decoupling. Tectonics, 36, pp. 3135–3154.

Malinverno, A.; Ryan, W.B.F. 1986. Extension in the Tyrrhenian Sea and shortening in the Apennines as result of arc migration driven by sinking of the lithosphere. Tectonics, 5, pp. 227–245.

Marani, M.P. 2004. Super-inflation of a spreading ridge through vertical accretion. Mem. Descr. Carta Geol. D'It., XLIV, pp. 185–194.

Marani, M.P.; Gamberi, F. 2004. Structural framework of the Tyrrhenian Sea unveiled by seafloor morphology. Mem. Descr. Carta Geol. Ital., 64, pp. 97–108.

Marroni, M.; Meneghini, F.; Pandolfi, L. 2017. A revised subduction inception model to explain the Late Cretaceous, double-vergent orogen in the precollisional western Tethys: Evidence from the Northern Apennines. Tectonics, 36, pp. 2227–2249.

Mazzoli, S.; Barkham, S.; Cello, G.; Gambini, R.; Mattioni, L.; Shiner, P.; Tondi, E. 2001. Reconstruction of continental margin architecture deformed by the contraction of the Lagonegro Basin, southern Apennines, Italy. J. Geol. Soc., 158, pp. 309–319.

Meloni, A.; Carmisciano, C.; Chiappini, M.; Faggioni, O.; Marson, I. 2007. Total Field Magnetic Anomaly Map of Italy and Sur-rounding Marine Areas at Sea Level. Recent Compilation and Scientific Significance. In Proceedings of the EGM 2007 In-ternational Workshop, Capri, Italy, 15–18 April.

Milia, A.; Torrente, M.M. 2014. Early-stage rifting of the Southern Tyrrhenian region: The Calabria–Sardinia breakup. J. Geodyn., 81, pp. 17–29, doi:10.1016/j.jog.2014. 06.001.

Milia,A.; Torrente, M.M.; Tesauro, M. 2017. From stretching to mantle exhumation in a triangular backarc basin (Vavilov basin, Tyrrhenian Sea, Western Mediterranean). Tectonophysics, 710–711, pp. 108–126.

Müller, R.D.; Cannon, J.; Qin, X.; Watson, R.J.; Gurnis, M.; Williams, S.; Pfaffelmoser, T.; Seton, M.; Russell, S.H.J.; Zahirovic, S. 2018. GPlates: Building a virtual Earth through deep time. Geochem. Geophys. Geosystems, 19, doi:10.1029/2018GC007584.

Müller, R.D.; Zahirovic, S.; Williams, S.E.; Cannon, J.; Seton, M.; Bower, D.J.; Gurnis, M. 2019. A global plate model including lithospheric deformation along major rifts and orogens since the Triassic. Tectonics, 38, pp. 1884–1907.

Nicolich, R. 1981. Crustal structures in the Italian Peninsula and Surrounding Seas: A review of DDS data. In Sedimentary Basins of the Mediter-ranean Margins. C.N.R. Italian Project of Oceanography; Wezel, F.C., Ed.; Tectoprint: Bologna, Italy, pp. 489–501.

Ogniben, L. 1969. Schema introduttivo alla geologia del confine calabro-lucano. Mem. Soc. Geol. It., 8, pp. 453–763.

Panza, G.F. 1984. Structure of the lithosphere–asthenosphere system in the Mediterranean region. Ann. Geophys., 2, pp. 137–138.

Panza, G.F.; Calcagnile, G. 1979-1980. The upper mantle structure in Balearic and Tyrrhe-nian bathyal plains and the Messinian sa-linity crisis. Palaeogeogr. Palaeoclimatol. Palaeoecol., 29, pp. 3–14.

Parotto, M.; Praturlon, A. 1975. Geological summary of the Central Apennines. In Structural Model of Italy. Quad. Ric. Sci.Ital., 90, pp. 257–311.

Pascucci, V. 2002. Tyrrhenian Sea extension north of the Elba Island between Corsica and western Tuscany (Italy). Boll. Soc. Geol. Ital., 1, pp. 819–828.

Pascucci, V.; Martini, I.P.; Sagri, M.; Sandrelli, F.; Nichols, G. 2007. Effects of transverse structural lineaments on the Neogene-Quaternary basins of Tuscany (inner Northern Apennines, Italy). Sediment. Process. Environ. Basins, 38, 155–182.

Patacca, E.; Scandone, P. 1989. Post-Tortonian mountain building in the Apennines. The role of the passive sinking of a relic lithospheric slab. In The Lithosphere in Italy: Advances in Earth Science Research; Boriani, A., Ed.; Accademia Nazionale dei Lincei: Rome, Italy; Volume 80, pp. 157–176.

Patacca, E.; Scandone, P. 1991. La zona di giunzione tra l'Arco Appenninico Settentrionale e l'Arco Appenninico Meridionale nell'Abruzzo e nel Molise. Studi Geol. Camerti, pp. 417–441, doi:10.15165/studgeocam-1043.

Patacca, E.; Scandone, P. 2001. Late thrust propagation and sedimentary response in the thrust-belt foredeep system of the Southern Apennines (Pliocene-Pleistocene). In Anatomy of an Orogen: The Apennines and Adjacent Mediterranean Basins; Vai, G.B., Martini, I.P., Eds.; Kluwer Academic, Dordrecht, The Netherlands; pp. 401–440

Patacca, E.; Scandone, P. 2007. Geology of the Southern Apennines. Boll. Soc. Geol. It. (Ital. J. Geosci.), 7, pp. 75–119.

Peccerillo, A.; Turco, E. 2004. Petrological and geochemical variations of Plio-Quaternary volcanism in the Tyrrhenian Sea area: Regional distribution of magma types, petrogenesis and geodynamic implications. Per. Miner., 73, pp. 231–251.

Pescatore, T.; Renda, P.; Schiattarella, M.; Tramutoli, M. 1999. Stratigraphic and structural relationships between Meso-Cenozoic Lagonegro basin and coeval carbonate platforms in southern Apennines, Italy. Tectonophysics, 315, pp. 269–286.

Piana, F. 1991. Configurazione geometrica ed evoluzione cinematica della zona di convergenza strutturale tra l'arco umbro ed il dominio laziale-abruzzese (Appennino Centrale). Studi Geol. Camerti, pp. 85–94, doi:10.15165/studgeocam-968.

Pierantoni, P.P.; Macchiavelli, C.; Penza, G.; Schettino, A.; Turco, E. 2020. Kinematics of the Tyrrhenian–Apennine system and implications for the origin of the Campanian magmatism. In Vesuvius, Campi Flegrei, and Campanian Volcanism, 1st ed.; De Vivo, B., Belkin, H.E., Rolandi, G., Eds.; Elsevier Inc.: Amsterdam, The Netherlands; p. 520.

Rosenbaum, G.; Lister, G.S.; Duboz, C. 2002. Reconstruction of the tectonic evolution of the western Mediterranean since the Oligocene. J. Virtual Explor., 8, pp. 107–126.

Rosenbaum, G.; Lister, G.S. 2004. Neogene and Quaternary rollback evolution of the Tyrrhenian Sea, the Apennines, and the Sicilian Maghrebides. Tectonics, 23, TC1013.

Roure, F.; Howell, D.G.; Müller, C.; Moretti, I. 1990. Late cenozoic subduction complex of Sicily. J. Struct. Geol., 12, pp. 259–266.

Sartori, R. 1990. The main results of ODP leg 107 in the frame of neogene to recent geology of peri-tyrrhenian areas. Proc. ODP Sci. Results, Volume 107, pp. 715–730.

Sartori, R. 2003. The Tyrrhenian back-arc basin and subduction of the Ionian lithosphere. Episodes, 26, pp. 217–221.

Sartori, R.; Torelli, L.; Zitellini, N.; Carrara, G.; Magaldi, M.; Mussoni, P. 2004. Crustal features along aW–E Tyrrhenian transect from Sardinia to Campania margins (Central Mediterranean). Tectonophysics, 383, pp. 171–192.

Scarsella, F. 1951. Sulla zona di incontro dell'Umbria e dell'Abruzzo. Boll. Serv. Geol. D'It., 71, pp. 155–165.

Schettino, A. 1998. Computer-aided paleogeographic reconstructions. Comput. Geosci., 24, pp. 259–267.

Schettino, A. 2014. Quantitative plate tectonics. Physics of the Earth–Plate Kinematics–Geodynamics, 1st ed.; Springer International Publishing: New York, NY, USA; pp. XIV.

Schettino, A.; Turco, E. 2006. Plate kinematics of the Western Mediterranean region during the Oligocene and Early Miocene. Geophysi. J. Int., 166, pp. 1398–1423.

Schettino, A.; Turco, E. 2011. Tectonic history of the western Tethys since the Late Triassic. GSA Bull., 123, pp. 89–105.

Selli, R. 1981. Thoughts on the geology of the Mediterranean region. In Proceedings of the Consiglio nazionale delle ricerche. International Conference, Rome, Italy, 22–23 May, pp. 489–501.

Spadini, G.; Cloething, S.; Bertotti, G. 1995. Thermo-mechanical modeling of the Tyrrhenian Sea: Lithosphere necking and kinematics of rifting. Tectonics, 14, pp. 629–644.

Speranza, F.; Cosentino, D.; Villa, I.M. 1999. Età della rotazione sardo-corsa: Nuovi dati paleomagnetici e geocronologici. Riassunti Convegno Geoitalia, 1, pp. 299–301.

Thinon, I.; Guennoc, P.; Serrano, O.; Maillard, A.; Lasseur, E.; Rehault, J.P. 2016. Seismic markers of the Messinian Salinity Crisis in an intermediate-depth basin: Data for understanding the Neogene evolution of the Corsica Basin (northern Tyrrhenian Sea). Mar. Pet. Geol., 77, pp. 1274–1296.

Turco, E.; Macchiavelli, C.; Mazzoli, S.; Schettino, A.; Pierantoni, P.P. 2012 Kinematic evolution of the Alpine Corsica in the framework of Mediterranean mountain belts. Tectonophysics, 579, pp. 193–206.

Turco, E.; Schettino, A.; Macchiavelli, C.; Pierantoni, P.P. 2013. A plate kinematics approach to the tectonic analysis of the Tyrrhenian–Apennines System. Geophys. Res. Abstr., 29, pp. 187–190.

Turco, E.; Schettino, A.; Pierantoni, P.P.; Santarelli, G. 2006. The Pleistocene extension of the Campania Plain in the framework of the southern Tyrrhenian tectonic evolution: Morphotectonic analysis, kinematic model and implications for volcanism. In Volcanism in the Campania Plain: Vesuvius, Campi Flegrei and Ignimbrites; De Vivo, B., Ed.; Elsevier: Amsterdam, The Netherlands; Volume 9, pp. 27–51.

Turco, E.; Zuppetta, A. 1998. A kinematic model for the Plio-Quaternary evolution of the Tyrrhenian–Apenninic system; implications for rifting processes and volcanism. J. Volcanol. Geoth. Res., 82, pp. 1–18.

Turco, E.; Macchiavelli, C.; Penza, G.; Schettino, A.; Pierantoni, P.P. 2021. Kinematics of Deformable Blocks: Application to the Opening of the Tyrrhenian Basin and the Formation of the Apennine Chain. Geosciences, 11, 177. https://doi.org/10.3390/geosciences11040177.

Van Dijk, J.P.; Bello, M.; Brancaleoni, G.P.; Cantarella, G.; Costa, V.; Frixa, A.; Zerilli, A. 2000. A regional structural model for the northern sector of the Calabrian Arc (southern Italy). Tectonophysics, 324, pp. 267–320.

Van Hinsbergen, D.J.; Torsvik, T.H.; Schmid, S.M.; Ma¸tenco, L.C.; Maffione, M.; Vissers, R.L.; Spakman, W. 2020. Orogenic architecture of the Mediterranean region and kinematic reconstruction of its tectonic evolution since the Triassic. Gondwana Res., 81, pp. 79–229.

Zuppetta, A.; Mazzoli, S. 1995. Analisi strutturale ed evoluzione paleotettonica dell'unità del Cilento nell'Appennino Campano. Studi Geol. Camerti, 13, pp. 103–114.

Chapter 3 -Adriatic-Ionian slab

Ch.3.1 - Introduction

The proposed kinematic model, which describes quantitatively the complex evolution of the system of deformable tectonic elements belonging to the Tyrrhenian–Apennine region, will be presented in Chapter 5. The main tectonic consequences of this model shed new light on the geodynamic processes that generated the Tyrrhenian extension and the corresponding formation of the Apennine chain. The slab retreat process, which is generally recognized as responsible for the origin of the Tyrrhenian rift (*Malinverno & Ryan, 1986; Royden et al., 1987; Doglioni, 1991; Faccenna et al., 1996)*, has complex geodynamic implications, not always sufficiently considered. It occurs when the speed between two converging plates is lower than the retreat speed of the slab inflection point, caused by the lithospheric sinking (*Dewey, 1975*).

From the kinematic point of view an adequate description can be made considering the rotation of the trench line about the Euler pole of the upper plate. But, besides the kinematic aspects, the slab-retreat process is associated with the formation of STEP faults and the elastic rebound that follows slab detachment and requires a description that takes into account all the boundary conditions.

The formation of STEP faults plays a crucial role in the formation of a new microplate that includes Sicily and its offshore and whose evolution, described in Chapter 4, is the specific object of this Phd thesis.

Ch.3.2 - Methods

In a context of slab-retreat, the geometry of the slab controls the tectonic setting of the upper plate. Therefore, even in absence of deep earthquake data, it is possible to outline the lower plate from the elements provided by the oceanic trench, the accretionary wedge, the back-arc extension and the volcanic arc. This is true when the tectonic framework can be attributed to a single continuous slab.

In order to determine the geometry and the evolution of the slab in the Tyrrhenian-Apennine system, where the structures of the upper plate are complex and the hypothesis of a single slab is excluded, *Pierantoni et al. (2020)* propose a method based on the research of the causes that determined the kinematic parameters of the tectonic setting of the upper plate.

The method involves the integration of two kinds of datasets:

* kinematic reconstructions of the upper plate, from *Turco et al. (2013 and 2021)*;
* features of the subducted lower plate such as COB and fracture zone trends, from *Schettino and Turco (2011*).

In the mentioned work by *Schettino & Turco (2011)*, the continent-ocean boundary (COB) has been traced doing the Pangea fit in the global rotation model. As a first assumption the COB has been considered perpendicular to the fracture zones which, in current coordinates, are E-W trending. The same trend can be extrapolated to the transfer faults that linked the rift basins during the Jurassic (Fig. 3.1, from *Schettino & Turco, 2011*).

The Late Cretaceous Adria-Eurasia collision is responsible for the reactivation of the Jurassic transfer faults that cut the entire post-rift succession on the Apulian platform.

The trend of the Apulian-Ionian COB is instead represented by the WNW-ESE trending Apulian slope that, in the rotation model, was the fracture zone during the Middle Triassic rifting (*Pierantoni et al., 2020*).

Figure 3.2 redrawn from *Schettino & Turco (2011)*, shows the reconstruction at 33.1 Ma of the western Tethys, where the Adriatic and Ionian COBs, with the relative synthetic isochrons and fracture zones, are represented. The same features have been traced on the lower plate paleo-maps from 19 to 0 Ma as shown in Figure 3.3. This type of representation allows visualization, in the various steps of evolution, of the quantity of continental lithosphere involved in the Adriatic-Ionian slab; this in turn determines the sinking velocity into the upper mantle.

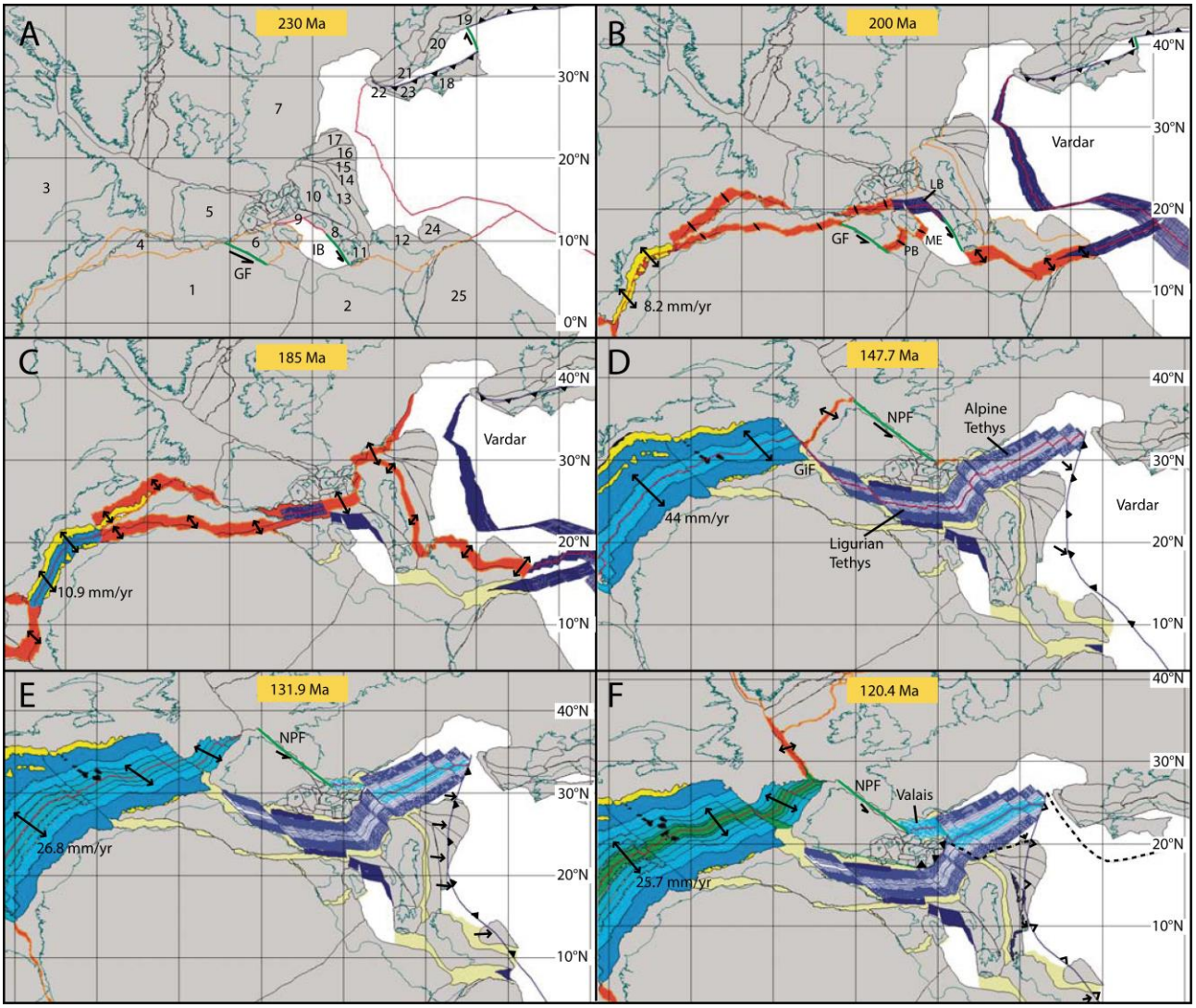

Figure. 3.1 – Late Triassic to Early Cretaceous plate reconstructions of the western Tethys from *Schettino & Turco, (2011)*. The areas affected by the first rifting events are bounded by orange lines. Transform faults are shown in green. Red lines are spreading centers. GF—Gafsa fault; IB—Ionian Basin; LB—Lagonegro Basin; PB—Pelagian Basin; ME—Malta Escarpment. Refer to Figure 1 in *Schettino & Turco (2011)* for further details.

The articulation of the Adriatic COB line of Figures 3.2 e 3.3 results in an asynchronous subduction. The continental lithosphere begins to subduct starting from the North and proceeds to the South with time intervals determined by the length of the COB steps. To the South, where the continental lithosphere is absent or scarce, the slab segments keep subducting into the upper mantle; on the contrary, the northernmost segments progressively decrease their sinking with the increase of the continental lithosphere included in the subduction, until the buoyancy equilibrium is reached.

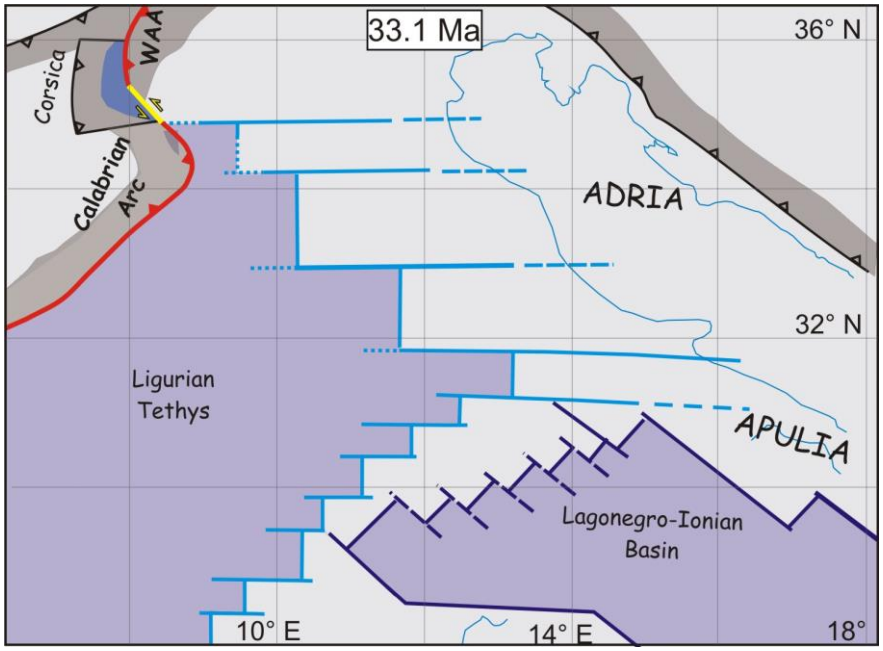

Figure. 3.2 - Plate reconstruction of the western Mediterranean region at 33.1 Ma. The Jurassic extension of the continental lithosphere is shown in light blue; dark blue is the Middle-Triassic extension. Modified from *Schettino & Turco, (2011).*

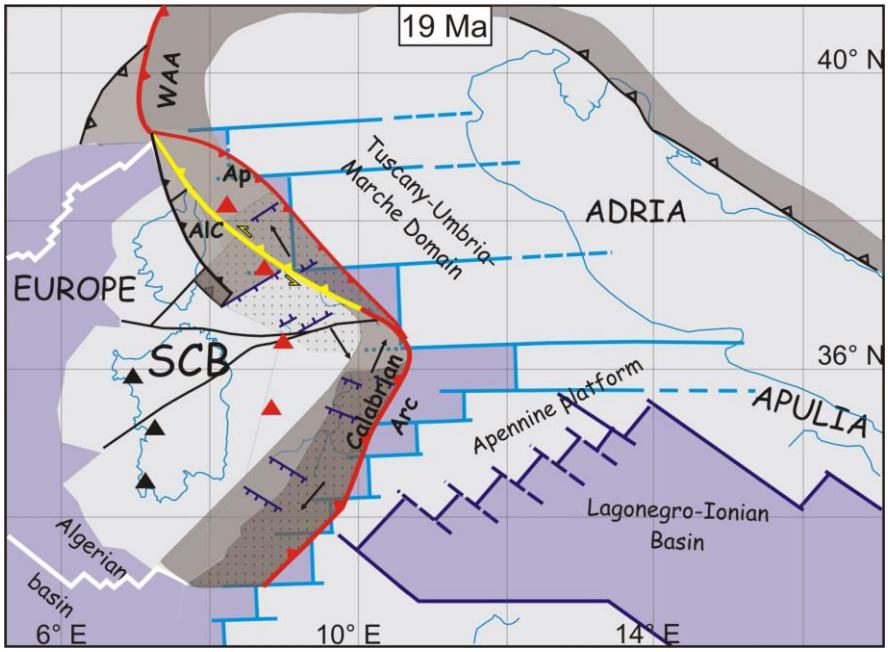

Figure. 3.3 - Plate reconstruction of the western Mediterranean region at 19 Ma. Lower Miocene Chains are shown in dark gray, the Africa-Adria and Europe continental lithosphere is in light gray, the oceanic crust is in blue. Red lines are active boundaries. Black lines are inactive boundaries. Yellow lines are transform faults. Light blue lines are the Jurassic COB (Continent Ocean Boundary) and transfer faults on the continental lithosphere. Dark blue lines are the Middle-Triassic COB and transfer faults on the continental lithosphere. Triangles are volcanoes. Ap, Proto-Apennine; WAA, Western Alps Arc. Modified from *Turco, et al., (2013).*

A STEP fault is produced where two neighbouring sectors do not have the same subduction velocity and it propagates along the trend of fracture zones and transform faults generated during the breakup of Pangea. This process follows the steps of the Adriatic COB. Figure 3.4 illustrates a possible present day 3D reconstruction of the segmented geometry of the Ligurian-Ionian slab, generated by the described process and based on kinematic considerations and seismic tomography (*Montuori et al., 2007; Di Stefano et al., 2009; Giacomuzzi et al., 2011;*).

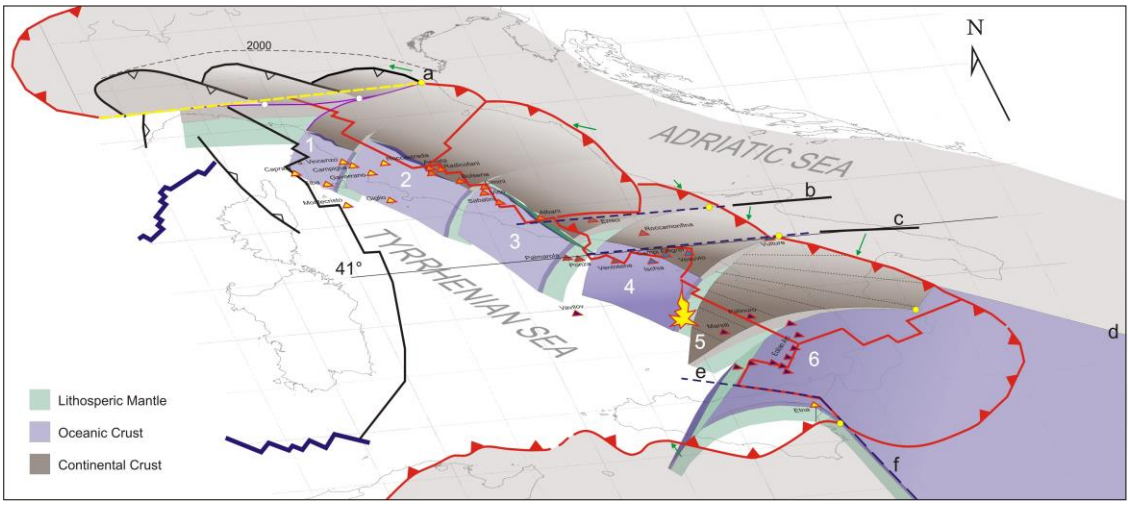

Figure. 3.4 - Proposed Adriatic-Ionian slab geometric reconstruction. The slab sectors are numbered from 1 to 6. (Dotted lines) are STEP faults labeled from a to f. (Yellow dot) is the active tip point of STEP fault, (white dot is paleo-tip point). (Triangles) are volcanoes. The entire slabs length is not represented. Green arrows are the velocity vectors between Adria and the adjacent sector; modified after *Pierantoni et al., (2020).*

STEP faults determine a downward flexure that partly affects the unsubducted plate, whose margin is dragged to some extent in the asthenosphere. Such a flexure propagates together with the rip between the slab and the continental margin. In the crust, the effects of this process are strictly related to the extent of the flexure, which in turn depends on the rigidity and strength of the lithosphere. In general, the marginal flexure of the continental lithosphere occurs along a hinge line that is oblique with respect to the STEP fault strike. The subsequent rebound determines the formation of crustal structures that are pairwise oblique with respect to the direction of slab retreat. In the Apennine area this effect is quite evident. In addition to this, the lithospheric flexure along a STEP fault produces important transpressive structures at crustal scale that simulate normal mountain chains (such as the northern Apennine).

Ch.3.3 - STEP faults evolution

First, the STEP fault to the North (a) is activated and propagates along the transfer structure of the Jurassic rifting that separated the lithosphere of the Ligurian basin from the Adriatic continental one. On the upper plate, the Adriatic slab tear fault detachment is reflected on the Northern Apennine sector. The curvature radius of the Apennine trench is still sufficiently large to suggest a continuous Adriatic-Ionian slab from North to South, mainly constituted by oceanic lithosphere. When the subduction velocity of the northern portion of the Adriatic slab slows, due to the subducted continental lithosphere, the slab geometry evolves separating the slab in segments with different buoyancy up to the STEP fault (c).

The sector 5-6 of the slab, still joined up to 3 Ma, is essentially composed by oceanic Ionian lithosphere, which gives this sector a remarkable subduction velocity. On the upper plate, the direct evidences of the STEP faults associated with this sector are not very clear, while on the lower plate (Apulia) the Jurassic structures, along which the faults propagated can be identified with the Mattinata line (b) and with the 41st parallel that passes through the Canal of Pyrrhus line and the Vulture Volcano (c). The indirect evidences are instead substantial and are represented by the implications on the kinematic of the upper plate blocks, described in Ch.5.

The STEP fault (d) propagates along the Middle-Triassic Apulian-Ionian COB. The activation and the consequent detachment produced by the tear fault (d) have effects in all the Tyrrhenian-Apennine and Calabrian Arc areas.

In the last million years, the oceanic lithosphere of the Apennine slab segments begins to detach from the continental lithosphere. Probably the slab 3 is completely detached, as witnessed by the general uplift of the Lazio-Abruzzi Chain (*Galadini et al., 2003*).

The last slab segment is the Ionian slab; outlined by a well-defined Benioff zone. It is constrained to the south by the STEP fault e-f. As shown in Figure 3.4, this fault has a double direction. The segment (e) starts tearing during the early pliocene and can be identified with the Taormina line; during the pleistocene the tearing was transferred to the Malta Escarpment (segment f).

Ch.3.4 - STEP Fault implications

On the basis of the considerations made in Ch.3.2 and Ch.3.3, it is possible to describe the consequences of the geodynamic processes involved in STEP faults evolution, within the Northern Apennine, the Southern Apennine and the Sicilian Chain.

Northern Apennine

In previous models, the northern and central Apennine are part of a unique arc that extends from the Sestri Voltaggio line to the Ortona–Roccamonfina line (*Royden et al., 1987*). These models are based on the hypothesis that a continuous Adriatic slab exists. Instead, the model described above suggests that the northern Apennine segment represents a transform structure of the upper plate with left-lateral motion, which links the western Alpine arc with the Apennine chain with opposite vergence. The flexure of the continental margin of Adria in the Padania Valley originated a submerged chain that was later exhumed by elastic rebound. A series of arcs formed, with a symmetry axis aligned with the hinge line of the flexure, thereby oblique with respect to the strike of the STEP fault. These arcs propagated eastwards and were eventually exhumed (the Monferrato arc) following the tear migration (Fig. 2.4 and *Bigi et al., 1991*).

Southern Apennine

The southern Apennine is aligned with the important STEP fault (d), that separates the continental margin of Apulia from the Ionian slab. Intially, the southwestern margin of Apulia bended downwards following the subduction of the Ionian oceanic lithosphere, while its northern margin is separated from Adria along the 41° parallel STEP fault (c). Starting from the late Tortonian, a tear formed between the slab segment 5 and 6. As soon as Apulia was not anymore pulled downwards by the Ionian slab, due to the detachment produced by the tear fault (d), the flexure line started rotating counterclockwise and assuming a strike slightly oblique with respect to the new southeastward propagating STEP fault. The contemporary elastic rebound of the more western parts of segment 5 enhanced this rotation of the flexure line and produced at the same time the rotation and exhumation of most of the southern Apennine (*Cinque et al., 1993*), and the formation of the Vavilov basin.

Sicilian Chain

The western Sicilian chain developed along three distinct STEP faults. The oldest (and most important) one had an E-W trend (in present day coordinates) and was placed along the northern continental Hyblean paleomargin. The next STEP coincided with the modern Taormina line (letter e in Figure 3.4). Finally, the modern STEP fault associated with the rip of the Ionian oceanic lithosphere from the African margin coincides with the Malta Escarpment (f). The eastward propagation of the tearing determined flexure along the Iblei and SSE migration of the external chain while the internal chain moved together with the Calabrian Arc (Figure 2.4 and 2.18). This process separated the two chains along the Monte Kumeta fault, which is characterized by right-lateral kinematics. The eastern termination of this fault is represented by the northeastern tip of the Caltanissetta extensional system. When the Taormina line started, the tectonic activity along the external and internal chains was essentially driven by the convergence between Africa and Eurasia. Finally, the tearing along the Malta Escarpment determined an eastern break in the continuity between the African continental margin and the Ionian lithosphere. I hypothesize that this event originated an eastward escape of Sicily with respect to stable Africa; Chapter 4 will address this point. Such a hypothesis is supported by the dextral kinematics along the Sicily Channel and by the submerged Elimi Chain (*Pondrelli et al. 2004; Neri et al., 2005*).

Volcanism

A widespread magmatic activity strongly affects the geodynamic evolution of this region, where magmatism developed almost continuously to present, producing different magmatic centres. The slab geometry represented in Figure 3.4 provides useful elements to understand the geodynamic context in which these magmatic sources are located.

Historically, this area has been divided into Magmatic Provinces based on magma compositions. From the geodynamic point of view, magmatism can be divided according to the position of the sources in the tectonic context, but there is not always a clear correlation with magma composition (*Peccerillo, 2020*).

From the slab reconstruction of Figure 3.4, it is possible to distinguish:

* classic volcanic arc sources located above the Ionian slab, as the Aeolian Arc;
* sources located above the Apennine slab, which includes Tethys oceanic lithosphere, with its transition to Adriatic continental lithosphere, as the Roman Province;
* oceanic type (MORB) sources, as the Vavilov and Marsili;
* sources probably placed in the asthenosphere of the lower plate, as the Vulture volcano and the Campanian province; these sources are located near the vertical projection of the STEP faults and are contaminated by the adjacent slab segment, in a rearward position.

The best example of the last source is represented by the magmatism of the Campanian plane, placed on the vertical projection of a particular asthenospheric window.

All the magmatism in Central Italy (from Tuscany to the Aeolian Islands) shows geochemical indications of source regions metasomatized by subduction processes (fluids and subducted terrigenous to marly sediments), superimposed on original mantle components that vary from Mid-Ocean Ridge Basalts (MORB)-like to Ocean Island Basalt (OIB)-like; examples of these two compositions are well represented by the Etna OIB and the Tyrrhenian sea MORB

These original mantle components result to be modified by subduction-related processes. This can be deduced from fractionated incompatible element patterns (Fig. 5.15 in *Peccerillo, 2020*) with positive spikes of Large-ion lithophile element (LILE) (Cs, Rb, Ba, K, Pb, LREE) and negative anomalies of high field strength elements (HFSE) (eg. Nb, Ta, Ti).

Moreover, LILE are easily transferred by subduction-related fluids and give indications on the nature and degree of enrichment processes that had different nature and much higher intensity for Roman than for Campania volcanoes. Various amounts of siliceous and carbonate sediments are also believed to be involved in the mantle metasomatism.

Due to their transferability, LILE cannot be used to investigate the pre-metasomatic mantle composition. Conversely, HFSE are known to be relatively immobile during arc metasomatism and their abundances and ratios furnish information on pristine mantle compositions.

In particular, in the Vulture, Stromboli and Campania volcanoes their values indicate a significant contribution of OIB-type components, whereas MORB-type components dominated beneath the Roman Province; Ernici-Roccamonfina falls between these two compositions.

Finally, it is important to specify that the magmatism of the Tuscan province is much older than that associated with the Adriatic subduction. From a compositional point of view, it is part of a

collisional context with substantial involvement of continental basement in the subduction. The magmatism associated with the Apennine subduction forms, instead, in a context of slab-retreat in which the continental collision is not contemplated. The magmatism of the Tuscan province is located only in the area in front of the Alpine Corsica. From the available data, *Pierantoni et al (2020)* believe that the Apennine slab only created the conditions for the melting of the asthenosphere, already contaminated by the Alpine Corsica continental collision, that had a subduction with an eastward polarity during the Upper Oligocene (*Turco et al., 2012*).

Ch.3.5 - References

Bigi, G.; Cosentino, D.; Parotto, M.; Sartori, R. Scandone, P. 1991. Structural model of Italy scale 1:500.000, sheet 5.In C.N.R.; Progetto Finalizzato Geodinamica. Structural Model of Italy, SELCA: Firenze, Italy.

Cinque, A., Patacca, E., Scandone, P., Tozzi, M., 1993. Quaternary kinematic evolution of the Southern Apennine. Relationships between surface geological features and deep lithospheric structures. Sec. Issue on the Workshop: "Modes of crustal deformation: from the brittle upper crust through detachments to the ductile lower crust" (Erice, 18-24 November 1991), Ann. Geofis., 36, pp. 249-260.

Dewey, J.F. Plate tectonics. Rev. Geophys. 1975, 13, pp. 326– 332, doi:10.1029/RG013i003p00326.

Di Stefano, R.; Kissling, E.; Chiarabba, C.; Amato, A.; Giardini, D. 2009. Shallow subduction beneath Italy: Three-dimensional images of the Adriatic-European-Tyrrhenian lithosphere system based on high-quality P wave arrival times. J. Geophys. Res., 114, doi:10.1029/2008JB005641.

Doglioni, C. 1991. A proposal for the kinematic modelling of W-dipping subductions-possible applications to the Tyrrhenian-Apennines system. Terra Nova, 3(4), pp. 423-434.

Faccenna, C.; Davy, P.; Brun, J.-P.; Funiciello, R.; Giardini, D.; Mattei, M.; Nalpas, T. 1996. The dynamics of back-arc extensions: An experimental approach to the opening of the Tyrrhenian Sea. Geophys. J. Int., 126, pp. 781–795.

Galadini, F., Messina, P., Giaccio, B., & Sposato, A. 2003. Early uplift history of the Abruzzi Apennines (central Italy): available geomorphological constraints. Quaternary International, 101, pp. 125-135.

Giacomuzzi, G.; Chiarabba, C.; De Gori, P. 2011. Linking the Alps and Apennines subduction systems: New constraints revealed by high-resolution teleseismic tomography. Earth Planet. Sci. Lett., 301, pp.531–543.

Malinverno, A.; Ryan, W.B.F. 1986. Extension in the Tyrrhenian Sea and shortening in the Apennines as result of arc migration driven by sinking of the lithosphere. Tectonics, 5, pp. 227–245.

Montuori, C.; Cimini, G.B.; Favali, P. 2007. Teleseismic tomography of the southern Tyrrhenian subduction zone: New results from seafloor and land recordings. J. Geophys. Res., 112, doi:10.1029/2005JB004114.

Neri, G.; Barberi, G.; Oliva, G.; Orecchio, B. 2005. Spatial variations of seismogenic stress orientations in Sicily, south Italy. Phys. Earth Planet. Inter., 148, pp. 175–191.

Peccerillo, A. 2020. Campania volcanoes: petrology, geochemistry, and geodynamic significance. In Vesuvius, Campi Flegrei, and Campanian Volcanism, 1st ed.; De vivo B., Belkin, H.E., Rolandi, G., Eds.; Elsevier Inc.: Amsterdam, The Netherlands.

Pierantoni, P.P.; Macchiavelli, C.; Penza, G.; Schettino, A.; Turco, E. 2020. Kinematics of the Tyrrhenian-Apennine system and implications for the origin of the Campanian magmatism. In Vesuvius, Campi Flegrei, and Campanian Volcanism, 1st ed.; De vivo B., Belkin, H.E., Rolandi, G., Eds.; Elsevier Inc.: Amsterdam, The Netherlands; pp. 520.

Pondrelli, S.; Piromallo, C.; Serpelloni, E. 2004. Convergence vs. retreat in Southern Tyrrhenian Sea: Insights from kinematics. Geophys. Res. Lett., 31, doi:10.1029/2003GL019223.

Royden, L.; Patacca, E.; Scandone, P. 1987. Segmentation and configuration of subducted lithosphere in Italy: An important control on thrust-belt and foredeep-basin evolution. Geology; 15,pp. 714–717, doi:10.1130/0091–7613(1987)15<714:SACOSL>2.0.CO;2.

Schettino, A.; Turco, E. 2011. Tectonic history of the western Tethys since the Late Triassic. GSA Bull., 123, pp. 89–105, doi:10.1130/B30064.1.

Turco, E.; Schettino, A.; Macchiavelli, C.; Pierantoni, P.P. 2013. A plate kinematics approach to the tectonic analysis of the Tyr-rhenian-Apennines System. Geophys. Res. Abstr., 29, pp. 187–190.

Turco, E.; Macchiavelli, C.; Penza, G.; Schettino, A.; Pierantoni, P.P. 2021. Kinematics of Deformable Blocks: Application to the Opening of the Tyrrhenian Basin and the Formation of the Apennine Chain. Geosciences, 11, 177. https://doi.org/10.3390/geosciences11040177.

Chapter 4 - Tectonic escape of Sicily microplate

Ch.4.1 - Introduction

Sicily is in the center of an area where complex geodynamic processes work together; these are the Tyrrhenian-Apennine System evolution, the Adriatic-Ionian slab subduction and the Africa-Europe collision. Some of these processes have been described in the previous chapters. In particular, the complex geometric configuration of the Adriatic-Ionian slab and the change in the direction of the Ionian slab retreat, along a STEP fault first E-W and then NW-SE and N-S oriented (Figs. 3.3-3.4), led me to think to an involvement of Sicily in a process of escape toward East/South-East.

As long the Ionian slab tearing runs along the Taormina line (STEP fault letter e in Fig. 3.4), the contrast between Sicily and the Calabrian sector allows only a small clockwise rotation. When the tearing moves at the tip of the Malta Escarpment, which divides the African continental margin from the Ionian lithosphere, the direction of the slab tear changes. This change is reflected on the upper plate, where two new structures are activated. From now on, the Calabrian accretionary prism is drawn to the deepest part of the Ionian sea; the eastern border of Sicily loses its contrast and is thus able to move toward south-east. This process also affects a part of the Northern Tunisian continent and its offshore.

The existence in the Sicily channel of deep troughs and a Quaternary volcanic activity have been associated to a rift zone (e.g. “Sicily rift zone” in Finetti, 1984; Cello, 1987; Argnani, 1990; “Pantelleria-Rift” in Reuther & Eisbacher, 1985) or to a wrench zone (“Medina Wrench zone” in Jongsma et al., 1985, 1987).

Aside from the many interpretations concerning the causes and the mechanism of formation of the channel, this part of the Pelagian basin has been deformed since Late Triassic. Until Lower Jurassic, a system of rift, ENE-WSW oriented, caused extension in the Pelagian basin and along the Malta Escarpment, separating the block Tunisia-Sicily from Africa. This block moved along the Gafsa fault with a left-lateral kinematic relative to Northwest Africa, determining a partitioning of the extension structures between the Pelagian basin and the Malta Escarpment. Since the Lower Jurassic the Tunisian-Sicily block moved with Africa (Fig. 3.1, a-c; *Schettino & Turco, 2011*).

According to *Jongsma et al. (1985, 1987)*, only after Miocene the Pelagian area was divided in two sectors: a platform, located south of the Tunisian Plateau and Medina Bank, attached to Africa and a Sicilian-Calabrian block moving toward east/southeast respect to Africa, with a movement similar but opposite to that of the Aegean microplate. This block includes southern Sicily and part of the Ionian Basin and is called "Messina Plate"; to the south it is bounded by the Medina Wrench Zone extending from the Sicily channel to the Medina ridge.
Also *Cello (1987)* suggests a separation of the Sicilian microplate from Northern Africa since Pliocene times, starting from the northern sector of the block and propagating to the sountheastern end of the "Strait of Sicily Rift Zone".

Other works suggest a motion of Sicily (or part of it) relative to Africa, oriented NE (*Goes et al., 2004; Van Hinsbergen et al., 2020; Milia et al., 2021;* and reference therein) or NW (*Catalano et al., 2009*), accommodated by rifting in the Sicily channel, or the development and opening of a large-scale pull-apart structure, without identifying a Sicilian block separated from Africa.
Recent works based on GPS velocities and elastic block models divide Sicily in three smaller tectonic blocks (southeastern, central and northeastern Sicily) rotating clockwise with respect to Eurasia and moving independently from Africa (Nubia) (*Mastrolembo Ventura et al., 2009, 2014; Serpelloni et al., 2007, 2010*).

It was not possible to compare or use the data from the aforementioned works as the three criteria for plate kinematics are not strictly respected: identification of plate boundaries, determination of rotation pole and angle. Indeed, some of these works determine rotation poles without identifying the plate boundaries, thus making it impossible to control what happens at the margins with the other plates involved in the kinematic; or they assign velocity vectors to a plate without specifying a pole and a rotation angle; others, more rigorous from the kinematic point of view, use data (e.g. GPS data) that refer to a period of time that is too short to be considered valid for millions of years.

The kinematic model proposed here considers Sicily as a microplate independent from Africa since 4.5 Ma ago. The boundaries with the main plates (Europe, Africa, Calabria) involved in the kinematic model have been traced along old or obvious discontinuities, sometimes already known in literature but with a different meaning. The model implies the identification of another new microplate that includes northern Tunisia. Euler poles of rotation for both microplates have been found and used to update the kinematic model of *Turco et al. (2021).*

Ch.4.2 - Geological setting

Ch.4.2.1 – Sicily

On land Sicilian successions are Permian to Quaternary in age and can be summarized in: "European"/Calabrian, "Tethyan" and "African" domains. These are derived from the deformation of the Meso-Cenozoic basins and platform carbonate successions that bordered the African continental margin. From the NE to the SW the tectonic units characterize the internal and external chain complex of the Sicily-Maghrebian fold and thrust belt.

The Calabrian element is represented by the Peloritani units (Fig. 4.1). These are formed by pre-Triassic low-grade metamorphic rock with middle to high grade crystalline rocks and Meso-Cenozoic sedimentary covers on top. Capo d'Orlando formation, a Upper Rupelian and Lower Burdigalian (*Turco et al., 2012; Weltje, 1992* and reference therein) detrital sequence of breccias and conglomerates, covered by sandstones fining upwards and laterally to mudstones, overlies the Peloritani thrust system.

The "Tethyan" rock units are characterized by rock bodies belonging to the Sicilide domain (*Ogniben, 1960*). This is composed of a stack of allochthonous units, interpreted by several authors (*Ogniben, 1985; Roure et al., 1990; Monaco and Tortorici, 1995*) as the remnant of an accretionary wedge related to Neo-Tethys oceanic crust subduction. The Meso-Cenozoic succession is characterized by basinal carbonates and sandy mudstones (Monte Soro sandstones and clays, Varicoloured clays, Troina sandstones and Polizzi Fm.) and terrigenous turbiditic successions and tuffitic marlstones (Tufiti di Tusa and Reitano Fm.) (*Basilone, 2015*). The Sicilide units crop out in northern and eastern Sicily (Fig. 4.1).

The "African" element includes Meso-Cenozoic sedimentary successions of deep-water carbonates and cherts (Imerese and Sicanian basins), located between carbonate platforms: Trapanese, Saccense, Pre-Panormide, Panormide and Hyblean-Pelagian platforms. These units were deformed during the Neogene and are now exposed within the Sicily fold and thrust belt.

The Imerese succession crops out in the Madonie, Sicani and "Palermo Mountains" (Monti di Palermo) (Fig. 4.1) and consists of Triassic (Carnian) to Oligocene thin-bedded limestones and bedded cherts, with Jurassic-Eocene debris flows generated by carbonate platform. Locally, siliciclastic deposits (marly shales, turbiditic sandstones and quartzarenites) of the Upper

Oligocene-Lower Miocene unconformably cover the carbonate succession. According to the tectonic stack visible in the Madonie Mountains, during the Middle Miocene the Panormide unit was superimposed on the Imerese unit (*Barreca and Monaco, 2013*).

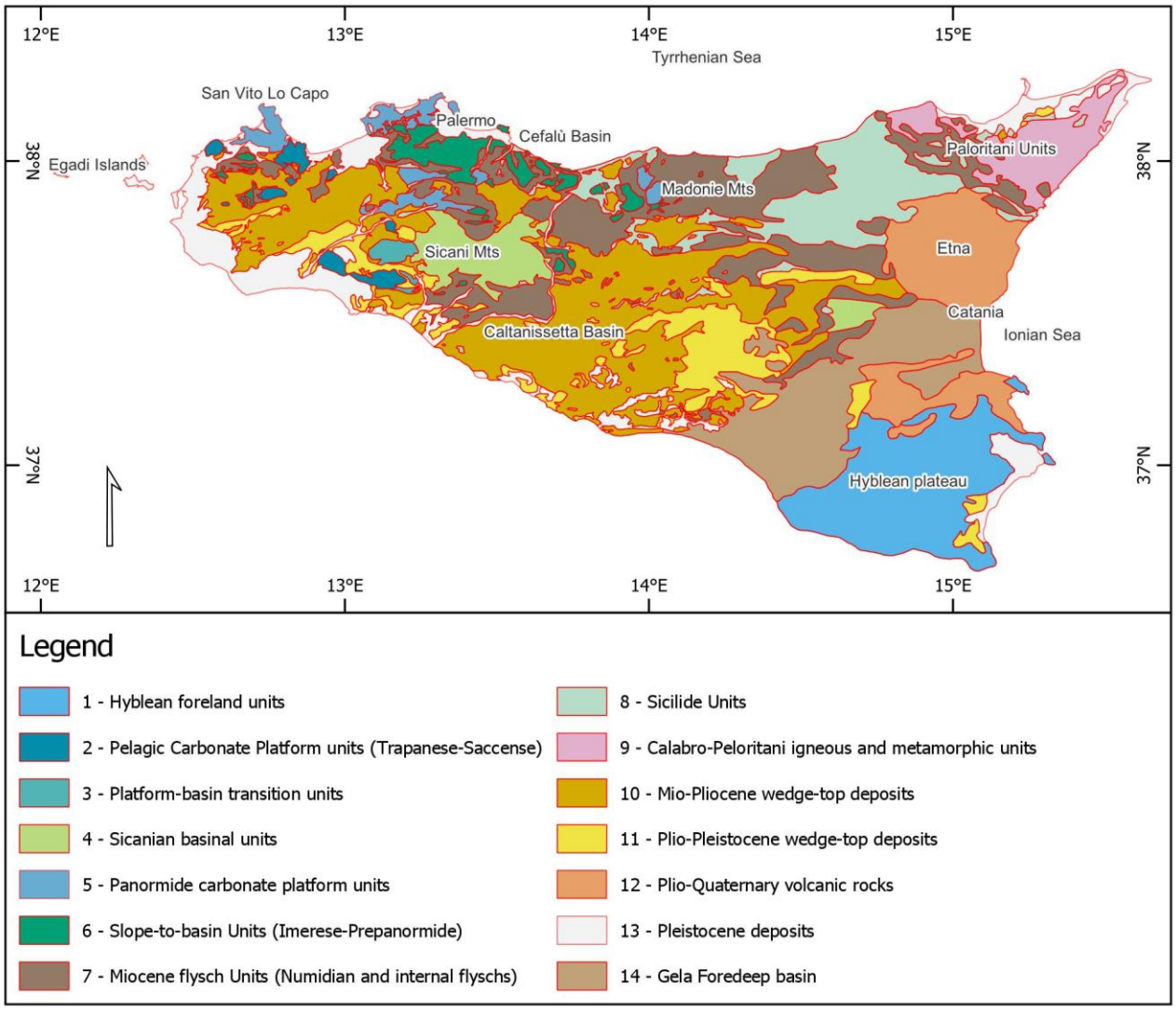

Figure 4.1 – Geological map of Sicily; modified after *Basilone (2012).*

The Sicanian units derive from the deformation of Paleozoic/Mesozoic-Tertiary basinal deposits of the Sicano domain (*Catalano and D'Argenio, 1978*). These units crop out in the homonymous mountains and consist of deep-water Upper Triassic (Carnian) to lower Miocene carbonates, followed by Middle Miocene clastic carbonates and marls. The old substratum of the Sicanian succession is composed of Lower Permian to Middle Triassic deep water clastic and carbonate deposits, with shallow water carbonate olistoliths. In the Sicanian succession is possible to recognize the same Middle Upper Triassic marls and cherty limestones typical of the Imerese

sequence but, the Jurassic-Eocene redeposited shallow water carbonates and the Upper Oligocene-Lower Miocene Numidian-type strata are missing.
The Panormide sequence, from bottom to top, is made of: Late Triassic marls, Upper Triassic (Norian) to Middle Cretaceous reef carbonates, Upper Cretaceous–Eocene wackestones and red marls, Oligocene fine-grained marls, quartzarenites and calcarenites, and Late Oligocene–Early Miocene Numidian flysch. The Panormide type successions is observable in Capo San Vito Peninsula and in the Palermo and Madonie Mountains (*Abate et al., 1991*) (Fig. 4.1), in boreholes in the Nebrodi Mountains (*Bianchi et al., 1987*) and in the Tyrrhenian Sea (*D'Argenio, 1999*).

The Trapanese-Saccense type successions outcrop in Western Sicily (Fig. 4.1). These are formed by Upper Triassic-Lower Jurassic carbonate platform dolomites and limestones, followed by Jurassic-Lower Oligocene pelagic platform deposits. Only in the Trapanese succession the Meso-Cenozoic deposits are unconformably covered by Upper Oligocene-Lower Miocene resedimented biocalcarenites and by open shelf to coastal, glauconitic sandstones.

The Hyblean-Pelagian platform succession crops out in the Sciacca area of western Sicily, and in the Hyblean plateau in southeastern Sicily (Fig. 4.1). A 25- to 35-km-thick continental crust is covered by a Meso–Cenozoic shallow-water to basin carbonate sequence, 7-8 km-thick, with several intercalations of volcanic products (Bianchi et al., 1987; Grasso et al., 2004).
From the Hyblean platform in southern Sicily to the Sicily Channel the Late Pliocene–Pleistocene NW-dipping Gela foredeep basin developed in between the chain and the foreland area, represented by the Hyblean plateau (Pelagian block). The basin is partially buried by the Gela Nappe, the frontal termination of the External Sicilian thrust system, and is filled by Plio-Pleistocene pelagic marly limestones of the Trubi Formation, followed by Ponte Dirillo clays, unconformably covered by turbidite sands and clays (*Ghielmi et al., 2012*).

A wide axial depression within the chain units, characterized by a strong negative Bouguer anomaly (more than -100 mGal) and known as the Caltanissetta basin (Fig. 4.1), represents an accumulation of Late Miocene-Quaternary sediments in central Sicily. Above a deformed substratum of Cretaceous to Oligocene shaly and varicoloured clays and Late Oligocene-Late Burdigalian Numidian Flysch turbidites, lies the Terravecchia Formation (Upper Tortonian-Lower Messinian) in the northern sector and the Licata Formation (Middle to Late Miocene) in the southern sector. Two major Messinian evaporitic cycles, the Trubi marly limestone, Enna marls and Capodarso calcarenites follow the deformed substratum. The basin is bounded to the south-

east by the Pleistocene thrust front of the Sicilian chain (Grasso and Butler, 1991), of which it represented the foredeep from the upper Miocene.

The Sicilian-Maghrebian chain is the major tectonic feature that characterizes Sicily and its nearest southwestern offshore ("External chain" in Fig. 4.2). The chain is Lower Miocene (Burdigalian)-Lower Pleistocene in age and is the result of the stacking of the basin and platform units, described above, on the Hyblean platform, in response to the Africa-Europe convergence *(Dewey et al., 1989; Oldow et al., 1990; Catalano et al., 1996, 2000, 2012; Bello et al., 2000; Avellone et al., 2010; Schettino and Turco, 2011*).

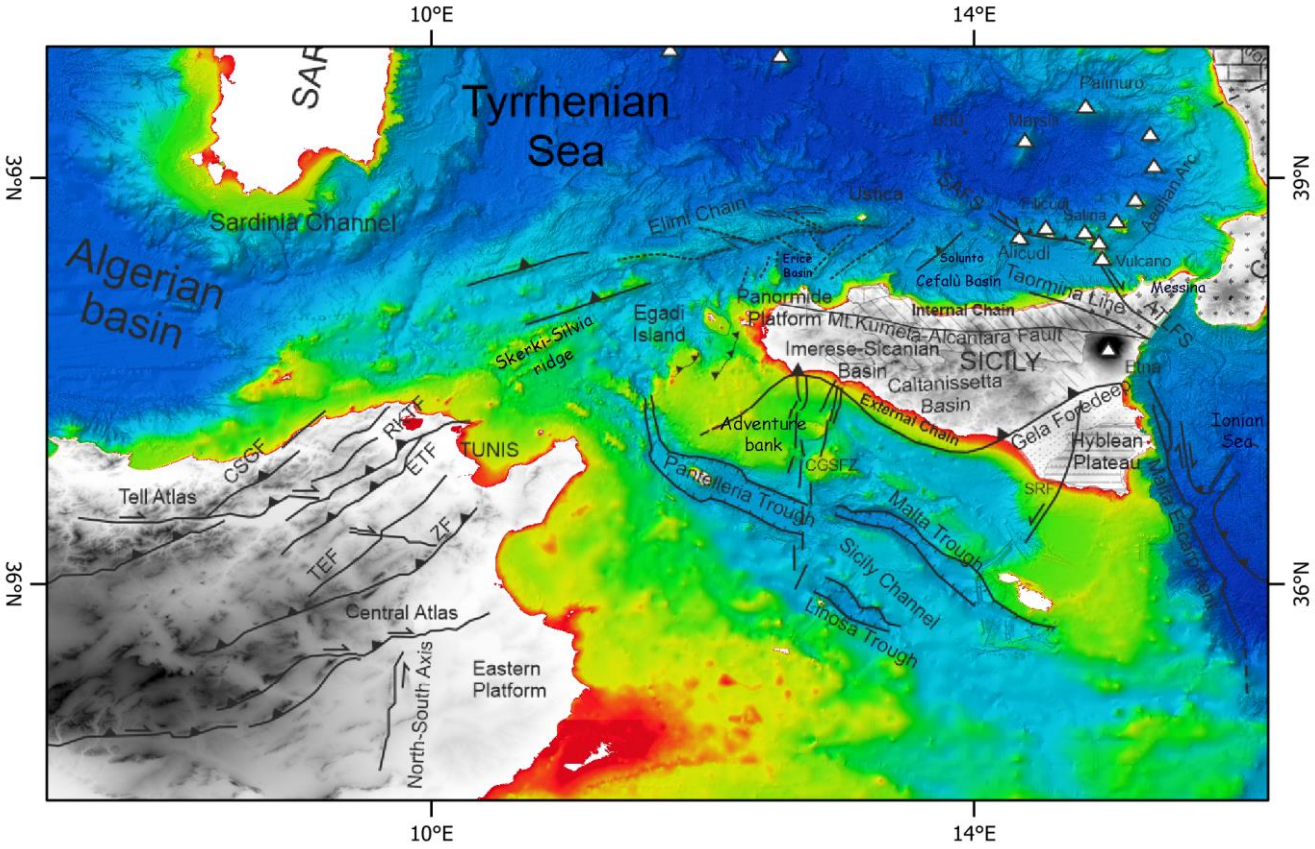

Figure 4.2 - Location map of the main structures and morpho-structures cited in Chapter 4.2. ATLFS: Aeolian-Tindari-Letojanni Fault System; CGSFZ: Capo Granitola-Sciacca Fault Zone; SAFS: Sisifo-Alicudi Fault System; SRF: Scicli-Ragusa Fault; CSGF: Cap Serrat-Gardimaou Fault; ETF: El Alia-Teboursouk Fault; RKTF: Ras El Kouran-Thibar Fault; TEF: Tunis Elles Fault; ZF: Zaghouan Fault. The bathymetry is after: EMODnet Bathymetry Consortium (2020). EMODnet Digital Bathymetry (DTM). DEM for Sicily and Africa are respectively after Tarquini et al. (2007) and Verdin (2017).

Northern Sicily is characterized by many morphostructures (Fig. 4.2) that in general are in continuity with the off-shore area, characterized by the alternation of structural highs (Banco Apologize, St. Vito High, Solunto High) interposed by deep sedimentary Plio-Pleistocene basins (Trapani, Erice, Castellammare and Cefalù Basins). Along the coastal area the principal

morphostructural highs are closely related to NW-SE trending strike-slip faults: Trapani, San Vito and Palermo faults (*Finetti and Del Ben, 1986 Gueguen et al., 2002,* and reference therein).

Toward the hinterland, a major E-W trending structure, known as Mt. Kumeta-Alcantara fault (*Ruggieri, 1966; Ghisetti and Vezzani, 1984*, and references therein) extends from the Trapani Mts. to Mt. Etna for over 300 km (Fig. 4.2). This fault has a general right-lateral kinematic character (*Ghisetti and Vezzani, 1984*) and is referred to the Early Pliocene-Recent interval *(Boccaletti and Dainelli, 1982; Ghisetti and Vezzani, 1984; Finetti and Del Ben, 1986; Nigro et al., 2000*).

Another important tectonic feature, the "Taormina line", extends from the Tyrrhenian to the Ionian coasts of Sicily, with a NW-SE direction (Fig. 4.2). This NNE dipping thrust is considered to be the contact between the Calabrian domain and the Sicilian–Maghrebian belt (e.g *Bonardi et al., 2001; Somma, 2006*); characterized by right-lateral slip (S*candone et al., 1974; Amodio Morelli et al., 1976; Lentini et al., 1994*).

Finally, the Hyblean Plateau is cut by a major N–S trending shear zone, extending for 70 km from the frontal thrust belt of the Appennine–Maghrebian Chain to the southern offshore, known as Scicli line or Scicli–Ragusa Fault System (*Ghisetti and Vezzani, 1980; Grasso and Reuther, 1988*) (Fig. 4.2). The system includes three N-S trending main fault segments and en-echelon second-order structures with NE–SW direction (*Catalano et al., 2010*). Restraining and releasing bends between the en-echelon segments of the fault system are evidence of a prolonged right-lateral strike slip movement (e.g. *Catalano et al., 2008; Musumeci et al., 2014)*, reactivated by left-lateral motions in recent times (*Bousquet and Lanzafame, 2004; Catalano et al., 2006*). Recent morphological features of the Hyblean Plateau are NE-SW and NW-SE oriented troughs (Scordia–Lentini Graben, Marina di Ragusa Basin, Augusta–Siracusa and Floridia basins) controlled by impressive normal fault segments (*Musumeci et al., 2014*), partially reversed (*Bousquet and Lanzafame, 2004; Catalano et al., 2006*).

Ch.4.2.2 - North and North-Western Sicily offshore

Elimi Chain

The SW–NE-trending Elimi chain (also known as Ustica ridge) is an arc-shaped submarine morphostructure that extends from the Sardinia Channel (southwestern Tyrrhenian sea) to the Ustica Island (Fig. 4.2). The Elimi chain area includes several seamounts, between them the Aceste, Drepano and Anchise seamounts are the most prominent. The emplacement of the Aceste volcano around 5 Ma ago (Serri et al., 2001; Rovere & Wurtz, 2015) and the magmatism progression

towards east is attributed to the E-SE Ionian slab migration. Oceanic Island-type basalts characterize the Aceste and Drepano seamounts while calcalkaline and shoshonite magmas are found in the Anchise Seamount *(Serri et al., 2001*), probably by contamination of the magma chamber by melts related to the slab subduction. Finally, in the middle-Pleistocene the Ustica island started to form (*Argnani, 2009*) and is characterized by Na-alkaline volcanism (*Calanchi et al., 1984; Trua et al., 2004*). The island is the only part of the Elimi chain above sea level; its uplifting is attributed by *Palmiotto et al. (2017)* to vertical movement of a lithospheric block.

The entire ridge is associated with a prominent magnetic anomaly and bordered by basins.
The sediment thickness ranges from < 100 m to >1500m: low values are detected along the eastern part of the Elimi chain, while high values occur within the Drepano and Erice basins (*Loreto et al., 2021*).
Both the ridge and the seafloor in the Elimi chain area are characterized by morphological features E-W, NW–SE and NE–SW oriented (Fig. 4.2). NE-SW and NW-SE trending normal faults, widespread within the sedimentary basins and bounding the seamounts, were probably active during the Plio-Pleistocene (*Palmiotto & Loreto, 2019*). Inversion structures as positive flower structures, anticlines with single or double vergence and inverted fault are detected within sediments covering the ridge (*Loreto et al., 2021*) and filling the basins (Fig. 4.3).
A North-dipping, South-vergent regional thrust, traceable at depth and referred as the Drepano Thrust front, has been recognized by previous studies based on seismic profiles interpretation (*Beccaluva et al., 1986; Compagnoni et al., 1989; Sulli, 2000; Pepe et al., 2003, 2005; Billi et al., 2007*). The thrust is considered to be Late Miocene in age, reactivated after the Messinian with involvement of the basement. It has been interpreted as the tectonic contact between the crystalline units of the Kabilian-Peloritan-Calabrian belt and the underlying Meso-Cenozoic sedimentary rocks (*Catalano et al., 1996*) of the Sicilian-Maghrebian belt. On land, the Drepano thrust front connects the Elimi chain to the Peloritani Mountains (*Pepe et al., 2005*).

The superposition of extensional to compressional regimes, inferable from the structures described above, is due to the absolute N/NE motion of the African plate and to the southeastward retreat of the Ionian slab. The deformation locally at the seafloor, the distribution of earthquakes and the focal mechanisms in the region, showing compressive and/or transcurrent tectonics (*Presti et al., 2013; Soumaya et al., 2015*) (Fig. 4.6A), and the strain field derived by GPS

measurements (*Serpelloni et al., 2005; Cuffaro et al., 2011*), are all in agreement with a recent activity of the compressive phase.

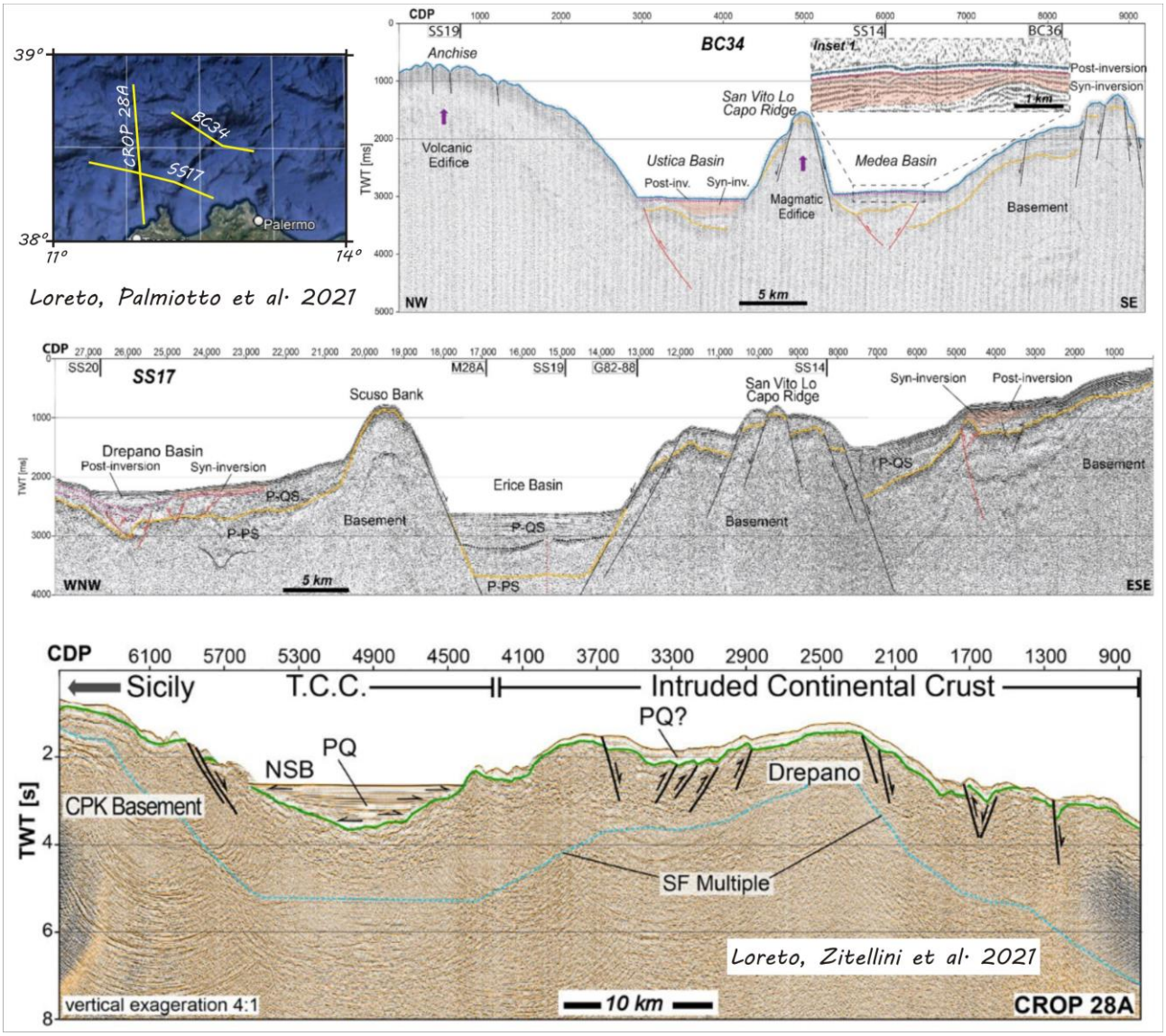

Figure 4.3 – Seismic sections showing inversion structures within sediments covering the ridge and filling the basins. Seismic line traces are the yellow lines in the insert (top-left). BC-34 and SS17 are after *Loreto, Palmiotto et al. (2021)*; CROP-28A is after *Loreto, Zitellini et al. (2021)*. Refer to the original papers for the legend.

Egadi area and Adventure Bank

The north-western Sicily offshore is characterized by a continental shelf incised by several canyons, and includes the Egadi shelf, with the Egadi Archipelago and the Adventure bank (or Adventure Plateau). The Sicily strait (or Sicily channel) divides the Sicily offshore from the Tunisian Platform; west of the Egadi valley the platform is interrupted by a NE oriented morphological high (Skerki-Silvia Bank) (Fig. 4.2).

The geological setting of the area is the result of a tectonic process that produced the ESE–verging Sicilian fold and thrust belt and its tectonic stack with a thickness of 10 km (*Sulli, 2000; Gasparo Morticelli et al., 2016; Lo Presti et al. 2019*); these directions are compatible with the direction of Africa-Sicily convergence during late Miocene.

The Egadi archipelago includes three major islands: Favignana, Levanzo and Marettimo; and two minors: Formica and Maraone. The archipelago is made up of Trias to Eocene, (*Milia et al., 2021*) carbonate successions and by terrigenous Oligocene to Miocene deposits, unconformably covered by Middle-Late Pliocene marls and shale, followed by Early Pleistocene grainstones and by Late Pleistocene calcarenites and biorudites (*Catalano et al., 1996; Incandela, 1996; Abate et al., 1997; Lo Presti et al., 2019; Pepe et al., 2018*). Pleistocene deposits are widespread along the whole island and locally appear in Levanzo and Marettimo.

The Adventure bank is a Mesozoic–Cenozoic shallow relatively flat carbonate platform; its southern limit is defined by the NW-SE-trending Pantelleria graben (Fig. 4.2, 4.5). The water depths rarely exceed 100 m and rise up to less than 10 m below sea level in the morphological highs. These elevations are Miocene sedimentary banks (Talbot, Ante-Talbot, Panope, Nereo and Pantelleria Vecchia) and submarine Early-Pliocene volcanic edifices (Galatea, Anfitrite and Tetide). The sedimentary succession is mostly composed of Triassic-Eocene carbonate units and Oligocene–Quaternary siliciclastic deposits and characterized by the occurrence of several hiatuses (*Civile et al., 2016* and reference therein).

Several wells (Tania and Narciso-Noemi-Ninfea-Nada) drilled in the Egadi and Adventure areas show thrust sheets emplaced during Late Miocene times (*Milia et al., 2021* and reference therein). Between them, the NNE-SSW-trending, SE-vergent Egadi thrust and the NE-SW-trending Adventure thrust fronts are part of the Egadi thrust system, located west of the Adventure Bank and the Adventure thrust system, extending on the eastern side of the Adventure bank in the offshore of Mazara del Vallo (Fig. 4.5). The Egadi thrust fault separates two paleogeographic domains: the Pre-Panormide and the Trapanese-Saccense, and it is covered by a very thick prograding unit Tortonian-Early Messinian in age (Terravecchia Formation). The Adventure thrust fault reactivated an inherited Mesozoic crustal boundary that separated Trapanese domain from the Saccense domain; during the Miocene it separated proximal from distal foredeep facies in the Terravecchia formation (*Argnani, 1993*).

In the northern and north-western offshore of Sicily, NW-SE, NNW-SSE, N-S, NNE-SSW, and NE-SW faults trends have been recognized (*Milia et al., 2021*). NW-SE, N-S and NE-SW faults bound numerous Pliocene sedimentary basins with two main orientations: NW-SE elongated basins are located south of the Egadi Islands and filled by >2000 m of sedimentary deposits; while north of the islands the basins are N-S elongated. The westernmost basin, calibrated by *Milia et al. (2021)* with the Tania well, is lower Pliocene in age; based on different onset of the basins fill, the same authors suggest a rejuvenation of the basins toward est, from lower Pliocene to lower Pleistocene. Similar basins have been observed by *Camafort et al. (2020)* between the northern Tunisian offshore and the Bizerte valley.

In the Adventure bank the late Miocene compressional deformation is highlighted by ESE-verging thrusts and back-thrusts (*Catalano et al. 2000*); a N-S trending lithospheric transfer zone (*Civile et al., 2016* and reference therein), with a predominantly strike-slip motion and several magmatic manifestations, controls the eastern boundary of the bank.

Along the Skerki Bank area, a stack composed of Numidian Flysch slices superimposed on Jurassic-Eocene deep-water marly carbonates overthrusts Triassic evaporites and shallow-water carbonate (*Tricart et al., 1993; Catalano et al., 1996; Milia et al., 2021*).

Aeolian Region

The Aeolian Islands volcanic arc is part of the Tyrrhenian back-arc basin. Most of the Aeolian volcanoes are located at the footwall of the faults separating the Marsili basin oceanic crust from the 15-20 Km thick continental crust of the Calabrian Arc (*Calanchi et al., 1995; Pepe et al., 2000; De Astis, 2003*).

According to *De Astis et al. (2003)*, three volcanological and structural sectors can be recognized: the western sector includes Glauco, Sisifo, Enarete and Eolo seamounts and Alicudi and Filicudi Islands; Salina, Lipari and Vulcano belong to the central sector; Panarea and Stromboli Islands and Lametini, Alcione and Palinuro seamounts are in the eastern sector (Fig. 4.2). The age of the volcanic activity ranges from 1.3 Ma to the present (*Gillot, 1987; Santo and Clark, 1994*) and propagated from the western to the eastern sectors, starting as a calcalkaline to HK-calcalkaline and changing into shoshonitic and potassium alkaline in the eastern and central sectors. Fumaroles, hot springs and shallow seismicity characterize the younger sectors where some of the islands are still active (Lipari, Vulcano, Panarea, Salina, Stromboli) (*Barberi et al., 1974; Keller,*

1980, 1982; Gamberi et al., 1997; Argnani et al., 2007). Isotopic data summarized by *Peccerillo* (2020, and references therein) suggest a different composition/origin between eastern Aeolian islands (Stromboli) and western and central Aeolian islands: the first are similar to Campi Flegrei-Vesuvius while the latter are similar to the Etna volcano (see Ch.3.4).

Many interpretations have been suggested to explain the formation of the Aeolian Islands:

- as a volcanic arc related to the active subduction of the Ionian slab beneath the Calabrian Arc (e.g., *Barberi et al., 1974; Beccaluva et al., 1982, 1985; Ferrari and Manetti, 1993*),
- associated to slab tearing along a STEP fault, the Tindari-Letojanni fault (De Astis et al., 2003; Cocchi et al., 2017) or;
- according to some authors (*Westaway, 1993; Hippolite et al., 1994; Milano et al., 1994; Carminati et al., 1998*), due to the post-subduction extensional tectonics, started around 1 Ma ago, that affected the Calabrian Arc and the Apennine chain; this, caused an heat flow anomaly probably related to the slab detachment beneath the Calabrian Arc and to the southeastern migration of the Tyrrhenian Sea opening;
- *Gvirtzman and Nur (1999, 2001)* suggest that they are formed by mantle upwelling, caused by the Ionian slab roll-back about 1-0.7 Ma ago and reflected also in the recent uplift of the forearc region.

Three main fault systems define the structural setting of the Aeolian Islands (e.g., C*alanchi et al., 1995; Neri et al., 1996; Lanzafame and Bousquet, 1997; Tibaldi, 2001; Bonaccorso, 2002*): the WNW-ESE trending "Sisifo-Alicudi'' system, the NNW-SSE trending ''Aeolian-Tindari-Letojanni" system and NE-SW trending system in the Stromboli and Panarea Islands.
In particular, the Aeolian-Tindari-Letojanni fault has been considered as a major tectonic element, active since lower-middle Pleistocene, extending from the Volcano island to the eastern coast of Sicily. (*Ghisetti, 1979; Lanzafame and Bousquet, 1997; Billi et al., 2006; Barreca, 2014; Cultrera et al., 2016, 2017*). Field, geodetic and seismological data allow to recognize a dextral transtension in the offshore northern branch (e.g. *Barreca et al., 2014; Cultrera et al., 2016, 2017*) and on land in the north-eastern Sicily branch of the Aeolian–Tindari–Letojanni fault system (e.g. *Neri et al., 2005; Billi et al., 2006; Mattia et al., 2008; Palano et al., 2012; De Guidi et al., 2013*); and a dextral strike-slip motion in the Sisifo–Alicudi fault system, with transtensive and transpressive sectors (Fig. 4.16).

Recent and still active extensional tectonic phase occurs in the north-eastern sector of the Aeolian Islands where Pleistocene elongated sedimentary basins (e.g. Paola and Gioia basin) formed. GPS-derived strain-rate axes (*Argnani et al., 2007; Serpelloni et al., 2007; Argnani, 2009*) and stress field obtained from focal mechanisms (e.g., *Neri et al., 2005*) confirm this recent deformation.

Ch.4.2.3 - Northern Tunisia

Northern continental Tunisia is mostly composed of Mesozoic and Cenozoic sedimentary rocks (*Ben Haj Ali et al., 1985*) and includes the E-W trending nappe tectonics of the northern Tell Atlas, the Central Atlas, characterized by NE-SW-striking thrust faults and NNW- SSE-trending Neogene and Quaternary grabens and the passive continental margin of the Eastern Platform (Sahel) (Fig. 4.2). These geological domains are part of the Maghrebide fold and thrust belt, affected by Plio-Quaternary N-S to NNE-SSW trending shortening (*Chihi, 1992; Rebaï et al., 1992; Ghribi and Bouaziz, 2010; Bahrouni et al., 2014*).

A N-S morphotectonic structure called North-South Axis extends for 200 Km, from the Zaghouan ridge in the north to the Chotts range in the south (Fig. 4.2) and resulted from the reactivation of an inherited basement fault. (*Boccaletti et al., 1990; Burollet, 1991; Rigane and Gourmelen, 2011*). To the north, the NE-SW trending, SE-vergent Zaghouan thrust belt extends for over 80 km (Fig. 4.2) with a vertical throw of 4000 m (*Castany, 1951*). Several authors (*Melki et al., 2012; Bejaoui et al., 2017; Booth-Rea et al., 2018*) observe a left-lateral component in the North–South Axis and Zaghouan faults and in other large NE-SW trending transpressive structures like the Cap Serrat-Gardimaou, Ras El Korane-Thibar and El Alia-Teboursouk (Fig. 4.2). On the other hand, E-W and NW-SE faults are mostly normal and right-lateral (*Zargouni, 1978; Melki et al., 2010; Zouaghi et al., 2011)*.

The same structural style can be observed in the Gulf of Tunis, located in the north-eastern part of the Tunisian offshore and strictly connected with the evolution of the Sicily Channel. The NE-SW features are organized in positive flower structures with sub-vertical fault planes, bending and converging into the basement and with a persistent displacement during the Meso-Cenozoic period (*Melki et al., 2010*). NW-SE features have extensional character and bound half-graben structures with tilted hanging wall blocks. The Jurassic-Early Cretaceous extensional faults and associated structures have been folded or inverted by the Pliocene shortening phase (related to

the Kabylian-North African collision); Quaternary sediments are also cut (Fig. 4.4) (*Belkhiria et al., 2017; Booth-Rea et al., 2018*).

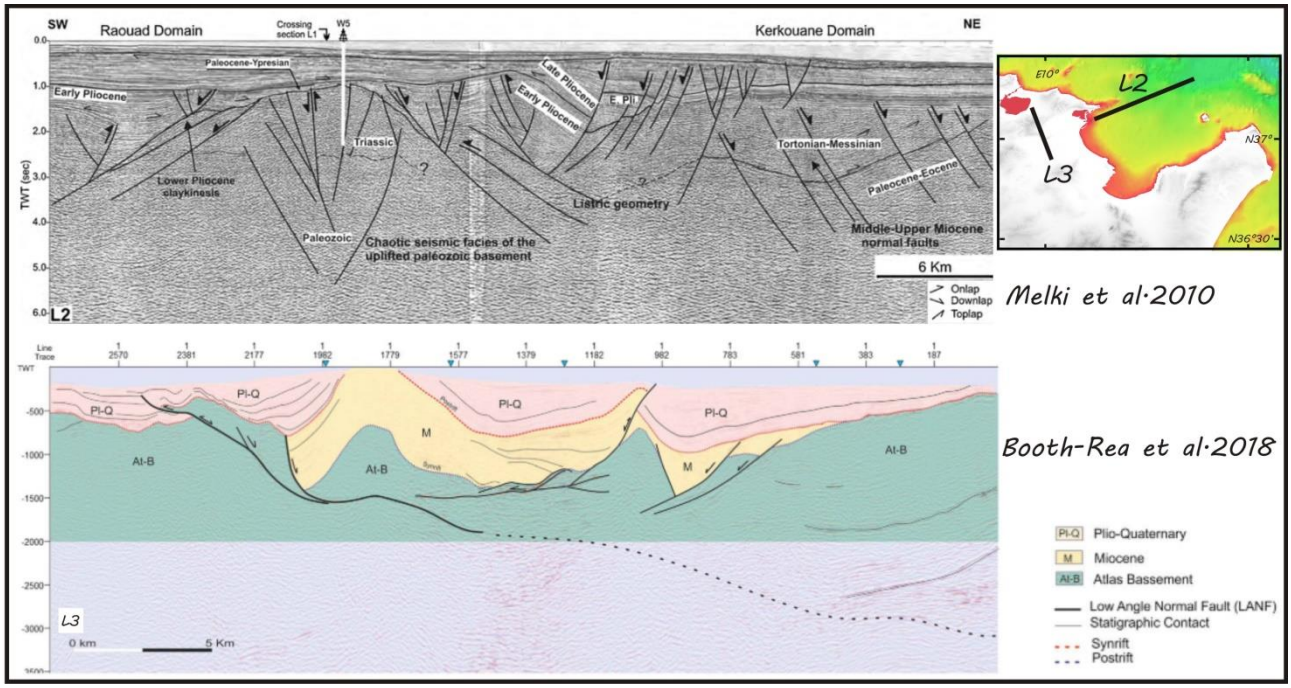

Figure 4.4 – Interpreted seismic lines showing NW-SE trending features with extensional character in the Gulf of Tunis (L2) and inversion tectonics in the norteastern end of Tunisia (L3). Seismic line traces are the black lines in the insert (top-right). L2 and L3 are respectively after *Melky et al. (2010)* and *Booth-Rea et al. (2018)*. Refer to the original papers for the legend.

However, within the Eastern platform and in the Gulf of Tunis, WNW-ESE and NW-SE trending minor extensional faults, formed during the late Miocene-Pliocene period, suggest a major variation in the stress field from a late Cretaceous-early Eocene predominant compression/transpression to an extension/transtension. It should be noted that this change is more important toward the Sicilian Channel, while in the Central Atlas the inversion tectonic was continuous during the Pliocene–Quaternary interval (*Letouzey, 1986; Ben Ayed, 1993; Melki et al., 2010; Belkhiria et al., 2017*) and even in the present-day (*Dlala and Rebaı¨, 1994; Boutib et al., 1997; Rekhiss, 2007; Melki et al., 2010*).

Ch.4.2.4 - Sicily channel

The Sicily Channel is located within the shallow Pelagian Sea, between Sicily and Tunisia. Three NW-SE oriented depressions, bordered by major faults, characterize the Channel: Pantelleria, Malta and Linosa troughs (Figs. 4.2 and 4.5). The Pantelleria trough narrows westward into a N-S trending depression that divides the Adventure Bank and the Tunisian Shelf; to the east, the Sicily

channel is bounded by the Malta plateau which drops off in the Ionian sea along the Malta Escarpment. The water depth in general is less than 400 m, except in the troughs where it exceeds 1000 m (*Morelli et al., 1975*). The crustal thickness ranges from 25 to35 km (*Scarascia et al., 2000*) and is reduced to less than 20 km in the basin areas (*Civile et al., 2008*); the heat flow reaches values up to 100 Mw/m 2 in the northwestern zones (*Zolotarev & Sochelnikov 1980, Boccaletti et al. 1984*), whereas gravimetric data show Bouguer anomaly values ranging from +40 to +80 reGal (*Morelli et al. 1975*)(Fig. 4.6C).

The stratigraphic succession of the Sicilian Channel consists of Triassic to Plio-Quaternary sedimentary deposits, 6-7 Km thick, overlying a crystalline basement (*Burollet, 1991*). The Meso-Cenozoic carbonate succession is made of shallow to deep-water carbonate deposits with intercalated volcanic rocks, followed by Miocene-Quaternary siliciclastic sediments; Messinian evaporites of the Gessoso-Solfifera Group can be locally present (*Civile et al., 2014*). Plio-Pleistocene turbidite deposits reaching thickness ranges of 1000-2000 m, (*Colantoni 1975; Maldonado & Stanley 1977; Winnock 1981)* fill the troughs.

The area is characterized by a widespread anorogenic volcanic activity of alkaline composition, mainly concentrated on the islands of Pantelleria and Linosa and by several submarine magmatic manifestations located in the Adventure, Graham and Nameless banks (*Beccaluva et al., 1981; Calanchi et al., 1989; Peccerillo, 2005; Rotolo et al., 2006; Falzone et al., 2009; Lodolo et al., 2012; Civile et al., 2015; Coltelli et al., 2016*), occurred until historical time.

The main structural features in the Sicily Channel were summarized in 5 main fault trends (*Boccaletti et al. 1987; Catalano et al., 2009*) (Fig. 4.5)

1. N110-120°E trending faults, characterized by dextral movements;
2. N140°E trending, mainly normal faults and well developed in the Malta Trough;
3. E-W oriented dextral strike-slip faults;
4. N-S oriented extensional structures, later reactivated as left-lateral strike-slip faults in the Maltese Islands and Cap Bon;
5. ENE-WSW-trending normal faults, present only in the Maltese Islands.

The three main troughs of Pantelleria, Malta and Linosa are bound by NW-SE trending structures which are dissected by N-S and ENE- WSW oriented transverse faults. Since the early Pliocene the faulting was contemporaneous with the deposition of Plio-Pleistocene sediments (*Colantoni, 1975;*

Maldonado & Stanley, 1977; Winnock, 1981; Boccaletti et al., 1987). Instrumental seismicity shows mainly strike-slip focal mechanisms, with some oblique-normal seismic events (*Calò and Parisi, 2014; Soumaya et al., 2015; Agius et al., 2020*) (Fig. 4.6A).

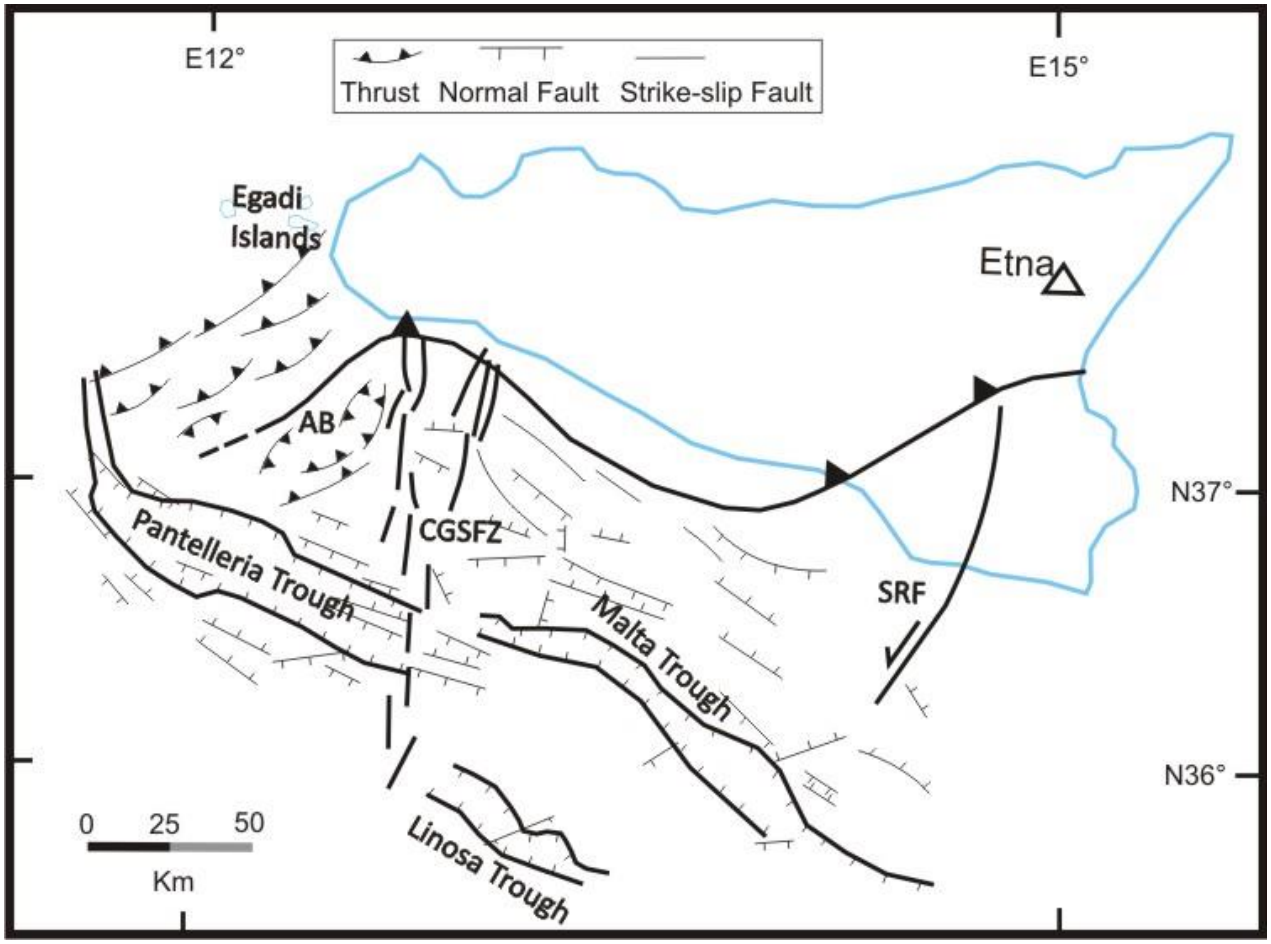

Figure 4.5 – Structural map of the Sicily Channel. AB: Adventure Bank; CGSFZ: Capo Granitola-Sciacca Fault Zone; SRF: Scicli-Ragusa Fault. Modified after *Civile et al. (2018)*.

Capo Granitola-Sciacca Fault Zone

The Sicilian channel is separated in a western area and an eastern sector by regional tectonic lineaments (eg. *Civile et al., 2010; 2018*), characterized by the proximity with several recent submarine volcanic centers (Nameless and Graham banks, Cimotoe volcano) (Figs. 4.2 and4.5) (e.g *Argnani, 1990, 1993a; Rotolo et al., 2006; Civile et al., 2008; Lodolo et al., 2012; Coltelli et al., 2016*) and present- day seismicity (e.g. the 1968 Belice earthquake) (*Calò and Parisi, 2014*).

These lineaments are known as Capo Granitola Fault System (or Belice fault system, A*ntonelli et al., 1988*) and Sciacca Fault system and bound a N-S trending transfer zone (Capo Granitola-Sciacca fault zone) (e.g. *Antonelli et al., 1988; Argnani, 1990, 1993a; Calò and Parisi, 2014; Civile et al., 2014*) (Fig.4.5) mainly developed during Pliocene time (*Civile et al., 2014*). The two fault system

are NNE-trending and are composed of faults with different length and a predominantly transpressive kinematics (e.g. *Cello, 1987; Antonelli et al., 1988; Argnani, 1990, 1993a; Civile et al., 2014*): left-lateral according to *Reuther et al. (1993)*, *Ghisetti et al. (2009)* and *Finetti and Del Ben (2005)*, right-lateral during the lower Pliocene and left-lateral since the Upper Pliocene according to *Fedorik et al. (2018);* whereas, in the southern part of the Capo Granitola Fault System a sub-vertical N-S oriented master fault show a pure strike-slip kinematic (*Civile et al., 2018*). In the southern part of the transfer zone, the Terribile Bank is dissected by Late Miocene WNW to NW-trending normal faults, later reactivated and currently active.

Sicily Channel Interpretations

Since the early geophysical exploration of the Mediterranean Sea (*Finetti and Morelli, 1972; Zarudzki, 1972*) the troughs of the Strait of Sicily have been documented as major topographic feature and interpreted as rift-related structures (Finetti and Morelli, 1972; Colantoni, 1975) or due to a large-scale wrench system (e.g. *Cello et al., 1984, 1985; Jongsma et al., 1985; Boccaletti et al., 1987*).

Several authors (*Argnani, 1990; Civile et al., 2010*) support the hypothesis of a "passive" rifting process, connected to mantle convections developed during the rollback of the Ionian slab (*Argnani 1990; Civile et al., 2010*); this process during the Plio-Quaternary generated the three troughs, controlled by NW-trending normal faults. Alternatively, a intraplate rifting formed the Miocene NE-SW structures, followed by a Mio-Quaternary second-order shear phase responsible for the activation of NW-SE-trending structures, related to the displacement of Sicily away from the African continent (*Illies,1981; Reuther and Eisbacher, 1985*). *Winnock (1981)* supports this second interpretation but suggests a Plio-Pleistocene as the age of shear, followed by a Quaternary rifting and volcanic activity.

Others, reinterpreted the Sicily Channel as a right-lateral transtensional zone, where crustal thinning and the magmatic activity in the Pantelleria trough are the result of the opening of complex pull-apart basins, bounded by NW-SE-trending structures (C*ello et al., 1985, 1987; Jongsma et alii, 1985; Boccaletti et al., 1987; Catalano et al., 2009; Finetti & Del ben, 2005; Atmaoui et al., 2006*). Moreover, *Aydin & Nur (1983)* and *Cello et al. (1985)* suggest the coalescence of several minor pull-apart basins as mechanism of formation.

A more complex interpretation, proposed by *Finetti (1984)*, involves extension perpendicular to a rift-axis extending from Pantelleria to the Malta Escarpment and a E-W directed right-lateral strike

slip motion along faults bounding the rift zone and delimiting the southern margin of Sicily, considered as a microplate separated from the North-African margin.

Ch.4.2.5 - Malta Escarpment and Messina strait

The Malta Escarpment is a steep NNW-SSE trending, 300 Km long, structural feature with a total bathymetric drop of more than 3000 m that bounds eastern Sicily south of Mount Etna up to the Sicily Channel (Fig. 4.2). It has been recognized to be a major tectonic feature separating the thinned oceanic Ionian Basin to the east and the Hyblean continental promontory to the west *(Dellong et al., 2018*). According to some authors (eg. *Scandone et al., 1981; Fabbri et al., 1982; Casero et al., 1984; Catalano et al., 2001; Gallais et al., 2011; Dellong et al., 2018*) this discontinuity is inherited from the Permian–Triassic opening of the Neo-Tethys and is active during the Jurassic–Cretaceous spreading stage. During the Neogene this paleomargin has been partly reactivated in the context of Africa-Europe collision.

The Malta Escarpment can be divided into two segments with different tectonic structures (*Argani & Bonazzi, 2005*). The segment north of Siracusa is characterized by NNW–SSE-trending, east-dipping, extensional faults bounding half-graben basins filled with Plio-Quaternary sediments (probably younger than late Pleistocene, according to *Argnani 2009*) (Fig. 4.15). On the eastern border of the Hyblean Plateau, structures related to the Malta Escarpment show a left-lateral kinematic, supported also by seismological data (e.g. *Amato et al., 1995; Adam et al., 2000; Musumeci et al., 2014; Gambino et al., 2022*) (Fig. 4.6A). These structures support the hypothesis of a large-scale sinistral strike-slip fault, trending roughly N-S, of which the uplifted area would represent a restraining bend (A*rgnani & Bonazzi, 2005*).

South of Siracusa no recent faulting has been observed above the Escarpment. The recent deformation is instead located about 20-30 km toward east; a NNW-SSE trending uplifted area is bounded by deep seated reverse faults and inverted normal faults, which extend northwards in the offshore of Mount Etna (*Argnani, 2009*). Other works suggest that the uplifted area is characterized by right-lateral and extensional faults (North and South Alfeo fault system in *Gutscher et al., 2016*; Alfeo-Etna fault in *Polonia et al., 2016*). Authors suggest a recent activity of this uplifted feature observing the growth geometry displayed by the adjacent sediments (*Argnani & Bonazzi, 2005; Argnani, 2009*) (Fig. 4.15). A morphologic high, the Alfeo Seamount, shows a

structural trend NE-SW oriented. It is thought that this relief was prior to the Calabrian Arc accretionary prism and reactivated in recent time (*Gutscher et al.,2016; Maesano et al., 2020*).

North of Catania, in the offshore of Mount Etna, a system of extensional faults, NW-SE trending, have been reactivated in contraction/right-lateral transpression (*Argnani & Bonazzi, 2005*). Northward, the Messina Strait separates Sicily from Calabria and is located between the Tyrrhenian basin and the Ionian basin. The area is seismically active (*Valensise and Pantosti, 2001; Calò & Parisi, 2014; Soumaya et al., 2015*) and has been affected by the Mw 7.1-1908 earthquake, with a related tsunami. A number of normal and right-lateral transtensional faults define the Messina strait. In the north-eastern part a ENE-trending graben is imaged in depth (*Doglioni et al., 2012*), while two systems of faults are arranged with ENE (Ganzirri-Scilla fault system, *Gargano, 1994; Lentini, 2000*) and NW direction between Messina and Reggio Calabria. To the south the right-lateral transtensional setting is expressed along the N-S segment of the strait; further south it merges with the Malta Escarpment.

Ch.4.3 - Method

The tools and methods of Plate Kinematics, in the absence of magnetic isochrons, have already been described in Chapter 1 with the fundamentals of Plate kinematics and in Chapter 2 describing the method used in *Turco et al. (2021)* to build the kinematic model of the Tyrrhenian Apennine system. The method used to reconstruct the kinematic evolution of Sicily microplate is also based on the structural geology but in this case the fan-shaped tectonic lineaments converging toward the Euler pole of rotation are missing (see Ch.2.3). Instead of the normal faults used in the other method, that here are discontinuous, transcurrent faults have been used. In the study area both transpressive and transtensive structures are observable in different places (e.g. the northwestern offshore of Sicily is characterized by transpressive structures, while transtensive structures are widespread in the southern offshore). Given the complexity of tranpressive features and the difficulty to observe and estimate the amount of compression, transtensive structures have been preferred as starting point for the construction of the kinematic model.

The first step is aimed at identifying the boundaries of the microplate, using various kinds of data and taking into account features already considered important in the literature. As a general rule high resolution bathymetric maps, joined with gravimetric and Moho depth maps are useful to seek morpho-structures, submerged mountain chains, alignments of volcanoes, sharp changes in the water depth and so on (Fig. 4.6) . Seismic sections are then useful to reconstruct the geometry, the relation with adjacent units and the age of the feature detected. Finally, focal mechanisms and GPS data can provide information on the very recent activity of the tectonic element that I consider as plate margin.

The tectonic elements that are selected as plate boundaries have been described in the geological setting (see Ch.4.2 and Fig. 4.2) and are:

- the Drepano-Elimi chain (Ustica ridge);
- the Taormina Line;
- “Sisifo-Alicudi’’ and ‘‘Aeolian-Tindari-Letojanni” lines;
- the Malta Escarpment;
- the Sicily Channel.

The polygon of the new microplate is drawn in Figure 4.6A. It is important to specify that the same plate boundary can accommodate the movement of Sicily with respect to a plate or another in

different times and that one tectonic element can stop its activity while another is activating. For example the northeastern margin of the plate is affected by the movement of Sicily with respect to Europe first and with Calabria later; the ‘‘Aeolian-Tindari-Letojanni” line becomes active as boundary between Sicily and Calabria when the Taormina line stops its activity.

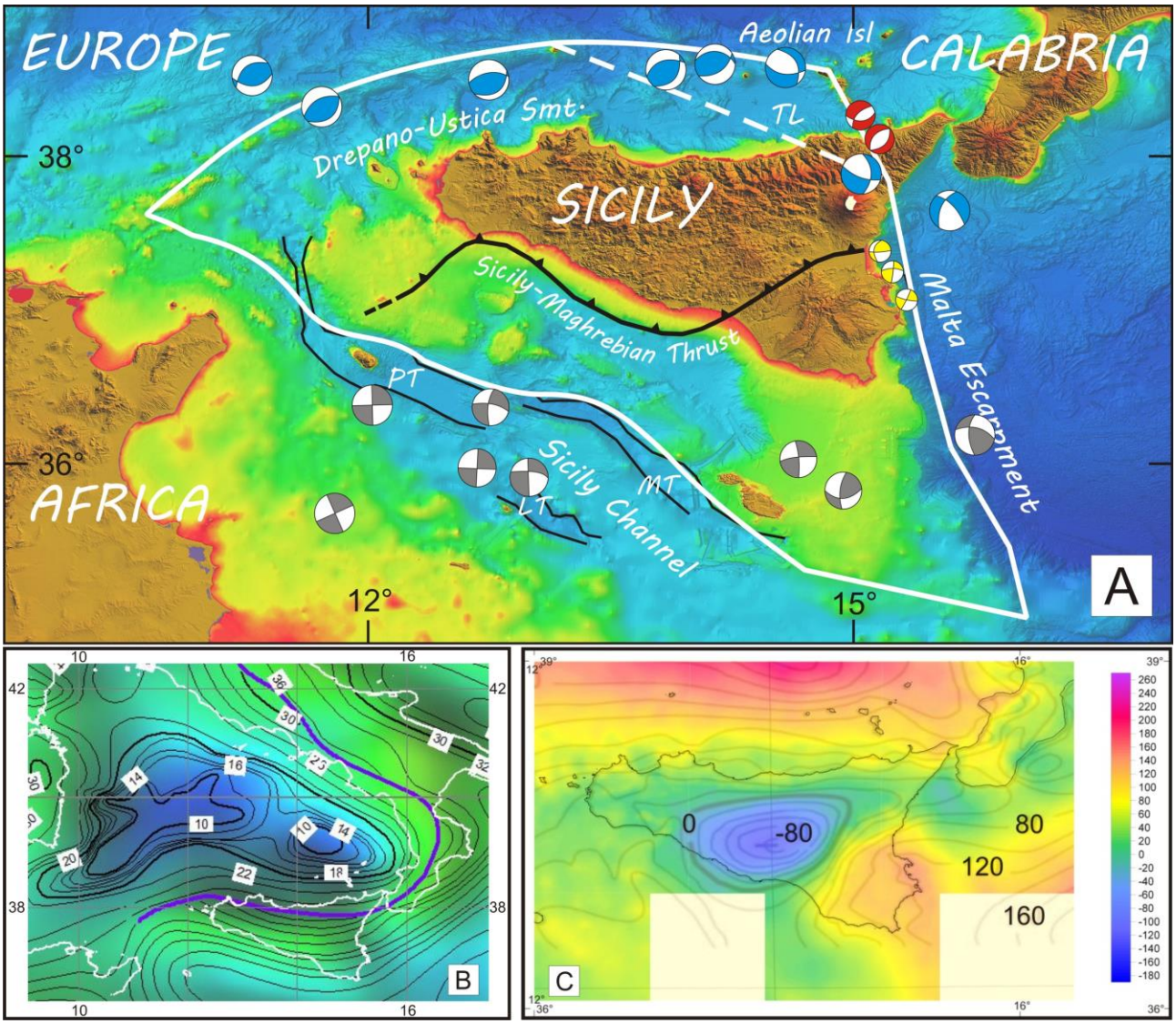

Figure. 4.6 – A: Boundary of Sicily microplate (solid and dashed white lines). The bathymetry is after: EMODnet Bathymetry Consortium (2020). EMODnet Digital Bathymetry (DTM). LT: Linosa Trough; MT: Malta Trough; PT: Pantelleria Trough; TL: Taormina Line. Focal mechanisms in light blue are from Soumaya et al. (2015), in red from Presti et al. (2013), in yellow from Gambino et al. (2020), in grey from Agius et al. (2020). B Moho depth map from Grad & Tire (2009); violet line is the Moho discontinuity. C: gravimetric map from ISPRA, ENI, OGS (2009), Cartografia Gravimetrica Digitale d’Italia alla scala 1:250.000 and Bouguer anomaly map from Mongelli et al. (1975); contour interval 20 mGal.

After the definition of the plate boundaries, the second step is to determine the Euler poles of rotation of Sicily microplate with respect to Africa, Europe and Calabria.

The movement between Sicily and Africa is expressed along the Sicily Channel and part of the Malta Escarpment. The peculiar geometry of the Sicily Channel fits well with the interpretation of several authors (*Cello et al., 1985, 1987; Jongsma et alii, 1985; Boccaletti et al., 1987; Finetti & Del Ben, 2005; Catalano et al., 2009*), so as a first assumption, Pantelleria, Linosa and Malta troughs have been considered as pull-apart basins developed in a dextral shear zone. Given this assumption, it was possible to find the Euler pole considering that before a certain time the three basins were closed. The method used to find the pole is sketched in Figure 4.7: the flanks of the troughs can be approximated to wide arcs of a circle whose center is the Euler pole. The small circles obtained in this way outline the direction of the movement between Sicily and Africa; the angle of rotation is constrained by the length of the troughs.

Several attempts have been made using this technique and the Euler poles are listed in Table 4.1. Sicily-Europe and Sicily-Calabria poles have been derived taking from the literature the Africa-Europe and Calabria-Europe poles. Velocity vectors have been obtained for each pole attempt and then compared with the respective boundary of the microplate, as shown in Figure 4.8.

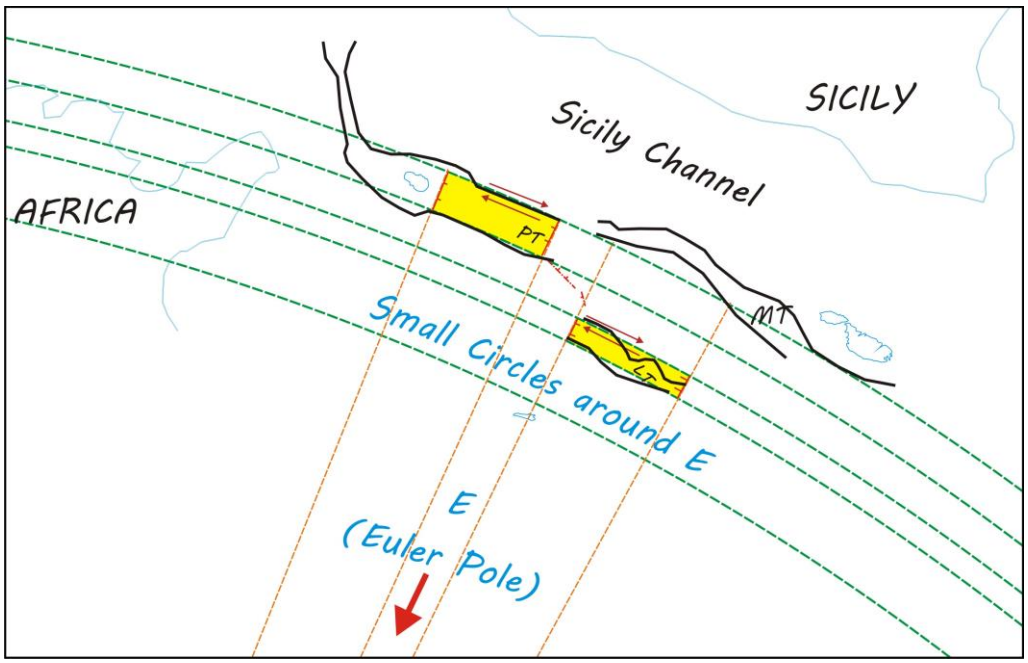

Figure. 4.7 – Simplified scheme of the methodology used to find the pole using small circles. Green lines are circle arcs, Orange lines are meridians of the Euler pole. LT: Linosa Trough; MT: Malta Trough; PT: Pantelleria Trough.

Table 4.1 – Euler Pole attempts for Sicily-Africa from 4.5 Ma.

Name	Latitude	Longitude	Ω	Ref.Plate
E5	44.25	19.09	-0.6	Africa
E4	11.36	-1.7	0.6	Africa
E4.1	11.36	-1.7	0.4	Africa
E4.2	11.36	-1.7	0.7	Africa
E4.3	11.36	-1.7	0.8	Africa
E3	7.73	-4.18	0.6	Africa
E2	63.43	94.73	-0.5	Africa
ET1	12.31	9	0.7	Africa
ET1.1	12.31	9	0.8	Africa
ET1.2	12.31	9	0.9	Africa
ET2	8.3	9	0.7	Africa
ET3	15.31	9	0.7	Africa
ET3.1	15.31	9	0.9	Africa
ET4	11	7	0.8	Africa
ER	31.57	15.85	1.57	Africa

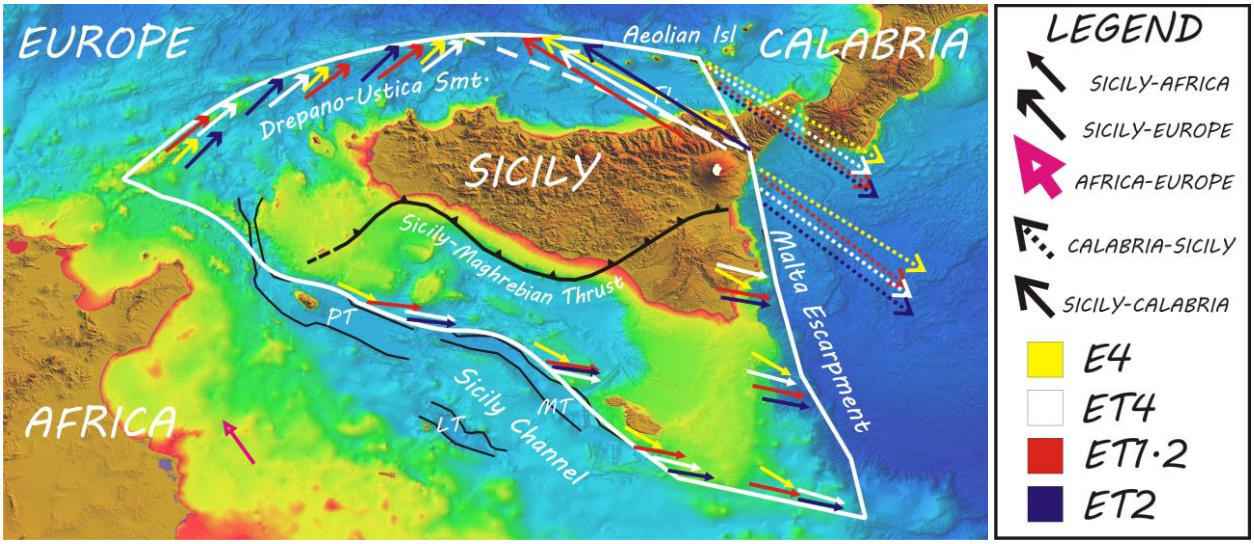

Figure. 4.8 –Comparison between some pole attempts of Table 4.1. Meanings of colors and arrows are in legend.

This step is useful to check which kind of kinematic and the amount of movement expected along the plate boundary. For instance the yellow arrows in Figure 4.8 have a consistent difference in direction and module respect to the others; the red arrows have the biggest module, that would mean a bigger amount of shear and transpression along the Sicily-Channel and the Elimi chain

respectively; blue and white arrows are comparable in magnitude but the direction is quite different.

Once the poles are entered in a rotation model, the new polygon is rotated back in time with the software GPlates (see Ch.1.4) (Fig. 4.9). In this way it is possible to see the position of the block at time t, with respect to a selected fixed plate, and understand and visualize the behavior of the plate margin. The Euler pole used in Figure 4.9A implies a right-lateral shear along the Sicily channel, according to the method of Figure 4.7; the presence of compression zones within the Channel is clearly visible, also from the bathymetry.

The results obtained from the modeling of the Sicily microplate considering the Sicily Channel as a rift zone, following the interpretation of *Argnani (1990)* and *Civile et al. (2010)*, is also shown in Figure 4.9B. Unlike the previous case, the small circles are perpendicular to the flanks of the troughs, according to a NE-SW direction of extension and the rotation pole could be located to the north-west or south-east of the Channel; the angle of rotation is constrained by the width of the troughs instead of their length. Observing, from the bathymetry, a bigger width of the Pantelleria trough respect to Linosa and Malta, is possible to assume a major extension for the first one, consequently poles attempts located to the south-east, thus closer to Linosa and Malta troughs, have been considered.

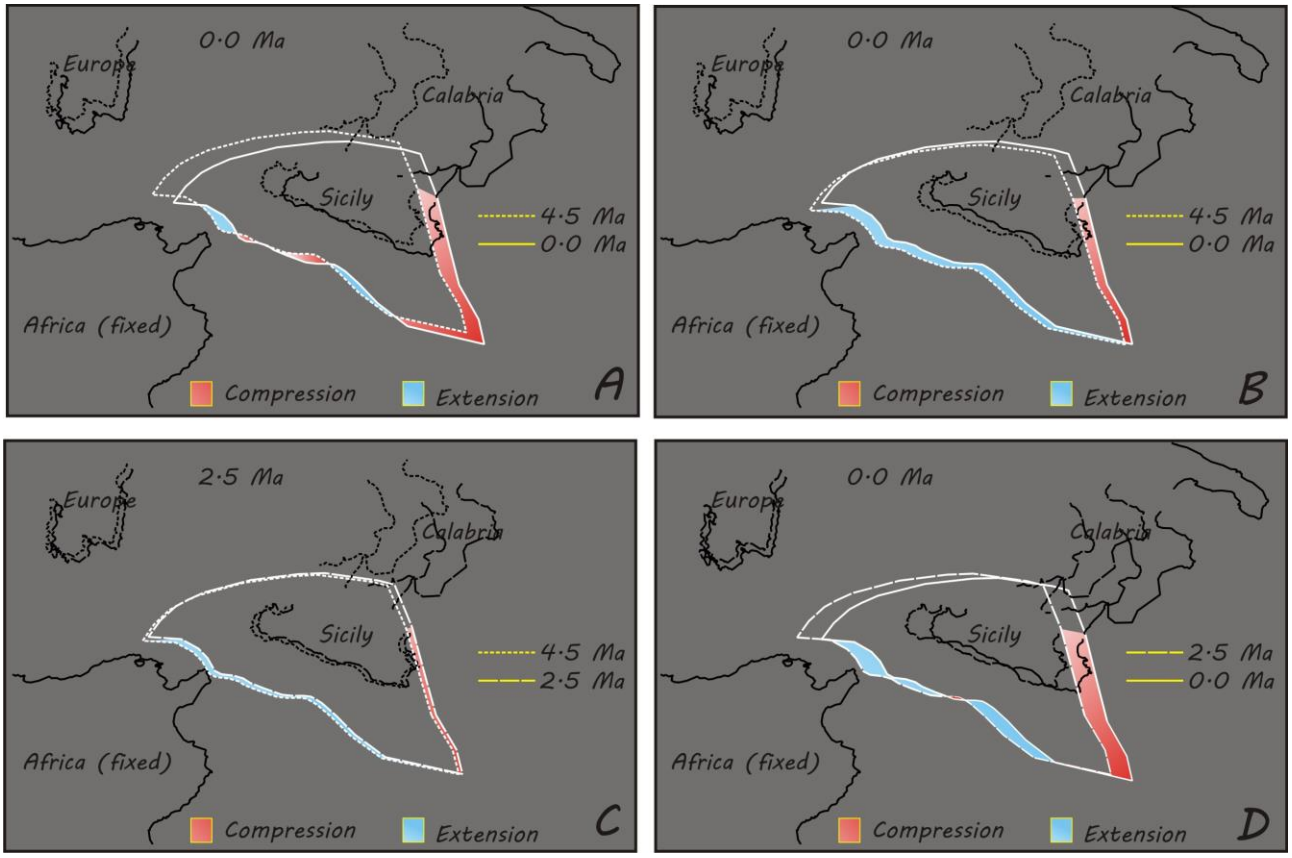

Figure. 4.9 – Comparison between some Euler pole attempts of Table 4.1: A) pole E4 from 4.5 Ma to present; B) pole ER from 4.5 Ma to present; and of Table 4.2: C) pole between 4.5 to 2.5 Ma; D) pole between 2.5 Ma to present. White (dashed, dotted and bold) line is the Sicily plate. Black lines are shorelines. Meanings of colors and dotted lines according to the time are in legend.Compression and extension are shown only along the margin with Africa.

Lastly, I concluded that one single pole did not fit with all the constraints imposed by the kinematics of the blocks around Sicily and also the complexity of the Sicily channel was not completely represented. Therefore, two kinds of kinematics have been combined, as also suggested by *Finetti (1984)*. The results of this last attempt are shown in Figure 4.9C-D: in a first stage the Sicily Channel is subject to a NE-SW directed extension (Fig. 4.9C), then to a ESE-WNW right-lateral shear (Fig. 4.9D); final poles are listed in Table 4.2 and shown in Figure 4.10.

Table 4.2 - Final chosen poles for Sicily and Tunisia microplates.

Time	Latitude	Longitude	Ω	Ref.Plate	
0-2.5 Ma	11	7	0.8	Africa	Sicily-Africa
2.5-4.5 Ma	21.311	11.187	1.57	Africa	Sicily-Africa
4.5-0 Ma	5.5	-83.51	-0.19	Europe	Tunisia-Europe

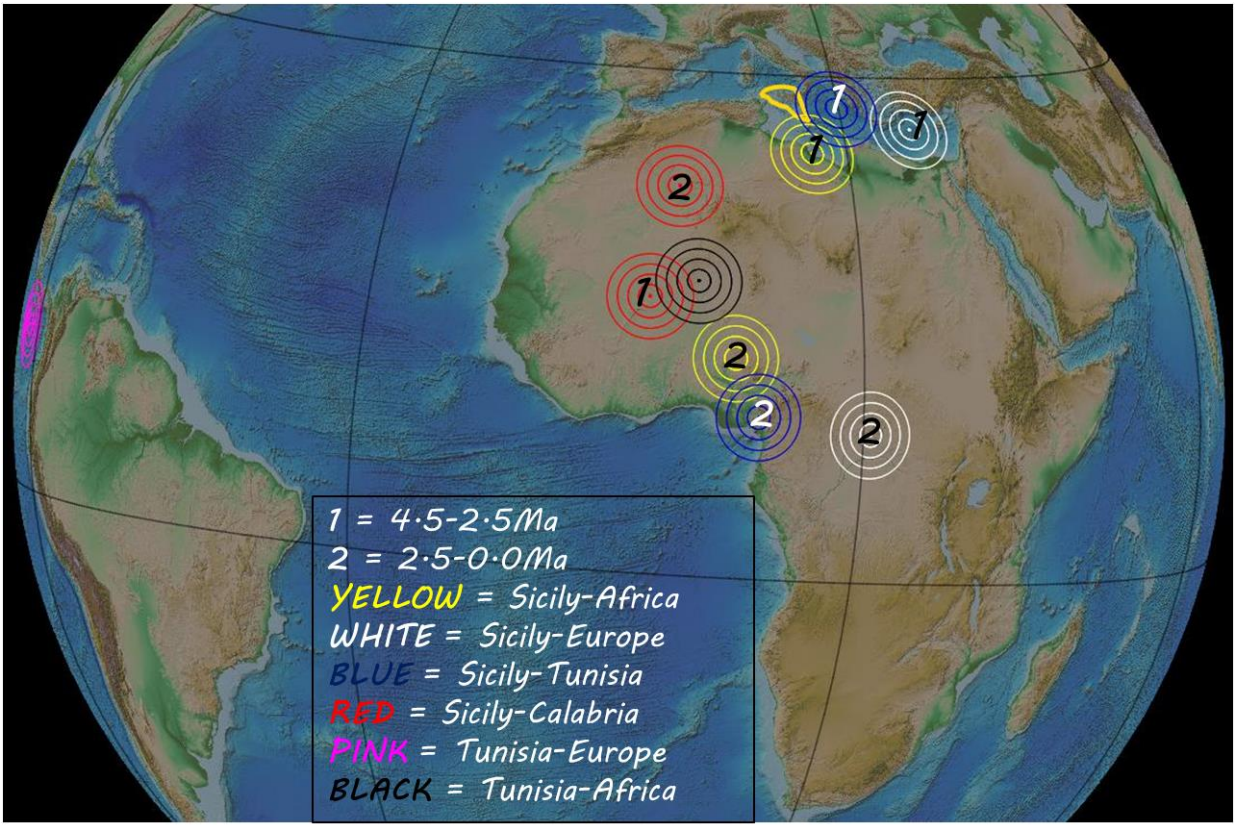

Figure. 4.10 – Location of the final chosen poles for Sicily and Tunisia of Table 4.2, visualized through GPlates.

The Tunisia microplate and its pole of rotation have been found applying the same method described above. The margins of the plate have been traced following the major morpho-structures observable on high resolution DEM, both onland and offshore (Fig. 4.2).

The time of the first Euler pole for Sicily has been constrained according to the Late Pliocene syn-rift deposits in the Sicily Channel; the second pole time is instead strictly related to the opening of the Marsili basin in the Southern Tyrrhenian sea and the change of direction of the Calabrian sector and the Ionian STEP fault along the Malta Escarpment, according to the kinematic model of the Tyrrhenian-Appenine system in which Sicily had to be included.

Ch.4.4 – Results and Geological implications

The poles found for Sicily and Tunisia microplates have been entered in the Rotation Model already used in *Turco et al. (2021)* and the two microplates have been modeled and included in the reconstruction of the Tyrrhenian-Apennine system; the proposed kinematic model will be described in Chapter 5. The result of the modeling for Sicily and Tunisia from 4.5 Ma to present-day is shown in Figures 4.11, 4.13 and 4.14.

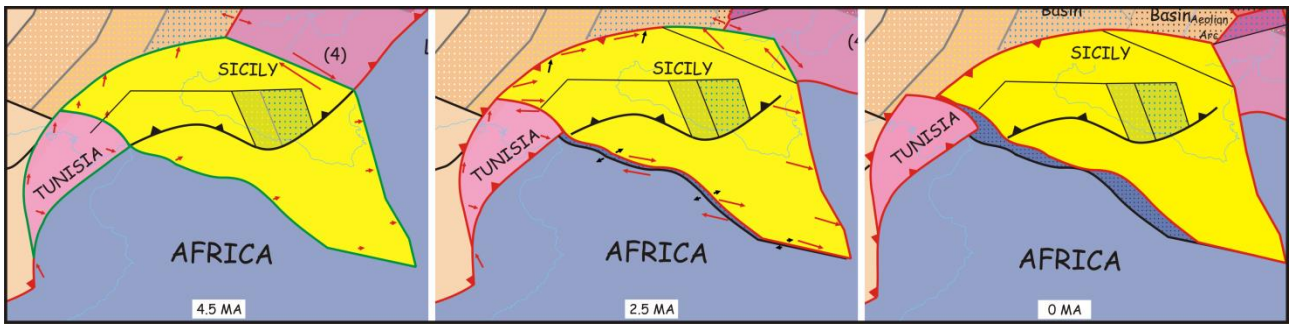

Figure. 4.11 – Detail of Sicily and Tunisia microplates, modeled according to the final chosen poles. See Figures 5.4-5.6-5.8 for the full pictures and legend.

The south-western boundary of Sicily with the African plate coincides with the Sicily channel, characterized by a right-lateral transtensive kinematic. The northern part of the Channel belongs to Tunisia and Sicily (Figs. 4.13-4.14).

Seismic lines M-24 and M-25 of the Crop project (Fig. 4.12), which run perpendicular to the main troughs, show a horst and graben system bounded by normal faults affecting Lower Pliocene Syn-rift deposits; negative flower structures, abrupt thickness changes in faulted deposits, vertical attitude of faults, and a straight trend in map view are evidences of strike-slip structures in Pantelleria, Malta and Linosa basins and in the central-southern Sicily offshore (*Argnani, 1990; Finetti et al., 2005, Civile et al., 2008; Civile et al., 2010; Cavallaro et al., 2017)*. A transtensive kinematic affected also the Eastern platform of Tunisia and the Gulf of Tunis (Figs. 4.4 and 4.14), where WNW-ESE and NW-SE trending minor extensional faults formed during early Pliocene (*e.g. Melki et al., 2010; Belkhiria et al., 2017*).

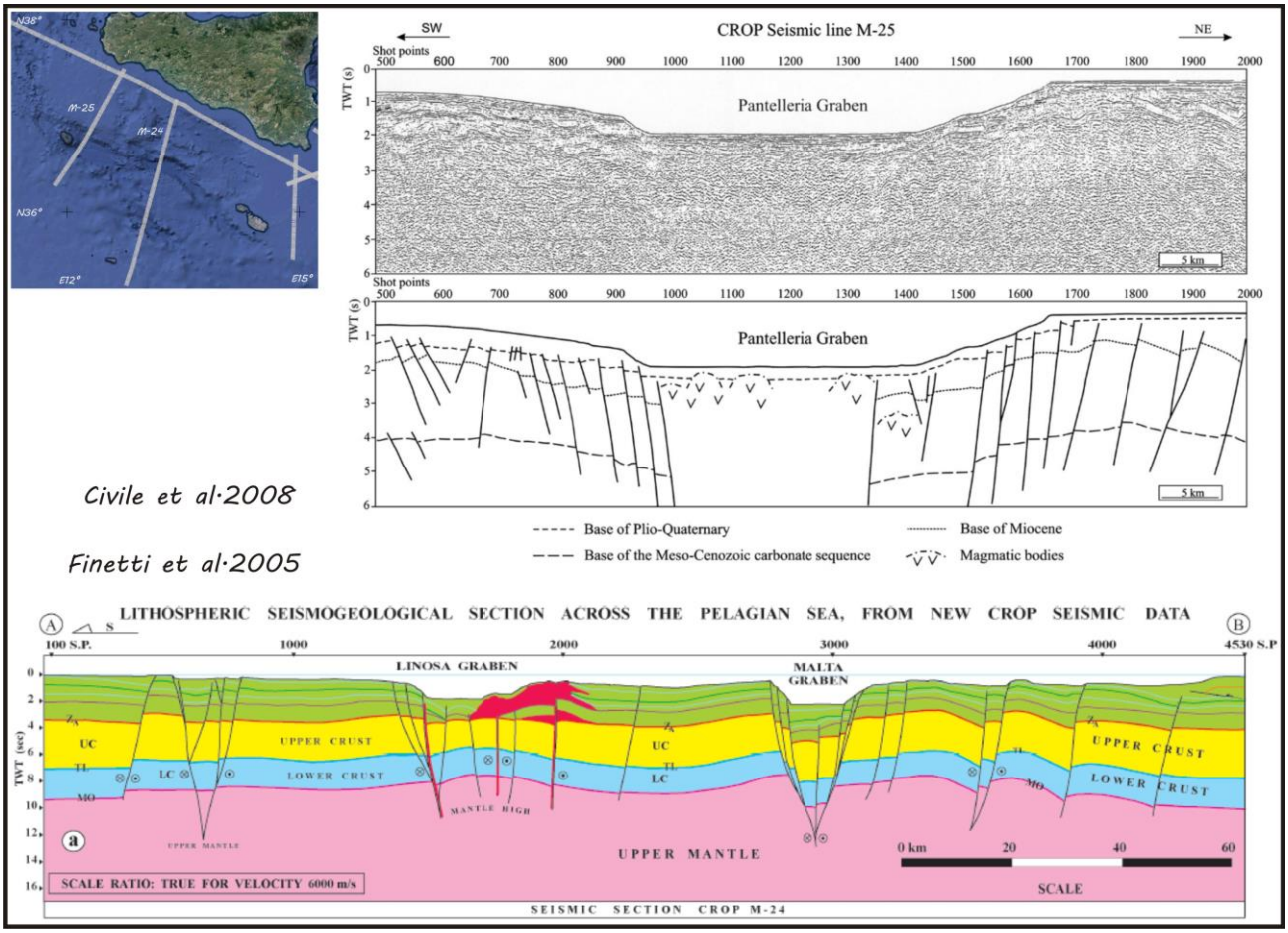

Figure 4.12 – Interpreted seismic sections across the Sicily Channel, showing the main structural features of the Pantelleria, Linosa and Malta grabens. Seismic line traces are the grey lines in the insert (top-left). CROP M-25 is after *Civile et al. (2008*); CROP M-24 is after *Finetti et al. (2005)*. Refer to the original papers for the legend.

The northern boundary of Sicily falls in a sector of the southern Tyrrhenian sea that, in the considered time frame, is part of the European plate. The rotation of Sicily with respect to Africa, implies a left-lateral transpression along most of the margin with Europe (Fig. 4.14). This margin passes through the Elimi chain (Ustica ridge), characterized by basins and ridges E-W, NW–SE and NE–SW oriented (Figs. 4.2 and 4.13). Inversion structures, as positive flower structures or anticlines with single or double vergence within sediments covering the ridge and filling the basins, have been detected in seismic profiles (Fig. 4.3) (*Catalano et al., 2013; Zitellini et al., 2020, Loreto et al., 2021*); also NW and NE trending normal faults bounding both basins and ridges have undergone a reversed phase. The incremental deformation obtained from present-day earthquakes aligned along the margin is mainly compressive (Fig. 4.6A).

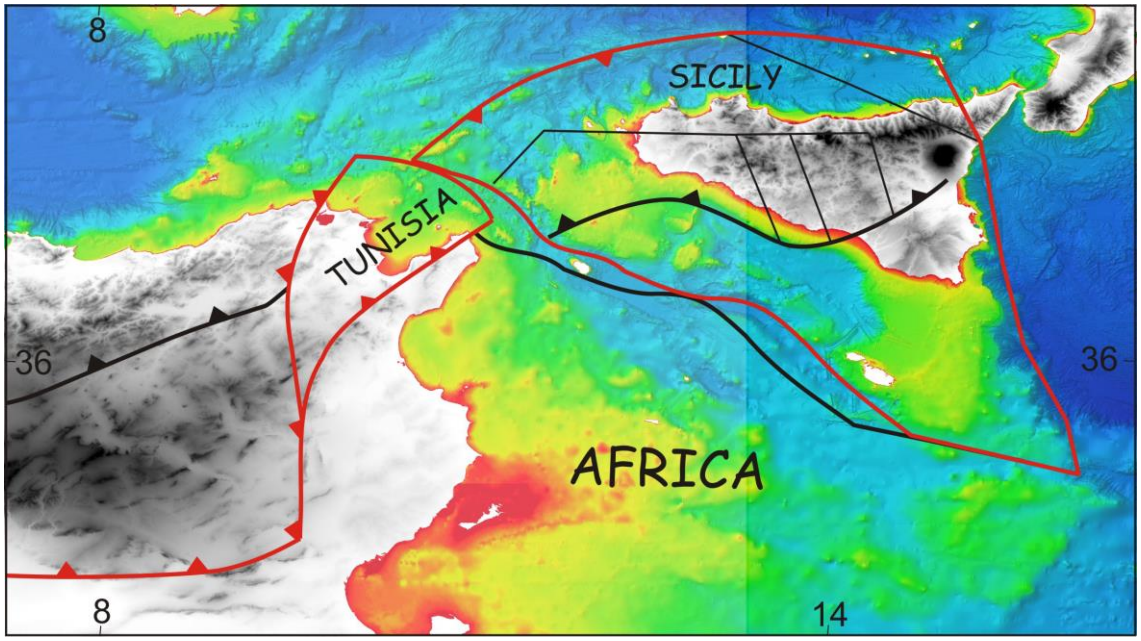

Figure. 4.13 – Location of the main tectonic elements at present day. The bathymetry is after: EMODnet Bathymetry Consortium (2020). EMODnet Digital Bathymetry (DTM). DEM for Sicily and Africa are respectively after *Tarquini et al. (2007)* and *Verdin (2017).*

The two mentioned features delimiting Sicily converge towards west, where they meet the northern margin of the Tunisian microplate; the triple junction Europe-Sicily-Tunisia runs along this margin (Fig. 4.14). The movement between Tunisia and Sicily creates extension in this sector, previously extended by the Tyrrhenian rifting, partially compensated by the northward motion of Tunisia with respect to Europe. Recently formed basins observed by *Camafort et al. (2020)* are in agreement with this kinematic. Tunisia-Europe N-S vector is accommodated along the several thrust faults NE-SW oriented that characterize the Central Atlas (e.g. Cap Serrat-Gardimaou, Ras El Korane-Thibar and El Alia-Teboursouk) and results in a left-lateral transpression (*Melki et al., 2012; Bejaoui et al., 2017; Booth-Rea et al., 2018*) (Figs. 4.2, 4.4, 4.13, 4.14). Instead, the margin between Tunisia and Africa is almost pure compressive and follows the Zaghouan thrust faults that continue in the Gulf of Tunis for several kilometers (Fig. 4.14). To the south, a left-lateral transpressive feature, the North-South Axis, links the eastern and western boundaries of Tunisia microplate with the thrusts of the Southern Tunisian Atlas (Figs. 4.2, 4.13, 4.14).

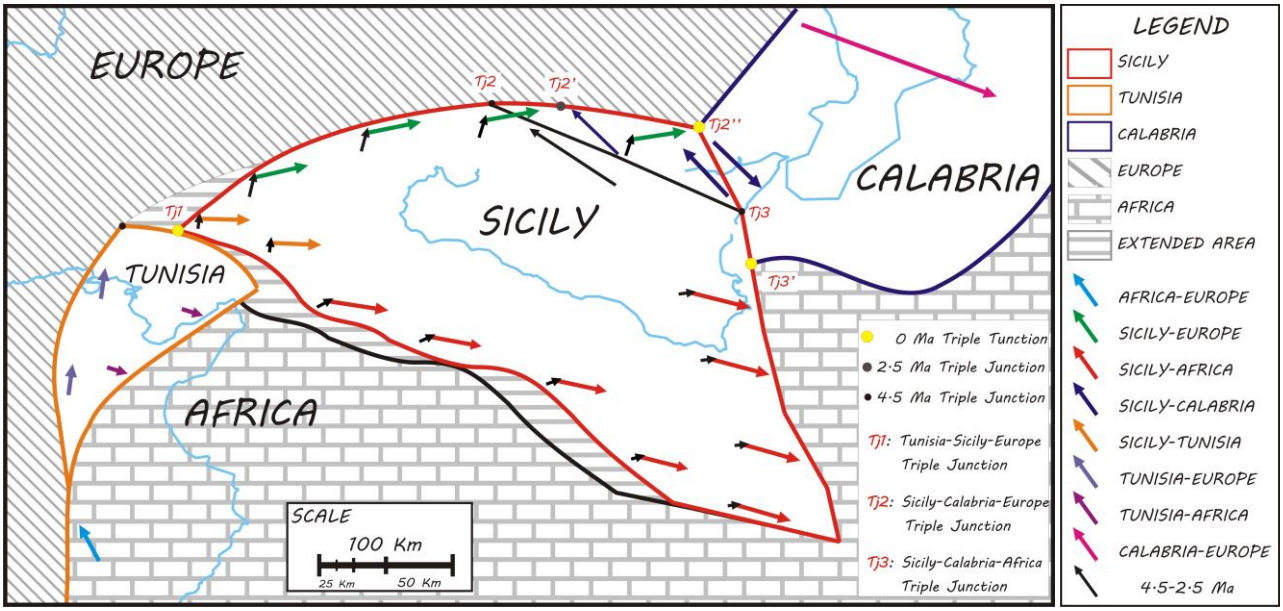

Figure. 4.14 – Sketch of plate configuration at present-day, triple junction migration and velocity vectors resulting from the final chosen poles of Table 4.2; black lines are inactive boundaries; black arrows are velocity vectors between 4.5 and 2.5 Ma; colored arrows are velocity vectors between 4.5 and 0 Ma; arrows are in scale.

The southern tip of Sicily microplate connects the Sicily Channel with the Malta Escarpment (Figs 4.2, 4.13, 4.14). This steep structural feature represents the boundary with Africa and is the place of a STEP fault where, about 2.5 Ma ago, the Ionian slab starts to break (*Argnani, 2000a; Pierantoni et al., 2020*), interrupting the continuity between the Sicilian and Ionian lithosphere. While the Calabrian arc continues to migrate toward southeast the northern portion of the Escarpment, up to Siracusa, becomes the margin between Sicily and Calabria (Fig. 4.11).

The difference in velocity between the triple junction Sicily-Africa-Calabria, moving along the Malta Escarpment, and the Calabrian arc, migrating toward south-east according to the Africa-Calabria vector, results in a hooked margin in the proximity of the Malta Escarpment (Figs. 4.11, 4.14); this shape of the margin is easily traceable on high-resolution bathymetric maps.

According to the poles for Sicily-Africa, the segment of the Malta Escarpment, south of Siracusa, experienced first a smaller amount of compression, equal to the amount of extension in the Sicily Channel between 4.5 and 2.5 Ma ago (Figs. 4.11 and 4.14), and then a bigger amount of left-lateral transpression, that reflects the right-lateral shear affecting the Channel in the time frame 2.5-0 Ma (Fig. 4.11).

Seismic profiles oriented E-W to NE-SW show verticalized extensional faults above the escarpment, NNW-SSE oriented faults, with evidences of a more or less pronounced contractional reactivation, and an uplifted region, with growth strata and bounded by deep seated reverse faults

(MESC-09/11/17, *Argnani & Bonazzi, 2005*; CROP M-3, *Polonia et al., 2016*) (Fig. 4.15), who may have accommodated compression. Features indicating inversion are also visible north of Siracusa where the western shoulder of a sedimentary basin has been reactivated in contraction (MESC-06, *Argnani & Bonazzi, 2005; Gambino et al., 2022*) (Fig. 4.15). A left-lateral movement along a roughly N-S oriented deep seated fault has been suggested by *Argnani & Bonazzi (2005)* and modeled using geodetic data by *Mastrolembo Ventura et al. (2014)*; earthquake focal mechanisms support a left-lateral strike-slip mechanism occurred along planes oriented NNE-SSW to NE-SW or a right lateral component along planes trending WNW-ESE to NW-SE.

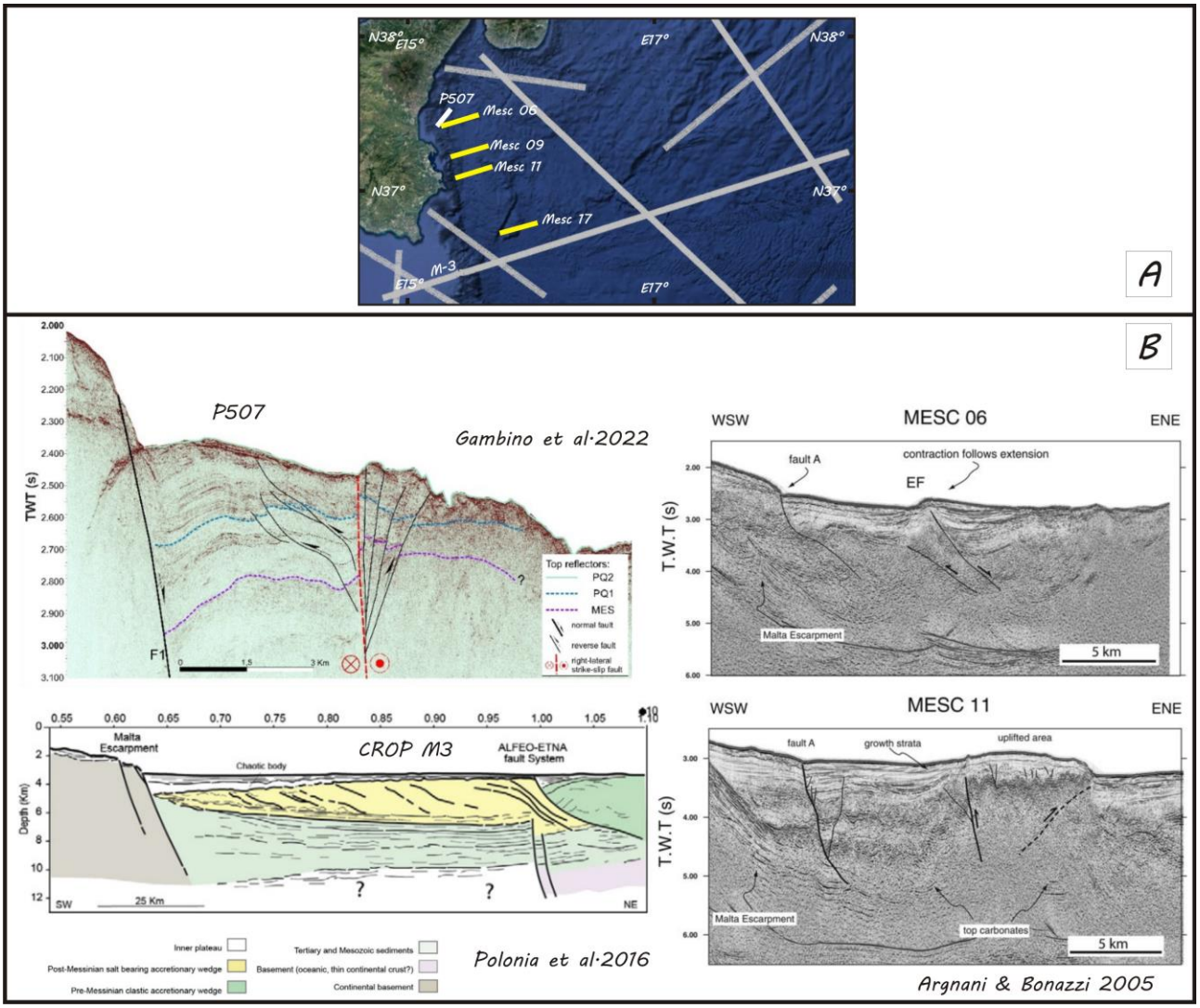

Figure 4.15 - Interpreted seismic sections showing structural features reactivated in contraction, uplifted region and growth strata along the Malta Escarpment. A) Seismic line traces. B) (top) north of Siracusa: P507 and MESC 06; (bottom) south of Siracusa: CROP M3 and MESC 11. P507 is after *Gambino et al. (2022)*; CROP M3 is after *Polonia et al. (2016*); MESC profiles are after *Argnani & Bonazzi (2005)*. Refer to the original papers for the legend.

Finally, the boundary between Sicily and Calabria evolves in time with changes happening in the southern Tyrrhenian sea. In the time frame 4.5-2.5 Ma the margin is located along the NW-SE oriented "Taormina Line" and its prolongation toward the northern Sicilian offshore; the triple junction Europe-Calabria-Sicily is around Ustica island and runs along the line (Figs 4.11, 4.14). As the triple junction moves toward southeast, following the migration of the Calabrian sector, part of the "Taormina Line" changes from right-lateral transpressive to compressive affecting a sector between Ustica and the western Aeolian islands, that is now related to the movement between Sicily and Europe (Fig. 4.14). The transpressive/compressive character of the "Taormina line" has been studied by several authors (e.g. *Scandone et al., 1974; Amodio Morelli et al., 1976; Lentini et al., 1994; Bonardi et al., 2001; Somma, 2006*).

At 2.5 Ma, the triple junction Europe-Calabria-Sicily jumps around Alicudi island and runs along the WNW-ESE "Sisifo-Alicudi line" with a dextral transpressive kinematic (*Barreca et al., 2014*), up to Lipari-Vulcano (Figs. 4.11, 4.14). Part of the Sicily-Calabria boundary is the "Aeolian–Tindari–Letojanni line" characterized by right-lateral transtension both offshore and onland, as testified by seismic sections and field and geodetic data (e.g. *De Guidi et al., 2013; Barreca et al., 2014; Mastrolembo-Ventura et al., 2014; Cultrera et al., 2017*) (Fig. 4.16).

The migration of the Calabrian sector involves an increasing sector of the Malta Escarpment in a dextral transtension (Fig. 4.11). NNW–SSE-trending, east-dipping, extensional faults bounding half-graben basins filled with Plio-Quaternary sediments have been observed by *Argnani & Bonazzi (2005)* (Fig. 4.15); the right-lateral character of these structures is due to the movement of the Calabrian Arc accretionary prism.

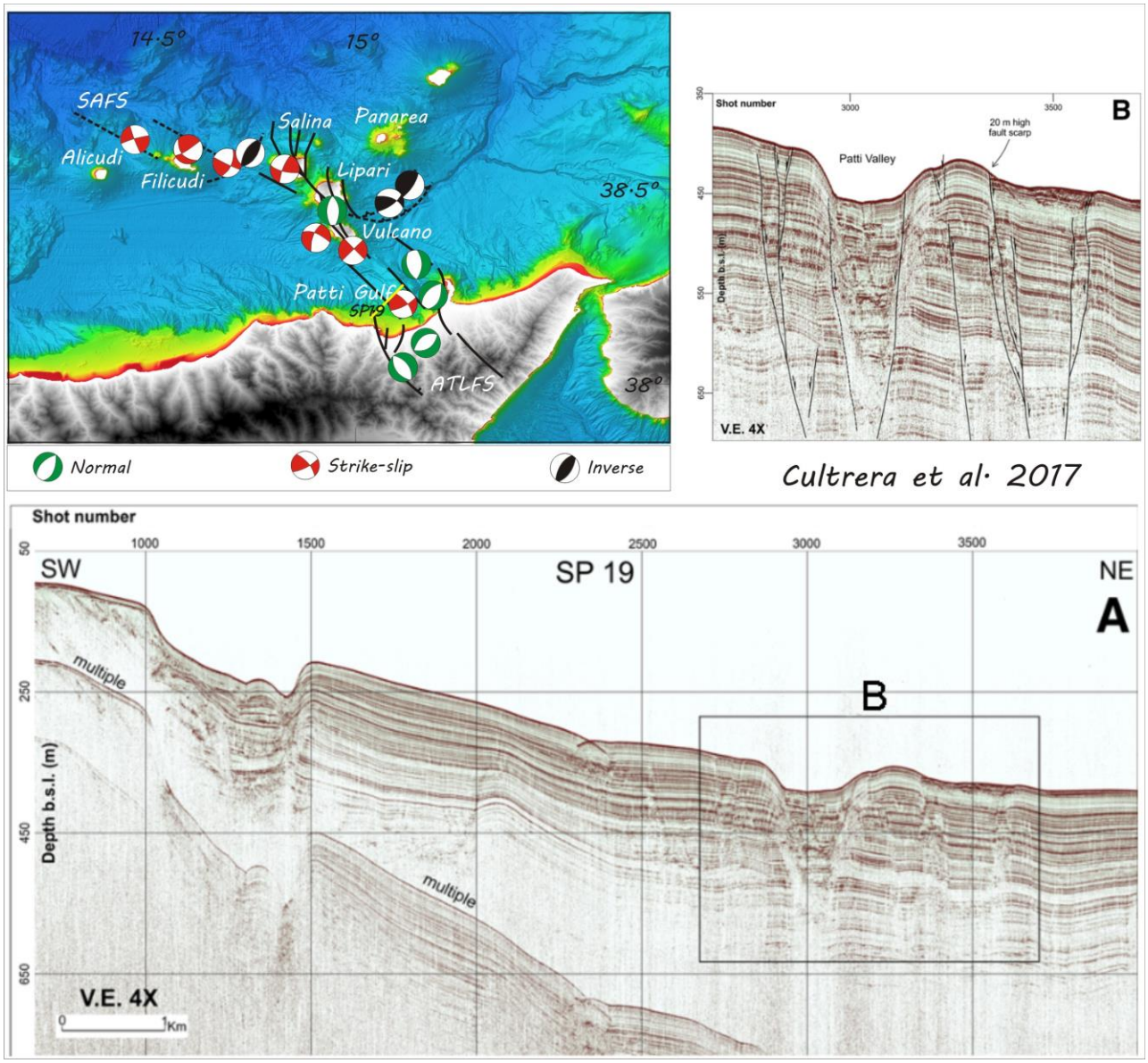

Figure 4.16 – Top-Left: Main structures and focal mechanisms of the "Sisifo-Alicudi" and "Aeolian-Tindari-Letojanni" Fault Systems; from *Barreca et al. (2014).* ATLFS: Aeolian-Tindari-Letojanni Fault System; SAFS: Sisifo-Alicudi Fault System. YELLOW LINE: SP19 line traces. A) Sparker profile SP 19 from *Cultrera et al. (2017)* showing horst and graben structures, B) locally involving Holocene deposits.

Ch.4.5 - Discussion

The results presented in Chapter 4.4 are strongly influenced by some initial assumptions and by parameters defined in the modeling phase. First of all, the choice of the method, forced by the available data: the absence of fan-shaped lineaments to be traced back to a single Euler pole, prompted me to use a method that implies the use of small circles to retrace the observed structure and to find the associated Euler pole. This method, although valid, can provide a big error in the position of the pole and needs a reiterative process of comparison with the geological data. Also, the definition of the plate boundaries affects the validity of the kinematic associated with them; an example of this is the current position of the Calabrian trench. In this work, the position of the Calabrian trench can determine whether the Malta Escarpment is the boundary with the Calabrian sector or with the Ionian plate (Africa); based on this, a right-lateral transtension or a left-lateral compression along the Escarpment will be obtained. The amount of extension considered in the troughs of the Sicily Channel alters the velocity of the Sicily microplate, while the Euler poles of the adjacent plates dictate the timing and the position of the microplate.
Some important features, such as the Capo Granitola-Sciacca Fault Zone, or the Scicli-Ragusa fault system have been neglected and considered as intraplate deformation, but the possibility of dividing the microplate in further micro blocks, independent from Africa, is not excluded.

The escape of Sicily, driven by the slab tearing, can be considered as a process that proceeds for incremental steps; when the STEP fault is stacked, the energy derived from the movement of Africa is concentrated and released along the margin with Europe. The lack of frequent and important current earthquakes in the Malta escarpment, south of Siracusa, where the major deformation is expected, suggests that the escape process is not active at the moment. Thus, Africa-Europe compression becomes the prevailing kinematic, as testified by focal mechanisms of earthquakes which are mainly concentrated along the Elimi Chain and show a compressive/right-lateral transpressive kinematic. The kinematic model presented here has a minimum range in time of 500 ka, therefore is not possible to make a direct correlation with the very short time range of earthquakes focal mechanisms.

Ch.4.6 - References

Abate, B., Di Maggio, C., Incandela, A., Renda, P., 1991. Nuovi dati sulla geologia della Penisola di Capo S. Vito (Sicilia nord–occidentale). Memorie Società Geologica Italiana 47, pp. 15–25.

Abate, B., Incandela, A., Renda, P., 1997. Carta Geologica delle Isole di Favignana e Levanzo. Dipartimento di Geologia, Università Di Palermo.

Agius, M. R., Galea, P., Farrugia, D., & D'Amico, S. 2020. An instrumental earthquake catalogue for the offshore Maltese islands region, 1995–2014. Annals of Geophysics, 63(6), SE658.

Amato, A., Azzara, R., Basili, A., Chiarabba, C., Cocco, M., Di Bona, M., et al. 1995. Main shock and aftershocks of the December 13, 1990 Eastern Sicily earthquake. Ann. Geophys. 38 (2), 255–266. doi:10.4401/ag-4122.

Amodio-Morelli, L., Bonardi, G., Colonna, V., Dietrich, D., Giunta, G., Ippolito, F., Liguori, V., Lorenzoni, S., Paglionico, A., Perrone, V., Piccarreta, G., Russo,M., Scandone,P., Zanetti-Lorenzoni, E., Zuppetta, A., 1976. L'Arco Calabro-Peloritano nell'orogene appenninico-maghrebide. Mem. Soc. Geol. Ital. 17, pp. 1–60.

Antonelli, M., Franciosi, R., Pezzi, G., Querci, A., Ronco, G.P., Vezzani, F., 1988. Paleogeographic evolution and structural setting of the northern side of the Sicily Channel. Memorie Società Geologica Italiana 41, pp. 141–157.

Argnani, A., 1990. The Strait of Sicily rift zone: foreland deformation related to the evolution of a back-arc basin. J. Geodyn. 12, pp. 311–331.

Argnani, A., 1993a. Neogene tectonics of the strait of sicily. In: Max, M.D., Colantoni, P. (Eds.), Geological Development of the Sicilian-Tunisian Platform, Proceedings of International Scientific Meeting. vol. 58. University of Urbino, Italy, pp. 55–60 4–6.

Argnani, A. 2000a. The southern Tyrrhenian subduc- tion system: Recent evolution and Neotectonic im- plications, Ann. Geofis., 43, pp. 585–607.

Argnani, A. 2009. Evolution of the southern Tyrrhenian slab tear and active tectonics along the western edge of the Tyrrhenian subducted slab. Geological Society Special Publication, 311, pp. 193–212. https://doi.org/10.1144/SP311.7.

Argnani, A., & Bonazzi, C. 2005. Malta Escarpment fault zone offshore eastern Sicily: Pliocene-quaternary tectonic evolution based on new multichannel seismic data. Tectonics, 24(4), 1–12. https://doi.org/10.1029/2004TC001656.

Argnani, A., Serpelloni, E., & Bonazzi, C. 2007. Pattern of deformation around the central Aeolian Islands: Evidence from multichannel seismics and GPS data. Terra Nova, 19(5), 317–323. https://doi.org/10.1111/j.1365-3121.2007.00753.x.

Atmaoui, N., Kukowski, N., Stöckhert, B., & König, D. 2006. Initiation and development of pull-apart basins with Riedel shear mechanism: Insights from scaled clay experiments. International Journal of Earth Sciences, 95(2), 225–238. https://doi.org/10.1007/s00531-005-0030-1.

Avellone, G., Barchi, M.R., Catalano, R., Gasparo Morticelli, M., Sulli, A., 2010. Interference between shallow and deep–seated structures in the Sicilian fold and thrust belt, Italy. Journal of the Geological Society 167, pp. 109–126.

Aydin, A. & Nur, A. 1982. Evolution of pull-apart basins and their scale independence. Tectonics 1, pp. 91-105.

Bahrouni, N., Bouaziz, S., Soumaya, A., Ben Ayed, N., Attafi, K., Houla, Y., El Ghali, A. and Rebai, N. 2014, Neotectonic and seismotectonic investigation of seismically active regions in Tunisia: A multidisciplinary approach, J. Seismol., 18(2), pp. 235–256.

Bahrouni, N., Masson, F., Meghraoui, M., Saleh, M., Maamri, R., Dhaha, F., & Arfaoui, M. 2020. Active tectonics and GPS data analysis of the Maghrebian thrust belt and Africa-Eurasia plate convergence in Tunisia. Tectonophysics, 785(April), 228440. https://doi.org/10.1016/j.tecto.2020.228440.

Barberi, F., Innocenti, F., Ferrara, G., Keller, J. and Villari, L. 1974. Evolution of Eolian Arc volcanism (Southern Tyrrhenian Sea), Earth. Planet. Sci. Lett., 21, pp. 269–276.

Barreca, G., Bruno, V., Cultrera, F., Mattia, M., Monaco, C., & Scarfì, L. 2014. New insights in the geodynamics of the Lipari-Vulcano area (Aeolian Archipelago, southern Italy) from geological, geodetic and seismological data. Journal of Geodynamics, 82(July), pp. 150–167. https://doi.org/10.1016/j.jog.2014.07.003.

Barreca, G., Monaco, C., 2013. Vertical–axis rotations in the Sicilian Fold and Thrust Belt; new structural constraints from the Madonie Mts. (central–northern Sicily, Italy). Italian Journal of Geosciences 132 (3), pp. 407–421, doi: 10.3301/IJG.2012.44.

Basilone, L. 2012.Litostratigrafia della Sicilia. Dipartimento di scienze della terra e del mare, Università degli studi di Palermo. p. 160.

Beccaluva, L., Colantoni, P., Di Girolamo, P. and Savelli, C., 1981. Upper-Miocene Submarine Volcanism in the Strait of Sicily (Banco Senza Nome). Bull. Volcanol., 44, pp. 573-581.

Beccaluva, L.,. Rossi, P. L and Serri, G. 1982. Neogene to Recent volcanism of the Southern Tyrrhenian-Sicilian area: Implications for the geodynamic evolution of the Calabrian Arc, Earth Evol. Sci., 3,pp. 222–238.

Beccaluva, L., Gabbianelli, G., Lucchini, F., Rossi, P. L and Savelli, C. 1985. Petrology and K/Ar ages of volcanic dredged from the Eolian seamounts: Implications for geodynamic evolution of the Southern Tyhrrenian basin, Earth Planet. Sci. Lett., 74, pp. 187–208.

Beccaluva, L., Morlotti, E., Torelli, L., 1986. Notes on the geology of the Elimi Chain area (south western margin of the Tyrrhenian Sea). Mem. Soc. Geol. Ital. 27, pp.213–232.

Bejaoui, H., Aïfa, T., Melki, F., & Zargouni, F. 2017. Structural evolution of Cenozoic basins in northeastern Tunisia, in response to sinistral strike-slip movement on the El Alia-Teboursouk Fault. Journal of African Earth Sciences, 134, pp. 174–197. https://doi.org/10.1016/ j.jafrearsci.2017.06.021.

Belkhiria, W., Boussiga, H. and Inoubli M. H. 2017. Thick-skinned tectonics within the intracontinental easternmost Atlas foreland-and-thrust belt (Tunisia): Meso-Cenozoic kinematics and implications for regional geodynamics, Tectonics, 36, pp. 981–1004, doi:10.1002/2016TC004340.

Bello, M., Franchino, A., Merlini, S., 2000. Structural model of Eastern Sicily. Memorie della Società Geologica Italiana 55, pp. 61–70.

Ben Ayed, N, 1993. Évolution tectonique de l'avant-pays de la chaıne alpine de Tunisie du début du Meˆ sozoı¨que a`l'Actuel, Ann. Mines Geol., éditions du Service géologique de Tunisie, no 32, p. 286.

Ben Haj Ali, M., Jedoui, Y., Dali, T., Ben Salem, H.and Memmi L. 1985. Carte Géologique de la Tunisie au 1/500.000. Office National des Mines, Service Géologique, Tunis.

Bianchi, F., Carbone, S., Grasso, M., Invernizzi, G., Lentini, F., Longaretti, G., Merlini, S., Mostardini, F. 1987. Sicilia Orientale: profilo geologico Nebrodi–Iblei. Memorie Società Geologica Italiana 38, pp. 429–458.

Billi, A., Barberi, G., Faccenna, C., Neri, G., Pepe, F., & Sulli, A. 2006. Tectonics and seismicity of the Tindari Fault System, southern Italy: Crustal deformations at the transition between ongoing contractional and extensional domains located above the edge of a subducting slab. Tectonics, 25(2), pp. 1–20. https://doi.org/10.1029/2004TC001763.

Billi, A., Presti, D., Faccenna, C., Neri, G. & Orecchio, B. 2007. Seismotectonics of the Nubia plate compressive margin in the south Tyrrhenian region, Italy: Clues for subduction inception. Journal of Geophysical Research: Solid Earth, 112(8), pp. 1–13. https://doi.org/10.1029/2006JB004837.

Boccaletti, M., Cello, G., Tortorici, L., 1987. Transtensional tectonics in the Sicily Channel. J. Struct. Geol. 9, pp. 869–876.

Boccaletti, M., Cello, G.and Tortorici L. 1990, First order kinematic elements in Tunisia and the Pelagian block, Tectonophysics, 176, pp. 215–228.

Boccaletti, M., Dainelli, P., 1982. Il sistema regmatico Neogenico–Quaternario nell'area Mediterranea: Esempio di deformazione plastico–rigida post–collisionale. Memorie Società Geologica Italiana 24, pp. 465–482.

Boccaletti, M., Nicolich, R. & Tortorici L. 1984. The Calabrian Arc and the Ionian Sea in the dynamic evolution of the Central Mediter- ranean. Mar. Geol. 55, pp. 219-245.

Booth-Rea, G., Gaidi, S., Melki, F., Marzougui, W., Azañón, J. M., Zargouni, F., Galvé, J. P., & Pérez-Peña, J. V. 2018. Late Miocene Extensional Collapse of Northern Tunisia. Tectonics, 37(6), pp. 1626–1647. https://doi.org/10.1029/2017TC004846.

Bonaccorso, A. 2002. Ground deformation of the southern sector of the Aeolian Islands volcanic arc from geodetic data, Tectonophysics, 351, 181–192.

Bonardi, G., Cavazza, W., Perrone, V., & Rossi, S. 2001. Calabria-Peloritani terrane and northern Ionian Sea. Anatomy of an Orogen: The Apennines and Adjacent Mediterranean Basins, pp. 287–306. https://doi.org/10.1007/978-94-015-9829-3_17.

Bousquet, J.C., Lanzafame, G., 2004. Compression and quaternary tectonic inversion on the Northern edge of the Hyblean Mountains, foreland of the Apennine– Maghrebian chain in Eastern Sicily (Italy): geodynamic implications for Mt. Etna. GeoActa 3, pp. 165–177.

Boutib, L., Melki, F., Zargouni, F., 1997. Tectonique récente et sismo- tectonique de la région du grand Tunis (Tunisie nord orientale): apport te´ le´ -analytique et donne´ es de terrains. Afr. Geoscience Rev. 4 (3 & 4), pp. 395–403.

Burollet, P.F. 1991. Structures and tectonics of Tunisia. Tectonophysics 195, pp.359–369.

Burollet, P. F., Mugniot, G. M. & Sweeney P. 1978. The geology of the Pelagian Block: the margins and basins of Southern Tunisia and Tripolitania. In: The Ocean Basins and Margins 4b (edited by Nairn A., Kanes W. & Stelhi F. G.). Plenum Press, New York, pp. 331-339.

Calanchi, N., Colantoni, P., Gabbianelli, G, Rossi, P.L. and Serri, G. 1984. Physiography of Anchise Seamount and of the subma- rine part of Ustica Island south Tyrrhenian., petrochemistry of dredged volcanic rocks and geochemical characteristics of their mantle sources. Miner. Petrogr. Acta, 28, pp. 215-224

Calanchi, N., Colantoni, P., Rossi, P. L., Saitta, M. and Serri, G., 1989. The Strait of Sicily Continental Rift System: Physiography and Petrochemistry of the Submarine Volcanic Centres. Marine Geology, 87, pp. 55-83.

Calanchi, N., Romagnoli, C. and Rossi, P. L. 1995. Morphos- tructural features and some petrochemical data from the submerged area around Alicudi and Filicudi volcanic islands (Aeolian Arc, Southern Tyrrhenian Sea), Mar. Geol., 123, pp. 215–238.

Calò, M., Parisi, L., 2014. Evidences of a lithospheric fault zone in the Sicily Channel continental rift (southern Italy) from instrumental seismicity data. Geophys. J. Int. 199 (1), pp. 219–225.

Camafort, M., Gràcia, E., & Ranero, C. R. 2020. Quaternary Seismostratigraphy and Tectonosedimentary Evolution of the North Tunisian Continental Margin. Tectonics, 39(11). https://doi.org/10.1029/2020TC006243.

Carminati, E., Wortel, M. J. R., Spakman, W. and Sabadini, R. 1998. The role of slab detachment processes in the opening of the western-central Mediterranean basins: Some geological and geophysical evidence, Earth Planet. Sci. Lett., 160, pp. 651–665.

Casero, P., Cita, M. B., Croce, M. and De Micheli A. 1984, Tentativo di interpretazione evolutiva della scarpata di Malta basata su dati geologici e geofisici, Mem. Soc. Geol. It., 27, pp. 233–253.

Castany, G. 1951. Etude Géologique de l'Atlas Tunisien Oriental, vol. 8, 632 pp., Ann. Mines Géol.

Catalano, R., D'Argenio, B., 1978. An essay of palinspastic restoration across the western Sicily. Geol. Rom., 17, pp. 145–159, Roma.

Catalano, S., De Guidi, G., Lanzafame, G., Monaco, C., Torrisi, S., Sturiale, G., Tortorici, G., Tortorici, L., 2006. Inversione tettonica positiva tardo-quaternaria nel Plateau Ibleo (Sicilia SE). Rend. Soc. Geol. It. 2 Nuova Serie, pp. 118–120.

Catalano, S., De Guidi, G., Romagnoli, G., Torrisi, S., Tortorici, G., Tortorici, L., 2008. The migration of plate boundaries in SE Sicily: influence on the large-scale kinematic model of the African promontory in southern Italy. Tectonophysics 449, pp. 41–62. http://dx.doi.org/10.1016/j.tecto.2007.12.003.

Catalano, S., De Guidi, G., Lanzafame, G., Monaco, C., & Tortorici, L. 2009. Late Quaternary deformation on the island on Pantelleria: New constraints for the recent tectonic evolution of the Sicily Channel Rift (southern Italy). Journal of Geodynamics, 48(2), pp. 75–82. https://doi.org/10.1016/j.jog.2009.06.005.

Catalano, R., Valenti, V., Albanese, C., Accaino, F., Sulli, A., Tinivella, U., Gasparo Morticelli, M., Zanolla, C., & Giustiniani, M. 2013. Sicily's fold-thrust belt and slab roll-back: The SI.RI.PRO. seismic crustal transect. Journal of the Geological Society, 170(3), pp. 451–464. https://doi.org/10.1144/jgs2012-099.

Catalano, R., Di Maggio, C., 1996. Sovrapposizione tettonica delle Unità Imeresi sulle Panormidi nei Monti di Palermo (Sicilia). Naturalista Siciliano. (3–4), pp. 147–166.

Catalano, R., Di Stefano, P., Sulli, A., Vitale, F.P. 1996. Paleogeography and structure of the central Mediterranean: Sicily and its offshore area. Tectonophysics 260, pp. 291-323.

Catalano, R., Doglioni, C., and Merlini, S. 2001. On the mesozoic ionian basin. Geophys. J. Int. 144, pp. 49–64. doi:10.1046/j.0956-540X.2000.01287.x.

Catalano, R., Franchino, A., Merlini, S. & Sulli, A. 2000. A crustal section from the Eastern Algerina basin to the Ionian ocean (Central Mediterranean). Memorie Società Geologica Italiana 55, pp. 71–85.

Catalano, S., Romagnoli, G., Tortorici, G. 2010. Kinematics and dynamics of the Late Quaternary rift flank deformation in the Hyblean Plateau (SE Sicily). Tectonophysics 486, pp. 1–14. http://dx.doi.org/10.1016/j.tecto.2010.01.013.

Catalano, R., Valenti, V., Albanese, C., Accaino, F., Sulli, A., Tinivella, U., Morticelli, M.G., Zanolla, C., Giustiniani, M., 2012. Sicily's fold–thrust belt and slab roll–back: the SI.RI.PRO. seismic crustal transect. Journal of the Geological Society, doi: 10.1144/jgs2012–099.

Cavallaro, D., Monaco, C., Polonia, A., Sulli, A., & Di Stefano, A. 2017. Evidence of positive tectonic inversion in the north-central sector of the Sicily Channel (Central Mediterranean). Natural Hazards, 86, pp. 233–251. https://doi.org/10.1007/s11069-016-2515-6.

Cello, G., 1987. Structure and deformation processes in the Strait of Sicily "rift zone". Tectonophysics 141, pp. 237–247.

Cello, G., Crisci, G. M., Marabini, S. & Tortorici, L. 1985. Transten- sive tectonics in the Strait of Sicily: structural and volcanological evidence from the island of Pantelleria. Tectonics 4, pp. 311-322.

Chihi, L., 1992. Seismotectonic study in Central and southern Tunisia. Tectonophysics 209 (1e4), pp. 175-178.

Civile, D., Lodolo, E., Tortorici, L., Lanzafame, G., Brancolini, G., 2008. Relationships between magmatism and tectonics in a continental rift: the Pantelleria Island region (Sicily Channel, Italy). Mar. Geol. 251, pp. 32–46.

Civile, D., Lodolo, E., Accettella, D., Geletti, R., Ben-Avraham, Z., Deponte, M., Facchin, L., Ramella, R., Romeo, R. 2010. The Pantelleria graben (Sicily Channel, Central Mediterranean): an example of intraplate 'passive' rift. Tectonophysics 490, pp. 173–183.

Civile, D., Lodolo, E., Alp, H., Ben-Avraham, Z., Cova, A., Baradello, L., Accettella, D., Burca, M., Centonze, J. 2014. Seismic stratigraphy and structural setting of the Adventure Plateau (Sicily Channel). Mar. Geophys. Res. 35 (1), pp. 37–53. http://dx.doi. org/10.1007/s11001-013-9205-5.

Civile, D., Lodolo, E., Zecchin, M., Ben-Avraham, Z., Baradello, L., Accettella, D., Cova, A., Caffau, M. 2015. The lost Adventure Archipelago (Sicilian Channel, Mediterranean Sea): morpho-bathymetry and Late Quaternary palaeogeographic evolution. Global Planet. Change 125, pp. 36–47.

Civile, D., Lodolo, E., Caffau, M., Baradello, L., & Ben-Avraham, Z. 2016. Anatomy of a submerged archipelago in the Sicilian Channel (central Mediterranean Sea). Geological Magazine, 153(1), pp. 160–178. https://doi.org/10.1017/S0016756815000485

Civile, D., Lodolo, E., Accaino, F., Geletti, R., Schiattarella, M., Giustiniani, M., Fedorik, J., Zecchin, M., & Zampa, L. 2018. Capo Granitola-Sciacca Fault Zone (Sicilian Channel, Central Mediterranean): Structure vs magmatism. Marine and Petroleum Geology, 96(February), pp. 627–644. https://doi.org/10.1016/j.marpetgeo.2018.05.016.

Cocchi, L., Passaro, S., Tontini, F. C. & Ventura, G. 2017. Volcanism in slab tear faults is larger than in island-arcs and back-arcs. Nature communications, 8(1), pp. 1-12.

Colantoni, P. 1975. Note di geologia marina sul Canale di Sicilia. G. Geol. 15, pp. 181-207.

Coltelli, M., Cavallaro, D., D'Anna, G., D'Alessandro, A., Grassa, F., Mangano, G., Patanè, D., Gresta, S., 2016. Exploring the submarine Graham Bank in the Sicily Channel. Ann. Geophys. 59 (2). http://dx.doi.org/10.4401/ag-6929. S0208.

Compagnoni, R., Morlotti, E., Torelli, L., 1989. Cristalline and sedimentary rocks from the scarps of the Sicily-Sardinia trough and Cornaglia Terrace (Soutwestern Tyrrhenian Sea): paleogeographic and geodynamic implication. Chem. Geol. 77, pp. 271-315.

Cuffaro, M., Riguzzi, F., Scrocca, D., Doglioni, C. 2011. Coexisting tectonic settings: The example of the southern Tyrrhenian Sea. Int. J. Earth Sci., 100, pp. 1915–1924.

Cultrera, F., Barreca, G., Burrato, P., Ferranti, L., Monaco, C., Passaro, S., Pepe, F., & Scarfì, L. 2016. Active faulting and continental slope instability in the gulf of patti (Tyrrhenian side of NE sicily, Italy): A field, marine and seismological joint analysis. Natural Hazards, 86, pp. S253–S272. https://doi.org/10.1007/s11069-016-2547-y.

Cultrera, F., Barreca, G., Ferranti, L., Monaco, C., Pepe, F., Passaro, S., Barberi, G., Bruno, V., Burrato, P., Mattia, M., Musumeci, C., & Scarfì, L. 2017. Structural architecture and active deformation pattern in the northern sector of the Aeolian-Tindari-Letojanni fault system (SE Tyrrhenian Sea-NE Sicily) from integrated analysis of field, marine geophysical, seismological and geodetic data. Italian Journal of Geosciences, 136(3), pp. 399–417. https://doi.org/10.3301/IJG.2016.17.

D'Argenio, A., 1999. Analisi stratigrafica delle successioni mesozoiche e terziarie dell'offshore della Sicilia nord–occidentale. Naturalista sicil., S. IV, XXIII (1–2), pp. 43–61.

De Astis, G., Ventura, G., & Vilardo, G. 2003. Geodynamic significance of the Aeolian volcanism (Southern Tyrrhenian Sea, Italy) in light of structural, seismological and geochemical data. Tectonics, 22(4), pp. 1–17. https://doi.org/10.1029/2003tc001506

De Guidi, G., Lanzafame, G., Palano, M., Puglisi, G., Scaltrito, A., Scarfì, L., 2013. Multidisciplinary study of the Tindari Fault (Sicily, Italy) separating ongoing contractional and extensional compartments along the active Africa–Eurasia convergent boundary. Tectonophysics 558, pp. 1–17.

Dellong, D., Klingelhoefer, F., Kopp, H., Graindorge, D., Margheriti, L., Moretti, M., Murphy, S., & Gutscher, M. A. 2018. Crustal Structure of the Ionian Basin and Eastern Sicily Margin: Results From a Wide-Angle Seismic Survey. Journal of Geophysical Research: Solid Earth, 123(3), pp. 2090–2114. https://doi.org/10.1002/2017JB015312.

Dewey, J.F., Helman, M.L., Turco, E., Hutton, D.H.W., Knott, S.D., 1989. Kinematics of the western Mediterranean, in Coward, M.P., Dietrich, D., and Park, R.G., eds., Alpine Tectonics, The Geological Society of London, Special Publication 45, pp. 265–283.

Dlala, M., Rebai¨, S., 1994. Relation compression–extension Miocène supérieur à Quaternaire en Tunisie: implication sismotectonique. C. R. Acad. Sci. Paris, Ser. IIa 319, pp. 945–950.

Doglioni, C., Ligi, M., Scrocca, D., Bigi, S., Bortoluzzi, G., Carminati, E., Cuffaro, M., D'Oriano, F., Forleo, V., Muccini, F., & Riguzzi, F. 2012. The tectonic puzzle of the Messina area (Southern Italy): Insights from new seismic reflection data. Scientific Reports, 2, pp. 2–10. https://doi.org/10.1038/srep00970.

Fabbri, A., Rossi, S., Sartori, R., and Barone, A. 1982. Evoluzione neogenica dei margini marini dell'Arco Calabro-Peloritano: implicazioni geodinamiche. Mem. Soc. Geol. It. 24, pp. 357–366.

Falzone, G., Lanzafame, G., Rossi, P.L., 2009. Il vulcano Ferdinandea nel Canale di Sicilia. Geoitalia 29, pp. 15–20.

Fedorik, J., Toscani, G., Lodolo, E., Civile, D., Bonini, L., Seno, S., 2018. Structural analysis and miocene-to-present tectonic evolution of a lithospheric-scale, transcur- rent lineament: the Sciacca Fault (Sicilian Channel, Central Mediterranean Sea). Tectonophysics 722, pp. 342–355.

Ferrari, L., and Manetti, P. 1993. Geodynamic framework of the Tyrrhenian volcanism: A review, Acta Vulcanol., 3, pp. 1–10.

Finetti, I. 1984. Geophysical study of the Sicily Channel rift zone. Boll. Geofis. teor. appl. 101-102, pp. 3-28.

Finetti, I.R., Del Ben, A., 1986. Geophysical study of the Tyrrhenian opening. Bollettino di Geofisica Teorica ed Applicata 27, pp. 74–151.

Finetti, I.R., Del Ben, A., 2005. Crustal tectono-stratigraphic setting of the Pelagian foreland from new CROP seismic data. In: Finetti, I.R. (Ed.), CROP Project: Deep Seismic Exploration of the Central Mediterranean and Italy. Elsevier, Amsterdam, pp. 581–595.

Finetti, I. R., Lentini, F., Carbone, S., Del Ben, A., Di Stefano, A., Forlin, E., Guarnieri, P.,Pipan, M. & Prizzon, A. 2005. Geological outline of Sicily and lithospheric tectono-dynamics of its Tyrrhenian margin from new CROP seismic data. CROP Project: deep seismic exploration of the central Mediterranean and Italy, 319-375. In: Finetti, I.R. (Ed.), CROP Project: Deep Seismic Exploration of the Central Mediterranean and Italy. Elsevier, Amsterdam, pp. 581–595.

Finetti, I. and Morelli, C. 1972. Wide scale digital seismic exploration of the Mediterranean Sea. Boll. Geofis. Teor. Appl., 14, pp. 291--342.

Gallais, F., Gutscher, M.-A., Graindorge, D., Chamot-Rooke, N., and Klaeschen, D. 2011. AMiocene tectonic inversion in the Ionian Sea (central Mediterranean): evidence from multichannel seismic data. J. Geophys. Res. 116, B12108. doi:10. 1029/2011JB008505.

Gamberi, F., Marani, M.and Savelli, C. 1997. Tectonic, vol- canic and hydrothermal features of a submarine portion of the Aeolian arc (Tyrrhenian Sea), Mar. Geol., 140, 167–181.

Gambino, S., Barreca, G., Bruno, V., De Guidi, G., Ferlito, C., Gross, F., Mattia, M., Scarfi, L. & Monaco, C. 2022. Transtension at the Northern Termination of the Alfeo-Etna Fault System (Western Ionian Sea, Italy): Seismotectonic Implications and Relation with Mt. Etna Volcanism. Geosciences, 12(3), pp. 128.

Gargano, C. 1994 Carta geologica della zona di Messina Monti Peloritani Sicilia NE. Scala 1:25.000 S.El.CA. Firenze.

Gasparo Morticelli, M., Sulli, A., Agate, M. 2016. Sea–land geology of Marettimo (Egadi Islands, Central Mediterranean Sea). J. Map. 12 (5), pp. 1093–1103.

Ghielmi, M., Amore, M. R., Bolla, E. M., Carubelli, P., Knezaurek, G., & Serraino, C. 2012. The Pliocene to Pleistocene Succession of the Hyblean Foredeep (Sicily, Italy). Search and Discovery Article, 30221, 30220.

Ghisetti, F.1979. Relazioni tra strutture e fasi trascorrenti e distensive lungo i sistemi Messina-Fiumefreddo, Tindari-Letojanni e Alia-Malvagna (Sicilia nordor- ientale): Uno studio microtettonico, Geol. Rom., 18, pp. 23–58.

Ghisetti, F.C., Gorman, A.R., Grasso, M., Vezzani, L. 2009. Imprint of foreland structure on the deformation of a thrust sheet: the Plio-Pleistocene Gela Nappe (southern Sicily, Italy). Tectonics 28 (4). http://dx.doi.org/10.1029/2008TC002385. TC4015.

Ghisetti, F., Vezzani, L., 1980. The structural features of the Iblean plateau and of the Monte Iudica area (South Eastern Sicily). A microtectonic contribution to the deformational history of the Calabrian Arc. Boll. Soc. Geol. Ital. 99, pp. 57–102.

Ghisetti, F., Vezzani, L. 1984. Thin–skinned deformation of the Western Sicily thrust belt and relationships with crustal shortening mesostructural data on the Mt. Kumeta–Alcantara fault zone and related structures. Bolletin Society Geology Italy 103, pp. 129–157.

Ghribi, R., Bouaziz, S. 2010. Neotectonic evolution of the eastern Tunisian platform from paleostress reconstruction. J. Hydrocarb. Mines Environ. Rres. Rennes 1 (1), pp. 14–25.

Gillot, P. Y. 1987. Histoire volcanique des Iles Eoliennes: Arc insulaire or complexe orogenique anulaire?, dissertation thesis, Paris Univ., Paris.

Goes, S., Jenny, S., Hollenstein, C., Kahle, H. G., & Geiger, A. 2004. A recent tectonic reorganization in the south-central Mediterranean. Earth and Planetary Science Letters, 226(3–4), pp. 335–345. https://doi.org/10.1016/j.epsl.2004.07.038.

Grasso, M., Behncke, B., Di Geronimo, I., Giuffrida, S., La Manna, F., Maniscalco, R., Pedley, H.M., Raffi, S., Schmincke, H.U., Strano, D., Sturiale, G., 2004. Carta geologica del bordo nord-occidentale dell'Avampaese Ibleo e del fronte della Falda di Gela. S.EL.C.A., Firenze.

Grasso, M., Butler, R.W.H., 1991. Tectonic controls on the deposition of late Tortonian sediments in the Caltanissetta basin of Central Sicily. Memorie Società Geologica Italiana 47, pp. 313–324.

Grasso, M., Reuther, C.D., 1988. The western margin of Hyblean plateau: a neotectonic transform system on the SE Sicilian foreland. Ann. Tectonicae 2, pp. 107–120.

Gueguen, E., Tavernelli, E., Renda, P., Tramutoli, M. 2002. The geodynamics of the Southern Tyrrhenian Sea margin as revealed by integrated geological, geophysical and geodetic data. Bollettino Società Geologica Italiana 121 (vol. Spec. 1), pp. 77– 85.

Gutscher, M. A., Dominguez, S., De Lepinay, B. M., Pinheiro, L., Gallais, F., Babonneau, N., Cattaneo, A., Le Faou, Y., Barreca, G., Micallef, A., & Rovere, M. 2016. Tectonic expression of an active slab tear from high-resolution seismic and bathymetric data offshore Sicily (Ionian Sea). Tectonics, 35(1), pp. 39–54. https://doi.org/10.1002/2015TC003898.

Gvirtzman, Z., and Nur, A. 1999. Formation ofMount Etna as a consequence of slab rollback, Nature, 401, 782–785.

Gvirtzman, Z., and Nur, A. 2001. Residual topography, litho- spheric thickness, and sunken slabs in the central Mediterranean, Earth Planet. Sci. Lett., 187,pp. 117– 130.

Hippolyte, J., Angelier, J. and Roure, F. 1994. A major change revealed by Quaternary stress patterns in the Southern Apennines, Tectonophysics, 230, 199–210.

Illies, J. H. 1981. Graben formation: the Maltese Islands a case history. Tectonophysics 73,pp. 151-168.

Incandela, A., 1996. Deformazioni neogeniche nelle Isole di Favignana e Levanzo (Isole Egadi). Mem. Soc. Geol. It. 51, pp. 129–135.

Jongsma, D., Van Hinte, J. E. and Woodside, J. M., 1985. Geologic structure and neotectonics of the north African continental margin south of Sicily. Marine and Petroleum Geology, 2, pp. 156-179.

Jongsma, D., Woodside, J. M., King, G. C. P., & van Hinte, J. E. 1987. The Medina Wrench: a key to the kinematics of the central and eastern Mediterranean over the past 5 Ma. Earth and Planetary Science Letters, 82(1–2), pp. 87–106. https://doi.org/10.1016/0012-821X(87)90109-9.

Keller, J. 1980. The Island of Salina, Rend. Soc. It. Miner. Petrol., 36, pp. 489–524.

Keller, J. 1982. Mediterranean island arcs, in Andesites, edited by R. S. Thorpe, John Wiley, Hoboken, N. J., pp. 307–325.

Lanzafame, G. and Bousquet, J. C. 1997. The Maltese es- carpment and its extension from Mt. Etna to Aeo- lian Islands (Sicily): Importance and evolution of a lithospheric discontinuity, Acta Vulcanol., 9, pp. 121– 135.

Lentini, F., Carbone, S.and Catalano, S. 1994, Main structural domains of the Central Mediterranean re- gion and their Neogene tectonic evolution, Boll. Geofis. Teor. Appl., 36, pp. 103–125.

Lentini, F. 2000. Carta Geologica della Provincia di Messina scala 1:50.000 e Nota Illustrativa a cura di Lentini F. Carbone S. e Catalano S. Ed. SELCA – Firenze.

Letouzey, J. 1986. Cenozoic paleo-stress pattern in the Alpine Foreland and Structural interpretation in a platform basin. Tectonophysics 132, pp. 215–235.

Lo Presti, V., Antonioli, F., Palombo, M. R., Agnesi, V., Biolchi, S., Calcagnile, L., Di Patti, C., Donati, S., Furlani, S., Merizzi, J., Pepe, F., Quarta, G., Renda, P., Sulli, A., & Tusa, S. 2019. Palaeogeographical evolution of the Egadi Islands (western Sicily, Italy). Implications for late Pleistocene and early Holocene sea crossings by humans and other mammals in the western Mediterranean. Earth-Science Reviews, 194(December 2018), pp. 160–181. https://doi.org/10.1016/j.earscirev.2019.04.027

Lodolo, E., Civile, D., Zanolla, C., Geletti, R., 2012. Magnetic signature of the sicily channel volcanism. Mar. Geophys. Res. 33, pp. 33–44.

Loreto, M.F.; Palmiotto, C.; Muccini, F.; Ferrante, V.; Zitellini, N. 2021. Inverted Basins by Africa–Eurasia Convergence at the Southern Back-Arc Tyrrhenian Basin. Geosciences, 11, 117. https:// doi.org/10.3390/geosciences11030117.

Loreto, M. F., Zitellini, N., Ranero, C. R., Palmiotto, C., Prada, M. 2021. Extensional tectonics during the Tyrrhenian back-arc basin formation and a new morpho-tectonic map. Basin Research, 33(1), pp.138-158.

Maesano, F. E., Tiberti, M. M., & Basili, R. 2020. Deformation and Fault Propagation at the Lateral Termination of a Subduction Zone: The Alfeo Fault System in the Calabrian Arc, Southern Italy. Frontiers in Earth Science, 8(April), pp. 1–16. https://doi.org/10.3389/feart.2020.00107.

Maldonado, A. & Stanley, D. I. 1977. Lithofacies as a function of depth in the Strait of Sicily. Geology 2, pp. 111-117.

Mastrolembo Ventura, B., Serpelloni, E., Argnani, A., Bonforte, M., Anzidei, P.B. and & Puglisi, G. 2009. Kinematics of Sicily in the framework of the Nubia-Eurasia plate convergence: new insights into microplate fragmentation and elastic strain accumulation at faults from modelling of gps velocities. Geological Society Special Publication, 316(November), pp. 155–172. https://doi.org/10.1144/SP316.9.

Mastrolembo Ventura, B., Serpelloni, E., Argnani, A., Bonforte, A., Bürgmann, R., Anzidei, M., Baldi, P., & Puglisi, G. 2014. Fast geodetic strain-rates in eastern Sicily (southern Italy): New insights into block tectonics and seismic potential in the area of the great 1693 earthquake. Earth and Planetary Science Letters, 404(February), pp. 77–88. https://doi.org/10.1016/j.epsl.2014.07.025

Mattia, M., Palano, M., Bruno, V., Cannavò, F., Bonaccorso, A., Gresta, S., 2008. Tectonic features of the Lipari–Vulcano complex (Aeolian Archipelago, Italy) from 10 years (1996–2006) of GPS data. Terra Nova 20, pp. 370–377.

Melki, F., Zouaghi, T., Chelbi, M. Ben, Bédir, M., & Zargouni, F. 2010. Tectono-sedimentary events and geodynamic evolution of the Mesozoic and Cenozoic basins of the Alpine Margin, Gulf of Tunis, north-eastern Tunisia offshore. Comptes Rendus - Geoscience, 342(9), pp. 741–753. https://doi.org/10.1016/j.crte.2010.04.005.

Melki, F., Zouaghi, T., Ben Chelbi, M., Bédir, M., & Zargouni, F. 2012. Role of the NE-SW Hercynian master fault systems and associated lineaments on the structuring and evolution of the Mesozoic and Cenozoic basins of the Alpine Margin, Northern Tunisia. Tectonics Evgenii Sharkov, pp. 131–168. IntechOpen. https://doi.org/10.5772/50145.

Milano, G., Vilardo, G.and Luongo, G. 1994. Continental collision and basin opening in southern Italy: A new plate subduction in the Tyrrhenian Sea?, Tec- tonophysics, 230, pp. 249–264.

Milia, A., Iannace, P., & Torrente, M.M. 2021. The meeting place of backarc and foreland rifting: The example of the offshore western Sicily (Central Mediterranean). Global and Planetary Change, 198(February 2020). https://doi.org/10.1016/j.gloplacha.2020.103408

Monaco, C., Tortorici, L., 1995. Tectonic role of ophiolite–bearing terranes in the development of the Southern Apennine orogenic belt. Terra Nova 7, pp. 153–160.

Morelli, C., Gantar, C. & Pisani M. 1975a. Bathymetry, gravity (and magnetism) in the Strait of Sicily and the Ionian Sea. Boll. Geofis. teor. appl. 17, pp. 39-58.

Morelli, C., Pisani, M. & Gantar, C. 1975b. Geophysical anomalies and tectonics in the Western Mediterranean. Boll. Geofis. teor. appl. 18, pp. 211-249.

Musumeci, C., Scarfì, L., Palano, M., and Patanè, D. 2014. Foreland segmentation along an active convergent margin: new constraints in southeastern Sicily (Italy) from seismic and geodetic observations. Tectonophysics 630, pp. 137–149. doi:10.1016/j.tecto.2014.05.017.

Neri, G., Caccamo, D., Cocina, O. and Montalto, A. 1996. Geodynamic implications of earthquake data in the Southern Tyrrhenian Sea, Tectonophysics, 258, pp. 233–249.

Neri, G., Barberi, G., Oliva, G., Orecchio, B. 2005. Spatial variations of seismo- genic stress orientations in Sicily, south Italy. Phys. Earth Planet. Inter. 148, pp. 175–191.

Nigro, F., Renda, P. 2000. Un modello di evoluzione tettono–sedimentaria dell'avanfossa neogenica siciliana. Bollettino Società Geologica Italiana, 119, pp. 667–686.

Ogniben, L. 1960. Note illustrative dello schema geologico della Sicilia nordorientale. Riv. Min. Sic. 64–65, pp. 183–212.

Ogniben, L. 1985. Relazione sul modello geodinamico "conservativo " della regione italiana, Commissione ENEA–ENEL per lo studio dei problemi sismici connessi con la realizzazione di impianti nucleari. ENEA, Roma.

Oldow, J.S., Channel, J.E.T., Catalano, R., D'Argenio, B. 1990. Contemporaneous thrusting and large–scale rotations in the western Sicilian fold and thrust belt. Tectonics, 9, pp. 661–681.

Palano, M., Ferranti, L., Monaco, C., Mattia, M., Aloisi, M., Bruno, V., Cannavò, F., Siligato, G. 2012. GPS velocity and strain fields in Sicily and southern Calabria, Italy: updated geodetic constraints on tectonic block interaction in the central Mediterranean. J. Geophys. Res. 117, B07401, http://dx.doi.org/10.1029/2012JB009254.

Palmiotto, C., Corda, L., Bonatti, E. 2017. Oceanic Tectonic Islands. Terra Nova 29, pp. 1–12.

Palmiotto, C. & Loreto, M. F. 2019. Regional scale morphological pattern of the Tyrrhenian Sea: New insights from EMODnet bathymetry. Geomorphology, 332, pp. 88–99. https://doi.org/10.1016/j.geomorph.2019.02.010.

Peccerillo, A. 2005. Plio-quaternary Volcanism in Italy. Petrology, Geochemistry, Geodynamics. Springer, Heidelberg, pp. 365.

Peccerillo, A. 2020. Campania volcanoes: petrology, geochemistry, and geodynamic significance. In Vesuvius, Campi Flegrei, and Campanian Volcanism, 1st ed.; De vivo B., Belkin, H.E., Rolandi, G., Eds.; Elsevier Inc.: Amsterdam, The Netherlands.

Pepe, F., Bertotti, G., Cella, F. and Marsella E. 2000. Rifted margins formation in the Southern Tyrrhenian Sea: A high-resolution seismic profile across the north Sicily continental margin, Tectonics, 19, pp. 241–257.

Pepe, F., Sulli, A., Catalano, R. & Valenti, V. 2003. New data on the structural setting of the Elimi Chain (South-western Tyrrhenian sea) from reprocessing of multichannel seismic profiles (MS grid). In EGS-AGU-EUG Joint Assembly, April (p. 5295).

Pepe, F., Sulli, A., Bertotti, G. & Catalano, R. 2005. Structural highs formation and their relationship to sedimentary basins in the north Sicily continental margin (southern Tyrrhenian Sea): Implication for the Drepano Thrust Front. Tectonophysics, 409(1–4), pp. 1–18. https://doi.org/10.1016/j.tecto.2005.05.009.

Pepe, F., Corradino, M., Parrino, N., Besio, G., Presti, V. Lo, Renda, P., Calcagnile, L., Quarta, G., Sulli, A., & Antonioli, F. 2018. Boulder coastal deposits at Favignana Island rocky coast (Sicily, Italy): Litho-structural and hydrodynamic control. Geomorphology, 303, pp. 191–209. https://doi.org/10.1016/j.geomorph.2017.11.017.

Pierantoni, P.P.; Macchiavelli, C.; Penza, G.; Schettino, A.; Turco, E. 2020. Kinematics of the Tyrrhenian-Apennine system and implications for the origin of the Campanian magmatism. In Vesuvius, Campi Flegrei, and Campanian Volcanism, 1st ed.; De vivo B., Belkin, H.E., Rolandi, G., Eds.; Elsevier Inc.: Amsterdam, The Netherlands; pp. 520.

Polonia, A., Torelli, L., Artoni, A., Carlini, M., Faccenna, C., Ferranti, L., Gasperini, L., Govers, R., Klaeschen, D., Monaco, C., Neri, G., Nijholt, N., Orecchio, B., & Wortel, R. 2016. The Ionian and Alfeo-Etna fault zones: New segments of an evolving plate boundary in the central Mediterranean Sea? Tectonophysics, 675, pp. 69–90. https://doi.org/10.1016/j.tecto.2016.03.016.

Presti, D.; Billi, A.; Orecchio, B.; Totaro, C.; Faccenna, C.; Neri, G. 2013. Earthquake focal mechanisms, seismogenic stress, and seismotectonics of the Calabrian Arc, Italy. Tectonophysics, 602, pp. 153–175

Rebaï, S., Philip, H., Taboada, A., 1992. Modern tectonic stress field in the Mediterranean region; evidence for variation in stress directions at different scales. Geophys. J. Int. 110, pp. 106–140.

Rekhiss, F. 2007. Mode d` le d'e´ volution structurale et géodynamique à l'extrémité´ orientale de la chaîne alpine d'Afrique du Nord, Thèse d'Etat en Géologie, université´ de Tunis El Manar, p.285.

Reuther, C.D., Ben-Avraham, Z., Grasso, M. 1993. Origin and role of major strike-slip transfers during plate collision in the central Mediterranean. Terra. Nova 5 (3), pp. 249–257.

Reuther, C. D. & Eisbachr. G. H. 1985. Pantelleria rift - crustal extension in a convergent intraplate setting. Geol. Rdsch. 74, pp. 585- 597.

Rigane, A., and Gourmelen, C. 2011, Inverted intracontinental basin and vertical tectonics: The Saharan Atlas in Tunisia, J. Afr. Earth Sci., 61, pp. 109–128, doi:10.1016/j.jafrearsci.2011.05.003.

Rotolo, S.G., Castorina, F., Cellula, D., Pompilio, M. 2006. Petrology and geochemistry of submarine volcanism in the Sicily Channel. J. Geol. 114, pp. 355–365.

Roure, F., Howell, D.G., Muller, C., Moretti, I. 1990. Late Cenozoic subduction complex of Sicily. Journal of Structural Geology, 12, pp. 259–266.

Rovere, M., Wurtz, M. 2015. Atlas of the Mediterranean Seamounts and Seamount-like Structures. IUCN, Gland, Switzerland and Málaga, Spain.

Ruggieri, G. 1966. Primi risultati di ricerche sulla tettonica della Sicilia Occidentale. Geologica Romana, 5, pp. 453–456.

Santo, A. P. and A. Clark, H. 1994. Volcanological evolution of Aeolian Arc (Italy): Inferences from 40Ar/39Ar ages of Filicudi rocks, paper presented at IAVCEI Congress, Int. Assoc. ofVolcanol. and Chem. of the Earth's Inter., Ankara.

Scandone, P., Giunta, G. and Liguori, V. 1974: The connection between Apulia and Sahara continental margins in the Southern Apennines and in Sicily. Mem. Soc. Geol. It., 13, pp. 317-323.

Scandone,P., Patacca,E., Radoicic,R., Ryan, W. B., Cita,M. B.,Rawson,M.,ChezaR,H., Miller,E., Mackenzie,J. & Rossi, S. 1981. Meso- zoic andCenozoic rocks fromMalta Escarpment (central Mediterranean). AAPG Bulletin, 65, pp. 1299–1319.

Scarascia, S., Cassinis, R., Lozej, A., Nebuloni, A., 2000. A seismic and gravimetric model of crustal structures across the Sicily Channel Rift Zone. Boll. Soc. Geol. Ital. 119, pp. 213–222.

Schettino, A., Turco, E. 2011. Tectonic history of the western Tethys since the late Triassic, Geological Society of America Bulletin, 123(1/2), pp. 89–105, doi:10.1130/B30064.1.

Serpelloni, E.; Anzidei, M.; Baldi, P.; Casula, G.; Galvani, A. 2005. Crustal velocity and strain-rate fields in Italy and surrounding regions: New results from the analysis of permanent and non-permanent GPS networks. Geoph. J. Int., 161, pp. 861–880.

Serpelloni, E., Vannucci, G., Pondrelli, S., Argnani, A., Casula, G., Anzidei, M., Baldi, P. & Gasperini, P. 2007. Kinematics of the Western Africa-Eurasia plate boundary from focal mechanisms and GPS data. Geophysical Journal International, 169, pp. 1180–1200.

Serpelloni, E., Bürgmann, R., Anzidei, M., Baldi, P., Mastrolembo Ventura, B., & Boschi, E. 2010. Strain accumulation across the Messina Straits and kinematics of Sicily and Calabria from GPS data and dislocation modeling. Earth and Planetary Science Letters, 298(3–4), pp. 347–360. https://doi.org/10.1016/j.epsl.2010.08.005.

Serri, G., Innocenti, F., & Manetti, P. 2001. Magmatism from Mesozoic to Present: petrogenesis, time-space distribution and geodynamic implications. Anatomy of an Orogen: The Apennines and Adjacent Mediterranean Basins, pp. 77–103. https://doi.org/10.1007/978-94-015-9829-3_8.

Somma R. 2006 - The south-western side of the Calabrian Arc (Peloritani Mountains): geological, structural and AMS evidence for passive clockwise rotations. Journal of Geodynamics, 41(4), pp. 422-439, doi: 10.1016/j.jog.2005.11.00.

Soumaya, A., Ben Ayed, N., Delvaux, D., Ghanmi, M., 2015. Spatial variation of present- day stress field and tectonic regime in Tunisia and surroundings from formal inver- sion of focal mechanisms: geodynamic implications for central Mediterranean. Tectonics 34, pp. 1154–1180.

Sulli, A. 2000. Structural framework and crustal characteristics of the Sardinia Channel Alpine transect in the central Mediterranean. Tectonophysics, 324(4), pp. 321–336. https://doi.org/10.1016/S0040-1951(00)00050-0

Tarquini S., Isola I., Favalli M., Battistini A. (2007) TINITALY, a digital elevation model of Italy with a 10 meters cell size (Version 1.0) [Data set]. Istituto Nazionale di Geofisica e Vulcanologia (INGV). https://doi.org/10.13127/TINITALY/1.0.

Tibaldi, A. 2001. Multiple sector collapses at Stromboli volcano, Italy: How they work, Bull. Volcanol., 63, pp. 112–125.

Tricart, P., Torelli, L., Bouillin, J.P., Rekhiss, F., Argnani, A., Brancolini, G., De Santis L., Peis, D. and Zitellini, N., 1993. Structure and Neogene dynamics of the Northern Tunisia margin. In: M.D. Max and P. Colantoni (Editors), Geological Development of the Sicilian-Tunisian Platform. UNESCO Rep. Mar. Sci., 58, pp. 71-76.

Trua T., Serri G. and P.L. Rossi, 2004. Coexistence of IAB-type and OIB-type magmas in the southern Tyrrhenian back-arc basin , evidence from recent seafloor sampling and geodynamic implications. Coesistenza di magmi di tipo IAB e di tipo OIB nel bacino di retro-arco. In: Marani M.P., Gamberi F. and E. Bonatti (eds.), From seafloor to deep mantle, architecture of the Tyrrhenian back- arc basin. Memorie Descrittive Carta Geologica d'Italia, 64. pp. 83-96.

Turco, E., Macchiavelli, C., Mazzoli, S., Schettino, A., Pierantoni, P.P., 2012. Kinematic evolution of Alpine Corsica in the framework of Mediterranean mountain belts, Tectonophysics, 579, pp. 193–206.

Turco, E.; Macchiavelli, C.; Penza, G.; Schettino, A.; Pierantoni, P.P. 2021. Kinematics of Deformable Blocks: Application to the Opening of the Tyrrhenian Basin and the Formation of the Apennine Chain. Geosciences, 11, 177. https://doi.org/10.3390/geosciences11040177.

Valensise, G., Pantosti, D. 1992. A 125 Kyr-long geological record of seismic source repeatability: the Messina Straits (southern Italy) and the 1908 earthquake (Ms 71/2). Terra Nova 4, pp. 472–483.

van Hinsbergen, D. J. J., Torsvik, T. H., Schmid, S. M., Maţenco, L. C., Maffione, M., Vissers, R. L. M., Gürer, D., & Spakman, W. 2020. Orogenic architecture of the Mediterranean region and kinematic reconstruction of its tectonic evolution since the Triassic. Gondwana Research, 81, pp. 79–229. https://doi.org/10.1016/j.gr.2019.07.009.

Ventura, G., Vilardo, G., Milano, G. and Pino, N.A. 1999. Relationships among crustal structure, volcanism and strike-slip tectonics in the Lipari-Vulcano volcanic complex (Aeolian Islands, Southern Tyrrhenian Sea, Italy), Phys. Earth Planet. Inter., 116, pp. 31– 52.

Verdin, K.L. 2017. Hydrologic Derivatives for Modeling and Applications (HDMA) database: U.S. Geological Survey data release, https://doi.org/10.5066/F7S180ZP.

Weltje, G. J., 1992. Oligocene to Early Miocene sedimentation and tectonics in the southern part of the Calabrian–Peloritan Arc (Aspromonte, southern Italy): a record of mixed–mode piggy–back basin evolution, Basin Research, 4, pp. 37–68.

Westaway, R. 1993. Quaternary uplift of southern Italy, J. Geophys. Res., 98, 21, pp.741–21,772.

Winnock, E. 1981. Structure du Bloc Pelagien. In: Sedimentary Basins of Mediterranean Margins (edited by Wezel F. C.). Technip, Bologna, pp. 445—464.

Zargouni, F. 197). Analyse structural de la chaîne de Lansarine zone des diapirs, Atlas Tunisien. Bulletin de la Société des Sciences Naturelles de Tunsie, 13, pp.97–104.

Zarudzki, E. F. K., 1972. The Strait of Sicily. A Geophysical Study. Rev. Geograph., Phys. et Geol. Dynam., 14, pp. 11-28.

Zitellini, N.; Ranero, C.R.; Loreto, M.F.; Ligi, M.; Pastore, M.; D'Oriano, F.; Prada, M. 2020. Recent inversion of the Tyrrhenian Basin. Geology, 48, pp.123–127.

Zolotarev, V. G. & Socheinikov, V. V. 1980. Geothermal conditions of the African-Sicilian rise. Izv. Earth Phys. 16, pp.202-206.

Zouaghi, T., Bedir, M., Melki, F., Gabtni, H., Gharsalli, R., Bessioud, A., & Zargouni, F. 2011. Neogene sediment deformations and tectonic features of northeastern Tunisia: Evidence for paleoseismicity. Arabian Journal ofGeosciences, 4(7–8), pp. 1301–1314. https://doi.org/10.1007/ s12517-010-0225-z.

Chapter 5 - Proposed kinematic model and Movie

Ch.5.1 - Introduction

The process of evolution of the Apennine Chain is originated by two big tectonic events: the rotation of the Sardinian–Corsican block and the formation of the Tyrrhenian basin.

First Apennine Event

According to (*Schettino & Turco, 2006; Turco et al., 2012*), the first phase of the Apennine evolution (33–19 Ma) generated a long left-lateral transpression along the boundary between the Adriatic Plate and the Sardinian-Corsican block. This transpression, with a major trascurrent component, drove apart the Western Alpine Arc and the Calabrian–Kabylide Arc, which aligned with opposite vergence when the rotation started (Figs. 3.2-3.3).

At the end of this phase the transpressive structure reached its maximum length (*Turco et al., 2012)*. The tectonic mélange that resulted from the deformation of the accretion wedges of the two arcs, locally covered by top-wedge successions (external Liguride flysch), was the proto-Apennine Chain (Fig. 3.3). Rocks belonging to this proto-chain outcrop in the actual Apennine chain along the Tyrrhenian margin from Liguria to northern Calabria (Falda Toscana, Apuane Alps, Argentario, Zannone island, and Cetraro and Verbicaro Units in Calabria). During this phase Adria was migrating toward NNW, while its slab was subducting into the upper mantle. As a consequence, at the end of the rotation phase the Adriatic slab was juxtaposed to the Corsica block, together with the deep portions of the Calabrian accretion wedge. The upper portion of the Calabrian wedge was still attached to the Calabrian arc.

On the southern side, the rotation phase of the Sardinian–Corsican block produced a huge stretch that was thinning the Calabrian–Kabylides Arc in its central portion. Moreover, considering the huge amount of volcanic sediments present in the internal Apennine flysch and external Ligurids successions (*Guerrera et al., 2015*), *Turco et al. (2021)* suppose that during the rotation of the Sardinian–Corsican block a second volcanic arc was forming due to the slab of Adriatic Plate. This arc was located on the eastern side of the block attached to the first embryo of the Apennine chain.

Second Apennine Event

The Tyrrhenian phase that results from the implications of the aforementioned kinematic model is described here. According to this model, this phase starts at the end of the Sardinia-Corsica block rotation, with an eastward jump of the axis of extension in the future Tyrrhenian area (Fig. 5.1). The beginning time of the Tyrrhenian rifting process is not well-constrained. The oldest stratigraphic record, made up of marine sediments in the western Tyrrhenian margin, is middle Tortonian in age (*Sartori, 2003; Milia & Torrente, 2014*; and reference therein). Thus, the onset of rifting could be a few million years older. The ending age of the Sardinia–Corsica block rotation (19 Ma) (*Schettino & Turco, 2006*) was assumed as the starting age of the rifting phase, although early Burdigalian sediments can be found in the Corsica Basin, thereby a basin already existed at that time to the east of Corsica. According to *Turco et al. (2021)*, the sediments associated with the N6 biozone (18 Ma) represent the first syn-rift deposits in the Corsica basin (*Thinon et al., 2016*), unconformably placed on older wedge-top basin sediments of the left-lateral transcurrent structure separating Corsica from Adria. However, it is important to note that the uncertainty about the starting age of Tyrrhenian extension does not affect the rotation model proposed here, because the structuring of the Apennine chain depends on the rotation speed ratios between the kinematic elements of the puzzle and not on their absolute speeds.

The Tyrrhenian rifting presumably started behind the existing Apennine Chain, following the trend of the eastern volcanic arc (Fig. 3.3). In the first phase of rifting, the Sardinia-Corsica margin necessarily underwent an important uplift, which inevitably caused strong erosion and further disruption of the volcanic chain already dismembered by the rifting. The Tyrrhenian extension also determined a separation between the Apennine chain and the Calabrian arc, which moved about different Euler poles with respect to the Sardinia-Corsica block. During this phase, the front of the Apennine Chain is no longer a transpressive structure, but acquires the character of an accretionary wedge. The subducting slab was made up of Adriatic lithosphere, probably teared along an E-W directed strike-slip structure that separated Adria from Apulia from the late Cretaceous to the Eocene (*Schettino & Turco, 2011*) (Fig. 5.1).

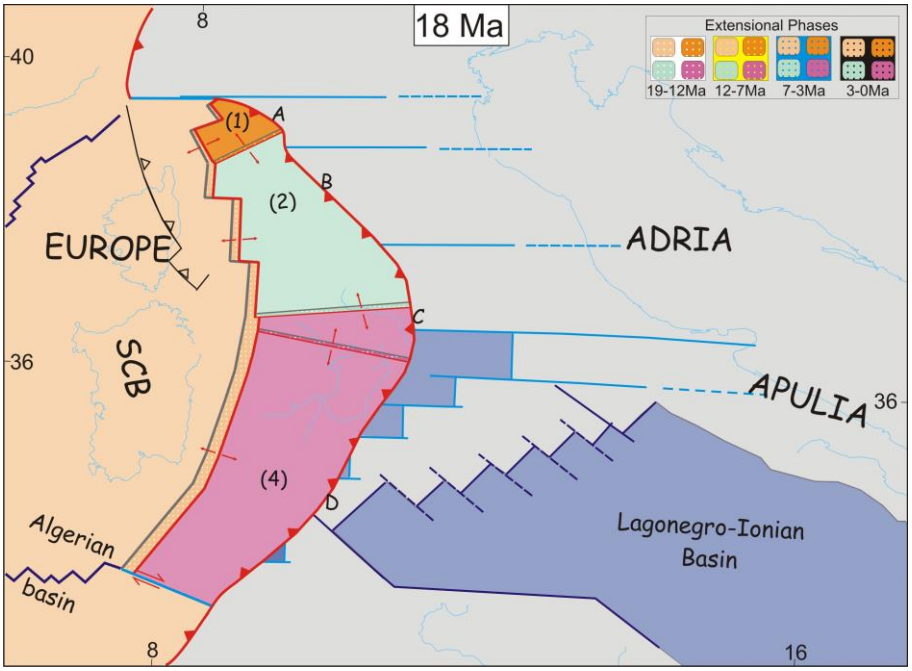

Figure 5.1 - Plate reconstruction of the western Mediterranean region at 18 Ma. The distribution of the continental lithosphere is shown in (gray); the oceanic crust is in blue. Present-day coastlines are shown for reference. The Northern Sector (1) is shown in (orange); the Central Sector (2) is in (aquamarine); the Calabrian Arc Sector (4) is in (dark pink); Europe is in (light orange). Dotted areas are in extension: 19-12 Ma (white dots), 12-7 Ma (yellow dots), 7-3 Ma (light blue dots), 3-0 Ma (black dots). (Red lines) are active boundaries. (Black and Grey lines) are inactive boundaries. (Light blue lines with arrows) are strike-slip faults. (Light blue lines) are transfer faults on the continental lithosphere and (Dark blue lines) are the Middle-Triassic COB. (Black arrows) indicate direction of extension. A: northern Apennine arc, B: central Apennine arc, C: northern Calabrian arc, D: southern Calabrian arc.

Later, the slab-retreat process produced important changes in the evolution of the Tyrrhenian-Apennine system, Sicily included. These changes have been attributed to new lithospheric tears that formed within the Ionian and Adriatic slabs (see Ch.3).

Four phases for the evolution of the Apennine–Tyrrhenian system were distinguished in *Turco et al. (2021)*; an intermediate phase has been added to show also the evolution of Sicily microplate. The five phases are: 1) Beginning of rifting and chain segmentation (19–12 Ma); 2) Separation of the Sicilian sector (12–7 Ma); 3) Vavilov basin formation (7–4.5 Ma); 4) Sicilian Channel extension (4.5-2.5 Ma); and 5) Marsili basin formation (2.5–0 Ma).

Ch.5.2 - Phases of the Evolution

Ch.5.2.1 - Phase 1. Start of Rifting (19–12 Ma)

The Tyrrhenian rift ends in the north against the left-lateral transform fault that links the Apennine chain from the Western Alps (Fig. 5.1). To the south, the rift ends with the right-lateral strike-slip fault that separates the Calabrian arc from Kabylides (Fig. 5.1). At the end of this first phase, the rifting process did not form important marine basins. Only on the Corsica side of the northern Tyrrhenian some marine successions can be attributed to this phase (*Thinon et al., 2016*). However, there are no known successions related to this phase in the southern Tyrrhenian area. As mentioned above, during this phase the Apennine chain was made of two arcs separated by a wide extension area that hosted the Sannite basin. The successions of this basin, described by *Patacca & Scandone (2007)*, form the actual Molise Arc. The model implies that the basin in this phase is located on the lithospheric flexure, generated by the tear fault between the two main slabs, which increased its subsidence (Fig. 5.2).

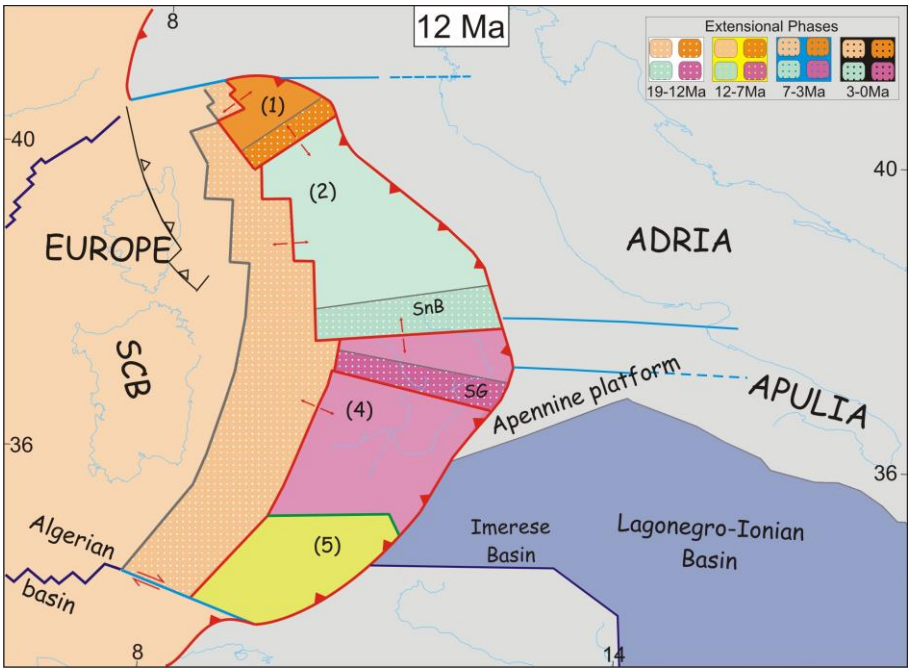

Figure 5.2 - Plate reconstruction of the western Mediterranean region at 12 Ma. The Northern Sector (1) is shown in (orange); the Central Sector (2) is in (aquamarine); the Calabrian Arc Sector (4) is in (dark pink), the Sicilian Sector (5) is in (light green); Europe is in (light orange). Dotted areas are in extension: 19-12 Ma (white dots), 12-7 Ma (yellow dots), 7-3 Ma (light blue dots), 3-0 Ma (black dots). (Green lines) are incipient boundaries. (Red lines) are active boundaries. (Black and Grey lines) are inactive boundaries. (Light blue lines with arrows) are strike-slip faults. (Light blue lines) are transfer faults on the continental lithosphere and (Dark blue lines) are the Middle-Triassic COB. (Black arrows) indicate direction of extension. SCB: Sardinian-Corsican block, SG: Squillace Gulf, SnB: Sannio basin.

Apennine Arc

During the first phase the arc was delimited to the north by a strike-slip fault that drove it apart from the Western Alpine arc. The fault was generated by the STEP fault of the Adriatic slab that at the same time formed an important eastward-migrating lithospheric flexure with NW-SE trend (Fig. 3.4), visible today in the Po river Valley. Along the flexure, an important left-lateral transpression was forming the northern Apennine sector. Geometries of the buried north Apennine structures that characterize the Po river valley are the expression of this complex process. At the beginning of the rifting, the Apennine chain was further divided in two sectors: a northern Apennine arc (A) and a central Apennine arc (B) (Fig. 5.1), separated in transverse direction by the extensional area covered by the Marnoso–Arenacea fm (*Mutti & Lucchi, 1972*) (Fig. 2.15b). The central sector of the Apennine chain is associated with the Adriatic slab-retreat, accompanied by the deformation of the Umbria–Marche succession, which in this phase includes the Lazio–Abruzzi platform. Probably the transversal basins that segmented the Apennine chain were fed by sediment coming from the Liguride units, that is, units of the previous top-wedges that covered the early Apennine chain. The part of the chain affected by this process today separates the two sectors of the Apennine arc and coincides essentially with the area where the Marnoso–Arenacea formation is exposed.

Calabrian Arc

The Calabrian arc is divided in two sectors: north Calabria (C) and south Calabria–Peloritani mounts (D), divided by the Catanzaro Trough (Fig. 5.1). The transversal extension between these two sectors is recorded by late Tortonian successions in the Gulf of Squillace (*Milia & Torrente, 2014*) (Fig. 5.2). To the west, the Calabrian arc is separated by Kabylies by a large right-lateral transtensional fault that thinned the chain and delimited the Tyrrhenian rift to SW. After the subduction of the last remnant of Liguride ocean, the Calabrian wedge thrusted onto the Panormide and Imerese domains, incorporating them in the accretionary wedge. During this phase the trench of the Calabrian arc still provided an access path to the Numidian sands, which continue to fill the entire trench.

Ch.5.2.2 - Phase 2. Sicilian Sector Separation (12–7 Ma)

The second phase of the Tyrrhenian extension is marked by the separation of the Western Sicily chain from the Calabrian arc. The separation takes place along a right-lateral strike-slip fault that transfers the extension between Calabrian Arc and Kabylies further to the East, in the Gela foredeep. Such a large transform structure that cuts the Sicilian upper plate is known as the Monte Kumeta–Alcantara fault. It separates the Sicilian Internal Chain from the External one (*Ghisetti & Vezzani, 1984*). The western Tethys reconstructions proposed in earlier works (e.g., *Schettino & Turco, 2011*) imply the existence of a STEP fault along the northern margin of Sicily until the Tortonian, where the Ionian lithosphere was cut away from the African margin. Here, the main feature of phase 2 of Tyrrhenian extension is related to the activity of this STEP fault. The associated flexure of the African lithosphere determined a southward migration of the External Sicilian chain. The external chain migrated southwards, while the Internal chain continued to migrate toward SE together with the Calabrian Arc (Fig. 5.3). The differential motion between these two sectors (Calabrian and Sicilian) formed the Monte Kumeta-Alcantara fault and caused a large E-W extension in the External Chain. In the section of the chain corresponding to the Gela foredeep, the decrease in thickness associated with the lithospheric flexure of the African plate was not compensated by the thrusting of the External Chain, thus generating a strong tectonic subsidence that started to form the Caltanissetta Basin (Fig. 2.18). The kinematic relations in the other sectors of the Chain and Tyrrhenian Rift remain unchanged in this phase. The Apennine trench passed the Carbonate platforms and Calabrian trench reached the Ionian–Lagonegrese basin.

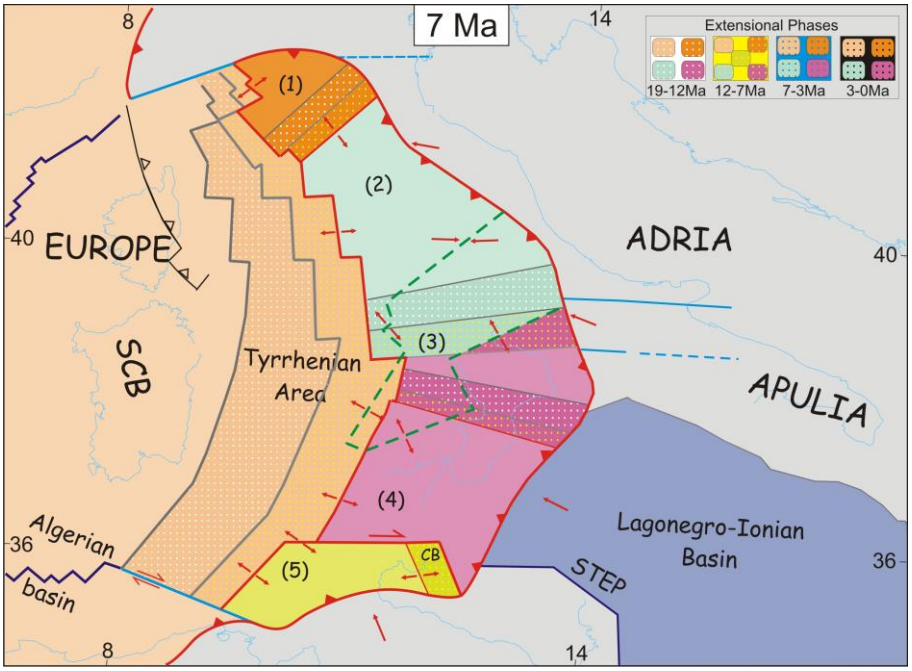

Figure 5.3 - Plate reconstruction of the western Mediterranean region at 7 Ma. The Northern Sector (1) is shown in (orange); the Central Sector (2) is in (aquamarine); the Calabrian Arc Sector (4) is in (dark pink), the Sicilian Sector (5) is in (light green); Europe is in (light orange). Dotted areas are in extension: 19-12 Ma (white dots), 12-7 Ma (yellow dots), 7-3 Ma (light blue dots), 3-0 Ma (black dots). (Green lines) are incipient boundaries. (Red lines) are active boundaries. (Black and Grey lines) are inactive boundaries. (Light blue lines with arrows) are strike-slip faults. (Light blue lines) are transfer faults on the continental lithosphere and (Dark blue lines) are the Middle-Triassic COB. (Black arrows) indicate direction of extension. (Red arrows) are the velocity vectors between Adria and the adjacent sector. SCB: Sardinian-Corsican block, CB, Caltanissetta Basin.

Ch.5.2.3 - Phase 3. Vavilov Basin Formation (7–4.5 Ma)

Phase 3 of Tyrrhenian extension was characterized by the formation of the Vavilov basin, which records major changes in the Ionian slab-retreat process. At the beginning of this phase, the entire Imerese Basin and the promontory of the Panormide Carbonate Platform were accreted to the Calabrian Arc accretionary wedge and the trench entered the narrow Ionian–Lagonegrese ocean corridor (Fig. 5.3). The kinematic model proposed here implies the tearing of the Ionian slab along the Apulian continental margin through a STEP fault, while the eastward propagation of the 41st parallel STEP fault slowed down. On the Sicilian margin, the Ionian tear fault propagated following the continental margin and assumed a different strike. Consequently, during this phase, the units of the Lagonegro basin were also accreted to the SE migrating Calabrian wedge.

The configuration shown in Figure 3.4 suggests that during phase 2 the flexure of the Apulian lithosphere induced a rotation of the future southern Apennine domain determining the opening

of the Vavilov Basin (Fig. 5.4). The particular geometry of the three slabs, whose flexure lines retreat rotating about different poles, gives the new nascent sector a striking rotation that is recorded by the simultaneous formation of the Vavilov Basin. Consequently, the Southern Apennine Sector rotated around a very close pole, located at the northern tip of the Vavilov Basin. At this stage, the Southern Apennine sector includes the Lazio–Abruzzi platform, separated from the Apennine Arc by the Ancona–Anzio Line. On the southern side, the boundary with the Calabrian Arc consists of an articulated low-angle fault that exhumes the Southern Apennines.

Given the reorganization of the phases, it must be specified that the Vavilov basin, the Ancona-Anzio line, The Laga Basin, Montagna dei Fiori and the Southern apennine are active during the entire phase 3 and part of the phase 4, up to 3 Ma ago.

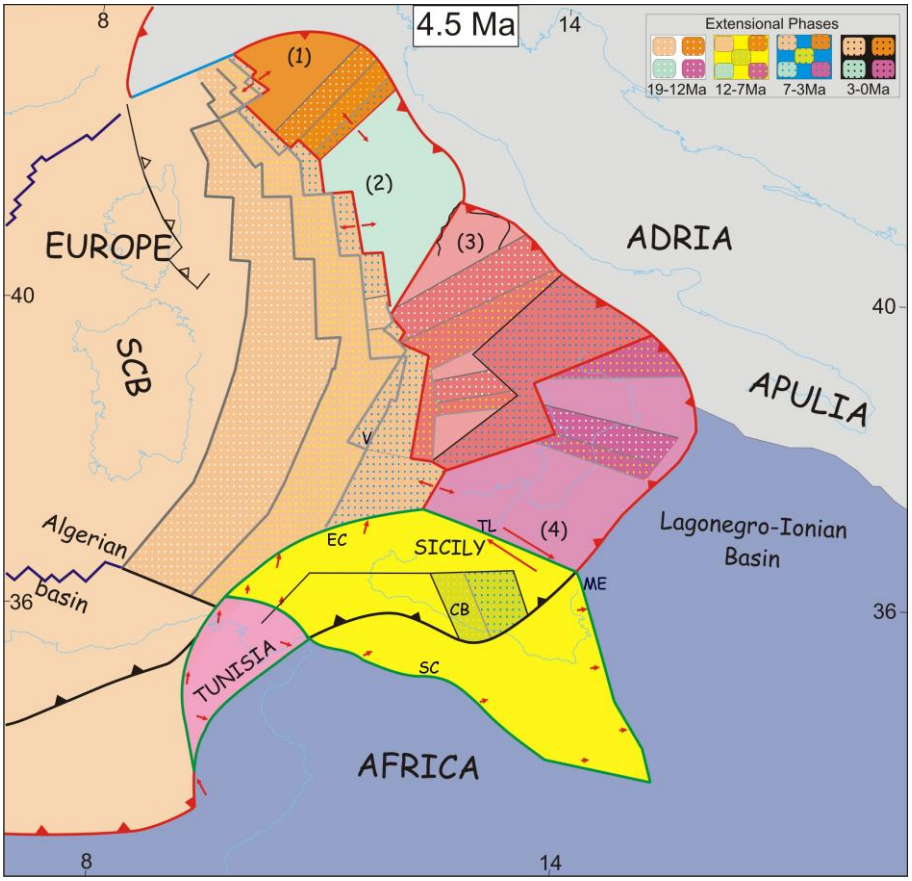

Figure 5.4 - Plate reconstruction of the western Mediterranean region at 4.5 Ma. The Northern Sector (1) is shown in (orange); the Central Sector (2) is in (aquamarine); the Calabrian Arc Sector (4) is in (dark pink), Sicily microplate is in (yellow), Tunisia microplate is in (pink); Europe is in (light orange). Dotted areas are in extension: 19-12 Ma (white dots), 12-7 Ma (yellow dots), 7-3 Ma (light blue dots), 3-0 Ma (black dots). (Green lines) are incipient boundaries. (Red lines) are active boundaries. (Black and Grey lines) are inactive boundaries. (Light blue lines) are strike-slip faults. (Red arrows) indicate direction of extension and compression. CB: Caltanissetta Basin; EC: Elimi Chain; ME: Malta Escarpment; SC: Sicily Channel; SCB: Sardinian-Corsican block; TL: Taormina Line; V: Vavilov Basin.

Vavilov Basin (7-3 Ma)

Phase 3 marks the beginning of the differentiation of the Tyrrhenian basin in two areas, roughly separated by the 41st parallel lineament (*Selli, 1981*). As mentioned above, the formation of the Vavilov Basin, located south of the lineament, arises from the rotation of the Southern Apennine Sector. The extension begins on the eastern margin and propagates with the rotation, significantly increasing the extension of the Southern Tyrrhenian Sea. The abyssal plain, more than 3500 m deep, probably made up of exhumed mantle or oceanic crust, is covered by limited thicknesses of Pliocene sediments (*Kastens & Mascle, 1987*). Therefore, the abyssal area of the basin began to form in the post-Messinian age. The Vavilov basin, with its triangular shape and the fan of extensional structures placed on the Apennine margin, provides the best kinematic record of the rotation of the Southern Apennine Sector. The magnetic features of the abyssal plain, on the other hand, appear less clear (Fig. 2.6a).

Ancona-Anzio Line (7-3 Ma)

The kinematics of the Ancona-Anzio line, which represents the boundary between the Umbria-Marche Apennine and the Lazio–Abruzzi Platform, was the facies line between the Carbonate Platform and Basin during the Mesozoic. The role of this structure has been much debated (*Dallan Nardi et al., 1971; Castellarin et al., 1982; Cipollari & Cosentino, 1991*). The Southern Apennine Sector represents, according to the used rotation model, a portion of the upper plate placed above three slabs. This boundary assumes an important kinematic role for the evolution of the Apennine Arc. The rotation of the two sectors around different poles generates a right-lateral transpression that cuts the Adriatic front of the chain, forming a triple junction between three transpressive trenches (Figs 3.3 and 3.4). The northern section of the trench forms the northern segment of the Ancona-Anzio line and coincides with the front of the Sibillini Mountains with eastern vergence. It represents the boundary between Adria and the Central Sector of the Apennine arc. The southern section of the line represents the boundary between the Central Sector and the Southern Apennine Sector. In this section, the transpression with western vergence is confirmed by the Antrodoco1 well (*Cappelletti et al., 2009-2017*). The opposite vergence between the two lines gives the Ancona–Anzio line its typical flexure. The third section is outlined by the front of the Gran Sasso, which represents the boundary between the Southern Apennine Sector and Adria foreland and is characterized by right transpressive kinematics.

Laga Basin and Montagna dei Fiori (7-3 Ma)

The Ancona-Anzio line, which cut the Adriatic front of the chain above the flexure of the Adriatic slab, forms a deep depression at the triple junction, not compensated by the essentially right-lateral Gran Sasso front. The Laga Basin formed at this location, fed by the pre-Tyrrhenian Apennine flysches. At the same time, the front of the Sibillini Mountains was migrating eastwards, forming the Montagna dei Fiori with an axis orthogonal to the Gran Sasso front.

Southern Apennine (7-3 Ma)

The formation of the Southern Apennines is perhaps the most interesting result of the kinematic model proposed by *Turco et al. (2021)*. At the beginning of phase 3, the Apennine Arc and the Calabrian Arc were separated by the Sannio Basin. The tectonic units that form the actual Southern Apennines (carbonatic platform and Lagonegrese Units) represented the basal part of the accretionary wedge of the Calabrian arc. The boundary between the Southern Apennine and the Calabrian arc sectors is characterized by an articulated low-angle fault, generated by the rotations between the two sectors (Fig. 2.15b). The activity of this fault produced a large extension that exhumed the carbonatic and Lagonegrese units from the accretionary wedge of the Calabrian Arc. At the same time, the exhumed units rotated with the Southern Apennine Sector, thereby migrating towards the Apulian flexure.

In summary, the Southern Apennine was generated by a sequence of events that took place in the following order: (1) accretion of the carbonate and Lagonegrese units in the Calabrian arc wedge; (2) exhumation from the accretionary wedge; (3) accretion of the exhumed units to the Southern Apennine Wedge. This singular process created the space occupied by the present chain, whose front developed along a NW-SE direction.

The direction of extension that generated the exhumation of the Apennine units, according to the kinematic model, varies from NW-SE to N-S as a function of the position of the instantaneous pole of rotation between the two sectors (Figs. 3.3 and 2.19). In addition, the extension is also evidenced by the formation of top-wedge basins present both in the Southern Apennines and in the Calabrian Arc (Irpino Basin, Gulf of Sibari, Crati Valley, Crotone Basin, etc.).

Northern Tyrrhenian and Apennine Arc

Along the Apennine Arc continues the rotation of the two sectors with the previous kinematics. Crustal thinning in the Northern Tyrrhenian area and between the two sectors of the Apennine Arc also continues. Tuscan magmatism is starting near the triple junction of the two rifts.

Ch.5.2.4 - Phase 4. Sicilian Channel extension (4.5-2.5 Ma)

This phase is characterized by the definition of Sicily and Tunisia microplates (Fig. 5.4).
When the Ionian STEP fault moved from the southern Tyrrhenian sea to the Taormina line, the Ionian slab retreat enabled a clockwise rotation of Sicily around a pole (referred to Africa) located in the Gulf of Sirte (Fig. 4.10). This rotation created an extension in the Sicily channel while the southern part of the block, the Medina bank area, acted as a fulcrum. As a consequence the Pantelleria basins experienced a major extension than the southern part of the block. Several basins formed in the Egadi area and in the north-western Sicily offshore, while the northern margin of the block, at the boundary with Europe, was affected by a NNE-SSW compression/transpression. At the same time the Tunisian block was pushed upward with respect to Europe, creating a left-lateral transpression along the western margin of the block; the indentation of Africa, instead, has been accommodated along the eastern margin of the block in an almost pure compression. At the boundary with the Sicilian block, the difference between the vectors Sicily-Europe and Tunisia-Europe results in an almost N-S oriented extension, smaller than the extension in the Sicily channel; thus, the movement of the Tunisian block prevented the northernmost part of the Channel from a complete opening.

The Internal and External Sicilian chains started rotating together with the new Sicily microplate. The activity of Monte Kumeta-Alcantara fault and the extension along the External Sicilian Chain ended. The latter was previously responsible for the formation of the Gela foredeep and the Caltanissetta basin.
During this phase, the Ancona-Anzio line stops its activity while, due to the propagation of the flexure of Adriatic lithosphere, the Adriatic trench jumps east of the Montagna dei Fiori and the Maiella Massif, up to the Ortona-Roccamonfina line. The Lazio–Abruzzi segment is again incorporated into the Central Sector of the Apennine Arc. The Ortona–Roccamonfina line from this moment forms the new boundary between the Apennine Arc and the Southern Apennine (Fig. 5.5). The line ends North of the Roccamonfina volcano, from where it transfers a convergent

movement on the southern tip of the Ancona-Anzio line through an articulated dextral transtensive structure. This E-W oriented structure runs along the Latina Valley, where the eruptive centers of the Ernici Mounts are located.

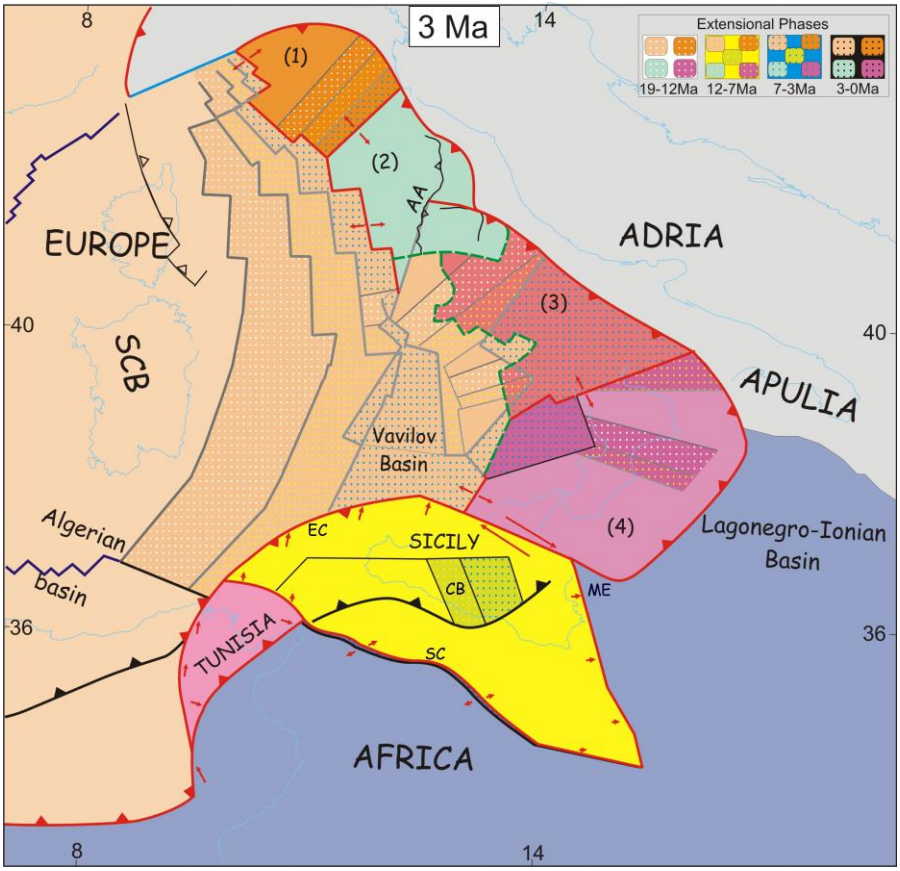

Figure 5.5 - Plate reconstruction of the western Mediterranean region at 3 Ma. The Northern Sector (1) is shown in (orange); the Central Sector (2) is in (aquamarine); the Calabrian Arc Sector (4) is in (dark pink), Sicily microplate is in (yellow), Tunisia microplate is in (pink); Europe is in (light orange). Dotted areas are in extension: 19-12 Ma (white dots), 12-7 Ma (yellow dots), 7-3 Ma (light blue dots), 3-0 Ma (black dots). (Green lines) are incipient boundaries. (Red lines) are active boundaries. (Black and Grey lines) are inactive boundaries. (Light blue lines) are strike-slip faults. (Red arrows) indicate direction of extension and compression. AA: Ancona-Anzio line; CB: Caltanissetta Basin; EC: Elimi Chain; ME: Malta Escarpment; SC: Sicily Channel; SCB: Sardinian-Corsican block.

Ch.5.2.5 - Phase 5. Marsili Basin Formation (2.5–0 Ma)

At the beginning of this phase extension jumped eastwards of the Vavilov basin and the southern branch of the triple junction of the Southern Tyrrhenian rifts started to form the Marsili basin in an area already thinned by transversal extension associated with the exhumation of the southern Apennines (Fig. 5.6). At the same time, the southern Apennine continues its exhumation from below the Calabrian Arc while migrating towards the Apulian flexure and generating transpessive structures in the exhumed Lagonegrese Units. Further away from the Apulian front, basins filled

with marine sediments (Potenza, Santarcangelo) formed on the exhumed units still in extension. On the Calabrian Arc, the same extensional event formed the Sibari–Corigliano Basin and the Paola Basin, while affecting the existing Crati Valley and Crotonese Basin (*Corradino et al., 2020*; and reference therein) (Fig. 2.15b). Further south the Catanzaro Trough was reactivated.

In Sicily, the Ionian STEP fault intersected the Malta Escarpment and the tear fault began to propagate along this structure. The model presented here suggests that this event started widening the narrow Ionian Slab and interrupted the continuity between the Sicilian and Ionian lithosphere. All this causes dramatic changes in Sicily. A right-lateral shear zone is activated in the Sicily Channel causing further extension of the Channel through the opening of pull-apart basins (Pantelleria, Malta and Linosa).

The margin between Sicily and Europe assumed a more trascurrent character, respect to the previous phase: according to the shape of the boundary, the eastern part is affected by transpression, the western part, instead, is affected by extension; this extension continues also at the boundary between Tunisia and Sicily. The triple junction between Tunisia, Sicily and Europe moves towards south-east along the transtensive margin in the north-eastern Tunisian offshore.

The Taormina line is no longer active and two lithospheric discontinuities, the WNW–ESE oriented "Sisifo-Alicudi" and the NNW–SSE striking "Aeolian-Tindari-Letojanni" lines are activated (Figs. 5.6-5.7). The Triple junction of the Southern Tyrrhenian (Europe) with Calabria and Sicily runs along the "Sisifo-Alicudi" line up to Lipari-Vulcano, while the triple junction of the Southern Tyrrhenian with Calabrian and Southern sector abandons the area of the Marsili and jumps near the eastern Aeolian Arc (Fig. 5.8). The slab-retreat process from this moment is exclusively guided by the Ionian slab.

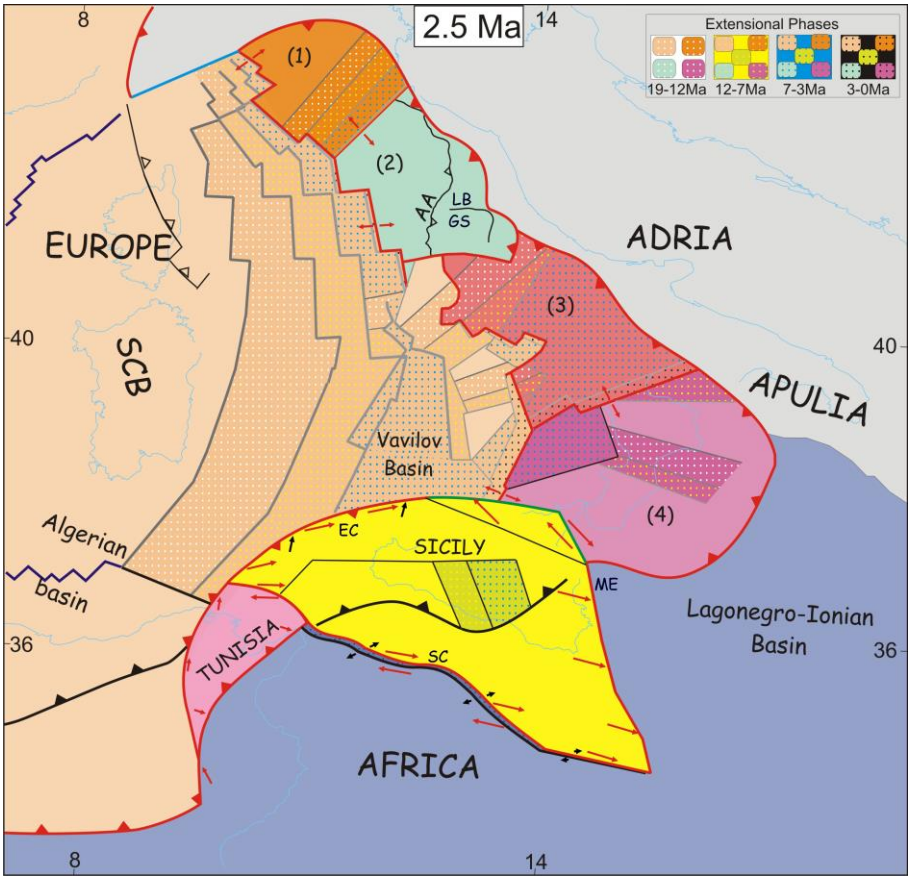

Figure 5.6 - Plate reconstruction of the western Mediterranean region at 2.5 Ma. The Northern Sector (1) is shown in (orange); the Central Sector (2) is in (aquamarine); the Calabrian Arc Sector (4) is in (dark pink), Sicily microplate is in (yellow), Tunisia microplate is in (pink); Europe is in (light orange). Dotted areas are in extension: 19-12 Ma (white dots), 12-7 Ma (yellow dots), 7-3 Ma (light blue dots), 3-0 Ma (black dots). (Green lines) are incipient boundaries. (Red lines) are active boundaries. (Black and Grey lines) are inactive boundaries. (Light blue lines) are strike-slip faults. (Red arrows) indicate direction of extension and compression. AA: Ancona-Anzio line; EC: Elimi Chain; GS: Gran Sasso; LB: Laga Basin; ME: Malta Escarpment; SC: Sicily Channel; SCB: Sardinian-Corsican block.

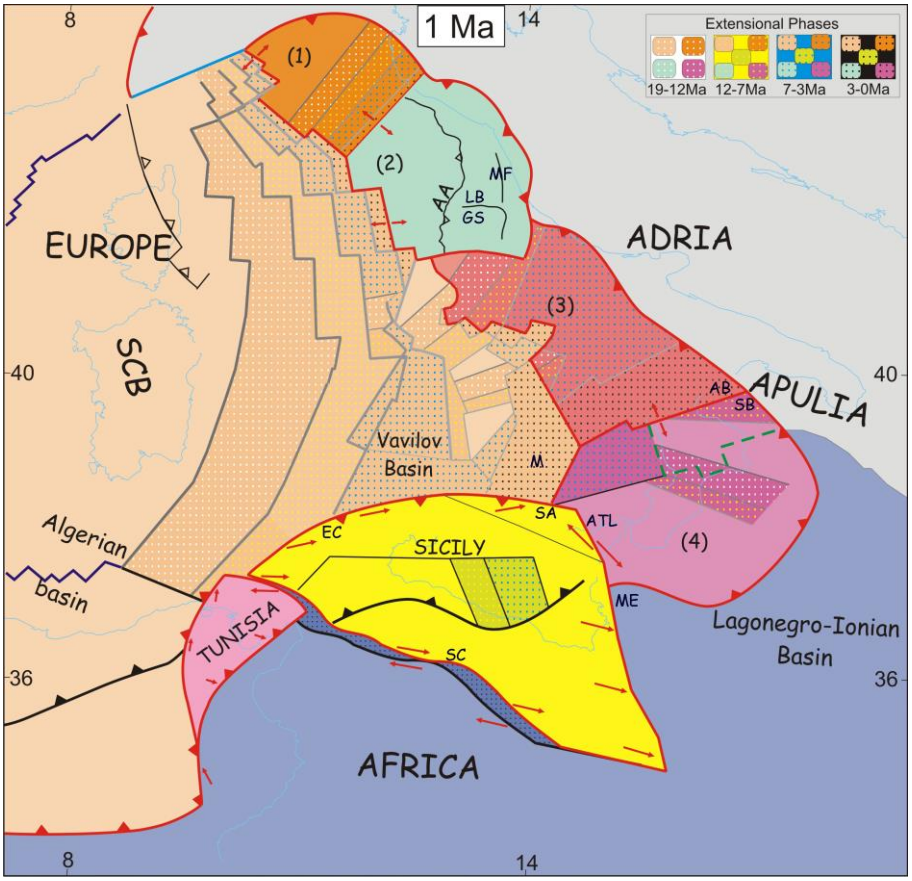

Figure 5.7 - Plate reconstruction of the western Mediterranean region at 1 Ma. The Northern Sector (1) is shown in (orange); the Central Sector (2) is in (aquamarine); the Calabrian Arc Sector (4) is in (dark pink), Sicily microplate is in (yellow), Tunisia microplate is in (pink); Europe is in (light orange). Dotted areas are in extension: 19-12 Ma (white dots), 12-7 Ma (yellow dots), 7-3 Ma (light blue dots), 3-0 Ma (black dots). (Green lines) are incipient boundaries. (Red lines) are active boundaries. (Black and Grey lines) are inactive boundaries. (Light blue lines) are strike-slip faults. (Red arrows) indicate direction of extension and compression. A-A: Ancona-Anzio line; AB: St. Arcangelo Basin; ATL: Aeolian-Tindari-Letojanni Line, EC: Elimi Chain; GS: Gran Sasso Front; LB: Laga Basin; ME: Malta Escarpment, MF: Montagna dei Fiori; SA: Sisifo-Alicudi Line, SB:Sibari Basin; SC: Sicily Channel, SCB: Sardinian-Corsican block.

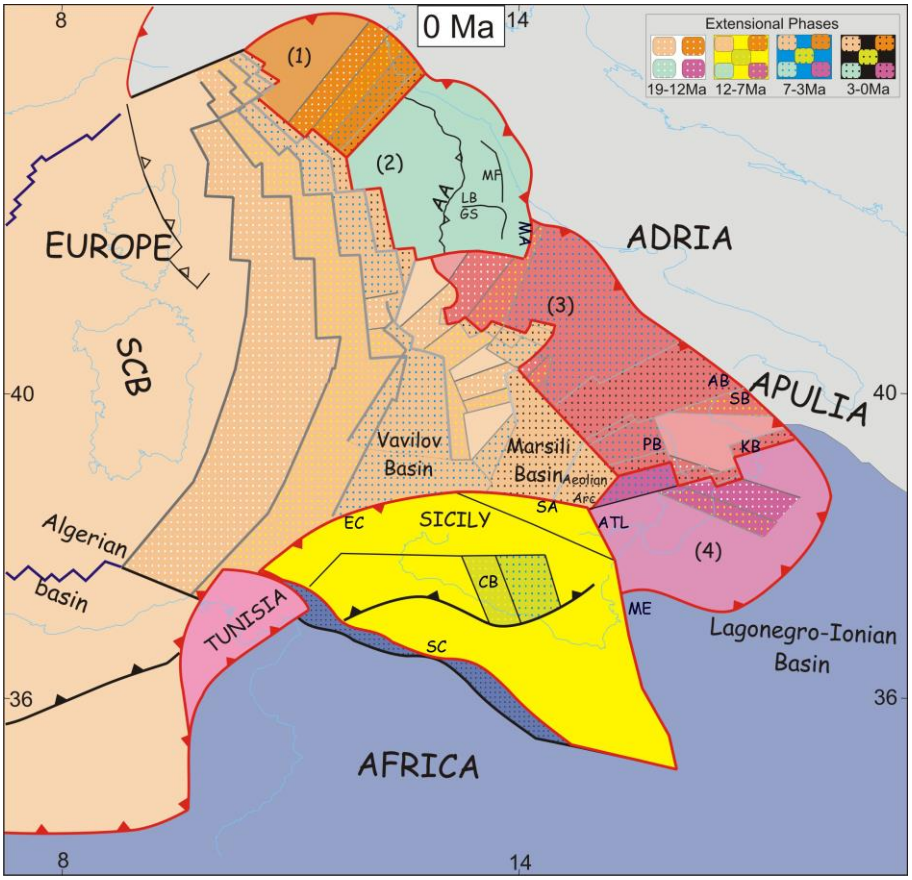

Figure 5.8 - Plate reconstruction of the western Mediterranean region at 0 Ma. The Northern Sector (1) is shown in (orange); the Central Sector (2) is in (aquamarine); the Calabrian Arc Sector (4) is in (dark pink), Sicily microplate is in (yellow), Tunisia microplate is in (pink); Europe is in (light orange). Dotted areas are in extension: 19-12 Ma (white dots), 12-7 Ma (yellow dots), 7-3 Ma (light blue dots), 3-0 Ma (black dots). (Green lines) are incipient boundaries. (Red lines) are active boundaries. (Black and Grey lines) are inactive boundaries. A-A: Ancona-Anzio line; AB: St. Arcangelo Basin; ATL: Aeolian-Tindari-Letojanni Line CB, Caltanissetta Basin, EC: Elimi Chain, KB: Crotone Basin; GS: Gran Sasso Front; LB: Laga Basin; MA: Maiella Front; ME: Malta Escarpment, MF: Montagna dei Fiori; PB: Paola Basin; SA: Sisifo-Alicudi Line, SB:Sibari Basin; SC: Sicily Channel, SCB: Sardinian-Corsican block.

Ch.5.3 - References

Cappelletti, F., Panei, L., Colucci, F., Guandalini, R., Moia, F., Stella, G. 2009-2017. ViDEPI project data utilization for sites characterization in range of CCS, geothermal and hydrocarbons projects in Italy.

Castellarin, A.; Colacicchi, R.; Praturlon, A.; Cantelli, C. 1982. The jurassic-lower pliocene history of the Ancona-Anzio Line (Central Italy). Mem. Soc. Geol. Ita., 24, pp. 325–336.

Cipollari, P.; Cosentino, D. 1991. La linea Olevano-Antrodoco: Contributo della biostratigrafia alla sua caratterizzazione cinematica. Studi Geol. Camerti, pp. 143–150, doi:10.15165/studgeocam-978.

Corradino, M.; Pepe, F.; Bertotti, G.; Picotti, V.; Monaco, C.; Nicolich, R. 2020. 3-D architecture and Plio-Quaternary evolution of the Paola Basin: Insights into the forearc of the Tyrrhenian-Ionian subduction system. Tectonics, 39, doi:10.1029/2019TC005898.

Dallan Nardi, L.; Elter, P.; Nardi, R. 1971. Considerazioni sull'arco dell'Appennino settentrionale e sulla" linea" Ancona-Anzio. Boll. Soc. Geol. Ital., 90, pp. 203–211.

Ghisetti, F.; Vezzani, L. 1984. Thin-skinned deformations of the western Sicily thrust belt and relationships with crustal short-ening; mesostructural data on the Mt. Kumeta-Alcantara fault zone and related structures. Boll. Soc. Geol. Ital., 103, pp. 129–157.

Guerrera, F.; Martín-Martín, M.; Raffaelli, G.; Tramontana, M. 2015. The Early Miocene "Bisciaro volcaniclastic event" (northern Apennines, Italy): A key study for the geodynamic evolution of the central-western Mediterranean. Int. J. Earth Sci., 104, pp. 1083–1106.

Kastens, K.A.; Mascle, J. 1987. Site 654: Upper sardinian margin. Proc. ODP Init. Rep., 107, 772.

Milia, A.; Torrente, M.M. 2014. Early-stage rifting of the Southern Tyrrhenian region: The Calabria–Sardinia breakup. J. Geodyn., 81, pp. 17–29, doi:10.1016/j.jog.2014. 06.001.

Mutti, E.; Lucchi, F.R. 1972. Le torbiditi dell'Appennino settentrionale: introduzione all'analisi di facies. Mem. Soc. Geol. It., 11, pp. 161–199.

Patacca, E.; Scandone, P. 2007. Geology of the Southern Apennines. Boll. Soc. Geol. It. (Ital. J. Geosci.), 7, pp. 75–119.

Pierantoni, P.P.; Macchiavelli, C.; Penza, G.; Schettino, A.; Turco, E. 2020. Kinematics of the Tyrrhenian-Apennine system and implications for the origin of the Campanian magmatism. In Vesuvius, Campi Flegrei, and Campanian Volcanism, 1st ed.; De vivo B., Belkin, H.E., Rolandi, G., Eds.; Elsevier Inc.: Amsterdam, The Netherlands; pp. 520.

Sartori, R. 2003. The Tyrrhenian back-arc basin and subduction of the Ionian lithosphere. Episodes, 26, pp. 217–221.

Schettino, A.; Turco, E. 2006. Plate kinematics of the Western Mediterranean region during the Oligocene and Early Miocene. Geophysi. J. Int., 166, pp. 1398–1423.

Schettino, A.; Turco, E. 2011. Tectonic history of the western Tethys since the Late Triassic. GSA Bull., 123, pp. 89–105, doi:10.1130/B30064.1

Selli, R. 1981. Thoughts on the geology of the Mediterranean region. In Proceedings of the Consiglio nazionale delle ricerche. International Conference, Rome, Italy, 22–23 May, pp. 489–501.

Turco, E.; Macchiavelli, C.; Mazzoli, S.; Schettino, A.; Pierantoni, P.P. 2012. Kinematic evolution of the Alpine Corsica in the framework of Mediterranean mountain belts. Tectonophysics, 579, pp. 193–206.

Thinon, I.; Guennoc, P.; Serrano, O.; Maillard, A.; Lasseur, E.; Rehault, J.P. 2016. Seismic markers of the Messinian Salinity Crisis in an intermediate-depth basin: Data for understanding the Neogene evolution of the Corsica Basin (northern Tyrrhenian Sea). Mar. Pet. Geol., 77, pp. 1274–1296.

General Conclusions

The tectonic reconstruction of the Tyrrhenian basin and the Apennine chain created the opportunity to propose a method that integrates plate kinematics tools with the methods of structural geology. The technique has proved to be adequate for performing quantitative deformation analyses at an intermediate scale such as that of the Mediterranean area. Structural geology has made significant contributions for the application of plate kinematics methods to continental tectonics. Among these: the identification of the components of the Apennine puzzle (microplates), the determination of the poles and angles of rotation, and the definition of the plate boundaries. With these fundamental parameters, the hypothesis of a rotation model of the puzzle of microplates has been formulated, built with the aid of the PCME and GPlates software tools. The model provided a framework of kinematic constraints that allowed to hypothesize innovative solutions to the problems inherent the tectonic reconstruction of the Apennine chain. The kinematic framework is also useful for future research that can confirm, improve, or modify the proposed model.

The model can be viewed through an animation (Movie 1) composed by a temporal sequence of images (Appendix 1), generated by the software. The characteristic of this approach, well known in the global tectonics studies, is to provide and visualize, for each point along plate boundaries, the relative velocity vectors between the microplates. Finally, this important feature allows the prediction of the tectonic and structural implications along the plate boundaries. The expected implications of the used rotation model have found a very satisfactory confirmation for the tectonic structure observed for the Apennine chain and the Tyrrhenian basin. Therefore, the initial hypotheses made on the recognition of microplates, on the determination of the rotation poles, on the activity times, and on the angles of rotation have been verified. The model also provides a precise balance of the areas, which is essential for paleogeographic reconstructions. Due to these important characteristics, the rotation models constructed with this methodology, thanks to their ability to predict implications of tectonic and structural processes in a very broad framework, represent powerful tools suitable for responding to interpretative disputes for complex areas still debated. However, the transition from the rotation model to its tectonic implications requires a certain aptitude to visualize the third dimension, not represented in the rotation models.

For the Apennine and Tyrrhenian areas, the rotation model has responded well to the historical issues. The most significant, starting from the North, are: the transversal structures that interrupt

the Umbria–Marche Arc and separate it from the Northern Apennine, while extending the Tyrrhenian, Tuscan–Lazio and Umbria areas in a direction transverse to the Apennine chain; the Ancona-Anzio transpressive lineament which, in the triple junction with the Sibillini and Gran Sasso front, form the Laga basin; the exhumation of the tectonic units of the Southern Apennine, which implies a great extension that pervades the entire chain; the formation of important basins, located near the foredeep of the southern chain (Santarcangelo, Sibari, Crotonese and Caltanissetta), the Paola basin and Crati Valley located in an innermost position and the Catanzaro trough that crosses the entire Calabrian arc. All these basins exhibit extension along the direction of the chain that is not appreciable in the tectonic reconstructions of transects.

Within this framework, two new microplates have been identified, generated as a direct consequence of the proposed kinematic model and the geodynamic implication associated with it. The separation of the African continental margin and the Ionian lithosphere, through a STEP fault placed along the Malta Escarpment, creates a lack of contrast that allows a part of the African continental margin (Sicily microplate) to escape toward south-east. This process of escape involves also part of Tunisian Atlas (Tunisia microplate); pushed by the Africa-Europe collision and dragged by the escape of Sicily, this micro plate acquires a northward direction of movement with respect to Europe.

The movements of Sicily and Tunisia have been modeled using plate kinematic techniques, the estimated poles have been included in the rotation file used for the Apennine microplates and the results are shown in the animation (movie1).

The escape of Sicily explains the activation of a dextral shear zone in the Sicily Channel, responsible for the formation of deep troughs, set along the direction of Upper-Triassic/Lower Jurassic faults.

Acknowledgments

I would like to thank the reviewers Giancarlo Molli and Eline Le Breton for their careful comments and valuable advice that certainly contributed to enhancing and improving the final work;

I am gratefull to the supervisor Pietro Paolo Pierantoni for giving me the chance to work on this project and for the valuable and effective advice;

a special thank to Professor Eugenio Tuco for encouraging and supporting me in the ideas, for sharing his immense knowledge and years of his work with me;

finally, I would like to point out that this work would not have been possible without the previous hard work of Chiara Macchiavelli, whom I thank infinitely for her patience, for revealing me her “tricks” and for always giving me the support I needed.

Appendix 1

The 27 frames from Movie1 are attached below.

Europe is the fixed plate.

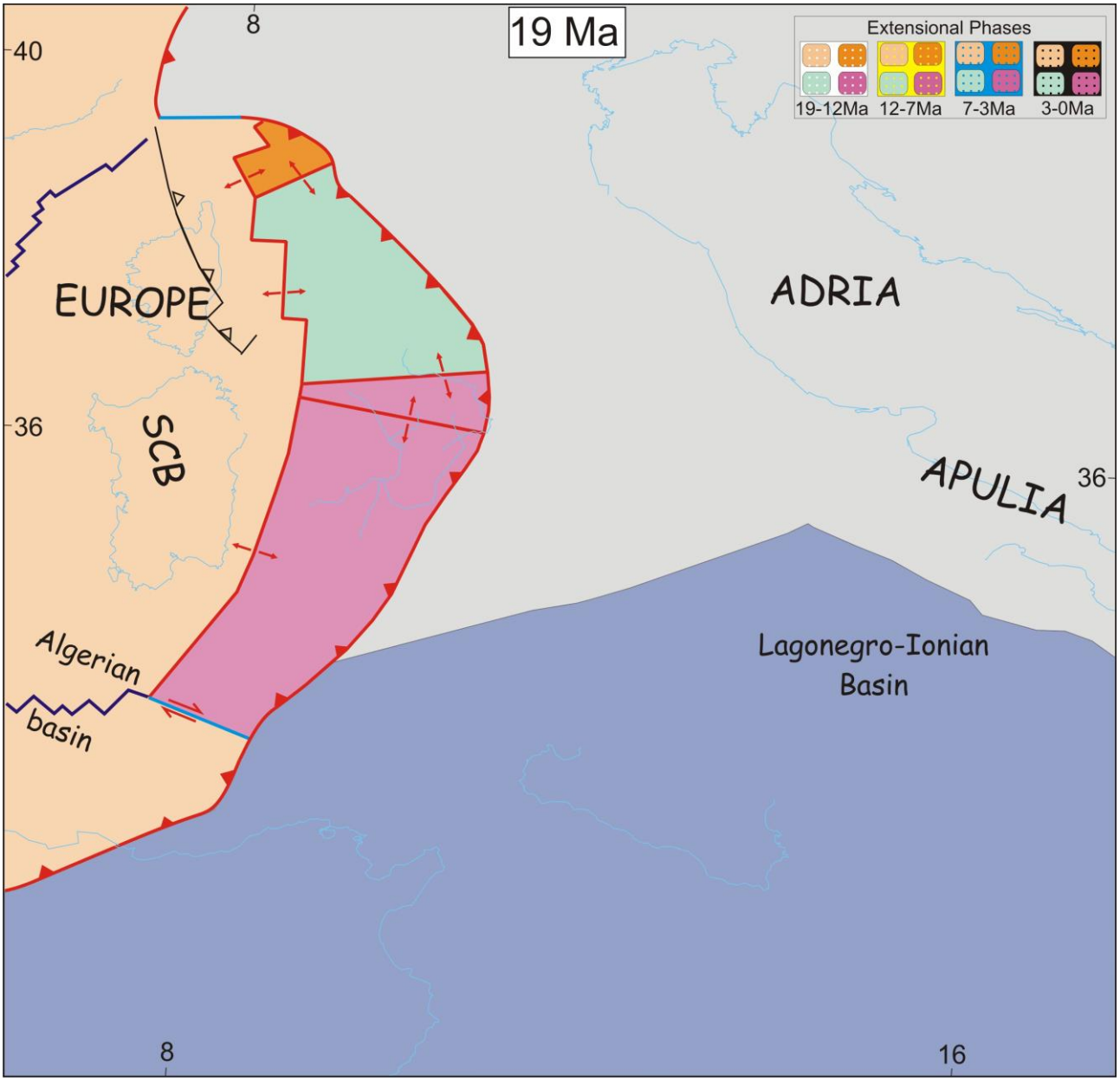
19 Ma
Extensional Phases
19-12Ma
12-7Ma
7-3Ma
3-0Ma
40
8
36
36
8
16
EUROPE
SCB
ADRIA
APULIA
Algerian
basin
Lagonegro-Ionian
Basin

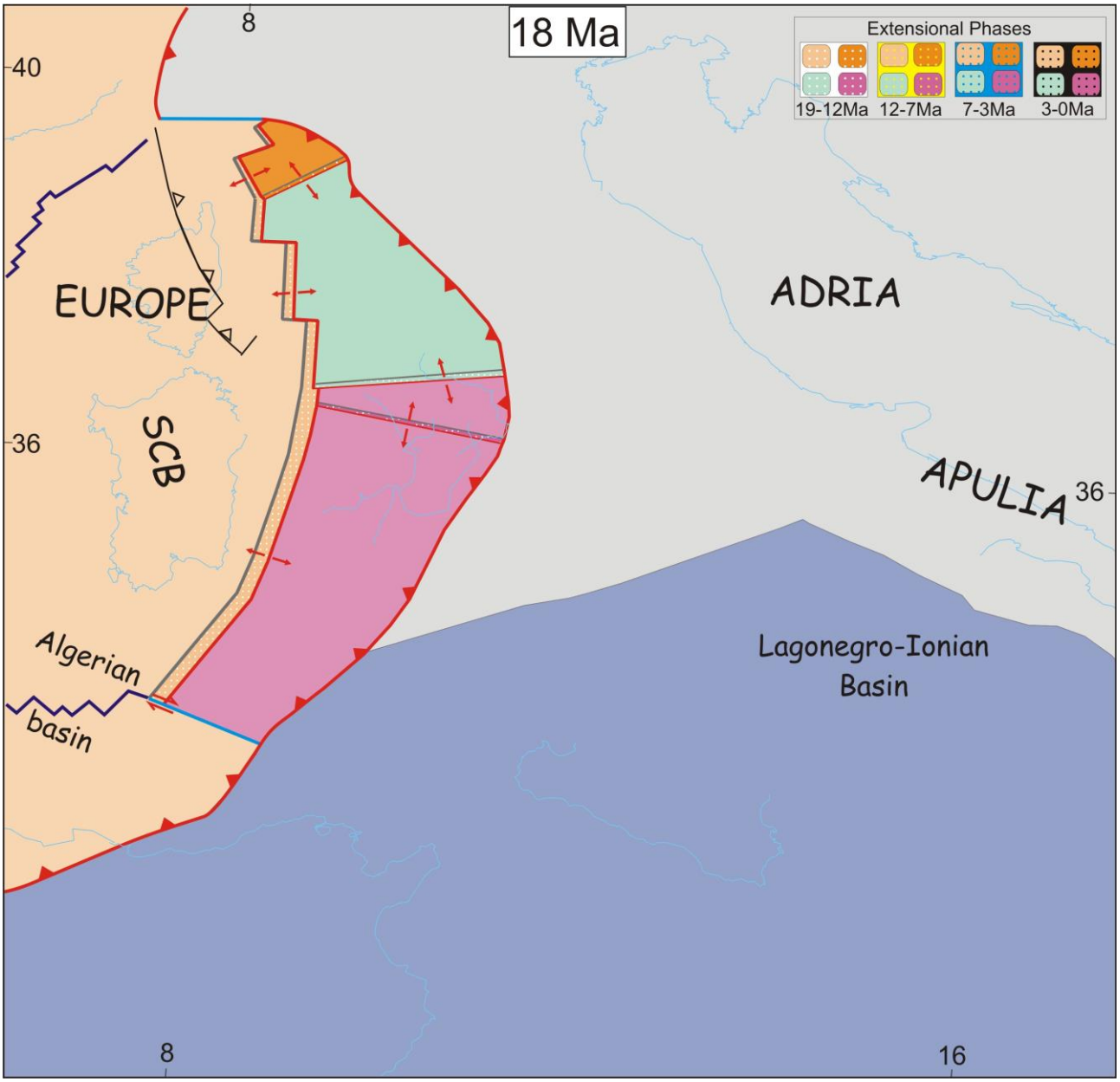
18 Ma
Extensional Phases
19-12Ma
12-7Ma
7-3Ma
3-0Ma
EUROPE
ADRIA
SCB
APULIA
Algerian
basin
Lagonegro-Ionian
Basin
40
36
8
16

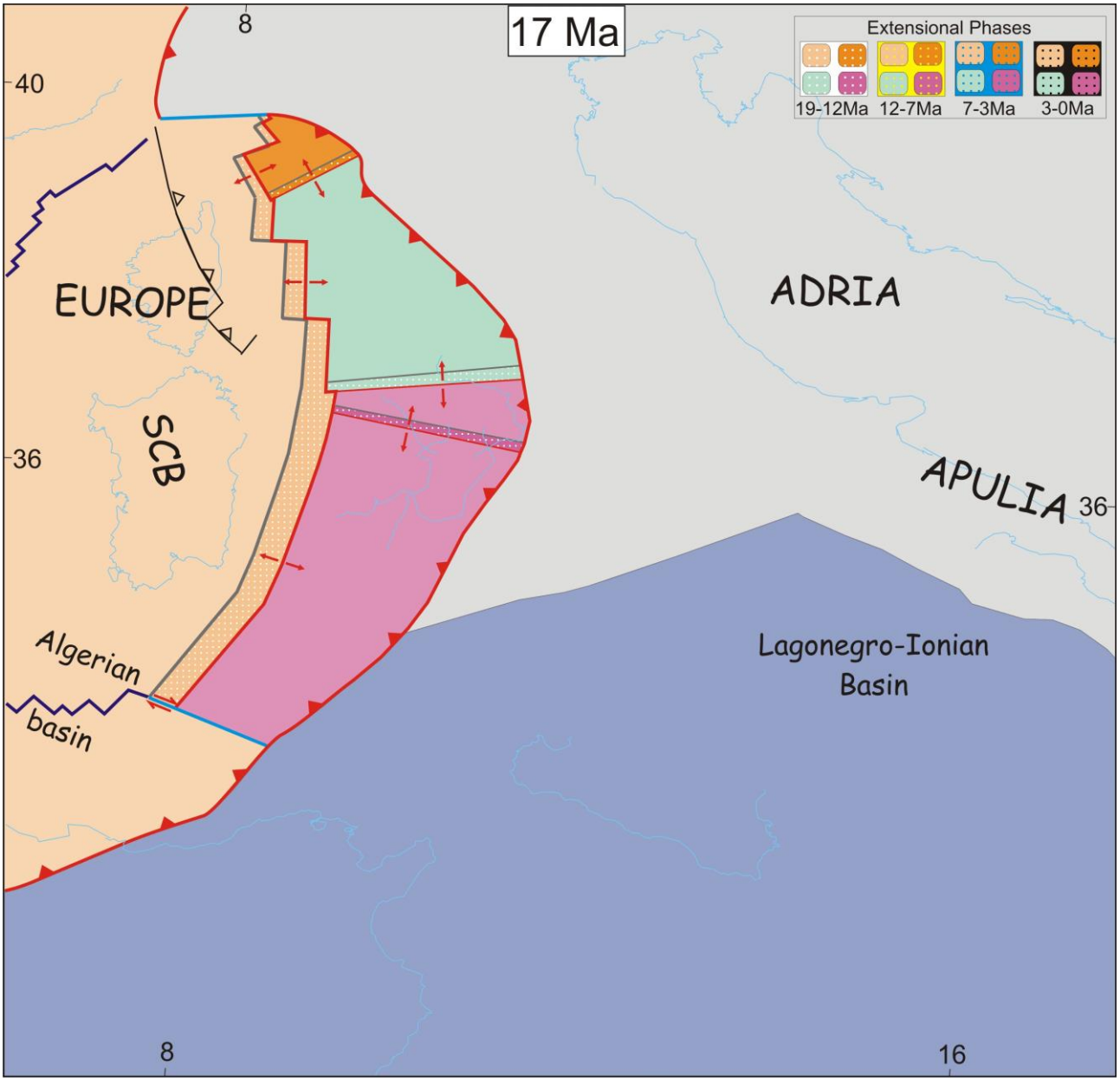
17 Ma
Extensional Phases
19-12Ma
12-7Ma
7-3Ma
3-0Ma
EUROPE
ADRIA
SCB
APULIA
Algerian
basin
Lagonegro-Ionian
Basin
40
36
8
16

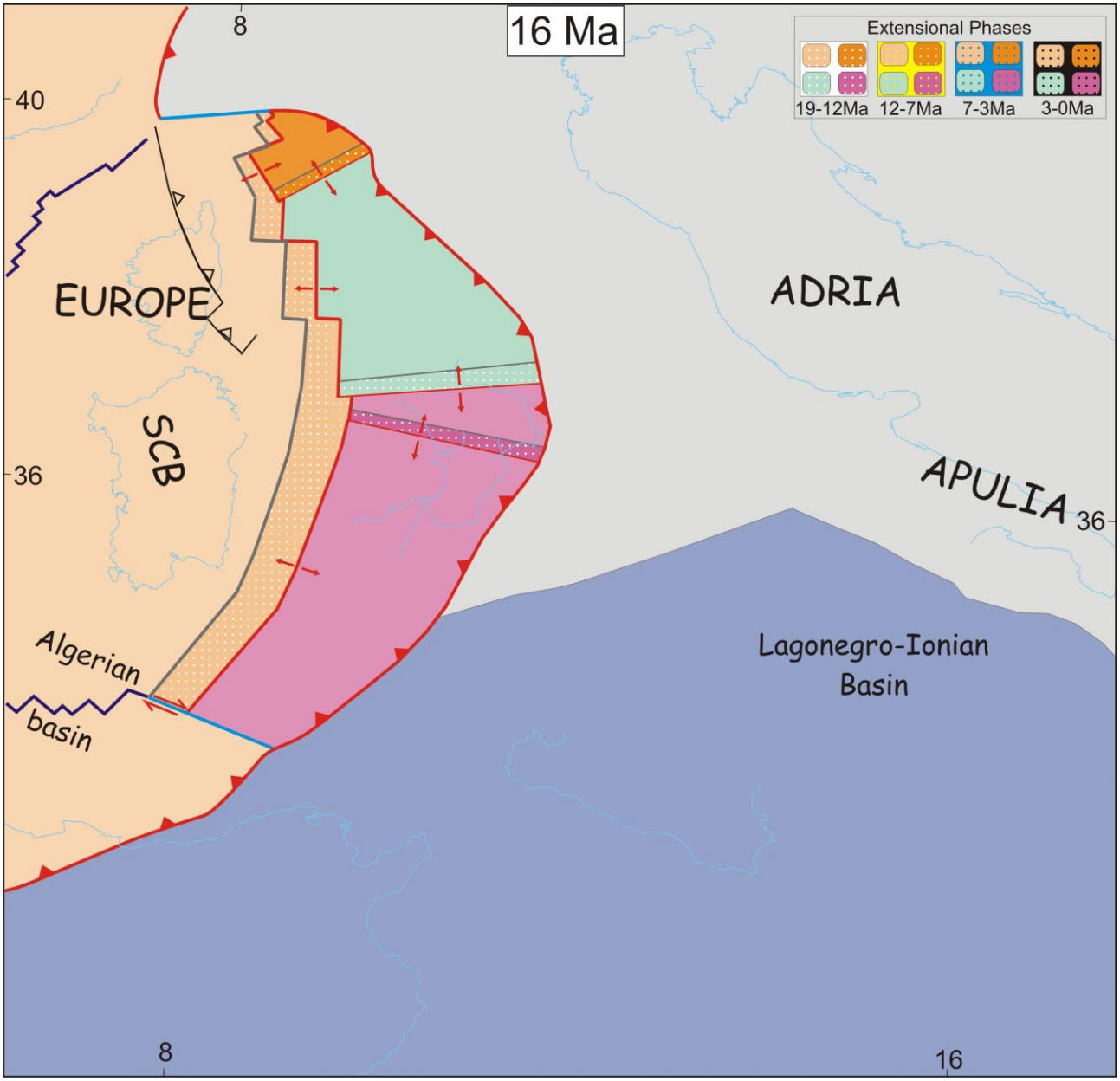
16 Ma
Extensional Phases
19-12Ma
12-7Ma
7-3Ma
3-0Ma
EUROPE
ADRIA
SCB
APULIA
Algerian
basin
Lagonegro-Ionian
Basin
8
40
36
8
16

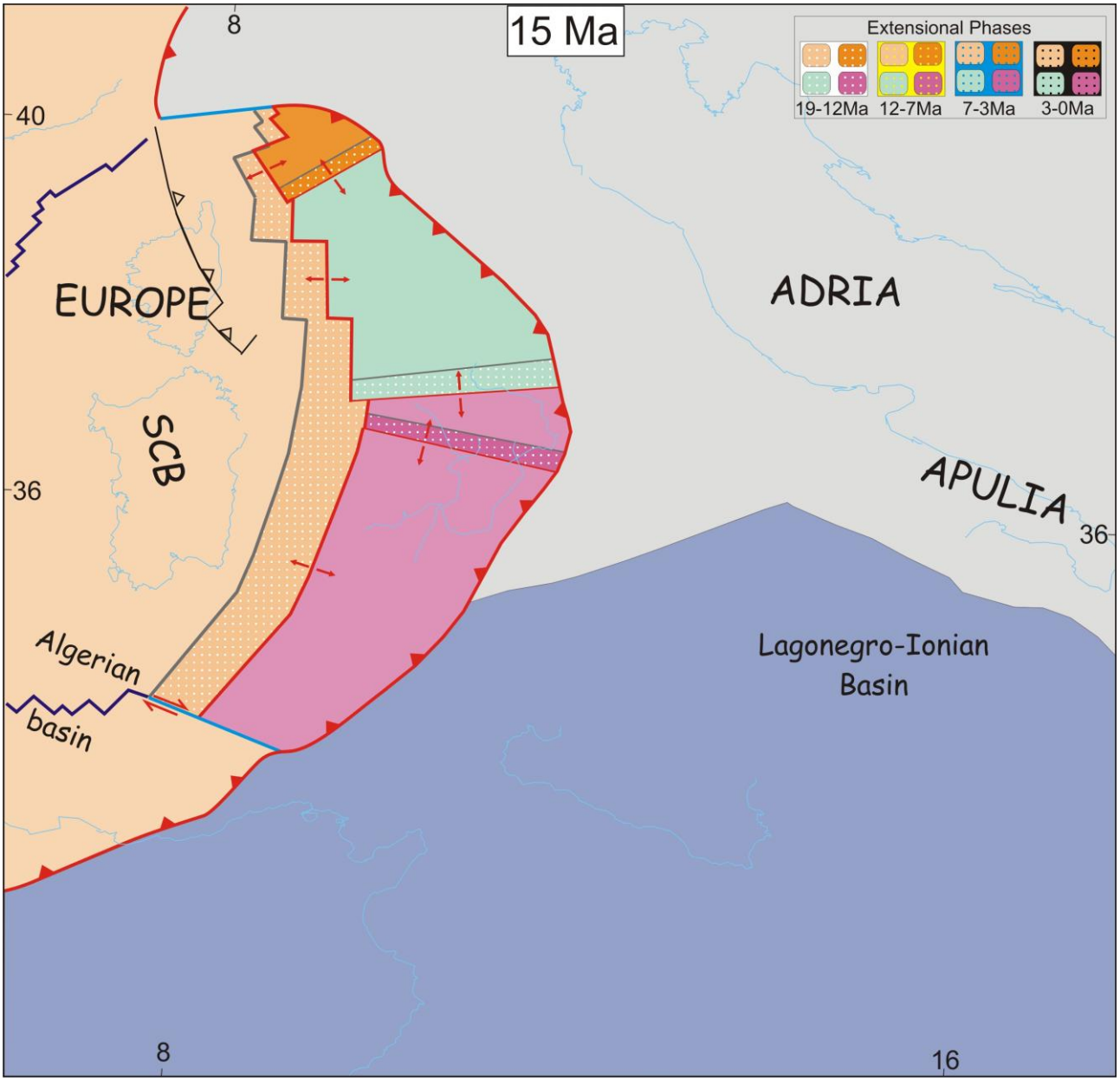
15 Ma
Extensional Phases
19-12Ma
12-7Ma
7-3Ma
3-0Ma
EUROPE
ADRIA
SCB
APULIA
Algerian
basin
Lagonegro-Ionian
Basin
8
40
36
8
16

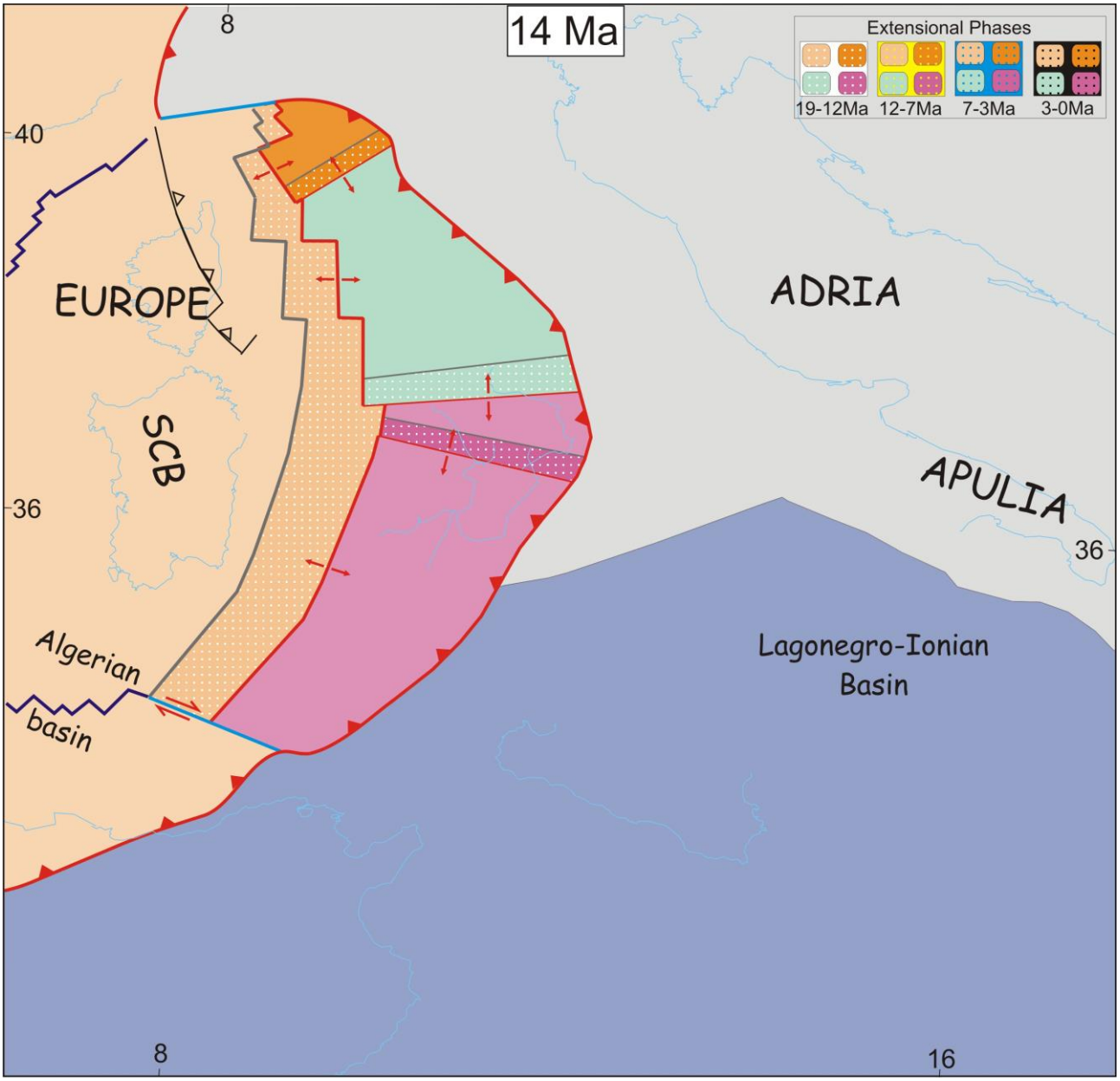
14 Ma
Extensional Phases
19-12Ma
12-7Ma
7-3Ma
3-0Ma
8
40
36
EUROPE
SCB
ADRIA
APULIA
36
Algerian
basin
Lagonegro-Ionian
Basin
8
16

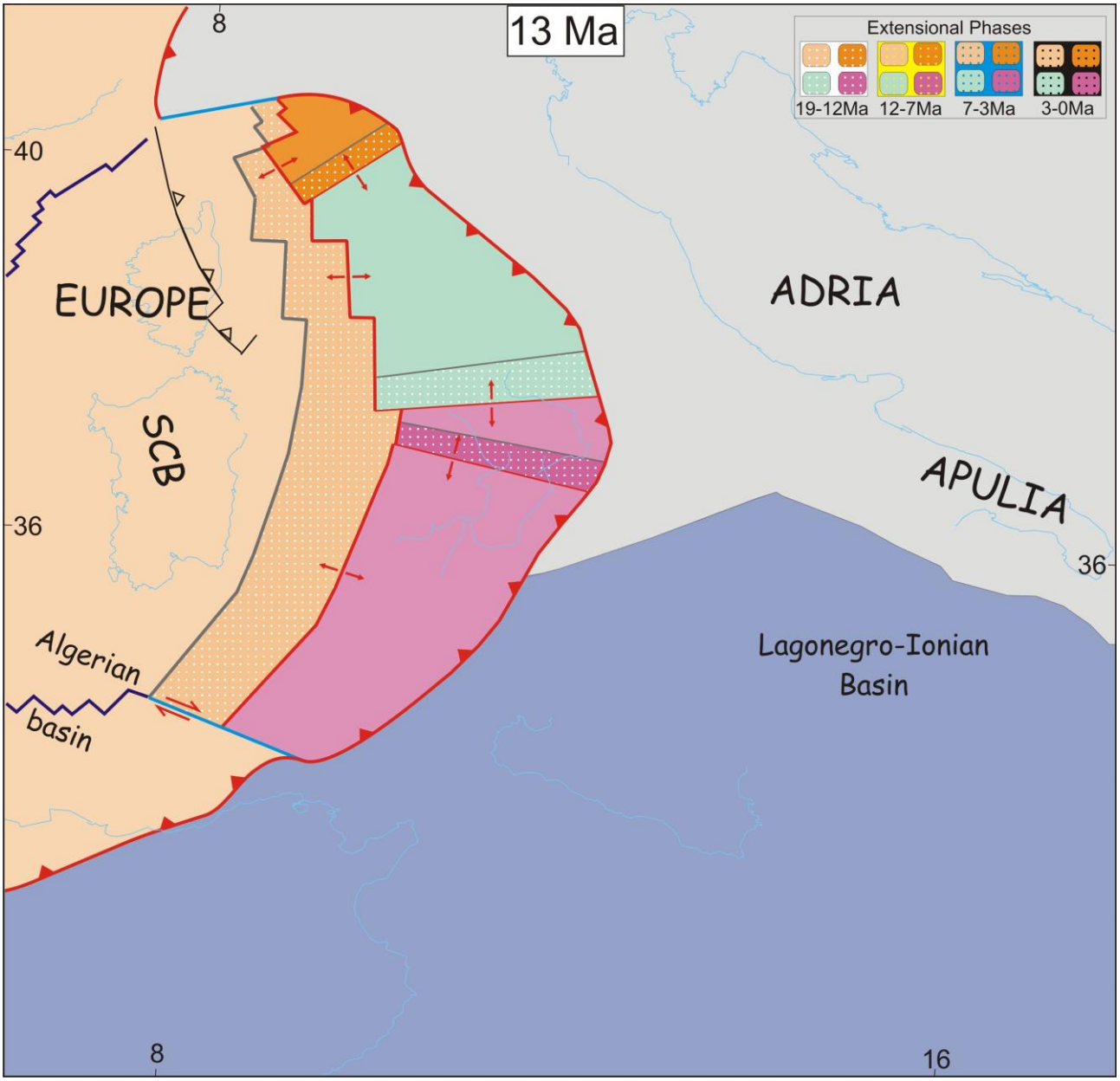
13 Ma
Extensional Phases
19-12Ma
12-7Ma
7-3Ma
3-0Ma
8
40
36
EUROPE
SCB
ADRIA
APULIA
36
Algerian
basin
Lagonegro-Ionian
Basin
8
16

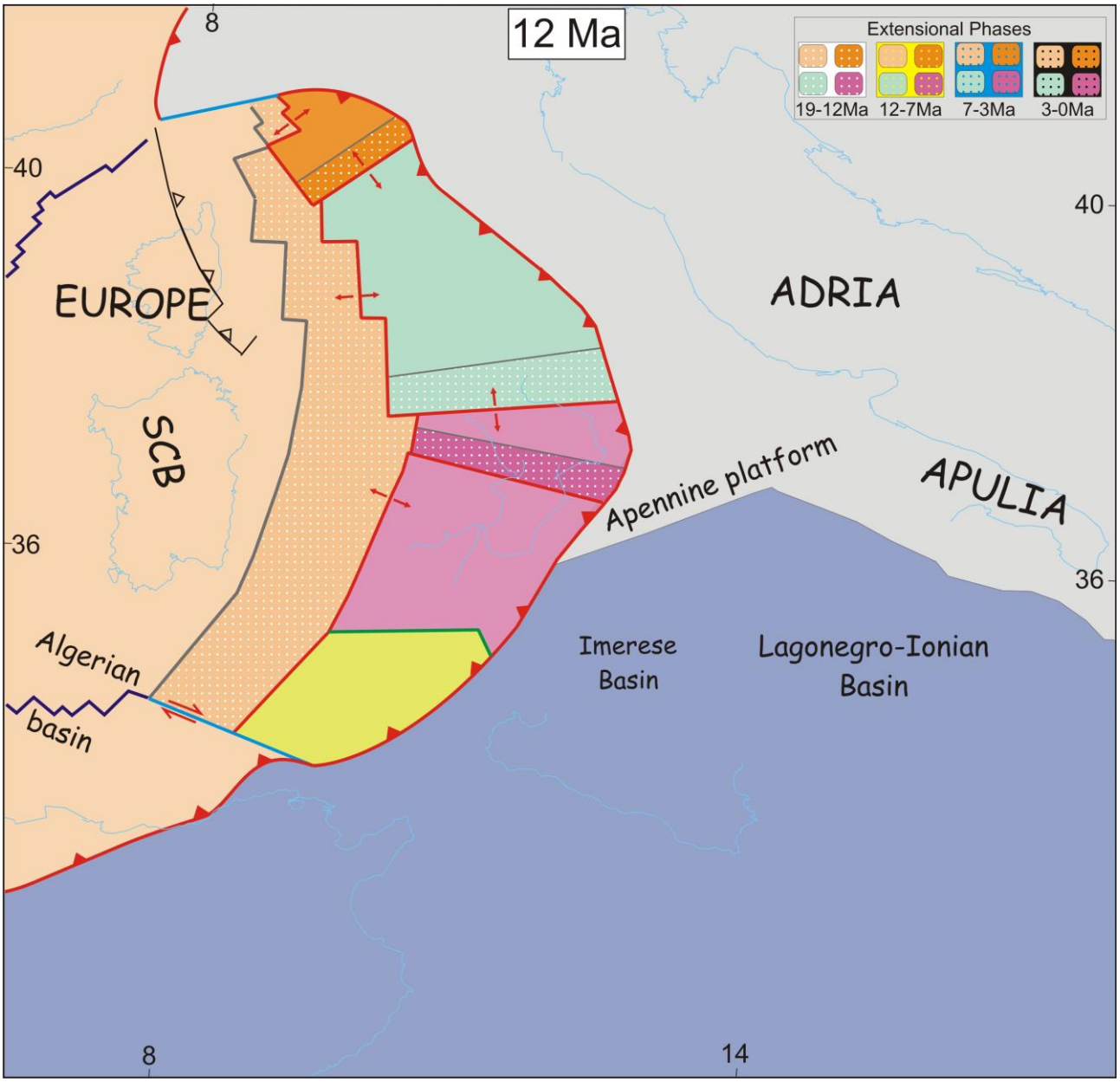
12 Ma
Extensional Phases
19-12Ma
12-7Ma
7-3Ma
3-0Ma
8
40
36
14
EUROPE
SCB
ADRIA
APULIA
Apennine platform
Algerian
basin
Imerese
Basin
Lagonegro-Ionian
Basin

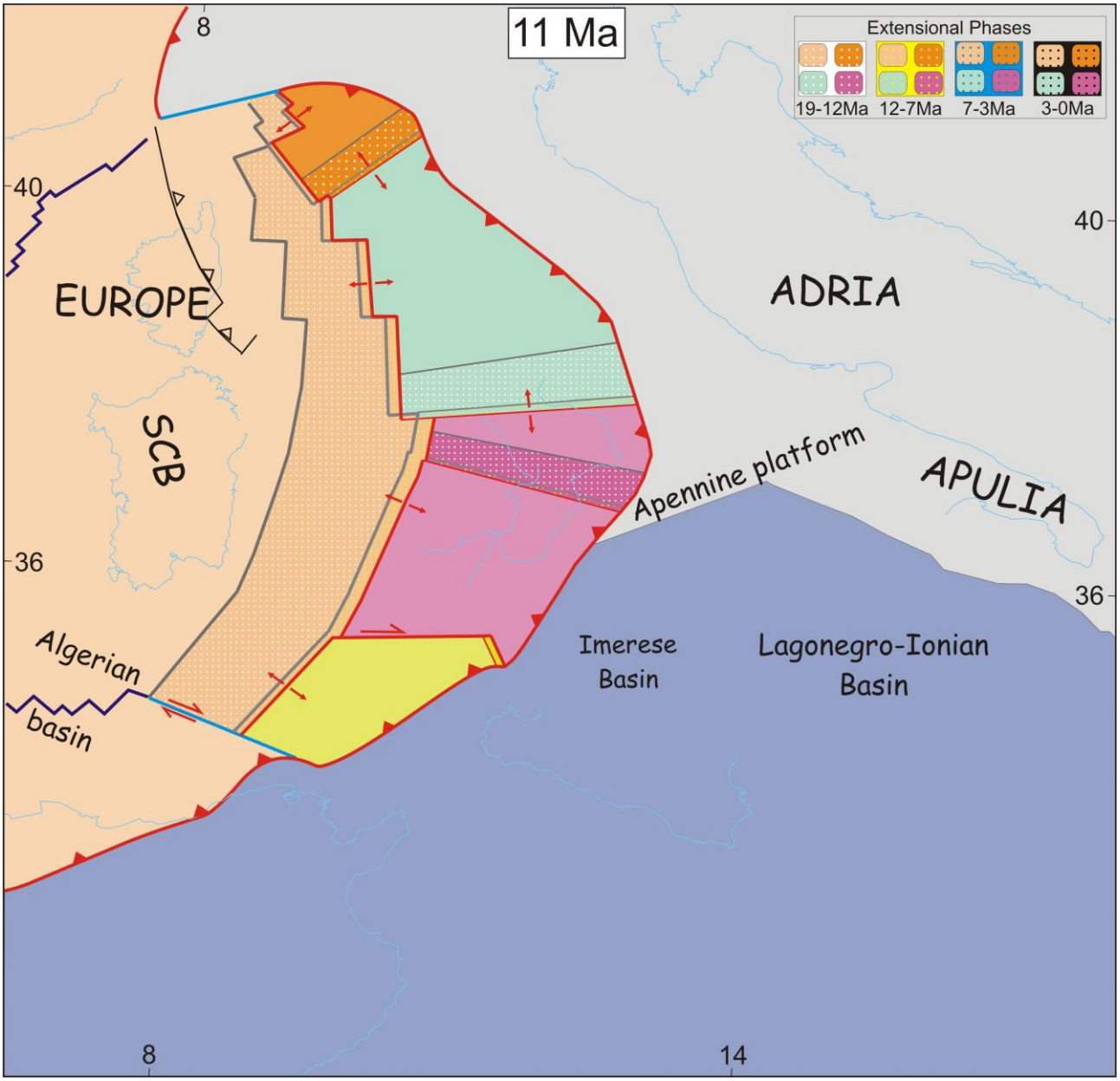
11 Ma
Extensional Phases
19-12Ma
12-7Ma
7-3Ma
3-0Ma
8
40
36
14
EUROPE
ADRIA
SCB
Apennine platform
APULIA
Algerian
basin
Imerese
Basin
Lagonegro-Ionian
Basin

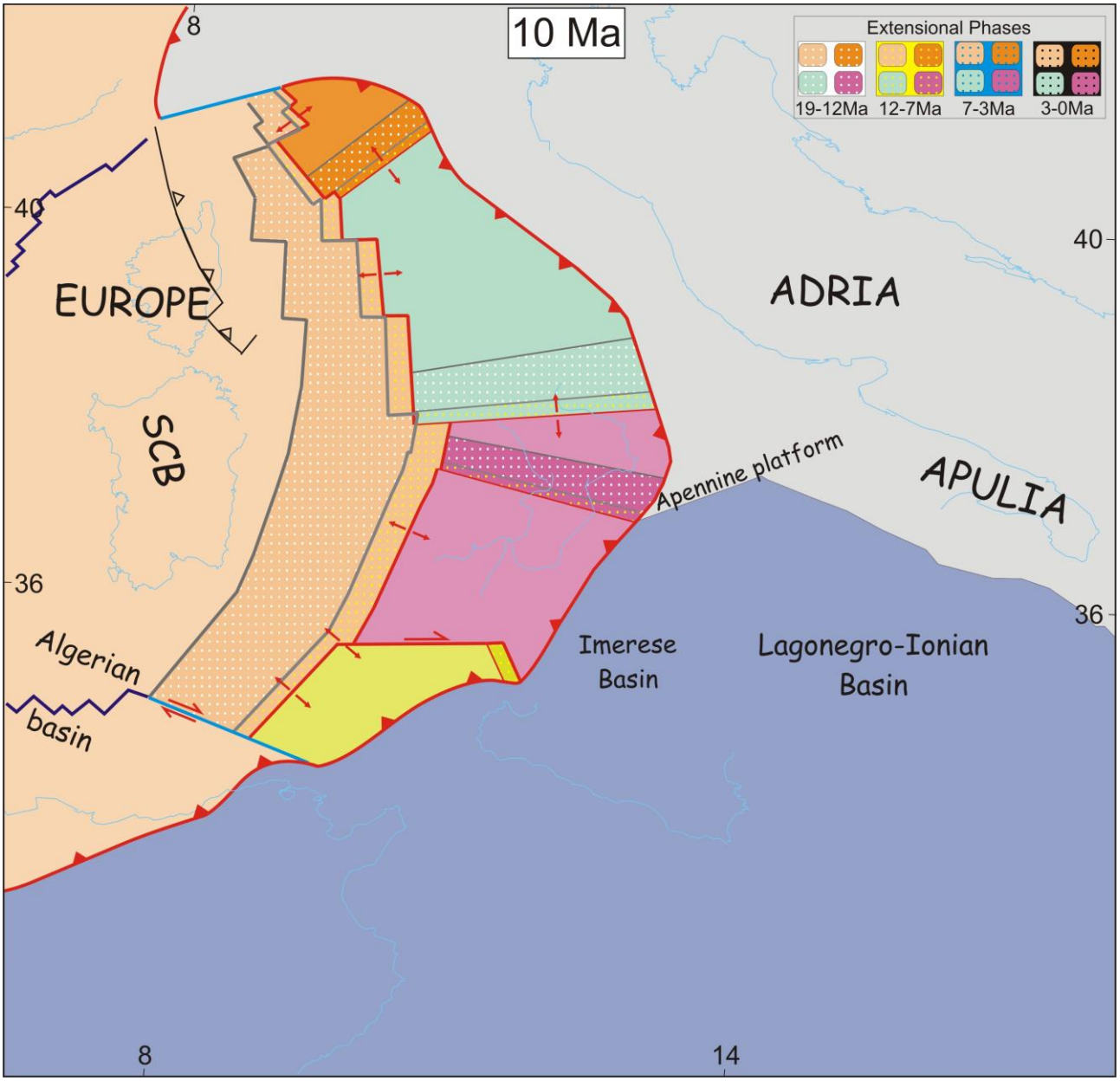
10 Ma
Extensional Phases
19-12Ma
12-7Ma
7-3Ma
3-0Ma
EUROPE
ADRIA
SCB
Apennine platform
APULIA
Algerian
basin
Imerese
Basin
Lagonegro-Ionian
Basin
8
40
36
14

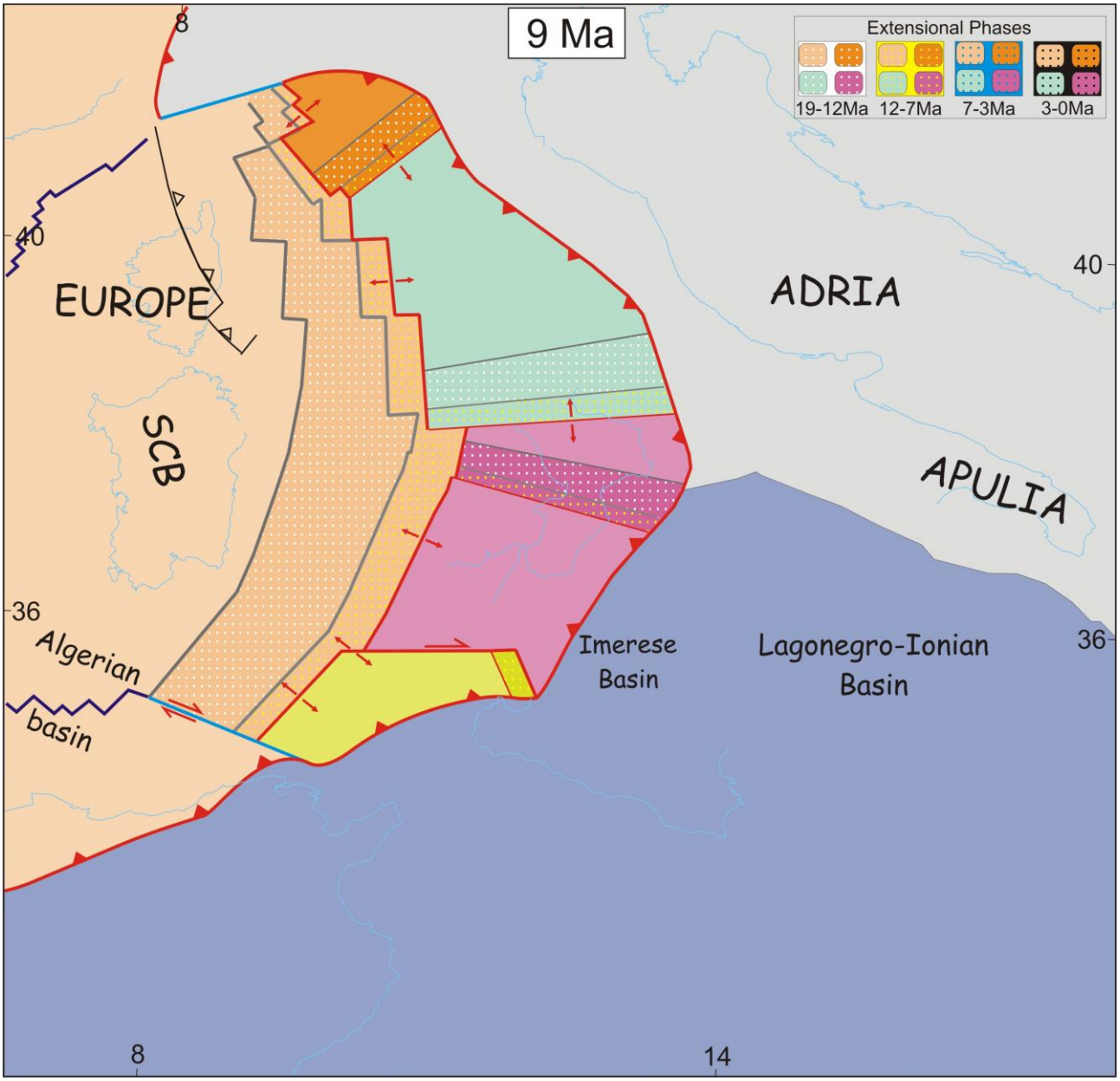
9 Ma
Extensional Phases
19-12Ma
12-7Ma
7-3Ma
3-0Ma
8
40
EUROPE
SCB
ADRIA
APULIA
36
Algerian
basin
Imerese
Basin
Lagonegro-Ionian
Basin
8
14

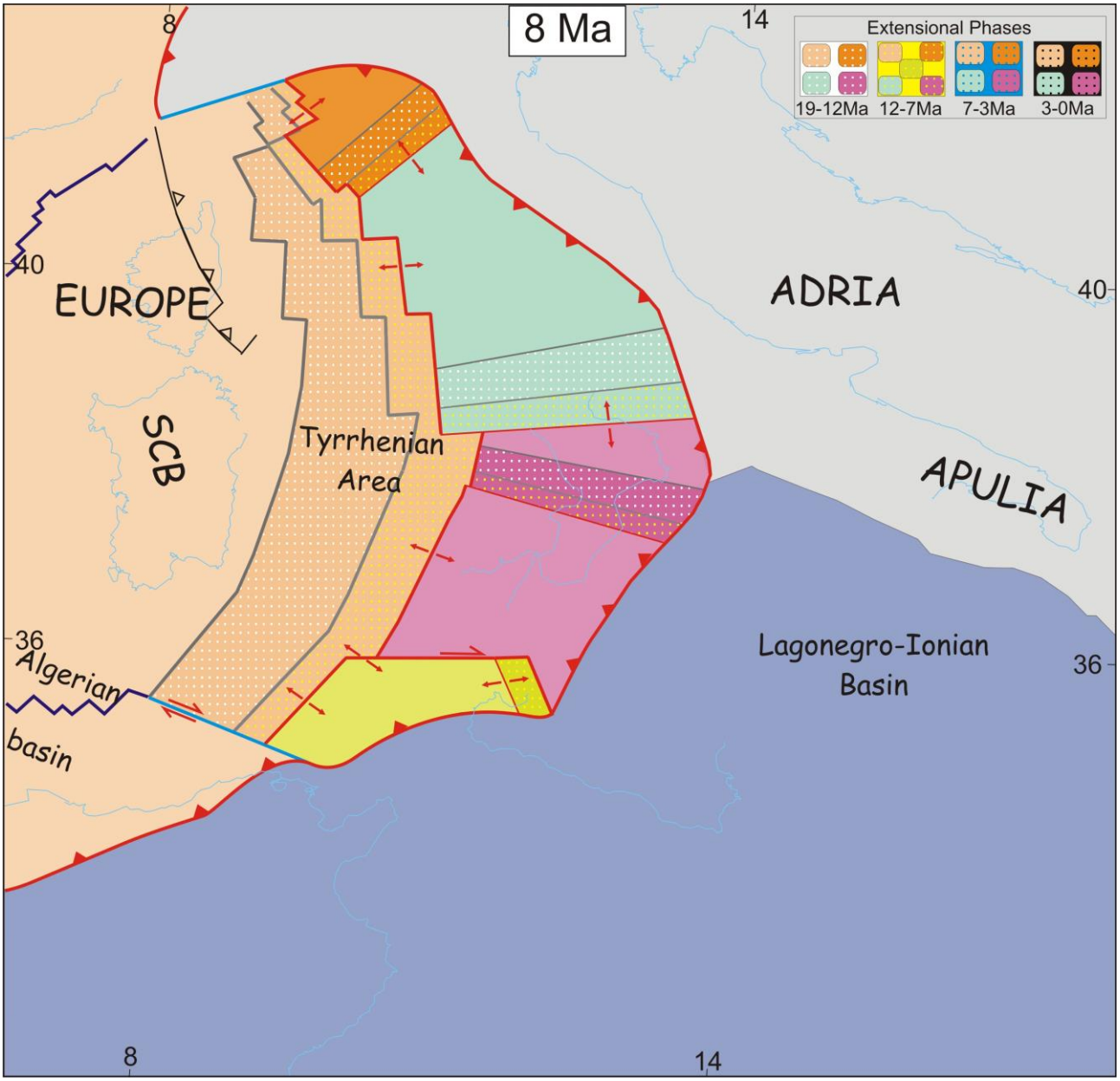
8 Ma
Extensional Phases
19-12Ma
12-7Ma
7-3Ma
3-0Ma
8
14
40
36
EUROPE
ADRIA
SCB
Tyrrhenian
Area
APULIA
Algerian
basin
Lagonegro-Ionian
Basin

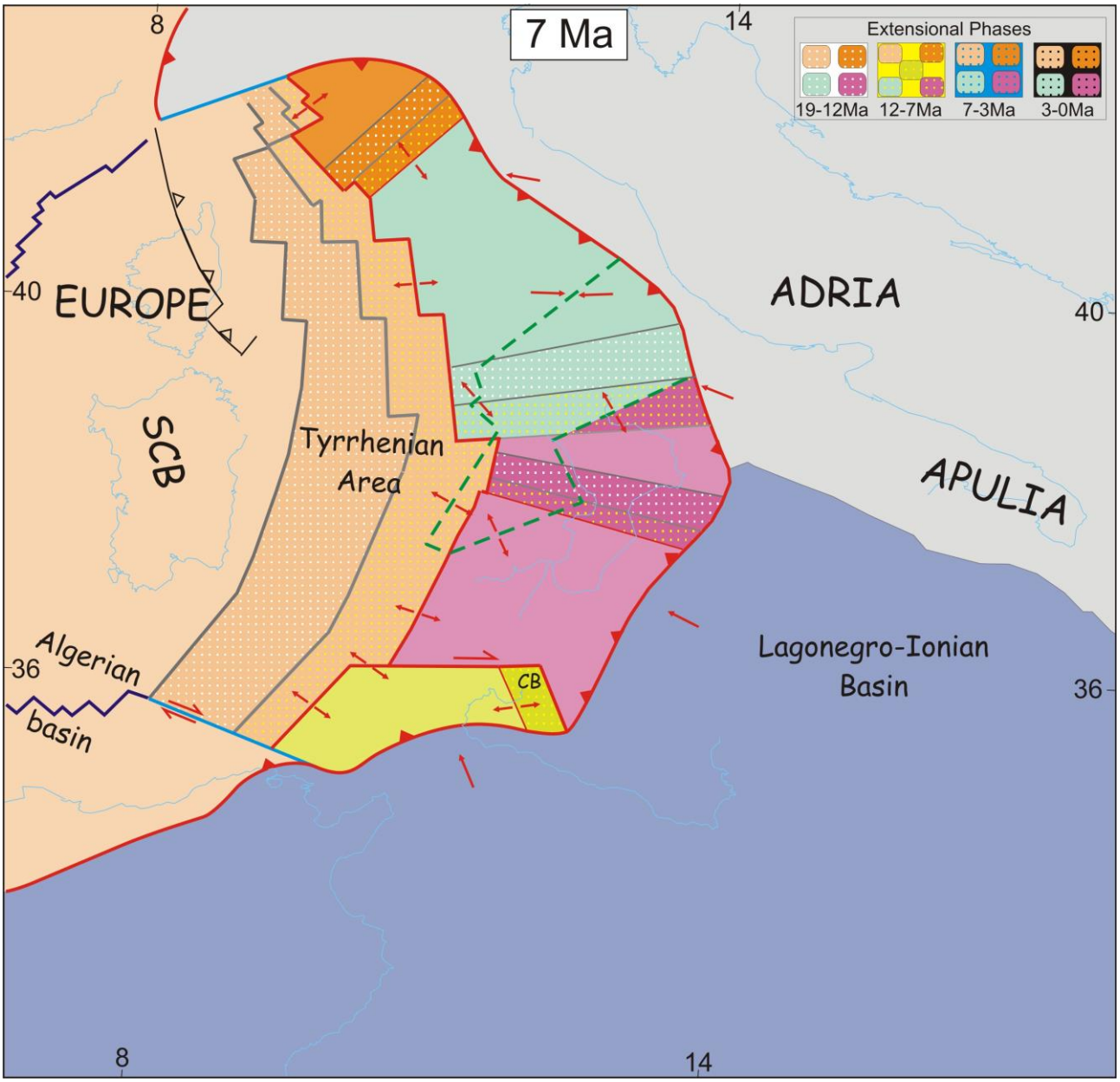
7 Ma
Extensional Phases
19-12Ma
12-7Ma
7-3Ma
3-0Ma
EUROPE
ADRIA
APULIA
SCB
Tyrrhenian
Area
Algerian
basin
CB
Lagonegro-Ionian
Basin
8
14
40
36

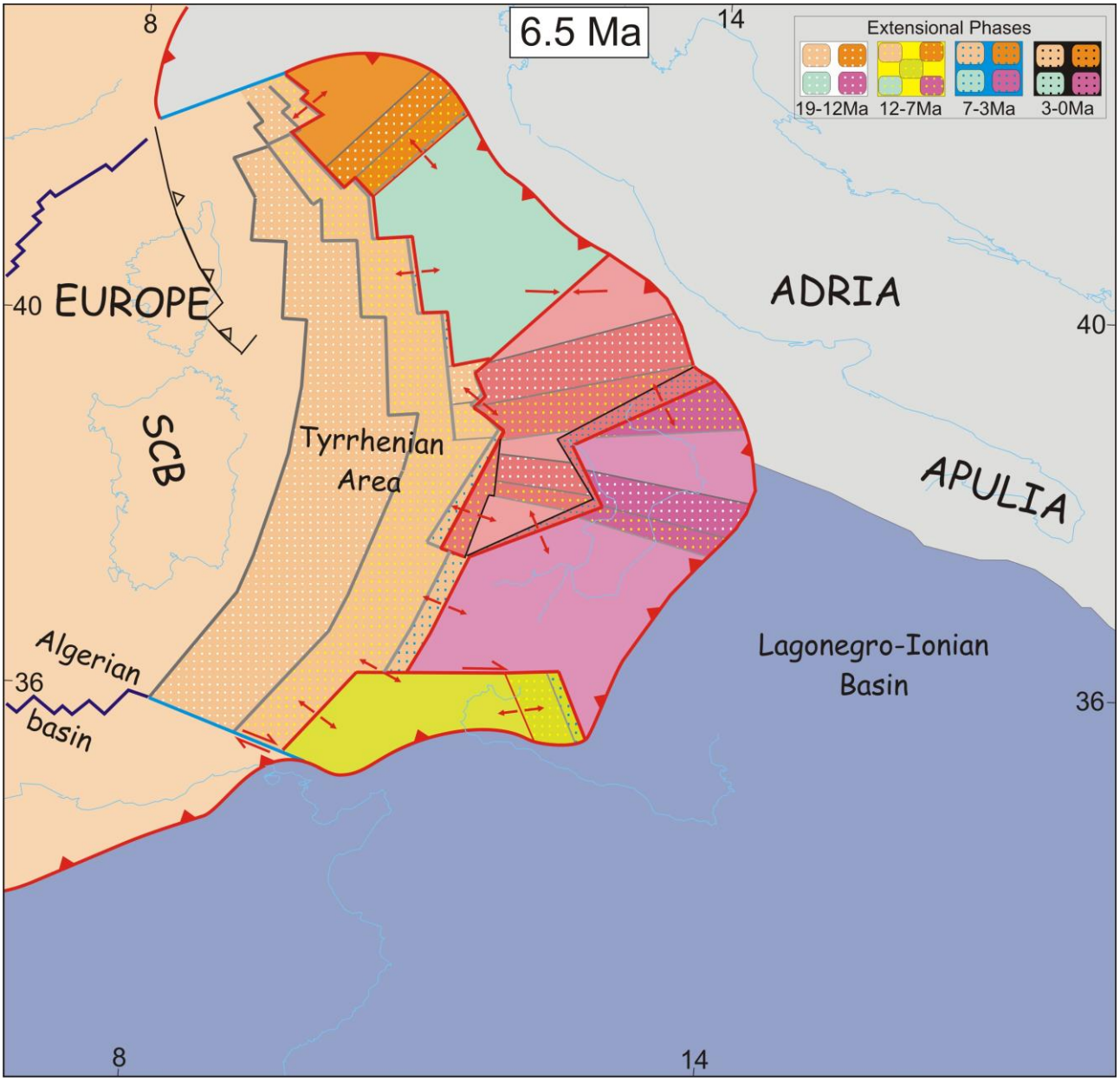
6.5 Ma
Extensional Phases
19-12Ma
12-7Ma
7-3Ma
3-0Ma
EUROPE
ADRIA
APULIA
SCB
Tyrrhenian
Area
Algerian
basin
Lagonegro-Ionian
Basin
8
14
40
36

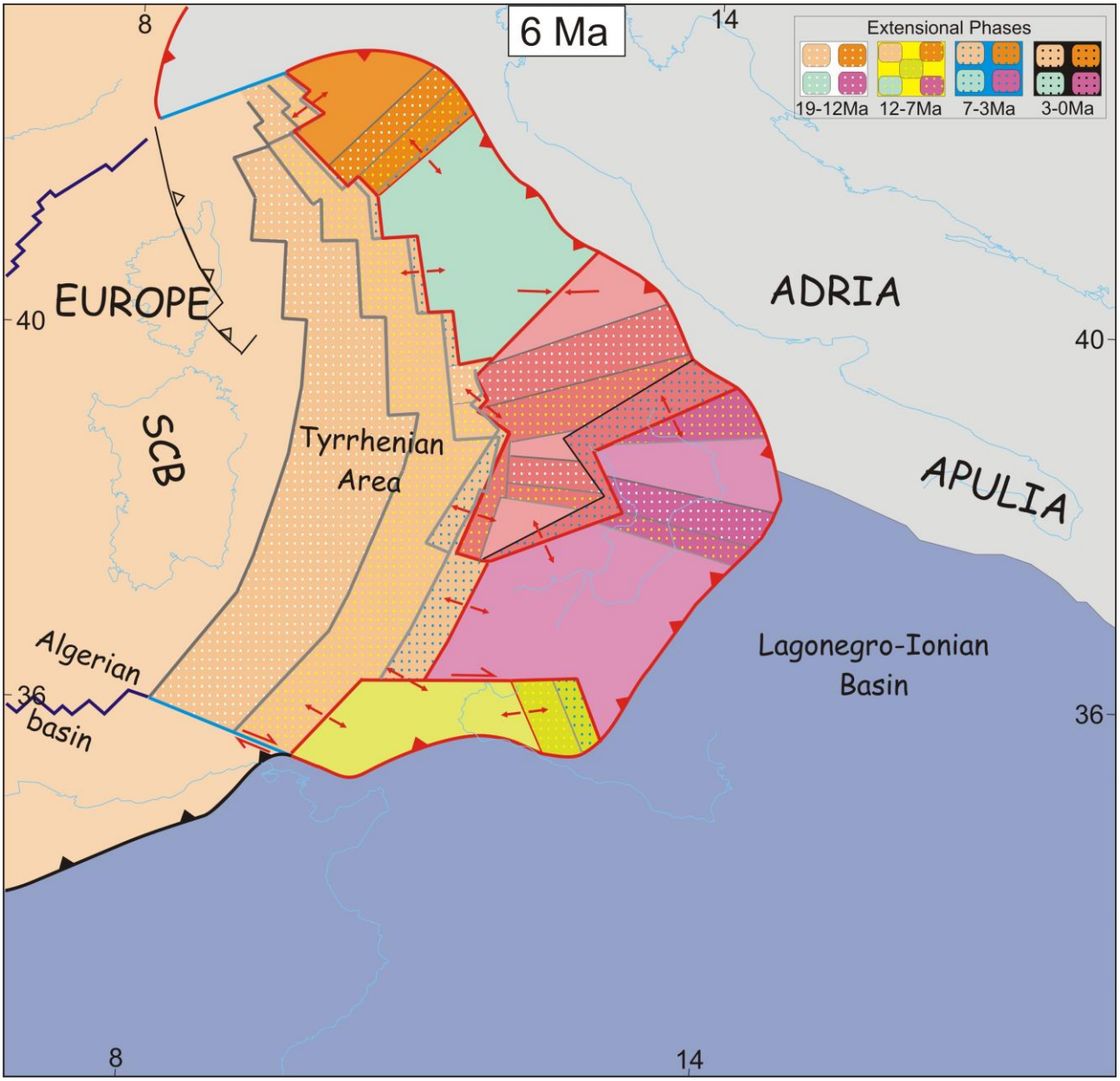
6 Ma
Extensional Phases
19-12Ma
12-7Ma
7-3Ma
3-0Ma
EUROPE
ADRIA
APULIA
SCB
Tyrrhenian
Area
Algerian
basin
Lagonegro-Ionian
Basin
8
14
40
36

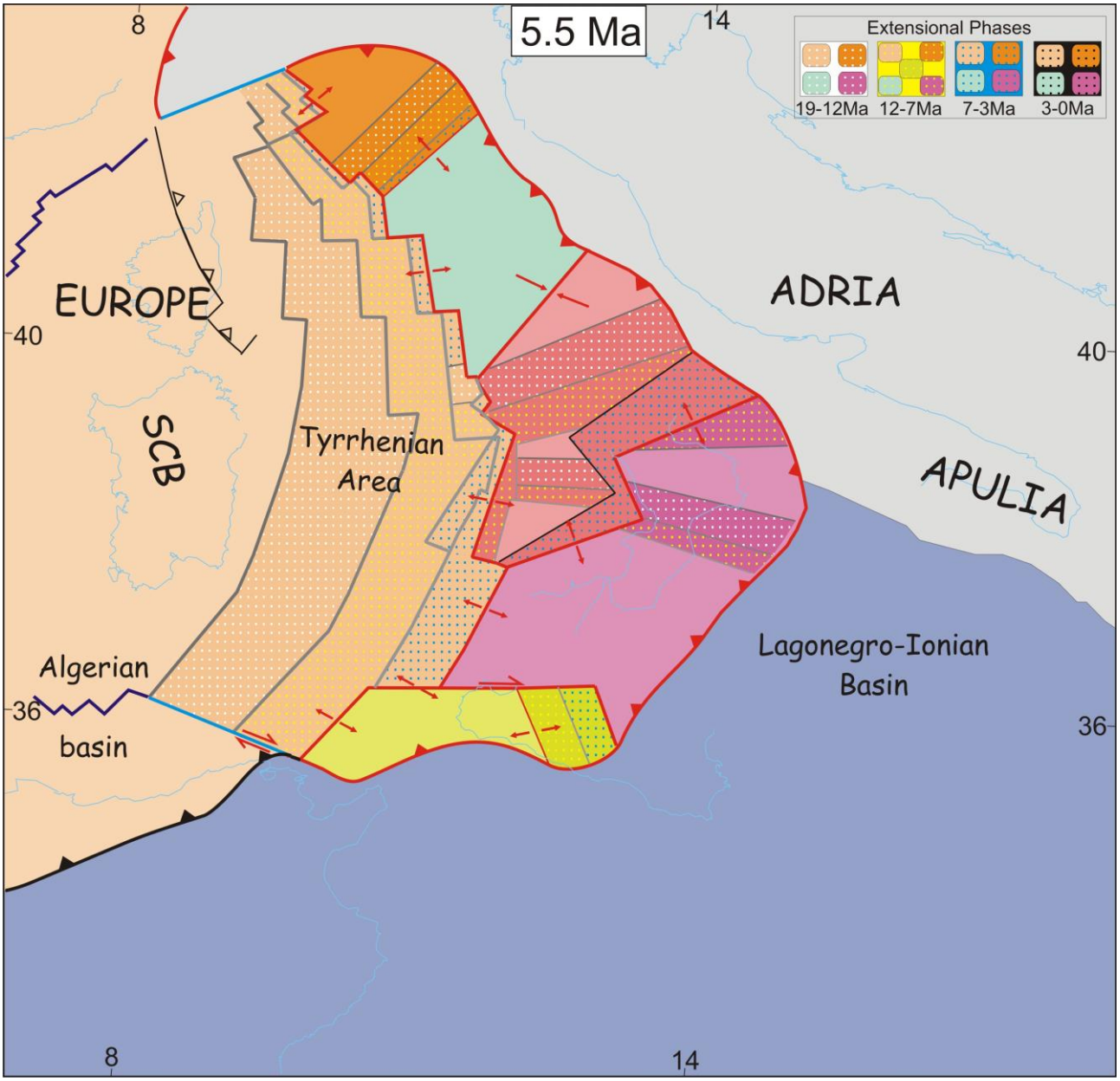
5.5 Ma
Extensional Phases
19-12Ma
12-7Ma
7-3Ma
3-0Ma
EUROPE
ADRIA
APULIA
SCB
Tyrrhenian
Area
Algerian
basin
Lagonegro-Ionian
Basin
8
14
40
36

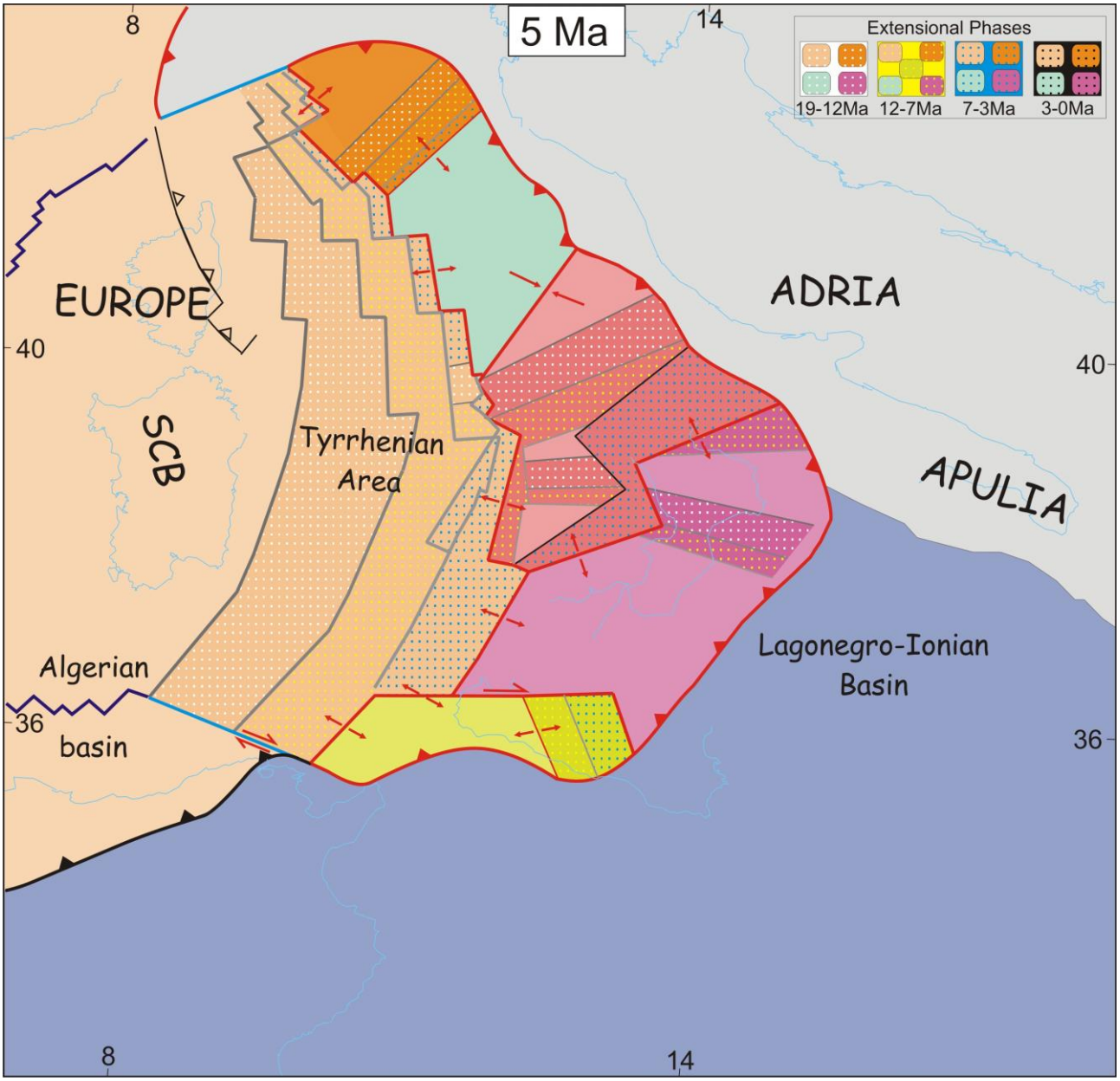
5 Ma
Extensional Phases
19-12Ma
12-7Ma
7-3Ma
3-0Ma
EUROPE
ADRIA
APULIA
SCB
Tyrrhenian
Area
Algerian
basin
Lagonegro-Ionian
Basin
8
14
40
36

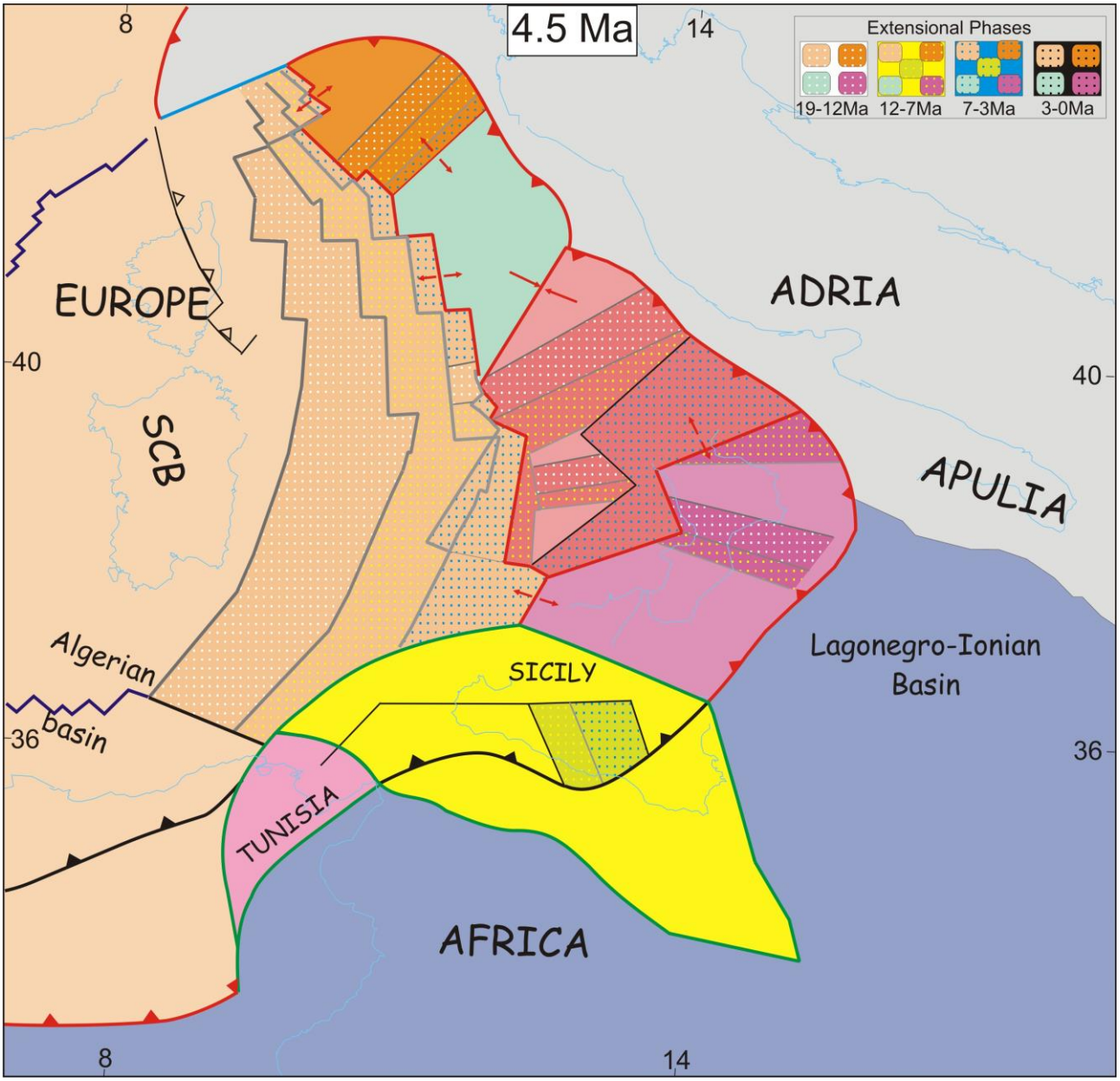
4.5 Ma
Extensional Phases
19-12Ma
12-7Ma
7-3Ma
3-0Ma
EUROPE
ADRIA
APULIA
SCB
Algerian
basin
SICILY
Lagonegro-Ionian
Basin
TUNISIA
AFRICA
8
14
40
36

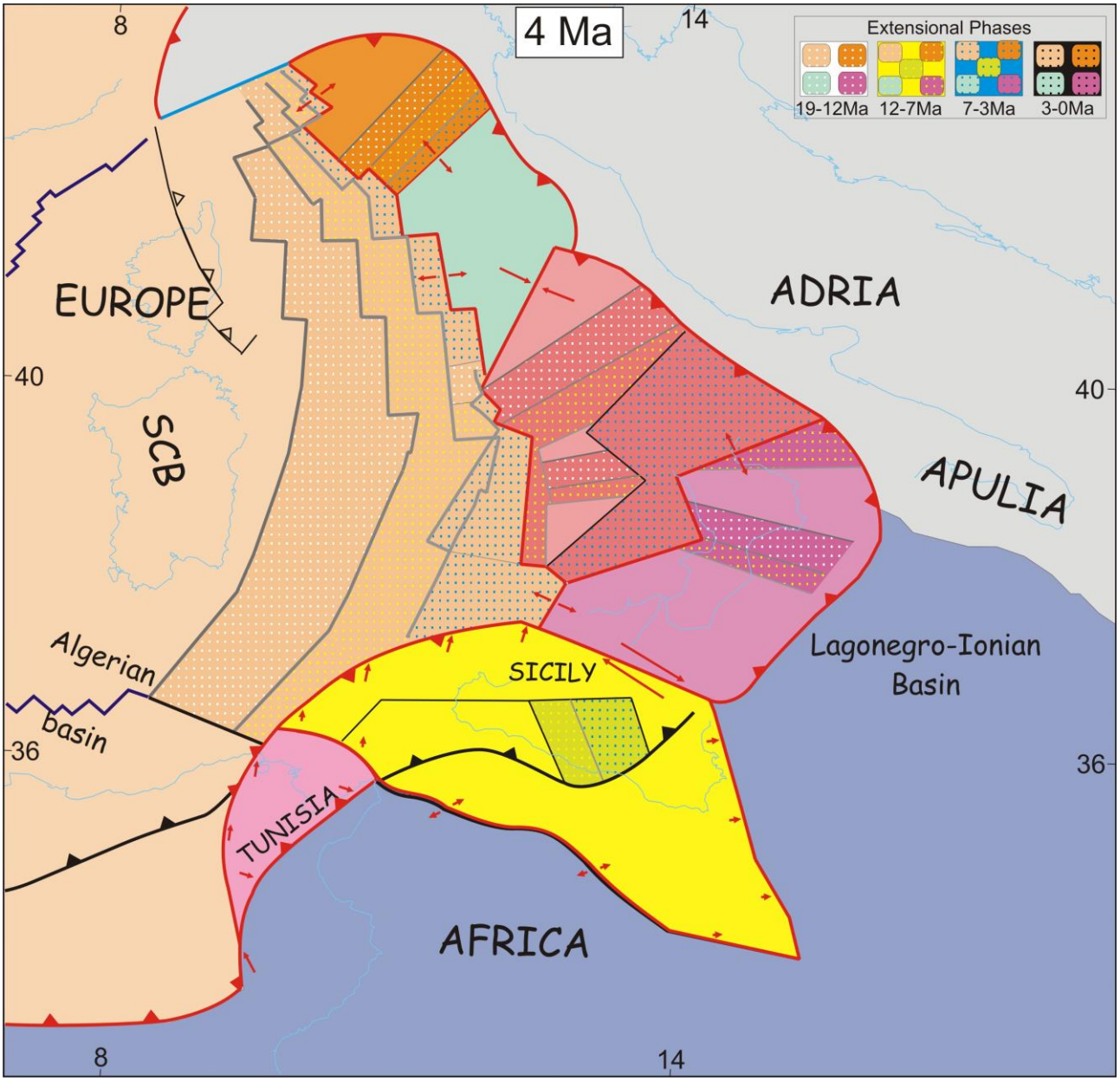
4 Ma
Extensional Phases
19-12Ma
12-7Ma
7-3Ma
3-0Ma
EUROPE
ADRIA
APULIA
SCB
Algerian
basin
SICILY
Lagonegro-Ionian
Basin
TUNISIA
AFRICA
8
14
40
36

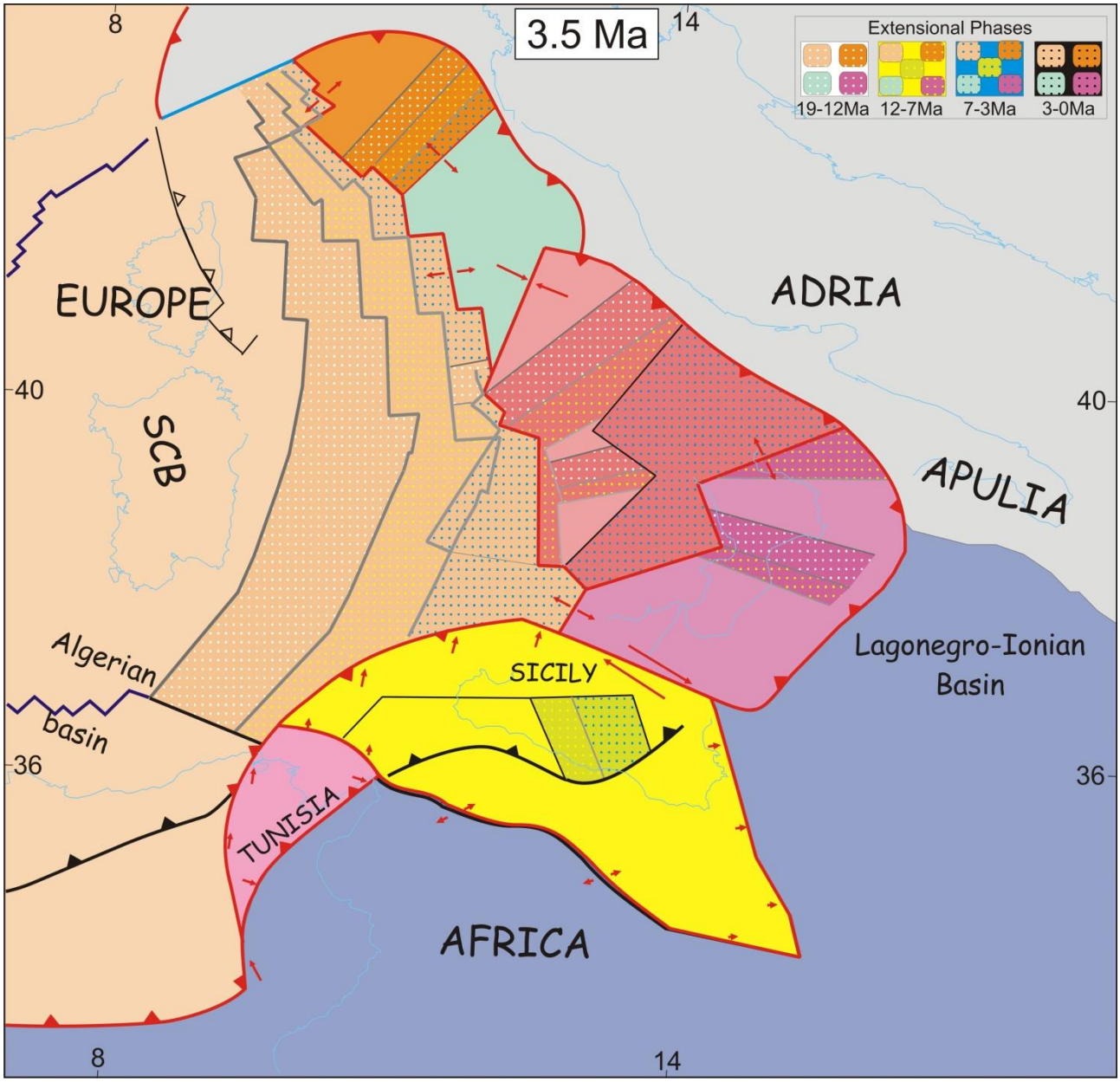
3.5 Ma
Extensional Phases
19-12Ma
12-7Ma
7-3Ma
3-0Ma
EUROPE
ADRIA
APULIA
SCB
Algerian
basin
SICILY
Lagonegro-Ionian
Basin
TUNISIA
AFRICA
8
14
40
36

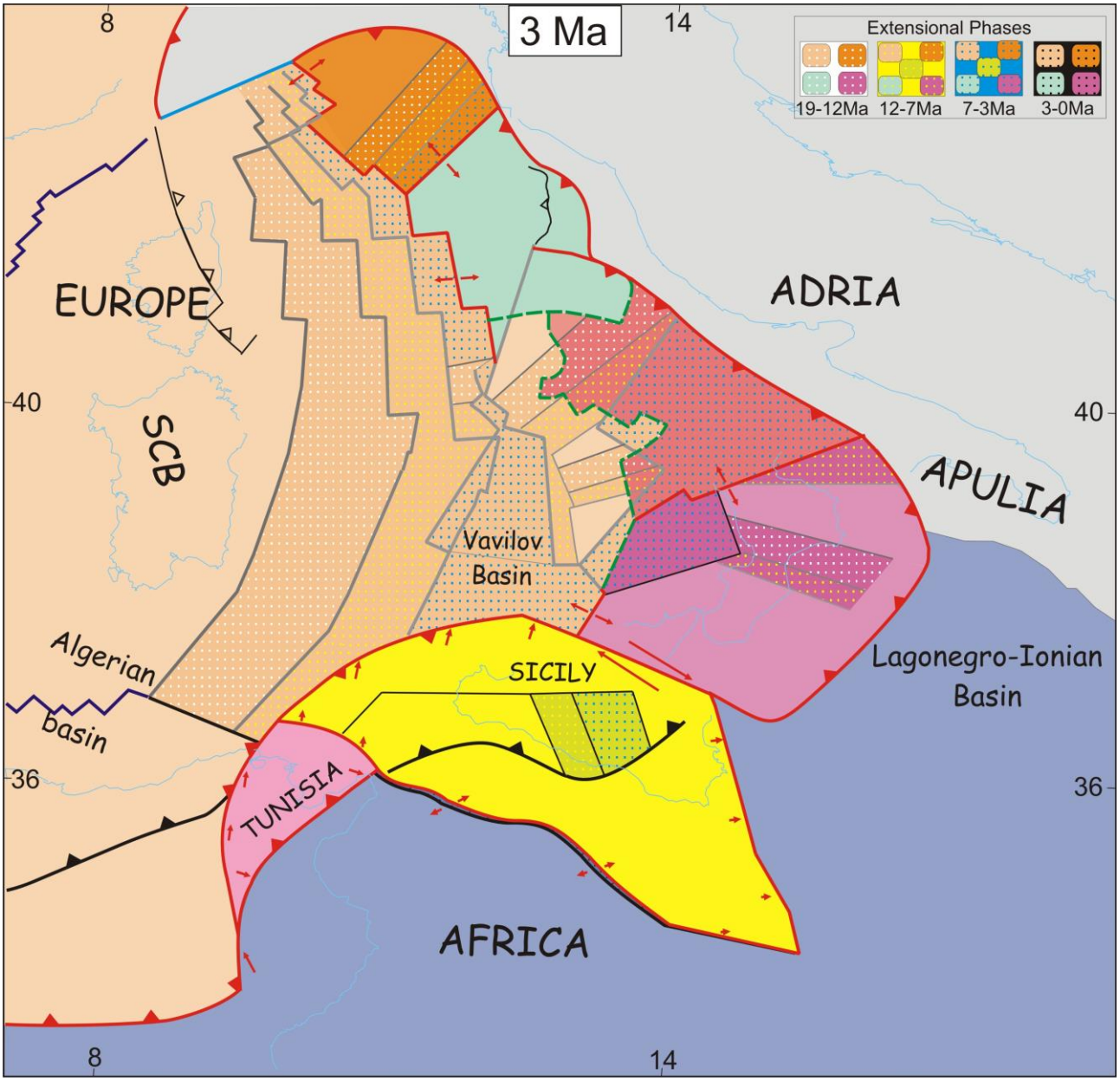
3 Ma
Extensional Phases
19-12Ma
12-7Ma
7-3Ma
3-0Ma
EUROPE
ADRIA
APULIA
SCB
Vavilov
Basin
Algerian
basin
SICILY
Lagonegro-Ionian
Basin
TUNISIA
AFRICA
8
14
40
36

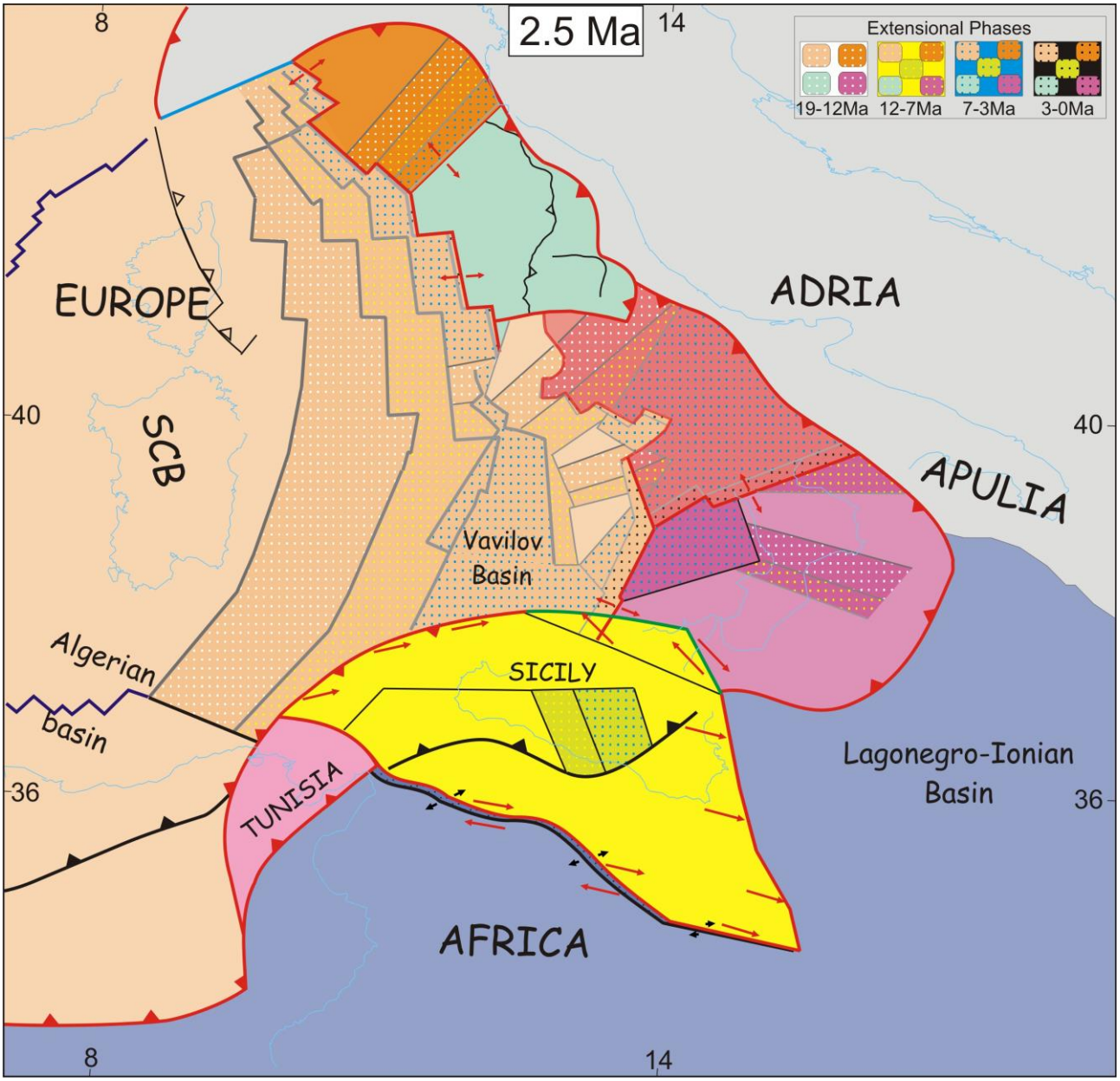
2.5 Ma
Extensional Phases
19-12Ma
12-7Ma
7-3Ma
3-0Ma
EUROPE
ADRIA
APULIA
SCB
Vavilov
Basin
Algerian
basin
SICILY
TUNISIA
Lagonegro-Ionian
Basin
AFRICA
8
14
40
36

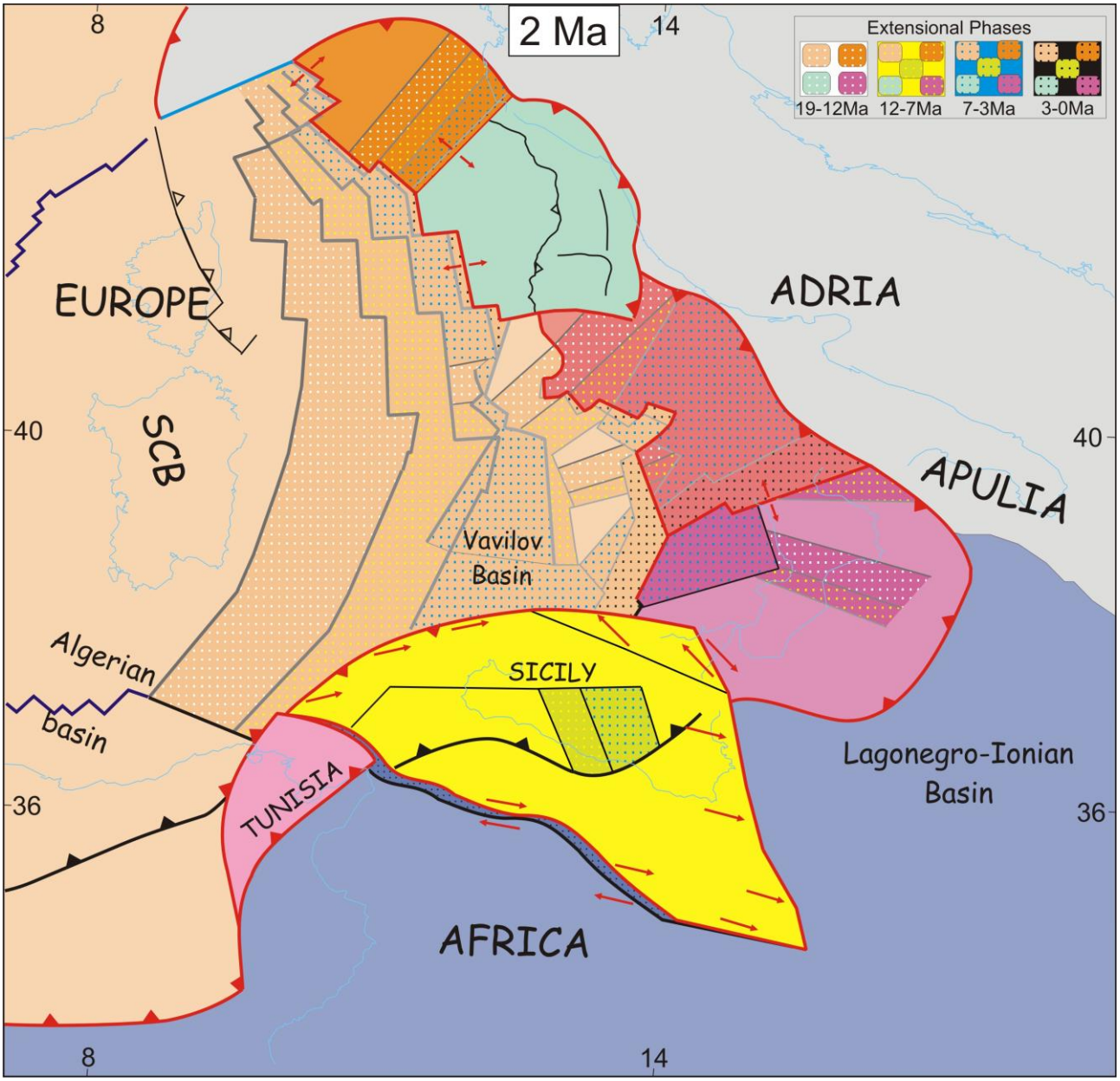
2 Ma
Extensional Phases
19-12Ma
12-7Ma
7-3Ma
3-0Ma
EUROPE
ADRIA
SCB
APULIA
Vavilov
Basin
Algerian
basin
SICILY
TUNISIA
Lagonegro-Ionian
Basin
AFRICA
8
14
40
36

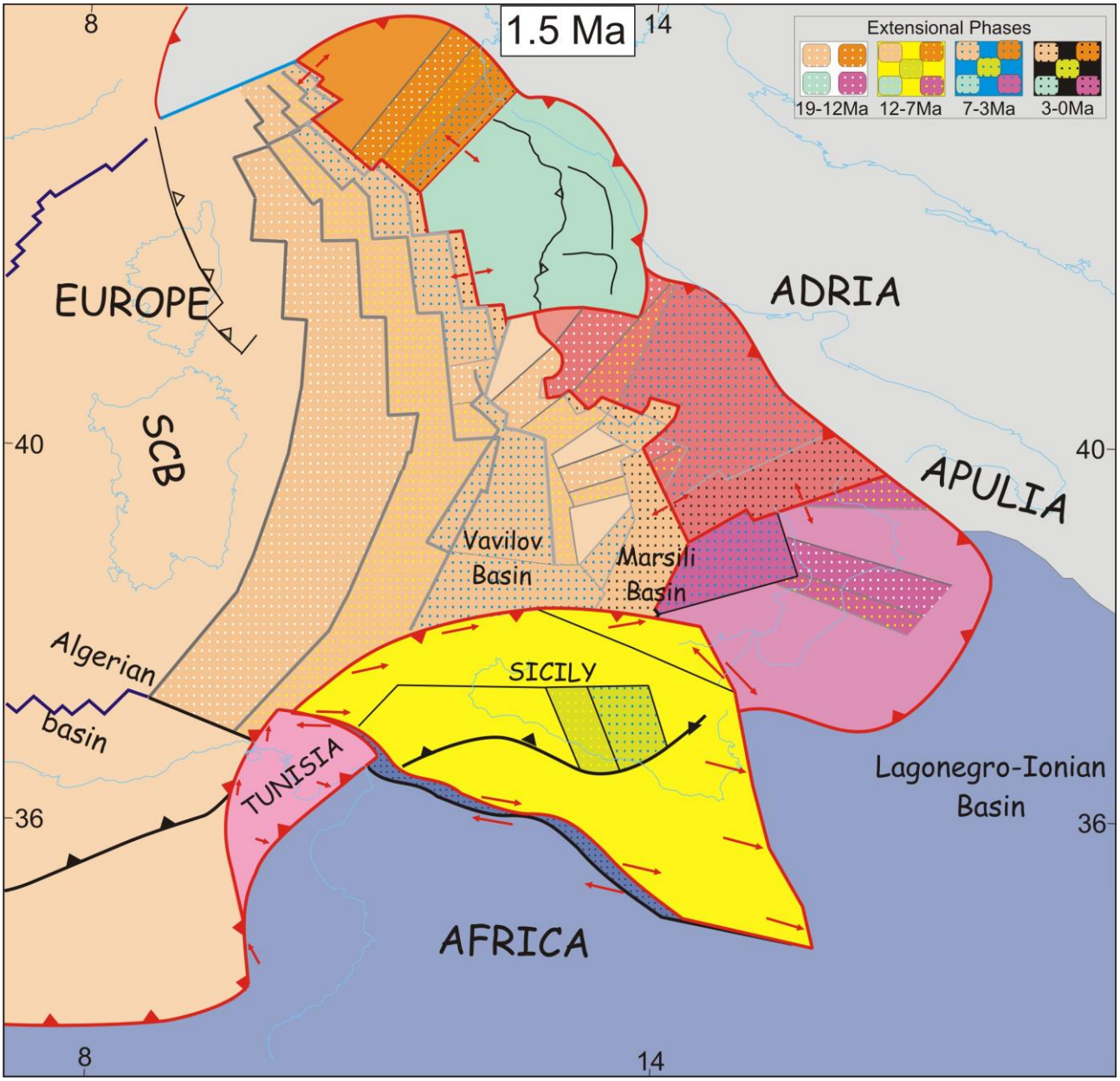
1.5 Ma
Extensional Phases
19-12Ma
12-7Ma
7-3Ma
3-0Ma
EUROPE
ADRIA
APULIA
SCB
Vavilov
Basin
Marsili
Basin
SICILY
Algerian
basin
TUNISIA
Lagonegro-Ionian
Basin
AFRICA
8
14
40
36

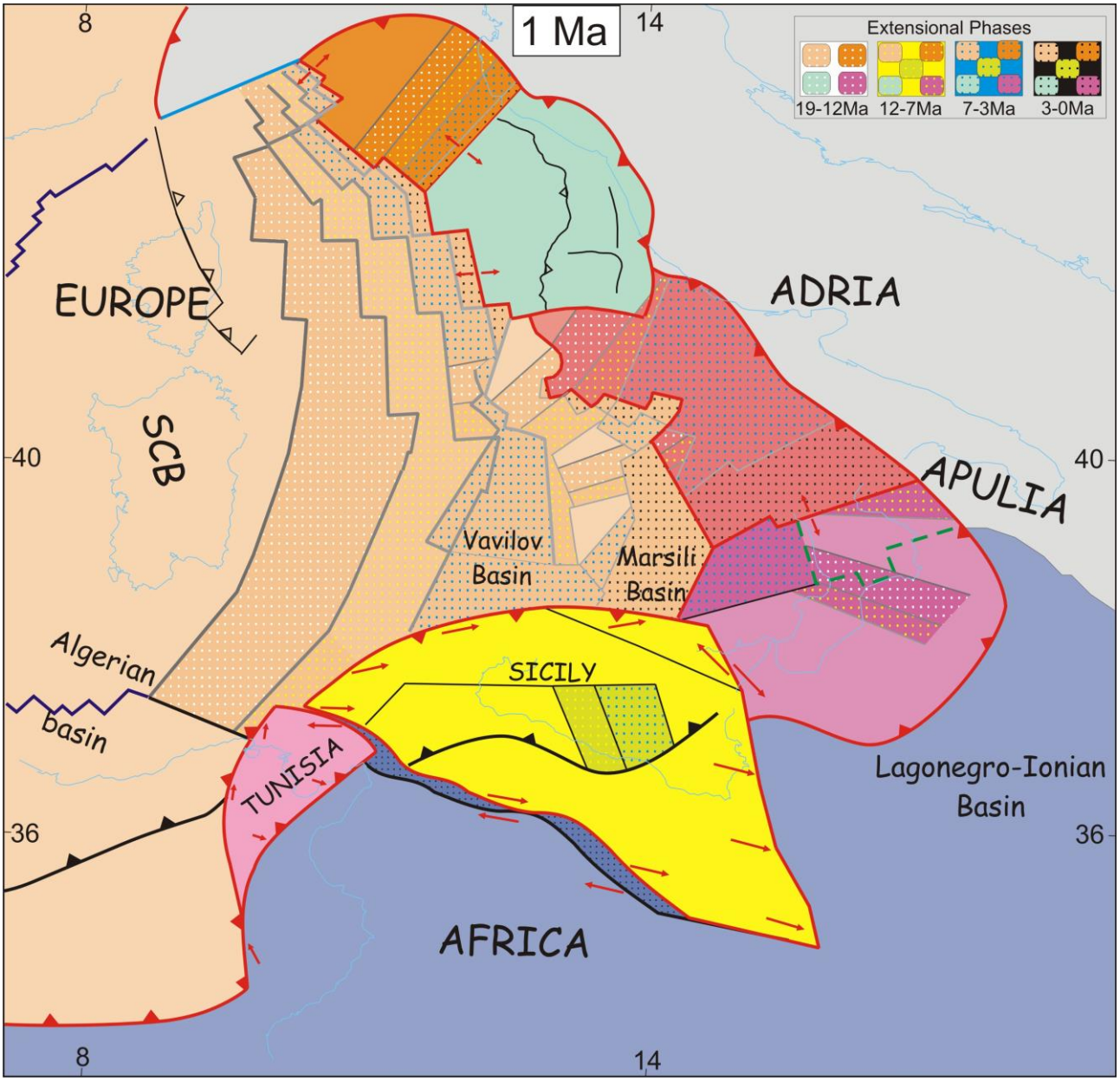
1 Ma
Extensional Phases
19-12Ma
12-7Ma
7-3Ma
3-0Ma
EUROPE
ADRIA
APULIA
SCB
Vavilov
Basin
Marsili
Basin
SICILY
Algerian
basin
TUNISIA
Lagonegro-Ionian
Basin
AFRICA
8
14
40
36

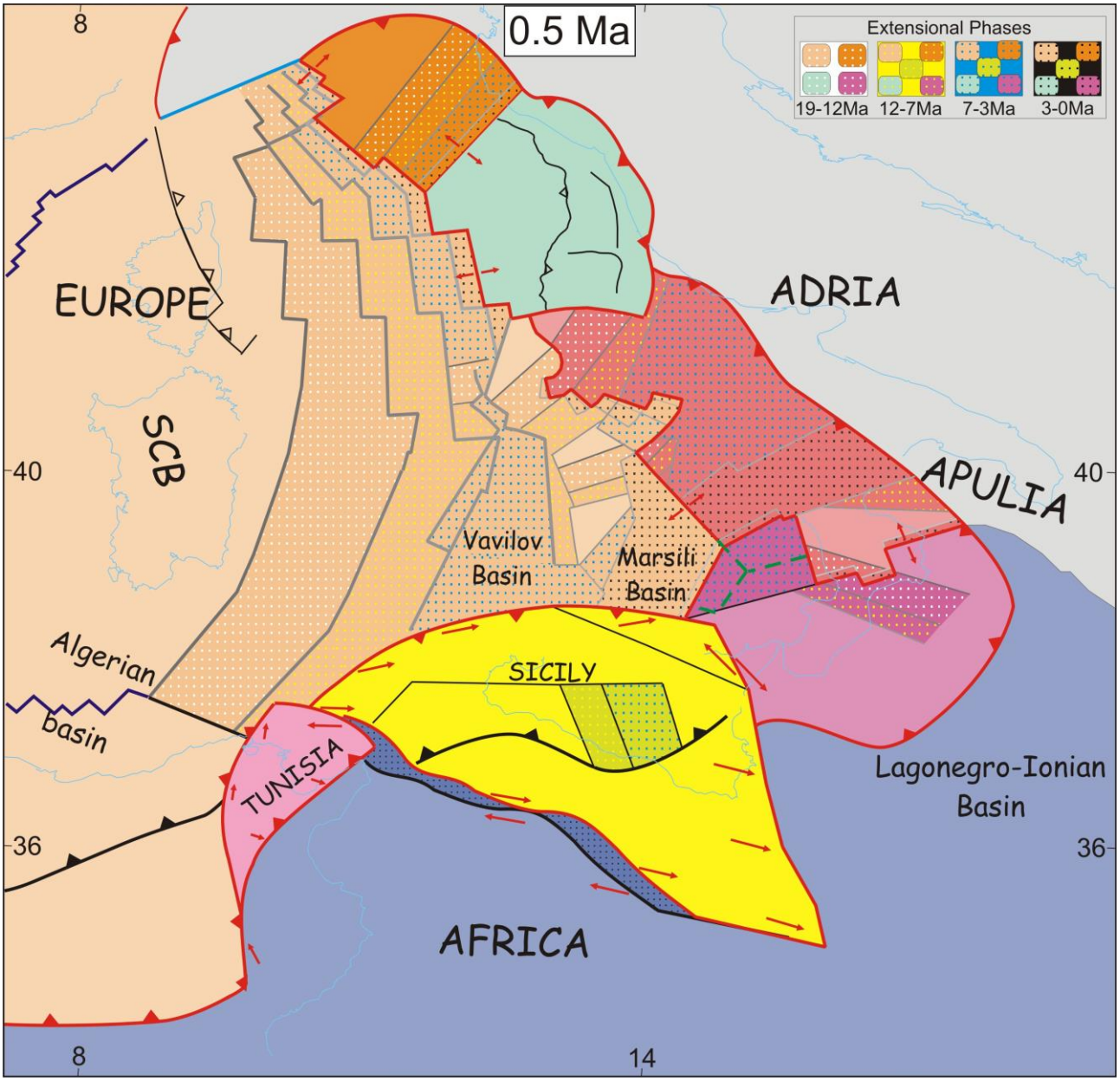
0.5 Ma
Extensional Phases
19-12Ma
12-7Ma
7-3Ma
3-0Ma
EUROPE
ADRIA
APULIA
SCB
Vavilov
Basin
Marsili
Basin
SICILY
Algerian
basin
TUNISIA
Lagonegro-Ionian
Basin
AFRICA
8
40
36
14

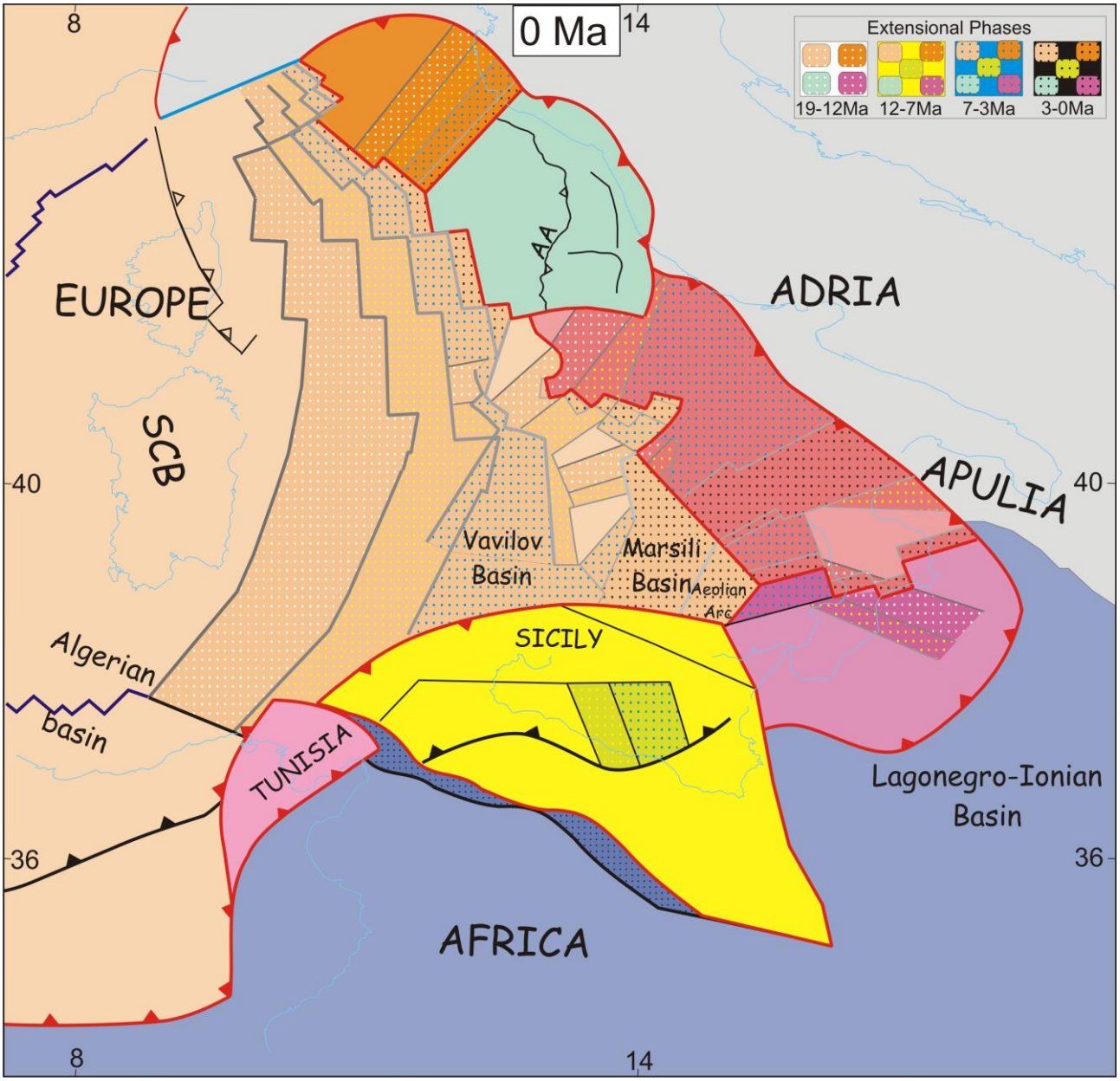
0 Ma
Extensional Phases
19-12Ma
12-7Ma
7-3Ma
3-0Ma
EUROPE
ADRIA
AA
SCB
APULIA
Vavilov
Basin
Marsili
Basin
Aeolian
Arc
SICILY
Algerian
basin
TUNISIA
Lagonegro-Ionian
Basin
AFRICA
8
14
40
36